LOCAL DELIVERY OF SMALL INTERFERING RNA TO INHIBIT

OSTEOPOROSIS USING A COMBINATION

DEVICE STRATEGY

by

Yuwei Wang

A dissertation submitted to the faculty of
The University of Utah
in partial fulfillment of the requirements for the degree of

Doctor of Philosophy

Department of Pharmaceutics and Pharmaceutical Chemistry

The University of Utah

December 2011

The University of Utah Graduate School

STATEMENT OF DISSERTATION APPROVAL

The dissertation of **Yuwei Wang**

has been approved by the following supervisory committee members:

David Grainger	, Chair	**8/11/11** Date Approved
Scott Miller	, Member	**8/9/11** Date Approved
Carol Lim	, Member	**8/8/11** Date Approved
Steven Kern	, Member	**8/8/11** Date Approved
Thomas Higgins	, Member	**8/8/11** Date Approved

and by **David Grainger** , Chair of

the Department of **Pharmaceutics and Pharmaceutical Chemistry**

and by Charles A. Wight, Dean of The Graduate School.

ABSTRACT

RNA interference (RNAi) is a powerful tool to knock down specific message RNA expression levels in cells by exploiting a natural intracellular regulatory phenomenon in mammalian species. Gene silencing using short interfering RNAs (siRNAs) has many potential therapeutic applications. Local or topical siRNA therapeutics have been most actively investigated.

Osteoporosis is rapidly becoming a global healthcare crisis worldwide. Most osteoporotic fractures require surgical intervention, reduction and stabilization, and various fixation devices are used as implants to improve fracture healing, necessitating the development of new treatment options for this condition. After orthopedic fixation device implantation, large numbers of osteoclast precursors recruited into the peri-implant tissue can rapidly differentiate into osteoclasts which accelerate bone loss and cause aseptic loosening and finally prosthetic failure. Injectable bone cements are clinically used to improve mechanical properties to improve fixation as bone augmentation biomaterials in osteoporosis, with several FDA-approved calcium phosphate cements (CPC) products in clinical use. Compared to nondegradable polymethylmethacrylate bone cement, CPC has several unique properties for bone, including intrinsic osteoconductivity, osteoinductivity and acceptable biocompatibility. Significantly, calcium-based bone cements in bone augmentation use provide a potential depot for local drug delivery directly to bone sites in osteoporosis.

The objective of this dissertation research was to investigate a new strategy to deliver siRNA locally to bone to inhibit osteoclast formation and function in improving osteoporotic bone healing. Our initial siRNA delivery data showed successful use of siRNA against receptor activator of nuclear factor-kappa B (RANK) and farnesyl pyrophosphate synthase (FPPS), resulting in knockdown of RANK in both osteoclast precursor and osteoclast cultures and knockdown of FPPS in both osteoclasts and osteoblasts, supporting a proof-of-concept to deliver siRNA to bone. In order to deliver siRNA to osteoclasts locally, resorbable poly(lactic-co-glycolic acid) (PLGA) microparticles were utilized as protective carriers. Cell-specific phagocytosis was achieved by PLGA particle size-cell phagocyte discrimination and selective uptake by bone phagocytes. PLGA-siRNA particles were dispersed equally into clinical-grade injectable CPC to serve as the delivery carrier and facilitate further active and passive in vivo degradation of cement and potentially for enhancing bone in-growth and healing at surgical sites.

This dissertation is dedicated to my parents, Jingtian Wang and Jingjie Luo, and my sister, Yuhong Wang, who have always been by my side and provided love and support.   Without them, I could not have completed this project.

TABLE OF CONTENTS

ACKNOWLEDGEMENTS

CHAPTER 1

RNA THERAPEUTICS TARGETING OSTEOCLAST-MEDIATED

EXCESSIVE BONE RESORPTION

Abstract

This chapter describes the diversity of molecular targets suitable for RNA interference (RNAi)-based gene knockdown in osteoclasts to control osteoclast-mediated excessive bone resorption. We identify strategies for developing targeted short interfering RNA (siRNA) delivery and efficient gene silencing, and describe opportunities and challenges of introducing siRNA as a therapeutic approach to hard and connective tissue disorders.

Introduction

Current treatments for osteoporosis can be divided into two categories: antiresorptive modulators and anabolic therapies. Estrogen, estrogen receptor modulators, calcitonin and bisphosphonates fall into the first category. Only one anabolic agent—teriparatide—is clinically approved, administrated by daily injection.[1] The limited number of options in antiresorptive therapy reflects inadequate efficacy, severe side effects, high dosing frequency or low patient compliance:[1-6] estrogen treatment exhibits known side effects on breast and uterus inappropriate for long-term use; long-term calcitonin treatment can induce tolerance since more than half of the patients produce circulating antibodies to calcitonin.[7] Bisphosphonates, the most common current

osteoporosis treatment, exhibit general side effects including gastrointestinal irritation, bone/joint pain and jaw osteonecrosis.[8-10] The latter two adverse effects can persist and even spread to new areas of unaffected bone after bisphosphonate therapy is discontinued. Because of bisphosphonate's long half-life, e.g., alendronate's half-life in bone is 10.9 years,[11] drug can remain active in bone for long periods after drug therapy is discontinued. Severe suppression of bone turnover has also been noted.[12, 13] Long-term bisphosphonate therapy increases fracture risk, including atypical fractures first reported in 2005.[14, 15] Recently, oral bisphosphonates were associated with 23 cases of esophageal cancer.[16] Therefore, maximum treatment duration for bisphosphonates is suggested to be 5 years.[17] Bisphosphonates are consequently counter-indicated in the context of fragility fracture healing. This enduring drug bioactivity presents substantial challenges for treatment of osteoporosis. Moreover, clinical studies of systemic bisphosphonate administration in combination with implants for 6 months or 2 years showed significant bone loss in the peri-implant area within 3 months postoperation.[18, 19] Similarly, in total hip arthroplasty, up to 14% bone loss was reported during the first 3 months postsurgery.[20]

Human clinical experience indicates that improved therapeutic strategies are needed in the context of osteoclastic bone resorption therapies. In 2010, denosumab (Prolia[TM], Amgen), a fully humanized monoclonal antibody targeting receptor activator of nuclear factor-kappa B ligand (RANKL), was approved by the FDA as a twice-yearly subcutaneous injection for treating postmenopausal osteoporosis. This antibody therapeutic appears well-tolerated and superior to the common bisphosphonate drug, aldendronate, in preserving bone mineral density in several clinical trials to date.[21, 22] Additional new therapeutics are actively under investigation to meet the

requirements of this fast-growing patient population worldwide.

RNA interference and siRNA delivery as a new therapeutic approach

RNA interference (RNAi) is a sequence-specific posttranscriptional gene silencing tool.[23] The process of gene-specific silencing through destruction of its message RNA transcript can be triggered by endogenous or exogenous small interfering RNAs (siRNAs).[24] Long double-stranded mRNAs derived from endogenous gene transcription or transfected transgene plasmids present in the cytoplasm can trigger the cleavage activity of the intracellular enzyme, Dicer, to cut mRNA into 19-nucleotide pairs with two nucleotide overhangs at both 3'-ends, called small interfering RNA (siRNA).[25] These double-stranded siRNA pieces then incorporate into RNA-induced silencing complexes (RISCs) which have a catalytic core comprising Argonaute (Ago) family proteins.[26, 27] Ago-2 then cleaves and removes the siRNA sense strand and thereafter RISC becomes activated with the remaining antisense siRNA strand. The antisense siRNA strand guides RISC activity in the cytoplasm to cleave its targeted complementary mRNA molecules, resulting in down-regulation of the targeted gene and corresponding protein expression. First introduced in 2001, RNAi has been exploited for its highly specific mechanism of mRNA transcript targeting, and as a target screening and validation tool for cell signaling studies of many types. RNAi is used for investigating and elucidating mammalian gene function as an alternative to knockout techniques. Specifically, siRNA also shows great potential for future targeted therapeutics for gene-associated diseases. Gene silencing using siRNA has several advantages intrinsic to RNAi, such as its high specificity, intrinsic biological response [28] and more efficient and specific silencing effects with

lower dosing requirements, compared to antisense-based gene silencing.[29]

However, as polyanions, synthetic or in situ transcribed siRNAs do not readily or reliably enter mammalian cells. The main challenge in developing siRNA therapies, like other nucleic acid therapeutics, is to deliver them specifically into targeted tissues or cells. Viral and nonviral vectors have been employed to address siRNA cell transfection inefficiency, and nonviral delivery is typically achieved by cationic lipoplexing reagents.[24, 30] Viral vector-based delivery is consistently associated with vector-based short hairpin RNA (shRNA) production systems, a DNA-based strategy to encode and obtain host-synthesized shRNAs in situ. These shRNAs can be further intracellularly processed into siRNA by Dicer. Both methods have their advantages and disadvantages. Nonviral delivery uses siRNA directly to generate potent silencing effects; therefore, it is simple and controllable. However, single-dose siRNA silencing effects are transient (up to 5 days in dividing cells),[24] and lipid-based siRNA delivery complexes can be removed from circulation by the liver rapidly, and lack tissue/cell specificity. The viral vector-based shRNA strategy has the potential of being able to provide stable, enduring gene silencing. Gene therapy can in principle continuously generate siRNA. The major bottleneck of the viral vector is its well-known safety issues.[24] Nevertheless, while nonviral delivery avoids the pitfalls of viral vector delivery, including high viral toxicity, possible carcinogenicity, proven immunogenicity and significant cost limitations,[31] it is extremely inefficient in targeting, transfection and expression. Because of the substantial challenges with reliable systemic siRNA delivery and targeting, almost all current clinical foci for siRNA-based therapeutics are based on local or topical siRNA therapeutics. Successful siRNA delivery approaches currently include ocular, respiratory, central

nervous system, dermal and vaginal delivery where local dosing accesses target cell populations directly.[32-36] One largely unexplored delivery route is via implantable combination devices facilitating local siRNA delivery directly from medical implants to adjacent tissue sites.[37]

RNAi applications in new osteoporosis therapies

As a nucleic acid therapeutic precedent, DNA-based gene therapy has developed rapidly for musculoskeletal applications in the last two decades. The therapeutic approach has been introduced to various disease categories: osteogenesis imperfecta,[38] lysosomal storage disorders,[39] rheumatoid arthritis,[40, 41] osteoarthritis,[42] and osteoporosis.[43-45] Specific to osteoporosis, gene transfer strategies deliver genetic material, either using intravenous injection of viral vectors carrying osteoprotegerin (OPG) cDNA[44, 45] or local injection of interleukin-1 receptor antagonist cDNA-transduced cells.[43] Due to desirable short-term transgene expression without the need to closely regulate transgene expression, DNA-based gene therapy has recently produced progress in musculoskeletal tissue healing. In a rat critical size defect model in femurs, BMP-2 cDNA-transduced cells seeded into collagenous scaffolds showed better healing compared with use of recombinant BMP-2 protein directly.[46] The feasibility of intralesional injection of viruses carrying cDNA encoding osteoinductive genes has been demonstrated in both rabbit and rat segmental defect models.[47, 48] Gene transfer strategies have been developed for many applications for musculoskeletal healing, such as spine fusion, articular cartilage and meniscus, intervertebral disc, ligament and tendon.[49] DNA-based transgene therapies continue to demonstrate the potential for treating musculoskeletal diseases, providing a solid foundation for

developing siRNA-based approaches in this field.

Applications of RNAi to musculoskeletal therapies can target a large and increasing number of signaling cascades in several tissue types, primarily bone and cartilage. In addition, RNAi can be utilized in several therapeutic categories: inflammation, degeneration and regeneration. RNAi use in the context of treating rheumatoid arthritis has been actively investigated to date.[50] Osteoporosis is less studied but represents a particularly interesting application for RNAi therapeutics, targeting a diverse number of possible pathways achieved by local delivery to fragility sites via bone augmentation strategies. Instead of complete gene knockout, both site-specific and temporally selective control over cellular signaling activity are perhaps more appealing for developing new osteoporosis therapies. FDA-approved denosumab demonstrates precedent success in this regard. The transient efficacy of siRNA means it can be turned off and on, facilitating this transient programmed benefit. Notably, siRNAs have new targets distinct from other drug classes, with their own unique characteristics: they interrupt intrinsic cellular pathways with high targeting specificity.

Osteoclastogenesis and osteoclastic bone resorption

Normal bone is constantly replaced by resorption of old bone by osteoclasts and deposition of new bone by osteoblasts. Continuous bone turnover results in the adult human skeleton being completely replaced every 10 years.[51] This balance of bone turnover is tightly regulated in healthy individuals. Osteoclasts residing at or near the bone surface are multinucleated phagocytic cells formed by the fusion of monocyte macrophage precursor cells.[52] They are responsible for

resorbing bone, working together with osteoblasts (bone producing cells) and playing a central role in normal bone remodeling. Two cytokines – nuclear factor kappa B (NF-κB) RANK ligand (RANKL, also called TRANCE/OPGL/ODF) and macrophage colony-stimulating factor (M-CSF) [53, 54] – are essential to this process.[55-57] Previously published evidence shows that osteoclast formation can be stimulated in vitro using cocultures of bone marrow cells and stromal cells/osteoblasts expressing those two cytokines.[58-60] M-CSF interacting with its c-fms receptor provides signals necessary for precursor cell survival and proliferation by receptor binding on early osteoclast precursor cells.[61] RANKL is the key cytokine for promoting osteoclastogenesis. Interactions between soluble RANKL and RANK receptor on the surface of osteoclast precursors are essential for expression of osteoclast-specific genes,[62] bone resorption and survival of mature osteoclasts.[63] Furthermore, osteoclastogenesis is negatively regulated by OPG (or osteoclastogenesis inhibitory factor, OCIF), also expressed by stromal cells and osteoblasts.[64] OPG is a decoy receptor that competes with RANK for binding RANKL.[65] Osteoclast production can be blocked by over-expression of OPG, resulting in osteopetrosis in mice.[64, 66] In this RANKL/RANK/OPG regulatory axis, positive regulator RANKL and negative regulator OPG are coordinated through interaction with RANK to regulate normal bone formation and degradation.

RANK is therefore a central factor in this bone metabolic regulatory pathway. It is central to much of the osteoclast functional phenotype and to bone metabolic balance. Therefore, RANK was chosen as the knockdown target to suppress osteoclast-mediated bone resorption.[67] Selective knockdown of RANK in mouse bone marrow cells can significantly block formation of Tartrate Resistant Acid Phosphatase (TRAP)-positive cells with RANKL and M-CSF in vitro.

Cell-cell fusion can be inhibited in RANK siRNA-transfected osteoclasts, consistent with the fact that RANKL stimulation is critical for cell fusion to osteoclasts.[68] Successful transfections have been seen in mature osteoclasts, and osteoclast-mediated bone resorption was dramatically inhibited by RANK siRNA using the pit formation assay in vitro.[67]

Activation of RANK by RANKL not only induces osteoclast differentiation and survival, but also leads to activation of bone resorption by mature osteoclasts. Once activated, differentiated osteoclasts move to the target matrix and attach to the bone surface. After attachment, an isolated extracellular microenvironment, called the sealing zone, formed between the interface of the underlying bone with osteoclast membranes, is actively generated by osteoclasts.[69] Osteoclasts polarize themselves to form a ruffled membrane adjacent to the bone surface which is their resorptive organelle in the sealing zone. Osteoclasts then acidify and dissolve the underlying bone matrix by pumping hydrogen ions mediated by a vacuolar H^+-adenosine triphosphatase (H^+-ATPase) through the ruffled membrane into the sealing zone. Osteoclast intracellular pH is maintained by HCO_3^-/Cl^- exchange across cell surfaces other than the ruffled membrane area.[70] These ion transporting events result in an acidic pH of ~4.5 only within the resorptive microenvironment.[71] The mineral phase of bone is first digested under this acidic milieu, followed by degradation of the collagen-rich demineralized organic component of bone by released hydrolytic enzymes.[72] Bone matrix degradation proteins are taken up by osteoclasts through the ruffled membrane from the resorption lacuna and released through the basolateral membrane into the extracellular space.[73] After local bone resorption is complete at this site, osteoclasts detach from the bone matrix and migrate to a new site to begin the next functional cycle. Because of this

central role in bone processing, osteoclasts are naturally a major target for most studies seeking to suppress bone resorption. In this review, siRNA targets for osteoporosis are sorted into three categories: osteoclastogenesis, osteoclastic bone resorption activity and osteoclast survival, including other potential associated targets identified to date. In addition, progress in developing efficient target silencing, delivery issues and emerging opportunities and challenges to exploit siRNA for therapeutic purposes are discussed.

<u>Targets for siRNA in Osteoporosis and Bone Metabolism</u>

Osteoclastogenesis

Transcription factors essential for osteoclastogenesis, including NF-κB downstream of RANK,[74] mediate osteoclast differentiation and inflammatory osteolysis.[75] Osteoclast differentiation failure is reported to be caused by mutant NF-κB in mice.[76] Its upstream regulator, IκB kinase (IKK) complex, contains IKKα and IKKβ as catalytic subunits and IKKγ as a regulatory subunit.[77, 78] IKKα and IKKβ are required for normal bone homeostasis. IKKβ is essential for osteoclastogenesis and osteoclast survival since deletion of IKKβ impairs osteoclast differentiation in vitro and in vivo.[79, 80] IKK alpha(-/-) mice did not show overall skeletal defects, but IKK alpha(-/-) hematopoietic cells failed to differentiate into multinucleated osteoclasts.[81] Nonetheless, the role of IKKγ is unclear. Recently, transient transfection of siRNA to inhibit IKKγ in bone marrow-derived osteoclast precursors was reported using a retroviral delivery approach.[82] When IKKγ was knocked down, formation of multinucleated osteoclasts was reduced 83% compared with controls. In addition, the role of IKKγ was confirmed through observation that RANKL-induced osteolysis

was impeded by preventing oligomerization of IKKγ monomers using peptides in mice.[82] The study

suggested that IKKγ is essential for osteoclastogenesis, and thus, all three IKK subunits could be

potential targets for inhibiting osteoclastogenesis and osteolysis using siRNA.

Interactions between RANKL and RANK are essential for osteoclastogenesis. RANK has

three TNF receptor-associated factor 6 (TRAF6) binding sites and recruits TRAF6 to activate the

transcription factors NF-κB and activator protein-1 (AP-1).[83, 84] Nuclear factor of activated T cells

(NFATc1) has been demonstrated as the transcription factor most strongly induced by NF-κB

activation.[85] NFATc1 is also known to be important in immune response and also play an essential

role in osteoclastogenesis.[85, 86] Therefore, siRNA targeting NFATc1 in both RAW264.7 cells and

RAW-induced osteoclasts under LPS stimulation was examined.[87] Specific knockdown of NFATc1

led to reduced formation of mature osteoclasts and significantly decreased osteoclast-specific

gene expression, including TRAP and cathepsin K, both responsible for effective osteoclastic bone

resorption.

Once RANK is activated by its ligand, several signaling cascades are induced during

osteoclast formation or activation, resulting in activation of several transcription factors mediated

by protein kinases,[88] such as c-Fos, NF-κB, c-Jun, and NFATc1.[84] Transcription factor c-Jun has

recently shown its essential role in osteoclastogenesis.[89] Interaction between RANK and RANKL

can stimulate JNK and activate c-Jun which complexes with c-Fos downstream to form AP-1.[84]

Moreover, c-Jun was reported to regulate osteoclastogenic activities of NFATc-1:

dominant-negative c-Jun transgenic mice were unable to form osteoclasts due to arrested

activation and expression of the NFAT family proteins.[90] Recently, using a proteomic approach, a

member of a family of growth regulatory genes, schlafen2 (Slfn2), was found to be highly induced by RANKL activation and capable of regulating c-Jun activation.[91] Using RNA silencing technology, knockdown of Slfn2 resulted in significantly reduced expression of c-Jun and NFATc1 and 50% less TRAP-positive multinucleated cells compared with control. Furthermore, over-expression of Slfn2 enhanced c-Jun phosphorylation. Slfn2 therefore functions downstream of RANK/RANKL signaling and upstream of c-Jun and NFATc1 in osteoclastogenic regulation.

Dendritic cell-specific transmembrane protein (DC-STAMP), a seven subunit-transmembrane protein originally found in dendritic cells [92] is highly expressed in osteoclasts but not in macrophages.[93] Expression levels of DC-STAMP can be rapidly up-regulated under RANKL-mediated osteoclastogenesis in osteoclast precursors.[94] Using siRNA to specifically knock down its expression in RAW-D cells completely abrogated the formation of multinucleated osteoclast-like cells stimulated with RANKL and TNF-α in vitro.[94] Consistent with this, osteoclastogenesis can also be enhanced by over-expression of DC-STAMP and   vice versa.[94] In addition, DC-STAMP has been further proven essential for both osteoclast and foreign body giant cell fusion.[93] No multinuclear osteoclasts were observed in bone sections from DC-STAMP-deficient mice, and their mononuclear cells were unable to differentiate to multinuclear osteoclasts under stimulation with RANKL and M-CSF in vitro, remaining mononuclear, TRAP-positive cells.[93] These cells are able to resorb bone, but with much lower efficiency, exhibiting the pathogenesis of moderate osteopetrosis.[93] Consistent with these results, bone mineral density and bone volume per tissue volume in DC-STAMP-/- mice increased compared with wild type controls.[93] DC-STAMP is therefore concluded to be indispensable for osteoclast

multinucleation.

A novel gene bearing significant similarity to the DC-STAMP family, called osteoclast stimulatory transmembrane protein (OC-STAMP), was identified in both primary bone marrow cells and RAW264.7 cells in 2007.[95] It is strongly up-regulated in response to RANKL stimulation as a multiple transmembrane protein in osteoclasts. Blocking OC-STAMP expression by either RNA interference or OC-STAMP antibodies showed similar results as blocked DC-STAMP: mononuclear, TRAP-positive cells.[95] The results suggest that both DC-STAMP and OC-STAMP are responsible for cell fusion and each of them can not compensate for the other since knockdown of only one of them impaired osteoclast multinucleation.

A study aimed at protecting biomaterials by inhibiting macrophage fusion at implant sites showed that using siRNA targeting Rac1 can limit fusion without limiting phagocytosis.[96] As the study attempted to find the fusion target shared by foreign body giant cells formed by monocyte fusion and also by osteoclasts, osteoclast formation theoretically should be inhibited as well. Further study is required to confirm the effect of Rac1 silencing on monocyte fusion to osteoclasts.

A membrane glycoprotein, CD9, one of the tetraspanins, has been reported to play an important role in cell fusion during osteoclastogenesis.[97] CD9 has been reported to be involved in cell-cell fusion and cell motility in different cells.[98, 99] In RAW264.7 cells, CD9 locates to the cell membrane and its expression is up-regulated by RANKL stimulation.[97] Targeted inhibition of CD9 using siRNA is able to significantly inhibit the formation of RAW264.7 differentiated osteoclasts by inhibiting cell fusion in cultures. Over-expression of CD9, interestingly, can promote cell fusion in RAW264.7 cultures without RANKL stimulation, but fused cells are TRAP-negative. In the same

study, CD9 is confirmed to be expressed in osteoclasts in vivo by immunohistochemical analysis of tissue sections from mouse femoral bone.

During the osteoclastogenesis cell-cell fusion process, sialic acid which is involved in a number of biologic responses, was hypothesized to play a role in this process.[100] Takahata et al.[101] found that alpha (2,6)-linked-sialic acid degraded during osteoclast differentiation and desialylated cells only could form mononuclear TRAP+ cells with normal expression of osteoclast markers. Using siRNA to knock down alpha (2,6)-sialyltransferase produced significant inhibition of osteoclast multinucleation, which suggests a role for alpha (2,6)-linked-sialic acid in cell-cell fusion processes during osteoclastogenesis.

A novel gene, nha-oc/NHA2 is significantly upregulated in RANKL-stimulated osteoclast precursors.[102] As the murine orthologue of the human gene HsNHA2,[103] encoding a cation-proton antiporter (CPA) localized on the mitochondria, it is proposed to regulate proton concentration in osteoclast mitochondria. NHA-oc/NHA2 selectively expressed in differentiated osteoclasts regulates Na^+-dependent mitochondrial pH changes and mitochondrial passive swelling. Importantly, nha-oc/NHA2 siRNA inhibits TRAP-positive multinucleated cell formation and resorption activity under RANKL stimulation. This reduction partially resulted from apoptosis induced from the loss of inhibition of caspase-9 activation by NHA-oc/NHA2. Therefore, NHA-oc/NHA2 is integrally involved in osteoclast formation, resorption and survival.

Ovarian cancer G-protein-coupled receptor 1 (OGR1) is a histidine-enriched proton-sensor. The OGR1 gene was found to be 7-fold up-regulated in the long bone of CSF-1-null osteopetrotic rats after CSF-1 injections compared to untreated mutants.[104] Expression of OGR1 can also be

induced in RAW264.7 cells under RANKL stimulation during osteoclast differentiation. Specifically knocking down OGR1 expression by siRNA (>1μg/ml) produced almost 50% inhibition of osteoclast formation in both mouse bone marrow mononuclear and RAW264.7 cells without significant cell death. Concomitant with confirming OGR1's role in regulating osteoclastogenesis, the expression and function of the regulators of G-protein signaling (RGS) proteins of osteoclastogenic RANKL signaling cascades were investigated. RGS proteins have been suggested to physiologically regulate G-protein cycles and G-protein signaling in hematopoietic cells.[105, 106] In this protein family, RGS18, specifically expressed in hematopoietic cells, showed consistent decreases in mRNA expression levels during RANKL stimulated osteoclastogenesis.[107, 108] Target-specific knockdown of RGS18 in RAW264.7 cells using siRNA resulted in enhanced osteoclast formation under RANKL induction. Additionally, antibodies against OGR1 with Zn^{2+} ion addition (antagonist of OGR1)[109] significantly reversed the effects of RGS18 siRNA. These observations suggest that the ability of RGS18 to suppress osteoclastogenesis depends on the OGR1 signaling pathway and inhibition of OGR1-mediated cell signaling.[108]

Another RGS member, RGS12, is reported to be significantly upregulated after RANKL stimulation, with its expression being dose-dependent on RANKL.[110] Using vector-based RNAi technology, stable RGS12-silenced RAW264.7 cells showed 18.7 times lower numbers of TRAP-positive multinucleated cells under RANKL stimulation compared with control groups. The mechanism of completely blocking osteoclast differentiation was suggested to lie in regulation of intracellular Ca^{2+} oscillations in the NFAT2 pathway during differentiation. Such Ca^{2+} oscillations can be completely blocked and the expression of NFAT2 simultaneously significantly inhibited in

RGS12-silenced cells.[110]

Triggering receptor expressed in myeloid cells-1 (TREM2) is produced in myeloid cells in bone marrow, and locates to these cell surfaces. Interactions between TREM2 and DAP12 produced from the TYROBP gene transmit signals to activate the cells. Osteoclast precursor cells harvested from DAP12$^{-/-}$ mice only form mononuclear TRAP-positive cells under stimulation with RANKL and M-CSF. These cells exhibit only 50% ability to resorb bone compared with wildtype cells.[111] siRNA against TREM2-transfected RAW264.7 cells largely reduces numbers of TRAP-positive cells, and most were small (<10 nuclei) or mononucleated cells. Thus, TREM2/DAP12 signaling plays an important role in osteoclast differentiation under RANKL stimulation.[112] The same study blocked TREM2 in murine primary cell-induced osteoclasts using antibodies and showed decreased bone resorption, providing evidence that the TREM2/DAP12 signal also regulates osteoclast function.

Extended space flight can cause severe bone loss in astronauts due to microgravity. Compared with normal gravity, microgravity can accelerate osteoclastogenesis about 2-fold.[113] Gene expression profiling of RAW264.7 cells under microgravity conditions has shown increased expression of the calcium-binding protein A8/calgranulin A (S100A8). siRNA knockdown of S100A8 in RAW264.7 cells significantly suppressed osteoclastogenesis under microgravity conditions. S100A8 can be a therapeutic target to prevent bone loss during extended space flights.

Retinoblastoma protein-interacting zinc finger 1 (RIZ1) protein also participates in RANKL-induced osteoclastogenesis,[114] binding with both retinoblastoma protein and estrogen receptors and reportedly involved in osteosarcoma.[115-117] RIZ1 expression increases under RANKL

induction at 24 hours, and RIZ1 siRNA-transfected RAW264.7 cells showed significantly inhibited NFATc1 activation 3 days post-RANKL and M-CSF treatment, but with no significant influence on TRAF6 expression. Thus, RIZ1 is suggested to positively regulate NFAT-1 activity at the last stages of osteoclastogenesis. RAW264.7 cells with reduced RIZ1 expression exhibited substantially reduced ability to form TRAP-positive multinucleated osteoclast-like cells under RANKL and M-CSF stimulation. Recently, c-Abl SH3 domain-binding protein-2 (3BP2) has been recognized as a key regulator of RANKL-induced osteoclastogenesis.[118] 3BP2 regulates several immunoreceptor signaling pathways in immune cells, such as T, B, and NK cells, and was reported to promote activation of NFAT in T and B cells.[119-123] Knockdown of 3BP2 in RAW264.7 cells decreased expression of NFATc1 and completely suppressed RANKL-induced TRAP-positive multinucleate cell formation.[118]

The family of disintegrin and metalloproteinases (ADAM) peptides are cell surface proteins involved in cell adhesion and cell fusion.[124] ADAM8 is a transmembrane glycoprotein expressed in monocytes and significantly up-regulated during osteoclastogenesis.[125, 126] Recently, ADAM8 has been shown to promote osteoclastogenesis whereby vitamin 1,25-(OH)D$_3$-stimulated osteoclast formation was inhibited by ADAM8 antisense treatment.[126] Its direct effect on osteoclastogenesis was also investigated using siRNA.[127] Silencing ADAM8 in RAW264.7 cells decreased osteoclast formation and cell size compared with controls, and modestly decreased osteoclast marker mRNA levels when stimulated with RANKL. In contrast, transfection of ADAM8 into RAW264.7 cultures increased osteoclast marker mRNA expression levels and increased the number of TRAP-positive cells. The study also showed that ADAM8 was highly expressed in rheumatoid arthritis (RA)

pannus macrophages and multinucleated cells adjacent to eroded cartilage. Therefore, ADAM8 was a recommended target for suppressing RA progression by preventing osteoclast formation.

Epidermal growth factor receptor (EGFR) has been the focus of increasing attention in osteoclastic bone resorption, shown to promote bone resorption in vitro.[128] Its inhibition in vitro resulted in suppression of bone marrow stromal cell induced osteoclast differentiation.[129] Yi et al.[130] investigated EGFR function in osteoclast formation and survival, and found that EGFR expression was highly up-regulated by RANKL. Knockdown of EGFR in bone marrow monocytes using lentivirus expressing shRNA completely suppressed osteoclastogenesis with RANKL and M-CSF. In addition, EGFR siRNA blocked NFATc1 expression completely under RANKL stimulation. This study also showed that EGFR co-immunoprecipitated with RANK and Gab2 which mediates the RANK signaling cascade. These data imply that EGFR may couple with RANK via the signaling mediator Gab2 to regulate RANK-stimulated downstream pathways, playing an important role in osteoclastogenesis.

Multinucleated osteoclasts are formed by fusion of monocyte macrophages. Therefore, the role of integrins important for trafficking monocytes in osteoclastogenesis has been assessed using siRNA. Only two integrin pairs are found on pre-osteoclast monocytes: CD11a/CD18 (LFA-1), and CD11b/CD18 (Mac-1) which is considered the premier marker of pre-osteoclasts.[131, 132] Antibodies against CD11b and CD18 to block Mac-1 both in RAW264.7 and primary cell culture can significantly inhibit osteoclastogenesis, but not antibodies against CD11a.[133] Specific knockdown of CD11b using siRNA in RAW264.7 cells, yielding a 50% decrease in CD11b expression, resulted in ~50% reduction in osteoclast area. This inhibition was suggested to occur

in the early stages of cell differentiation since it was accompanied by a 3-fold increase in the mRNA expression level of NFATc1, a major regulator of osteoclastogenesis.[133] Taken together, integrin Mac-1 is suggested to play an important role in early stage osteoclast differentiation via pre-osteoclast cell-cell interactions.

A new member of the TNF family that induces cell apoptosis, called TNF-related apoptosis-inducing ligand (TRAIL), shares a 25% amino acid homology with RANKL[134] and is reported to inhibit osteoclastogenesis in both human peripheral blood mononuclear cells (PBMC) and RAW264.7 cells, possibly by inhibiting the p38/MAPK pathway.[135] It is also involved in human osteoclast apoptosis.[136] More recently, TRAIL has been found to inhibit the accumulation of RANKL-dependent p27^{Kip1} in PBMC.[137] p27^{Kip1} is a cyclin-dependent kinase inhibitor shown to be progressively upregulated to play an important role in mediating RANKL-induced murine osteoclastogenesis.[138, 139] Addition of TRAIL into pre-osteoclast cultures incubated with RANKL and M-CSF resulted in the 6-fold decrease in formation of TRAP-positive cells and significant reduction in the expression of p27^{Kip1}.[137] Using siRNA to specifically knock down p27^{Kip1} in PBMC culture dramatically reduces formation of TRAP-positive cells induced by RANKL and M-CSF, consistent with the results of p27^{Kip1}-deficient mice.[139] Taken together, p27^{Kip1} function alone appears essential for RANKL-mediated osteoclastogenesis.

Bone resorption targets

After osteoclasts mobilize the bone mineral phase, several hydrolytic enzymes degrade the organic bone component. The principal protease involved in this process is cathepsin K,[72, 140] a

lysosomal protease mainly expressed in osteoclasts and released from the ruffled membrane to the resorption lacunae in the sealed zone. Cathepsin K mRNA and protein expression levels are stimulated by RANKL in a time- and dose-dependent manner, and increase with osteoclast differentiation and activation.[141-143] Cathepsin K efficiently degrades type I and II collagen, and gene mutation can cause osteopetrosis and exhibit features of pycnodystosis.[140, 144, 145] Specific down-regulation of cathepsin K mRNA expression decreased both the number and area of bone pits more than 50% without significantly changing cell viability.[146] The unchanged osteoclast number may benefit maintenance of bone homeostasis since osteoclast and osteoblast activities are closely correlated, and disruption of this communication may cause other issues.[147] In mature osteoclasts, cathepsin K expression is increased by RANKL, both in vitro and in vivo.[141] RANK-RANKL binding activates at least five distinct downstream signaling pathways.[148] TRAF6 acts as a critical adaptor in binding with the cytoplasmic domain of RANK; its mutations cause osteopetrosis.[149, 150] Activation of transcription factor AP-1 has been suggested to result from TRAF6 signaling.[143] AP-1 is a heterodimeric protein composed of Jun (c-Jun, JunB or JunD) and Fos.[151] Transfecting RAW264.7 cells with either the dominant negative form of c-fos or siRNA against either c-jun or junB down-regulated RANKL-mediated cathepsin K gene expression. Both transfections inhibited CTSK promoter activity, suggesting that AP-1 stimulated the cathepsin K promoter.[143] In addition, c-Fos is known to play a critical role in osteoclastogenesis: over-expression of c-Fos rescues RANKL-induced osteoclast formation previously blocked by N,N-dimethyl-d-erythro-sphingosine treatment.[152]

H^+-ATPase in the osteoclast ruffled membrane is responsible for reducing and maintaining the

low pH in the sealed resorption lacuna during the process of osteoclast-mediated extracellular acidification. The ATPases have multiple subunits. One subunit isoform located in the ruffled membrane, subunit a3, is reported to be highly expressed and essential to osteoclast resorption function. Defects in this subunit of the vacuolar proton pump induce severe osteopetrosis.[153, 154] Hu et al.[155] showed successful carrier-free a3 siRNA transfection of primary rat osteoclast cultures, reporting that actin ring structures characteristic of actively resorbing osteoclasts were reduced to 20% of controls after siRNA transfection, but re-emerge after halting transfections. Bone resorption pits were significantly reduced 48 hours after transfections and type I collagen C-terminal cross-linked telopeptides in the culture media were decreased more than 50% compared to controls or nontargeting siRNA-treated groups. H^+-ATPase knockdown is similar with cathepsin K knockdown: specific gene down-regulation reduces osteoclastic resorption activity without inducing cell death.

H^+-ATPases have two domains: V1 located on the cytoplasm side and V0 bound within the membrane.[156] ATP-hydrolytic domain V1 has 8 individual subunits, A-H.[157, 158] Subunit C in murine H^+-ATPase has three isoforms: Atp6v1c1 (C1), Atp6v1c2a (C2a), and Atp6v1c2b (C2b).[159] Only C1 is highly expressed in osteoclasts compared to the other two, and is highly up-regulated after RANKL and M-CSF stimulation during differentiation.[160] Feng et al.[160] depleted C1 expression in murine bone marrow macrophages with no significant difference in numbers of TRAP-positive multinucleated cells compared with untreated cultures. However, osteoclastic ability to actively produce H^+ to acidify the extracellular sealing zone environment was largely impaired, and areas of resorption pits on dentin slices by siRNA-treated osteoclasts were 0.5~0.75% of control cultures.

Co-immunoprecipitation studies showed that C1 interacted with another essential ruffled border H^{+}-ATPase subunit a3 and colocalizes with microtubules, but distinct from a3 deficiency,[62] C1 depletion was able to impair F-actin ring formation.[160] C1 was therefore suggested to be a regulator of F-actin sealing ring formation during osteoclast activation. Taken together, C1 knockdown does not affect osteoclastogenesis, but inhibits osteoclastic bone resorption.

Electrostatic neutralization of the membrane potential gradient during osteoclast acid secretion is maintained by Cl^{-} ion channels on the osteoclast's ruffled border.[161] ClC-7 Cl^{-} channels are highly expressed in osteoclasts and localize to the ruffled border membrane. Disruption of ClC-7 in both humans and mice produced severe osteopetrosis.[161] With the exception of ClC-7, ClC-3 in the CLC family of channels was identified in osteoclasts as the functional Cl^{-} ion-specific channel in intracellular organelles, such as endosomes and lysosomes.[162] Both organelle acidity and bone resorption activity are reduced using siRNA against ClC-3. Okamoto et al. concluded that observed osteoclastic bone resorption relied on such internal organelle acidification, since ClC-3 only locates to intracellular organelles, influencing this organelle acidity exclusively. However, bone resorption activity remains in the absence of ClC-3 activity in osteoclasts, attributed to the role of ClC-7 or other redundant Cl^{-} ion channels.[162, 163] Since ClC-7 causes severe osteopetrosis in chloride channel-deficient mice,[161] the functional role of K^{+}/Cl^{-} cotransporters (KCCs) in mouse osteoclast-mediated bone resorption has been a focus. KCCs exist in many tissues and cells, transporting K^{+} and Cl^{-} ions each driven by their respective individual chemical gradients.[164, 165] A previous study showed that both ClC-7 and KCC1 mRNA was expressed in murine osteoclasts, with KCC1 locating to the cell membrane.[163] The KCC

inhibitor, R(+)-butylindazone (DIOA) was able to increase the intracellular concentration of both Cl^-

and H^+ in resorbing osteoclasts. Thus, inhibiting KCCs can suppress Cl^- secretion in resorbing

osteoclasts, which eventually produces reduced H^+ pumping activity. Transfecting bone marrow

cell-induced osteoclasts with siRNA against KCC1 dramatically reduces of the area of bone

resorption pits compared with controls and these results are similar, but slightly less potent, to

those from ClC-7 inhibition.[163]

The Na^+/Ca^{2+} ion exchanger (NCX) is a bidirectional membrane transporter regulating Ca^{2+}

homeostasis in many tissues on cell plasma membrane.[166] The NCX family comprises

homologous proteins: NCX 1, NCX 2, NCX 3.[167, 168] In murine osteoclasts, three splice variants of

NCX1 and NCX3, called NCX1.3, NCX1.41 and NCX3.2, were detected.[169] NCX mediates both

Ca^{2+} efflux and influx and is predicted to locate to the ruffled border and control Ca^{2+} influx in

resorbing osteoclasts.[169] SiRNA delivered against each NCX1.3, NCX1.41 and NCX3.2 at 100nM

in mouse bone marrow cell-induced osteoclasts all significantly reduced the area of bone

resorption pits per osteoclast approximately 50%.[169] These data support the essential role of these

three NCX in Ca^{2+} transport and their important role in regulating bone resorption.

The c-Src gene, encoding a cytosolic protein tyrosine kinase (PTK), [170] is also essential for

osteoclast activity. Lack of c-Src expression in mice resulted in osteopetrosis characterized by

inactive osteoclasts.[171] Previous work indicates that c-Src is functional as an adaptor in

osteoclasts, regulating cell attachment and migration by recruiting essential signaling proteins.[172]

Strong c-Src PTK activity has been found in ruffled borders in active osteoclasts.[173]

Osteoclast-mediated bone resorption can be abolished both in vivo and in vitro by blocking c-Src

PTK activity in osteoclasts.[174] Knockdown of Src expression in RAW264.7 cells reduces both size and number of actin rings, and decreased cell spreading and fusion rates.[175] c-Src PTK activity is activated by dephosphorylation, and a structurally unique osteoclast-specific transmembrane protein-tyrosine phosphatase (PTP-oc) in osteoclasts is known.[176] RAW/C4 osteoclast-like precursor cells transfected with PTP-oc siRNA in serum-containing media and showed RANKL-mediated suppression of osteoclast differentiation. Both osteoclast number and size was significantly reduced by decreasing endogenous PTP-oc mRNA levels.[177] In addition, apoptosis was induced significantly by PTP-oc siRNA compared to control siRNA. Enhanced apoptosis from such knockdown also suggests its role in osteoclasts. Additionally, PTP-oc is also indicated to be involoved in regulating RANKL-mediated osteoclastic differentiation.[178] A homologous recombination strategy was used to inhibit PTP-oc function in RAW264.7 cell culture. PTP-oc knockout cells could not form TRAP-positive multinucleated osteoclast-like cells under RANKL treatment after 7 days. Therefore, PTP-oc is a target not only on mature osteoclasts to inhibit bone resorption, but also on osteoclast precursors to limit differentiation into osteoclasts.

The osteoclast sealing zone requires tight attachment between osteoclasts and the bone surface for successful bone resorption[179] and this depends upon formation of a dense belt-like actin ring surrounding the ruffled membrane.[180] These osteoclast actin rings have high concentrations of actin filaments assembled locally into dynamic structures as podosomes in bone attachment sites. With its significant prerequisite role in osteoclastic bone resorption, actin ring formation is a target for inhibiting osteoclasts and has been investigated in many studies. Gelsolin is an important actin regulator, necessary for podosome formation but not necessary for actin ring

formation, which means that gelsolin-null osteoclasts are able to resorb bone, but with reduced

potency.[181-183] However, Wiscott-Aldrich syndrome protein (WASP) critical for podosome assembly

exists in the actin ring of gelsolin-null osteoclasts.[182] WASP interacts with phosphatidylinositol

4,5-bisphosphate (PIP_2) and Cdc42 in response to integrin $\alpha v\beta 3$ signaling, enhancing the sealing

zone formation and bone resorption.[182] Mice without WASP expression exhibited defects in

formation of podosomes and actin rings in the sealing zone and bone formation.[184] Attenuation of

WASP using siRNA demonstrated the absence of podosome formation of actin rings and reduced

bone resorption. WASP is activated by the coordinated binding of Cdc42 and PIP_2, and full

activation stimulates the actin-nucleating function of the actin-related protein (Arp)2/3 complex by

associating with Arp2/3.[185-188] The Arp2/3 complex initiates actin nucleation and crosslinking, and

has been reported to be 3-fold upregulated in RAW264.7 cells in response to RANKL.[189, 190]

Knockdown of Arp2 in RANKL-stimulated RAW264.7 cells using siRNA generated an average

70% protein reduction 30 hours posttransfection.[190] Fewer podosome-like structures appeared,

and compared with control, less than 1% actin rings were observed after knockdown, proving the

vital role for Arp2/3 in actin ring formation and its potential to be a new target for therapeutic agents.

Actin nucleation requires phosphorylation of WASP's C-terminal VCA domain during WASP

binding to Arp2/3 complex after integrating a number of signals.[191-193] The PTP-PEST

(protein-tyrosine phosphatase-proline, glutamic acid, serine, threonine amino acid sequence) has

been shown to be involved in WASP and Src phosphorylation and dephosphorylation.[194] This

regulates phosphorylation of proteins associated with WASP and enhances interactions between

WASP, actin monomers, and the Arp2/3 complex by increasing the WASP conformational

stability.[194] At the same time, it regulates Src activity through (de)phosphorylation.[195] Reducing

PTP-PEST expression levels using siRNA in osteoclasts eliminated actin rings and significantly

inhibited formation of the sealing zone, formation of WASP-cortactin-Arp2 complexes[195] and bone

resorption.[194] This indicates a direct role of PTP-PEST in the formation of cell-sealing zones while

interacting with WASP.

Simultaneously with WASP, cortactin, a c-Src substrate, binds with Arp2/3 at its N-terminal

acidic domain to promote Arp2/3-induced actin assembly and stabilize actin filaments by binding to

their repeat regions.[196] Cortactin was not found in hematopoietic cell precursors, but is induced in

differentiated osteoclasts. Depletion of cortactin in primary mouse osteoclasts using siRNA

resulted in the absence of podosomes, sealing rings and loss of bone-resorbing ability, suggesting

an indispensable role for cortactin in osteoclastic bone resorption. Cortactin's mechanism for

regulating sealing ring formation has been further studied.[197] Instead of inhibiting the initial actin

aggregate phase, knockdown of cortactin using siRNA suppressed the subsequent sealing zone

maturation process.

Osteoclast ability to attach to bone surfaces is essential for successful bone resorption. An

intracellular calcium channel, inositol-1,4,5-triphosphate receptor-1 (IP3R1) is involved in the

regulation of reversible osteoclast attachment.[198] IP3R1 can bind an endosomal isoform of

IP3R-associated cGMP-dependent kinase substrate (IRAG). Using siRNA against IRAG in human

osteoclasts in vitro reduced cell spreading diameters and displayed distributed podosomes.[199]

Loss of podosome ring structures explained reduced cell adhesion. Knockdown of the orphan

nuclear receptor ERRα in RAW264.7 cells[200] generated similar effects as IRAG. Expression of

osteopontin and the β3 integrin subunit is down-regulated after silencing ERRα. Transfected cells detach from the substrate easily and no podosome belts are observed. Though cell adhesion and migration is impaired, their differentiation and precursor cell proliferation are not influenced by ERRα knockdown.

Given the essential role of actin assembly in osteoclastic bone resorption, the motor protein family of myosins responsible for actin-based motility was examined in osteoclasts.[201, 202] Myosin X (Myo10) maintains low expression levels in most vertebrate tissues,[203] binding actin and microtubules.[204] Assembly of podosomes and sealing zones in osteoclasts depends on a complete intact microtubule system.[205, 206] RNAi-mediated inhibition of Myo10 in both RAW264.7 and mouse bone marrow-derived osteoclasts reduced the sizes of sealing zones and cell perimeters, but did not influence cell fusion.[202]

Brain-type creatine kinase (Ckb) exhibits high up-regulation upon osteoclast maturation as witnessed with proteomic technology.[207] Increased expression occurs in both mice bone marrow cells and RAW264.7 cells exposed to RANKL and M-CSF. Ckb regulates ATP distribution and supply in cells, required in osteoclast actin formation and maintenance.[208, 209] Down-regulation of Ckb in cell cultures produced prominent reduction in areas of resorption pits on dentin slices.[207] Reduced resorption ability was suggested to be partially due to impaired actin ring structures observed in transfected osteoclasts. In addition, Ckb was also shown to affect V-ATPase activity,[207] a major proton pump essential for osteoclastic resorption. Normal osteoclasts can recover their intracellular pH under challenge with strong acid over about 400 seconds. However, the lack of such intercellular pH recovery observed when inhibiting Ckb, infers that Ckb influences

osteoclast bone resorption by affecting V-ATPase. In vitro cell culture data were confirmed in vivo through reduced bone surface erosion in ovarectomized Ckb$^{-/-}$ mice. Interestingly, no significant differences in numbers of osteoclasts were observed between Ckb$^{-/-}$ and wildtype mice.[207] Therefore, Ckb is a target for altering osteoclast activity, not osteoclastogenesis.

Osteoclast viability targets

In addition to targeting osteoclastogenesis and osteoclastic bone resorption, targeted induction of osteoclast apoptosis is also an efficient strategy to suppress excessive bone loss. EGFR is a target for regulating osteoclast differentiation (mentioned in Section 4.1). Inhibition of EGFR expression was also reported to cause apoptosis of mature osteoclasts through a caspase-9/caspase-3-dependent pathway by inhibiting the activation of P13K-Ake/PKB.[130] Taken together, siRNA against EGFR can not only inhibit osteoclast differentiation, but also suppress mature osteoclast survival.

RANK siRNA can be similarly characterized, as RANKL/RANK interaction is responsible for osteoclast differentiation, bone resorption and mature osteoclast survival as well. Therefore, mature osteoclasts transfected with RANK siRNA resulted in cell death.[67] Taken together, transfection of either osteoclast precursors or mature osteoclasts with RANK siRNA can reduce osteoclast-mediated bone resorption by inhibiting osteoclast differentiation, resorption activity and osteoclast survival.

Bisphosphonates, the most commonly used pharmacological approach for targeting osteoporosis currently, have several side effects which have clouded their therapeutic efficacy.[9, 10,

[15] As an alternative, siRNA against alendronate's (a nitrogen-containing bisphosphonate, N-BP) known molecular target,[210] farnesyl pyrophosphate synthase (FPPS), was investigated to inhibit osteoclasts and promote osteoblast activity simultaneously. FPPS plays an important role in the mevalonate pathway which produces lipids essential for cell survival.[211] Additionally, N-BPs are reported to induce human osteoblast differentiation and mineralization in culture by inhibiting the mevalonate pathway.[212] siRNA targeting FPPS significantly suppressed osteoclast cell viability with a single transfection and significantly increased osteoblast differentiation with effects sustained 5 days posttransfection in osteoblasts. However, this treatment does not significantly change osteoblast proliferation and mineralization compared to controls.[213] Therefore, selective knockdown of FPPS expression has the potential to inhibit osteoclasts while at the same time promoting osteoblastic activity.

Other siRNA targets described above influence osteoclast survival as well. NHA-oc/NHA2, mentioned as a target for osteoclastogenesis, inhibits osteoclast resorption activity partially because reduced NHA-oc/NHA2 express induces apoptosis by loss of inhibition of caspase-9 activation;[102] significant osteoclast death can also be induced by OGR1 siRNA transfection; siRNA against structurally unique osteoclast-specific transmembrane PTP-oc induces significant apoptosis in RAW/C4 osteoclast-like precursor cells. In addition, many other general cell apoptosis signals are reported. Using siRNA targeting these proteins regulating these pathways, cell-specific delivery is essential to avoid undesired side effects.

Other potential osteoporosis targets

Recognition of bone by osteoclasts is regulated by cell integrin receptors.[214] Integrins, as calcium-dependent, heterodimeric transmembrane protein receptors, mediate cell attachment with extracellular matrix or with other cells. Four different integrins are actively expressed in osteoclasts.[215] Among them, αvβ3 is highly expressed in osteoclasts and exhibits an important role in facilitating osteoclast attachment to bone and subsequent bone resorptive processes.[216] Osteoclast-mediated bone resorption was shown to be significantly inhibited by anti-αvβ3 antibody treatment in vitro [217] and increased skeletal mass, absence of actin rings and abnormal osteoclast ruffled membranes were all observed in osteoclasts in αvβ3-deficient mice.[216] Integrin αvβ3 recognizes the extracellular RGD peptide sequence and therefore RGD peptide has been used to label and target αvβ3-positive cells in vivo.[218] In addition, inhibition of αvβ3 using a soluble RGD mimic as a receptor antagonist reduced osteoclastic bone resorption both in vitro and in vivo, suggesting that αvβ3 blockade prevents rapid bone loss caused by estrogen withdrawal.[219] In a study seeking to identify human peripheral blood monocyte subsets differentiating into osteoclasts, integrin-β3 subunit siRNA was transfected into human CD16$^+$ monocytes.[220] This transfection significantly reduced TRAP-positive multinucleated cells in a dose-dependent manner. Silencing the β3 subunit in myeloma cells from human patients suppresses bone resorption activity (i.e., osteoclast-like activity) of these cells in vitro.[221] These data reflect the importance of β3 integrin subunit in RANKL-induced osteoclastogenesis. Therefore, αvβ3 could be an attractive target to attenuate or modulate osteoclastic bone resorption.

The soluble cell signaling protein, p53, is well known to protect cells from malignant tumor

transformation by coordinating several intracellular signaling networks.[222] The ubiquitin ligase,

murine double minute 2 (MDM2), regulates p53 activation by controlling p53 half-life.[223] Recently,

a small molecule inhibitor, Nutlin, is reported to competitively bind MDM2 to interrupt p53-MDM2

interaction and activate the p53 pathway.[224, 225] In order to investigate the effect of Nutlin-3 on

pre-osteoclastic precursor cell survival, proliferation and differentiation, human peripheral blood

mononuclear cell pre-osteoclasts were transfected with p53 siRNA.[226] Results showed that

Nutlin-3 anti-osteoclastogenesis activity was greatly compromised by p53 siRNA, indicating that

the inhibitory effects of Nutlin-3 on osteoclast precursors require the p53 activation pathway. Using

siRNA technology to interrupt p53-MDM2 interactions may therefore have therapeutic implications

for controlling excessive osteoclastic activity.

OGR1 was mentioned (vida supra) as a possible target for controlling osteoclastogenesis.

This seven-pass transmembrane protein binds protons and exhibits pH-sensing activity.[109] Given

that increased extracellular proton concentrations led to nuclear translocation of NFATc1, a

downstream mediator of RANKL stimulation in osteoclasts,[227] OGR1's role, while still unclear,

could be linked to bone pH homeostasis working as a proton sensor in response to external

acidosis.[109] Therefore, further studies investigating OGR1 function in bone resorption sites is

necessary to validate OGR1 as a target for osteoclast-mediated excessive bone resorption.

FPPS has been used as an siRNA target to inhibit osteoclast viability, mimicking the

pharmacology of N-BPs (vida supra). However, depletion of intracellular geranylgeranyl

pyrophosphate (GGPP) has also been reported to produce analogous phenotypic effects of

bisphosphonate treatment on both osteoclasts and osteoblasts.[228, 229] Therefore, siRNA inhibition

of GGPP synthase may induce apoptosis in osteoclasts while simultaneously promoting osteoblastic activities. Using siRNA against GGPP synthase could also potentially suppress excessive bone loss by stimulating osteoblastic bone production.

As osteoclasts form from cell fusion, cell-to-cell contact is critical for osteoclastogenesis. Cell adhesion molecules such as intercellular adhesion molecule-1 (ICAM-1), whose expression is regulated by intracellular signalling through NF-κB and JNK, is involved in cell-cell contact between osteoclast precursors and osteoblasts/stromal cells, or among osteoclast precursors.[230, 231] ICAM-1 binds to integrin pairs, LFA-1 (CD11a/CD18), blocking interactions between ICAM-1 and LFA-1, inhibiting osteoclast formation.[230] Hidetaka et al. reported that siRNA knockdown of LFA-1 in RAW264.7 cells had no effects on osteoclastogenesis. Alternatively, ICAM-1 could be an siRNA target to inhibit osteoclasts as ICAM-1 is not only expressed on osteoclast precursors and mature osteoclasts, but also on osteoblasts.[232, 233] Therefore, cell-specific targeted delivery will be essential for the specific bioactivity and siRNA selectivity to osteoclasts as desired.

siRNA Delivery to Bone

Challenges and strategies

RNAi as a novel therapeutic approach has considerable potential to silence abnormal genes, especially for gene targets not effectively targeted by conventional therapeutics (i.e., by small molecules, proteins and antibodies). The major obstacle for developing siRNA for therapeutics is also its targeted delivery with clinically acceptable formulations and reliable routes of administration. This is particularly true of siRNA delivery to bone with its intrinsically poor drug

penetration and vascular perfusion. Bone is primarily composed of three cell types: osteoclasts, osteoblasts and osteocytes. Bone's unique extracellular matrix is strongly mineralized with calcium phosphate, forming ~70 wt% apatite, a major reservoir of the body's calcium most actively involved with physiological calcium and phosphorus homeostasis. Increasing molecular and cellular understanding of bone biology has produced continuous reports of new potential therapeutic targets for various bone pathologies. Nonetheless, despite new targets identified as osteoclast-specific, targeting methods are not yet reliably tissue-based specifically with requisite bone-specificity necessary for these therapeutic agents. Serious complications from cross-reactivity with other nontarget tissues or poor efficacy due to low drug target tissue concentration require a reliable targeting strategy. Many attempts to improve the targeting of drugs to bone mineral fraction (apatite) include drug conjugation with bone-targeting ligands, such as tetracycline,[234] estradiol, and bisphosphonate.[235, 236] Bisphosphonates, especially N-BPs, as antiresorptive drugs having intrinsic high affinity to the bone apatite surface, are very attractive for delivery of conjugated nonspecific bone therapeutic agents. However, their exploitation as bone-targeting agents must consider that free bisphosphonate itself also will increase antiresorptive activity.

SiRNAs are well known for their very short circulating half-lives in vivo.[237] Unmodified naked siRNA cannot be directly administered directly in vivo, exhibiting only a 6 min half-life after systemic administration to rats due to degradation by serum nucleases.[237] Many studies seek to overcome the challenges of siRNA delivery by the chemical modification of siRNA nucleotides, lipid/liposomal/polymer-based complexes, and collagen (atelocollagen)-based[238, 239] formulations

for siRNA, as well as viral vectors and polymer-complexed siRNA carriers.[240] These methods each have their advantages and disadvantages, but nonviral delivery is considered a more clinically relevant delivery mechanism, avoiding the known problems of current viral vector delivery: high viral toxicity, possible carcinogenicity, proven immunogenicity and significant cost limitations.[31] Delivery of siRNA-targeted specifically to bone is not an entirely new story. To date, in vivo siRNA studies in humans have focused on rheumatoid arthritis (RA) by local delivery (intra-articular injection[241, 242], electroporated siRNA[243], topical cream[34]), or by systemic delivery, each with modest effects.[244] Delivery of siRNA to bone osteoclasts in vivo, either targeted to or addressing, is not yet reported.

To improve siRNA stability in vivo, various chemical modifications have been investigated. SiRNA stability against nuclease degradation can be improved by introducing a phosphorothioate (P=S) backbone linkage or modifying the ribose 2'-hydroxyl position as 2'-OMe or 2'-F, as well as a 4'-thioribose modification.[245] All show significant improvements over unmodified siRNA.[246-248] Combination of 2'- and 4'-thioribose modification results in substantially improved siRNA bioactivity and plasma stability.[249] This improved siRNA plasma stability facilitates more reliable systemic dosing and versatile delivery options. In addition, specific siRNA chemical modifications can potentially be used to improve conjugation and targeting as well. Bone-targeting ligands, antibodies[250] or small molecule drugs (vida supra) can be conjugated with siRNA molecules with various chemistries for systemic delivery of siRNA-based bone disease therapeutics. For example, bisphosphonates, can be conjugated to ribose hydroxyl groups in siRNA sugars. Modification of the ribose 2'-OH at the 3' end of the guide siRNA strand appears effective for improving siRNA

activity.[240] In this case, bisphosphonate performs both as a drug and also as a targeting moiety to deliver siRNA specifically to bone.

Using tissue-specific targeting methods, both locally and systemically delivered siRNA can be more reliably dosed by judicious combination of other "homing" molecules. Established drug delivery strategies can be utilized for both targeted systemic and local siRNA delivery, including siRNA conjugation to cell membrane-targeting ligands, antibodies, water-soluble polymers [251] or cell-penetrating peptides. These methods seek to improve amount of siRNA delivered specifically to targeted bone cells, and to limit drug off-target effects in cells other than osteoclasts.

RANK expressed on osteoclast precursors as well as on mature osteoclasts serves as a popular molecular target for osteoporosis therapies. Antibodies against RANK have been tested for effective osteoclast targeting by conjugation with calcitonin, an antiresorptive protein drug.[252] The conjugate showed efficacy inhibiting osteoclast formation and bone resorption. The strategy, using receptor ligand binding peptides as the targeting moiety, provides a general approach to generating an osteoclast-targeting platform for specific drug delivery to osteoclasts. Other osteoclast-specific proteins can also be utilized for this purpose, such as cathepsin K and NHA-oc/NHA2. In addition, many calcium-binding proteins, recently reviewed,[253] including acidic proline-rich salivary proteins, osteocalcin, sialoprotein and osteopontin, have the potential as novel bone-targeting moieties.[253] The hexapeptide $(Asp)_6$ exhibited high affinity to bone and was used as bone-targeting moiety conjugated with estradiol in ovariectomized mice. The conjugates maintained bone density similarly to unconjugated estradiol, but without displaying increased liver and uterus weight.[254, 255]

In addition to specific chemical modifications, protection of siRNA in plasma is also provided by formulating siRNA into nano/macro-sized particles for delivery, as recently reviewed.[256-258] Most drug delivery strategies to date primarily target the liver, either deliberately or nondiscriminately, a natural result of first-pass metabolism and highly efficient liver-based drug and colloidal clearance. This is an advantage for liver targeted therapies: for example, hydrodynamic tail-vein injection of Fas siRNA successfully protected mice from liver failure and fibrosis.[259] However, the liver and other reticuloendothelial (MPS/RES) system tissues efficiently filter most drug carrier particles (i.e., >90%) despite active targeting to other target tissue sites. To avoid this massive dose removal, locally delivered siRNA-particle formulations can be used in bone-targeted therapeutics. Specifically to target osteoclast or osteoclast precursors, siRNA delivery can exploit drug carrier particle size-selective cell-specific uptake to numerous phagocyte target cells in bone tissue using local delivery. In the context of osteoporosis therapy, targeted cells are pre-osteoclastic monocytes and osteoclasts -- all naturally phagocytic cells. Phagocytes efficiently take up particles with diameters up to 10 μm.[260] However, particles with diameters greater than 300 nm are too large to penetrate nonphagocytic cell membranes (i.e., osteoblasts, fibroblasts) either passively or by endocytosis or pinocytosis.[261] Therefore, siRNA-loaded microparticles with controlled sizes could be exploited for selective internalization by osteoclastic phagocytic mechanisms, and to target siRNA to these cells in new osteoporotic therapeutic strategies without a conjugated targeting moiety. These particles could be delivered locally to bone sites in clinical cases, especially in bone augmentation and implant surgeries. Additionally, for some bone molecular drug targets appropriate both for osteoclasts and osteoblasts, siRNA-containing nanoparticles capable of being

taken up by both cell types might be effective for increasing bone mass by inhibiting osteoclasts while simultaneously stimulating osteoblasts. Particle opsonisation by host plasma proteins, commonly a problem for drug carriers, may confound target cell phagocytosis since opsonisation (particularly, nonspecific adsorption of immunoglobulins and complement onto the particles) may activate macrophages and T-cells and cause inflammation in surrounding tissues and damage to healthy cells.[262]

Currently, local siRNA administration is more efficient than its systemic delivery for short-term therapeutic purposes.[263] Nonetheless, local delivery must also consider target specificity. For example, intra-articular injection of siRNA for RA is not an effective route of administration for transfecting osteoclasts located near or on bone surfaces at most common osteoporotic bone sites, notably pelvis, vertebrae and wrist.[264] To maximize drug availability to specific bone sites and obtain a reliable, reproducible and predictable pharmcokinetic profiles, bioactive materials, including porous chitosan/collagen scaffolds[265] and injectable FDA-approved calcium phosphate bone cements (CPC) are being developed as drug carriers for local bone delivery. Polymethylmethacrylate (PMMA) bone cements used clinically for implant fixation, kyphoplasty [266] and bone augmentation,[267] exhibit very poor control over entrapped dose release kinetics, often leaving up to 40% of the drug trapped in PMMA.[268, 269] Injectable CPC exhibits several unique properties for bone drug delivery, including peri-operative preparation and drug loading, liquid-solid setting in situ, intrinsic osteoconductivity (degradable by osteoclasts), osteoinductivity (infiltrated by osteoblasts and replaced with new bone), and acceptable biocompatibility.[270-272] CPC's self-setting ability at ambient or body temperature within the bone cavity [273] enables

injectable formulation, largely expanding its therapeutic utility.[274, 275] To date, a large body of evidence supports the feasibility and value of using CPC as a local drug carrier in bone augmentation. Pharmacologically active molecules are readily dispersed or distributed throughout CPC prior to setting and surgical placement, providing a sustainable and controlled drug release medium. Several conventional small molecule and protein-based drugs have been delivered using CPC in bone, including antibiotics to decrease postsurgical infections,[276-279] anticancer drugs to reduce tumorogenesis[280, 281] and growth factors to promote bone healing.[282, 283] Therefore, despite its limited mechanical properties, CPC could also be used to deliver siRNA to bone as a local delivery matrix. A degradable cationic hydrogel comprising of gelatin and chitosan has been used for local delivery of an antisense oligonucleotide targeting murine TNF-α to suppress endotoxin-induced osteolysis in mouse calvaria.[284] Cationic polymeric chitosan complexes with anionic nucleotides and also facilitates cell transfection. Osteoclast numbers and bone resorption were significantly suppressed 4 weeks postimplantation. The same idea can also be extended to siRNA local delivery to bone.   The intrinsically low pH in osteoclast resorption lacuna and in the cell lysosome is attractive as a basis for targeting drugs conjugated to carriers containing acid-cleavable hydrazone bonds.[285] Additionally, various acid-sensitive, cathepsin K-specific and MMPs-specific peptide linkages (reviewed recently[253]) also provide disease- and environmentally specific bone-targeting strategies appropriate for targeted siRNA bone delivery.

Nonspecific siRNA-cell bioactivities and off-target side effects

The first clinical trials involving siRNA were applied by local intraocular injection in patients with choroidal neovascularization (CNV).[33, 286] CNV is an age-related eye disorder characterized by the choroidal vessel invasion to the retina beneath retinal pigmented epithelium. Naked siRNA targeting VEGFA or VEGFR1 showed significant suppression in a laser-injury-induced CNV mice model.[33, 286] However, in 2008, new data showed that this therapeutic suppression is a general siRNA-class effect, independent of siRNA sequence.[25] The observed therapy was based on interactions between cell-surface (but not endosomal) toll-like receptor 3 (TLR3), a cell membrane double-stranded viral RNA sensor found on numerous cell types,[287] and siRNA, regardless of RNA sequences, target, and internalization. However, to bind TLR3, siRNA of 21 nucleotides or longer was required to form a 2:1 TLR3-RNA conjugate. TLR3 plays an indispensable role in the TRIF--NF-κB cell signalling cascade where TRIF is the TLR3 adaptor protein.[288] This important discovery has revealed generic properties of siRNAs on vascular tissues, and improved the global understanding of siRNA general bioactivities, both desired and potentially undesired, through non-specific signalling pathways.

In this regard, primary human choroidal endothelial cells showed decreased survival in serum-containing media cultured with serum-stable 2'O-methyl-Lus-siRNA (without transfection reagents).[25] Such extracellular siRNA-induced cytotoxicity might affect other organs, including bone. Osteoclast precursors but not mature osteoclasts express TLR3.[59] Poly(I:C)dsRNA, which acts as a TLR3 ligand to stimulate cell surface TLR3, produced strong inhibition of osteoclast differentiation in both mouse bone marrow cultures and human peripheral blood monocytes at 1

µg/ml in a dose-dependent manner under induction by M-CSF and RANKL. TLR stimulation induces the production of various proinflammatory cytokines such as TNF-α[289] and prompts high levels of phagocytic activity in osteoclast precursors,[59] indicating an enhanced immune response after TLR stimulation in osteoclast precursors. Taken together, both the unanticipated vascular and immune-general siRNA-class effects should be carefully considered for siRNA therapies, especially when delivered systemically.

Conclusions

Gene silencing using siRNA has many potential therapeutic applications due to several advantages intrinsic to RNAi, such as its high target specificity and intrinsic biological response.[28] Effective siRNA delivery and selective targeting to desired tissue sites remains problematic. siRNA delivery to bone has developed relatively slowly compared to its delivery to other tissues. In this regard, osteoporosis is an increasingly challenging problem globally with a need for improved therapeutics. Many new cellular targets in osteoclasts are continually reported and attractive for siRNA knockdown. Efficient siRNA delivery methods and selective targeting to bone connective tissue and osteoclasts must be developed, improved and optimized. siRNA's efficacy, bioavailability and therapeutic duration in the context of osteoclast-mediated bone resorption are largely unexplored, but this strategy has attractive options for development of new therapeutics.

References

1. Deal, C.; Gideon, J. Recombinant human PTH 1-34 (Forteo): an anabolic drug for osteoporosis. *Cleve Clin J Med* **2003,** 70, (7), 585-6, 589-90, 592-4 passim.

2. Rodan, G. A.; Martin, T. J. Therapeutic approaches to bone diseases. *Science* **2000,** 289,

(5484), 1508-14.

3.   Lambrinoudaki, I.; Christodoulakos, G.; Botsis, D. Bisphosphonates. *Ann N Y Acad Sci* **2006,** 1092, 397-402.

4.   Rossouw JE; Anderson GL; Prentice RL; et al. Risks and benefits of estrogen plus progestin in healthy postmeopausal women: principal results from the women's health initiative randomized controlled trial. *JAMA* **2002,** 288, (3), 321-333.

5.   Walsh, B. W.; Kuller, L. H.; Wild, R. A.; Paul, S.; Farmer, M.; Lawrence, J. B.; Shah, A. S.; Anderson, P. W. Effects of raloxifene on serum lipids and coagulation factors in healthy postmenopausal women. *Jama* **1998,** 279, (18), 1445-51.

6.   Drugs for prevention and treatment of postmenopausal osteoporosis. *Treat Guidel Med Lett* **2005,** 3, (38), 69-74.

7.   Wada, S.; Udagawa, N.; Nagata, N.; Martin, T. J.; Findlay, D. M. Physiological levels of calcitonin regulate the mouse osteoclast calcitonin receptor by a protein kinase Alpha-mediated mechanism. *Endocrinology* **1996,** 137, (1), 312-20.

8.   Dodson, T. B.; Guralnick, W. C.; Donoff, R. B.; Kaban, L. B. Massachusetts General Hospital/Harvard Medical School MD oral and maxillofacial surgery program: a 30-year review. *J Oral Maxillofac Surg* **2004,** 62, (1), 62-5.

9.   Marx, R. E. Pamidronate (Aredia) and zoledronate (Zometa) induced avascular necrosis of the jaws: a growing epidemic. *J Oral Maxillofac Surg* **2003,** 61, (9), 1115-7.

10. Ruggiero, S. L.; Mehrotra, B.; Rosenberg, T. J.; Engroff, S. L. Osteonecrosis of the jaws associated with the use of bisphosphonates: a review of 63 cases. *J Oral Maxillofac Surg* **2004,** 62, (5), 527-34.

11. Khan, S. A.; Kanis, J. A.; Vasikaran, S.; Kline, W. F.; Matuszewski, B. K.; McCloskey, E. V.; Beneton, M. N.; Gertz, B. J.; Sciberras, D. G.; Holland, S. D.; Orgee, J.; Coombes, G. M.; Rogers, S. R.; Porras, A. G. Elimination and biochemical responses to intravenous alendronate in postmenopausal osteoporosis. *J Bone Miner Res* **1997,** 12, (10), 1700-7.

12. Yang, K. H.; Won, J. H.; Yoon, H. K.; Ryu, J. H.; Choo, K. S.; Kim, J. S. High concentrations of pamidronate in bone weaken the mechanical properties of intact femora in a rat model. *Yonsei Med J* **2007,** 48, (4), 653-8.

13. Sebba, A. Osteoporosis: how long should we treat? *Curr Opin Endocrinol Diabetes Obes*

2008, 15, (6), 502-7.

14. Sellmeyer, D. E. Atypical fractures as a potential complication of long-term bisphosphonate therapy. *Jama* **2010,** 304, (13), 1480-4.

15. Odvina, C. V.; Zerwekh, J. E.; Rao, D. S.; Maalouf, N.; Gottschalk, F. A.; Pak, C. Y. Severely suppressed bone turnover: a potential complication of alendronate therapy. *J Clin Endocrinol Metab* **2005,** 90, (3), 1294-301.

16. Wysowski, D. K. Reports of esophageal cancer with oral bisphosphonate use. *N Engl J Med* **2009,** 360, (1), 89-90.

17. Ott, S. M. Long-term safety of bisphosphonates. *J Clin Endocrinol Metab* **2005,** 90, (3), 1897-9.

18. Venesmaa, P. K.; Kroger, H. P.; Miettinen, H. J.; Jurvelin, J. S.; Suomalainen, O. T.; Alhav, E. M. Alendronate reduces periprosthetic bone loss after uncemented primary total hip arthroplasty: a prospective randomized study. *J Bone Miner Res* **2001,** 16, (11), 2126-31.

19. Nehme, A.; Maalouf, G.; Tricoire, J. L.; Giordano, G.; Chiron, P.; Puget, J. Effect of alendronate on periprosthetic bone loss after cemented primary total hip arthroplasty: a prospective randomized study. *Rev Chir Orthop Reparatrice Appar Mot* **2003,** 89, (7), 593-8.

20. Venesmaa, P. K.; Kroger, H. P.; Miettinen, H. J.; Jurvelin, J. S.; Suomalainen, O. T.; Alhava, E. M. Monitoring of periprosthetic BMD after uncemented total hip arthroplasty with dual-energy X-ray absorptiometry--a 3-year follow-up study. *J Bone Miner Res* **2001,** 16, (6), 1056-61.

21. Brown, J. P.; Prince, R. L.; Deal, C.; Recker, R. R.; Kiel, D. P.; de Gregorio, L. H.; Hadji, P.; Hofbauer, L. C.; Alvaro-Gracia, J. M.; Wang, H.; Austin, M.; Wagman, R. B.; Newmark, R.; Libanati, C.; San Martin, J.; Bone, H. G. Comparison of the effect of denosumab and alendronate on BMD and biochemical markers of bone turnover in postmenopausal women with low bone mass: a randomized, blinded, phase 3 trial. *J Bone Miner Res* **2009,** 24, (1), 153-61.

22. Kendler, D. L.; Roux, C.; Benhamou, C. L.; Brown, J. P.; Lillestol, M.; Siddhanti, S.; Man, H. S.; San Martin, J.; Bone, H. G. Effects of denosumab on bone mineral density and bone turnover in postmenopausal women transitioning from alendronate therapy. *J Bone Miner Res* **2010,** 25, (1), 72-81.

23. Fire, A.; Xu, S.; Montgomery, M. K.; Kostas, S. A.; Driver, S. E.; Mello, C. C. Potent and specific genetic interference by double-stranded RNA in Caenorhabditis elegans. *Nature* **1998,** 391, (6669), 806-11.

24. Aagaard, L.; Rossi, J. J. RNAi therapeutics: principles, prospects and challenges. *Adv Drug Deliv Rev* **2007,** 59, (2-3), 75-86.

25. Kleinman, M. E.; Yamada, K.; Takeda, A.; Chandrasekaran, V.; Nozaki, M.; Baffi, J. Z.; Albuquerque, R. J.; Yamasaki, S.; Itaya, M.; Pan, Y.; Appukuttan, B.; Gibbs, D.; Yang, Z.; Kariko, K.; Ambati, B. K.; Wilgus, T. A.; DiPietro, L. A.; Sakurai, E.; Zhang, K.; Smith, J. R.; Taylor, E. W.; Ambati, J. Sequence- and target-independent angiogenesis suppression by siRNA via TLR3. *Nature* **2008,** 452, (7187), 591-7.

26. Hammond, S. M.; Bernstein, E.; Beach, D.; Hannon, G. J. An RNA-directed nuclease mediates post-transcriptional gene silencing in Drosophila cells. *Nature* **2000,** 404, (6775), 293-6.

27. Beer, M. A.; Tavazoie, S. Predicting gene expression from sequence. *Cell* **2004,** 117, (2), 185-98.

28. Novina, C. D.; Sharp, P. A. The RNAi revolution. *Nature* **2004,** 430, (6996), 161-4.

29. Achenbach, T. V.; Brunner, B.; Heermeier, K. Oligonucleotide-based knockdown technologies: antisense versus RNA interference. *Chembiochem* **2003,** 4, (10), 928-35.

30. Kumar, L. D.; Clarke, A. R. Gene manipulation through the use of small interfering RNA (siRNA): from in vitro to in vivo applications. *Adv Drug Deliv Rev* **2007,** 59, (2-3), 87-100.

31. Wang, Q. Z.; Lv, Y. H.; Diao, Y.; Xu, R. The design of vectors for RNAi delivery system. *Curr Pharm Des* **2008,** 14, (13), 1327-40.

32. Woodrow, K. A.; Cu, Y.; Booth, C. J.; Saucier-Sawyer, J. K.; Wood, M. J.; Saltzman, W. M. Intravaginal gene silencing using biodegradable polymer nanoparticles densely loaded with small-interfering RNA. *Nat Mater* **2009,** 8, (6), 526-33.

33. Reich, S. J.; Fosnot, J.; Kuroki, A.; Tang, W.; Yang, X.; Maguire, A. M.; Bennett, J.; Tolentino, M. J. Small interfering RNA (siRNA) targeting VEGF effectively inhibits ocular neovascularization in a mouse model. *Mol Vis* **2003,** 9, 210-6.

34. Takanashi, M.; Oikawa, K.; Sudo, K.; Tanaka, M.; Fujita, K.; Ishikawa, A.; Nakae, S.; Kaspar, R. L.; Matsuzaki, M.; Kudo, M.; Kuroda, M. Therapeutic silencing of an endogenous gene by siRNA cream in an arthritis model mouse. *Gene Ther* **2009,** 16, (8), 982-9.

35. Massaro, D.; Massaro, G. D.; Clerch, L. B. Noninvasive delivery of small inhibitory RNA and other reagents to pulmonary alveoli in mice. *Am J Physiol Lung Cell Mol Physiol* **2004,** 287, (5), L1066-70.

36. Thakker, D. R.; Natt, F.; Husken, D.; Maier, R.; Muller, M.; van der Putten, H.; Hoyer, D.; Cryan, J. F. Neurochemical and behavioral consequences of widespread gene knockdown in the adult mouse brain by using nonviral RNA interference. *Proc Natl Acad Sci U S A* **2004,** 101, (49), 17270-5.

37. Wu, P.; Grainger, D. W. Drug/device combinations for local drug therapies and infection prophylaxis. *Biomaterials* **2006,** 27, (11), 2450-67.

38. Niyibizi, C.; Smith, P.; Mi, Z.; Phillips, C. L.; Robbins, P. Transfer of proalpha2(I) cDNA into cells of a murine model of human Osteogenesis Imperfecta restores synthesis of type I collagen comprised of alpha1(I) and alpha2(I) heterotrimers in vitro and in vivo. *J Cell Biochem* **2001,** 83, (1), 84-91.

39. Barranger, J. A.; Rice, E. O.; Dunigan, J.; Sansieri, C.; Takiyama, N.; Beeler, M.; Lancia, J.; Lucot, S.; Scheirer-Fochler, S.; Mohney, T.; Swaney, W.; Bahnson, A.; Ball, E. Gaucher's disease: studies of gene transfer to haematopoietic cells. *Baillieres Clin Haematol* **1997,** 10, (4), 765-78.

40. Evans, C. H.; Ghivizzani, S. C.; Herndon, J. H.; Wasko, M. C.; Reinecke, J.; Wehling, P.; Robbins, P. D. Clinical trials in the gene therapy of arthritis. *Clin Orthop Relat Res* **2000**, (379 Suppl), S300-7.

41. Evans, C. H.; Robbins, P. D.; Ghivizzani, S. C.; Herndon, J. H.; Kang, R.; Bahnson, A. B.; Barranger, J. A.; Elders, E. M.; Gay, S.; Tomaino, M. M.; Wasko, M. C.; Watkins, S. C.; Whiteside, T. L.; Glorioso, J. C.; Lotze, M. T.; Wright, T. M. Clinical trial to assess the safety, feasibility, and efficacy of transferring a potentially anti-arthritic cytokine gene to human joints with rheumatoid arthritis. *Hum Gene Ther* **1996,** 7, (10), 1261-80.

42. Evans, C. H. Gene therapies for osteoarthritis. *Curr Rheumatol Rep* **2004,** 6, (1), 31-40.

43. Baltzer, A. W.; Whalen, J. D.; Wooley, P.; Latterman, C.; Truchan, L. M.; Robbins, P. D.; Evans, C. H. Gene therapy for osteoporosis: evaluation in a murine ovariectomy model. *Gene Ther* **2001,** 8, (23), 1770-6.

44. Bolon, B.; Carter, C.; Daris, M.; Morony, S.; Capparelli, C.; Hsieh, A.; Mao, M.; Kostenuik, P.; Dunstan, C. R.; Lacey, D. L.; Sheng, J. Z. Adenoviral delivery of osteoprotegerin ameliorates bone resorption in a mouse ovariectomy model of osteoporosis. *Mol Ther* **2001,** 3, (2), 197-205.

45. Kostenuik, P. J.; Bolon, B.; Morony, S.; Daris, M.; Geng, Z.; Carter, C.; Sheng, J. Gene therapy with human recombinant osteoprotegerin reverses established osteopenia in ovariectomized mice. *Bone* **2004,** 34, (4), 656-64.

46. Lieberman, J. R.; Daluiski, A.; Stevenson, S.; Wu, L.; McAllister, P.; Lee, Y. P.; Kabo, J. M.; Finerman, G. A.; Berk, A. J.; Witte, O. N. The effect of regional gene therapy with bone morphogenetic protein-2-producing bone-marrow cells on the repair of segmental femoral defects in rats. *J Bone Joint Surg Am* **1999,** 81, (7), 905-17.

47. Baltzer, A. W.; Lattermann, C.; Whalen, J. D.; Wooley, P.; Weiss, K.; Grimm, M.; Ghivizzani, S. C.; Robbins, P. D.; Evans, C. H. Genetic enhancement of fracture repair: healing of an experimental segmental defect by adenoviral transfer of the BMP-2 gene. *Gene Ther* **2000,** 7, (9), 734-9.

48. Betz O, V. M., Baltzer A, Lieberman JR, Robbins PD, Evans CH, *Bone Regeneration and Repair: Biology and Clinical Applicaitons*. ed.; Humana Press: Totowa, NJ, 2005; 'Vol.' p 157-168.

49. Evans, C. H.; Ghivizzani, S. C.; Herndon, J. H.; Robbins, P. D. Gene therapy for the treatment of musculoskeletal diseases. *J Am Acad Orthop Surg* **2005,** 13, (4), 230-42.

50. Courties, G.; Presumey, J.; Duroux-Richard, I.; Jorgensen, C.; Apparailly, F. RNA interference-based gene therapy for successful treatment of rheumatoid arthritis. *Expert Opin Biol Ther* **2009,** 9, (5), 535-8.

51. Anil K Jain, S. S. Y. Bone health - An investment. *Indian Journal of Orthopaedics* **2009,** 43, (3), 223-224.

52. Vaananen, K. Mechanism of osteoclast mediated bone resorption--rationale for the design of new therapeutics. *Adv Drug Deliv Rev* **2005,** 57, (7), 959-71.

53. Yasuda, H.; Shima, N.; Nakagawa, N.; Yamaguchi, K.; Kinosaki, M.; Mochizuki, S.; Tomoyasu, A.; Yano, K.; Goto, M.; Murakami, A.; Tsuda, E.; Morinaga, T.; Higashio, K.; Udagawa, N.; Takahashi, N.; Suda, T. Osteoclast differentiation factor is a ligand for osteoprotegerin/osteoclastogenesis-inhibitory factor and is identical to TRANCE/RANKL. *Proc Natl Acad Sci U S A* **1998,** 95, (7), 3597-602.

54. Lacey, D. L.; Timms, E.; Tan, H. L.; Kelley, M. J.; Dunstan, C. R.; Burgess, T.; Elliott, R.; Colombero, A.; Elliott, G.; Scully, S.; Hsu, H.; Sullivan, J.; Hawkins, N.; Davy, E.; Capparelli, C.; Eli, A.; Qian, Y. X.; Kaufman, S.; Sarosi, I.; Shalhoub, V.; Senaldi, G.; Guo, J.; Delaney, J.; Boyle, W. J. Osteoprotegerin ligand is a cytokine that regulates osteoclast differentiation and activation. *Cell* **1998,** 93, (2), 165-76.

55. Takahashi, N.; Yamana, H.; Yoshiki, S.; Roodman, G. D.; Mundy, G. R.; Jones, S. J.; Boyde, A.; Suda, T. Osteoclast-like cell formation and its regulation by osteotropic hormones in mouse bone marrow cultures. *Endocrinology* **1988,** 122, (4), 1373-82.

56. Amizuka N, T. N., Udagawa N, Suda T, Ozawa H. An ultrastructural study of cell-cell contact between mouse spleen cells and calvaria-derived osteoblastic cells in a co-culture system for osteoclast formation. *Acta Histochem Cytochem* **1997,** 30, 351-362.

57. Nicolin, V.; Baldini, G.; Bareggi, R.; Zweyer, M.; Zauli, G.; Vaccarezza, M.; Narducci, P. Morphological features of osteoclasts derived from a co-culture system. *J Mol Histol* **2006,** 37, (3-4), 171-7.

58. Chamberlain, L. M.; Godek, M. L.; Gonzalez-Juarrero, M.; Grainger, D. W. Phenotypic non-equivalence of murine (monocyte-) macrophage cells in biomaterial and inflammatory models. *J Biomed Mater Res A* **2009,** 88, (4), 858-71.

59. Takami, M.; Kim, N.; Rho, J.; Choi, Y. Stimulation by toll-like receptors inhibits osteoclast differentiation. *J Immunol* **2002,** 169, (3), 1516-23.

60. Wang, Y.; Lebowitz, D.; Sun, C.; Thang, H.; Grynpas, M. D.; Glogauer, M. Identifying the relative contributions of Rac1 and Rac2 to osteoclastogenesis. *J Bone Miner Res* **2008,** 23, (2), 260-70.

61. Corral, D. A.; Amling, M.; Priemel, M.; Loyer, E.; Fuchs, S.; Ducy, P.; Baron, R.; Karsenty, G. Dissociation between bone resorption and bone formation in osteopenic transgenic mice. *Proc Natl Acad Sci U S A* **1998,** 95, (23), 13835-40.

62. Dougall, W. C.; Glaccum, M.; Charrier, K.; Rohrbach, K.; Brasel, K.; De Smedt, T.; Daro, E.; Smith, J.; Tometsko, M. E.; Maliszewski, C. R.; Armstrong, A.; Shen, V.; Bain, S.; Cosman, D.; Anderson, D.; Morrissey, P. J.; Peschon, J. J.; Schuh, J. RANK is essential for osteoclast and lymph node development. *Genes Dev* **1999,** 13, (18), 2412-24.

63. Lacey, D. L.; Tan, H. L.; Lu, J.; Kaufman, S.; Van, G.; Qiu, W.; Rattan, A.; Scully, S.; Fletcher, F.; Juan, T.; Kelley, M.; Burgess, T. L.; Boyle, W. J.; Polverino, A. J. Osteoprotegerin ligand modulates murine osteoclast survival in vitro and in vivo. *Am J Pathol* **2000,** 157, (2), 435-48.

64. Simonet, W. S.; Lacey, D. L.; Dunstan, C. R.; Kelley, M.; Chang, M. S.; Luthy, R.; Nguyen, H. Q.; Wooden, S.; Bennett, L.; Boone, T.; Shimamoto, G.; DeRose, M.; Elliott, R.; Colombero, A.; Tan, H. L.; Trail, G.; Sullivan, J.; Davy, E.; Bucay, N.; Renshaw-Gegg, L.; Hughes, T. M.; Hill, D.; Pattison, W.; Campbell, P.; Sander, S.; Van, G.; Tarpley, J.; Derby, P.; Lee, R.; Boyle, W. J. Osteoprotegerin: a novel secreted protein involved in the regulation of bone density. *Cell* **1997,** 89, (2), 309-19.

65. Yasuda, H.; Shima, N.; Nakagawa, N.; Mochizuki, S. I.; Yano, K.; Fujise, N.; Sato, Y.; Goto, M.; Yamaguchi, K.; Kuriyama, M.; Kanno, T.; Murakami, A.; Tsuda, E.; Morinaga, T.; Higashio, K.

Identity of osteoclastogenesis inhibitory factor (OCIF) and osteoprotegerin (OPG): a mechanism by which OPG/OCIF inhibits osteoclastogenesis in vitro. *Endocrinology* **1998,** 139, (3), 1329-37.

66. Wagner, E. F.; Karsenty, G. Genetic control of skeletal development. *Curr Opin Genet Dev* **2001,** 11, (5), 527-32.

67. Wang, Y.; Grainger, D. W. siRNA knock-down of RANK signaling to control osteoclast-mediated bone resorption. *Pharm Res* **2010,** 27, (7), 1273-84.

68. Iwasaki, R.; Ninomiya, K.; Miyamoto, K.; Suzuki, T.; Sato, Y.; Kawana, H.; Nakagawa, T.; Suda, T.; Miyamoto, T. Cell fusion in osteoclasts plays a critical role in controlling bone mass and osteoblastic activity. *Biochem Biophys Res Commun* **2008,** 377, (3), 899-904.

69. Mundlos, S.; Otto, F.; Mundlos, C.; Mulliken, J. B.; Aylsworth, A. S.; Albright, S.; Lindhout, D.; Cole, W. G.; Henn, W.; Knoll, J. H.; Owen, M. J.; Mertelsmann, R.; Zabel, B. U.; Olsen, B. R. Mutations involving the transcription factor CBFA1 cause cleidocranial dysplasia. *Cell* **1997,** 89, (5), 773-9.

70. Teti, A.; Blair, H. C.; Teitelbaum, S. L.; Kahn, A. J.; Koziol, C.; Konsek, J.; Zambonin-Zallone, A.; Schlesinger, P. H. Cytoplasmic pH regulation and chloride/bicarbonate exchange in avian osteoclasts. *J Clin Invest* **1989,** 83, (1), 227-33.

71. Emery, J. G.; McDonnell, P.; Burke, M. B.; Deen, K. C.; Lyn, S.; Silverman, C.; Dul, E.; Appelbaum, E. R.; Eichman, C.; DiPrinzio, R.; Dodds, R. A.; James, I. E.; Rosenberg, M.; Lee, J. C.; Young, P. R. Osteoprotegerin is a receptor for the cytotoxic ligand TRAIL. *J Biol Chem* **1998,** 273, (23), 14363-7.

72. Gowen, M.; Lazner, F.; Dodds, R.; Kapadia, R.; Feild, J.; Tavaria, M.; Bertoncello, I.; Drake, F.; Zavarselk, S.; Tellis, I.; Hertzog, P.; Debouck, C.; Kola, I. Cathepsin K knockout mice develop osteopetrosis due to a deficit in matrix degradation but not demineralization. *J Bone Miner Res* **1999,** 14, (10), 1654-63.

73. Nesbitt, S. A.; Horton, M. A. Trafficking of matrix collagens through bone-resorbing osteoclasts. *Science* **1997,** 276, (5310), 266-9.

74. Darnay, B. G.; Haridas, V.; Ni, J.; Moore, P. A.; Aggarwal, B. B. Characterization of the intracellular domain of receptor activator of NF-kappaB (RANK). Interaction with tumor necrosis factor receptor-associated factors and activation of NF-kappab and c-Jun N-terminal kinase. *J Biol Chem* **1998,** 273, (32), 20551-5.

75. Dai, S.; Hirayama, T.; Abbas, S.; Abu-Amer, Y. The IkappaB kinase (IKK) inhibitor,

NEMO-binding domain peptide, blocks osteoclastogenesis and bone erosion in inflammatory arthritis. *J Biol Chem* **2004,** 279, (36), 37219-22.

76. Iotsova, V.; Caamano, J.; Loy, J.; Yang, Y.; Lewin, A.; Bravo, R. Osteopetrosis in mice lacking NF-kappaB1 and NF-kappaB2. *Nat Med* **1997,** 3, (11), 1285-9.

77. DiDonato, J. A.; Hayakawa, M.; Rothwarf, D. M.; Zandi, E.; Karin, M. A cytokine-responsive IkappaB kinase that activates the transcription factor NF-kappaB. *Nature* **1997,** 388, (6642), 548-54.

78. Mercurio, F.; Zhu, H.; Murray, B. W.; Shevchenko, A.; Bennett, B. L.; Li, J.; Young, D. B.; Barbosa, M.; Mann, M.; Manning, A.; Rao, A. IKK-1 and IKK-2: cytokine-activated IkappaB kinases essential for NF-kappaB activation. *Science* **1997,** 278, (5339), 860-6.

79. Ruocco, M. G.; Maeda, S.; Park, J. M.; Lawrence, T.; Hsu, L. C.; Cao, Y.; Schett, G.; Wagner, E. F.; Karin, M. I{kappa}B kinase (IKK){beta}, but not IKK{alpha}, is a critical mediator of osteoclast survival and is required for inflammation-induced bone loss. *J Exp Med* **2005,** 201, (10), 1677-87.

80. Otero, J. E.; Dai, S.; Foglia, D.; Alhawagri, M.; Vacher, J.; Pasparakis, M.; Abu-Amer, Y. Defective osteoclastogenesis by IKKbeta-null precursors is a result of receptor activator of NF-kappaB ligand (RANKL)-induced JNK-dependent apoptosis and impaired differentiation. *J Biol Chem* **2008,** 283, (36), 24546-53.

81. Chaisson, M. L.; Branstetter, D. G.; Derry, J. M.; Armstrong, A. P.; Tometsko, M. E.; Takeda, K.; Akira, S.; Dougall, W. C. Osteoclast differentiation is impaired in the absence of inhibitor of kappa B kinase alpha. *J Biol Chem* **2004,** 279, (52), 54841-8.

82. Darwech, I.; Otero, J.; Alhawagri, M.; Dai, S.; Abu-Amer, Y. Impediment of NEMO oligomerization inhibits osteoclastogenesis and osteolysis. *J Cell Biochem* **2009,** 108, (6), 1337-45.

83. Gohda, J.; Akiyama, T.; Koga, T.; Takayanagi, H.; Tanaka, S.; Inoue, J. RANK-mediated amplification of TRAF6 signaling leads to NFATc1 induction during osteoclastogenesis. *Embo J* **2005,** 24, (4), 790-9.

84. Boyle, W. J.; Simonet, W. S.; Lacey, D. L. Osteoclast differentiation and activation. *Nature* **2003,** 423, (6937), 337-42.

85. Takayanagi, H. The role of NFAT in osteoclast formation. *Ann N Y Acad Sci* **2007,** 1116, 227-37.

86. Ishida, N.; Hayashi, K.; Hoshijima, M.; Ogawa, T.; Koga, S.; Miyatake, Y.; Kumegawa, M.; Kimura, T.; Takeya, T. Large scale gene expression analysis of osteoclastogenesis in vitro and elucidation of NFAT2 as a key regulator. *J Biol Chem* **2002,** 277, (43), 41147-56.

87. Fahid, F. S.; Jiang, J.; Zhu, Q.; Zhang, C.; Filbert, E.; Safavi, K. E.; Spangberg, L. S. Application of small interfering RNA for inhibition of lipopolysaccharide-induced osteoclast formation and cytokine stimulation. *J Endod* **2008,** 34, (5), 563-9.

88. David, J. P.; Sabapathy, K.; Hoffmann, O.; Idarraga, M. H.; Wagner, E. F. JNK1 modulates osteoclastogenesis through both c-Jun phosphorylation-dependent and -independent mechanisms. *J Cell Sci* **2002,** 115, (Pt 22), 4317-25.

89. Kenner, L.; Hoebertz, A.; Beil, T.; Keon, N.; Karreth, F.; Eferl, R.; Scheuch, H.; Szremska, A.; Amling, M.; Schorpp-Kistner, M.; Angel, P.; Wagner, E. F. Mice lacking JunB are osteopenic due to cell-autonomous osteoblast and osteoclast defects. *J Cell Biol* **2004,** 164, (4), 613-23.

90. Ikeda, F.; Nishimura, R.; Matsubara, T.; Tanaka, S.; Inoue, J.; Reddy, S. V.; Hata, K.; Yamashita, K.; Hiraga, T.; Watanabe, T.; Kukita, T.; Yoshioka, K.; Rao, A.; Yoneda, T. Critical roles of c-Jun signaling in regulation of NFAT family and RANKL-regulated osteoclast differentiation. *J Clin Invest* **2004,** 114, (4), 475-84.

91. Lee, N. K.; Choi, H. K.; Yoo, H. J.; Shin, J.; Lee, S. Y. RANKL-induced schlafen2 is a positive regulator of osteoclastogenesis. *Cell Signal* **2008,** 20, (12), 2302-8.

92. Hartgers, F. C.; Vissers, J. L.; Looman, M. W.; van Zoelen, C.; Huffine, C.; Figdor, C. G.; Adema, G. J. DC-STAMP, a novel multimembrane-spanning molecule preferentially expressed by dendritic cells. *Eur J Immunol* **2000,** 30, (12), 3585-90.

93. Yagi, M.; Miyamoto, T.; Sawatani, Y.; Iwamoto, K.; Hosogane, N.; Fujita, N.; Morita, K.; Ninomiya, K.; Suzuki, T.; Miyamoto, K.; Oike, Y.; Takeya, M.; Toyama, Y.; Suda, T. DC-STAMP is essential for cell-cell fusion in osteoclasts and foreign body giant cells. *J Exp Med* **2005,** 202, (3), 345-51.

94. Kukita, T.; Wada, N.; Kukita, A.; Kakimoto, T.; Sandra, F.; Toh, K.; Nagata, K.; Iijima, T.; Horiuchi, M.; Matsusaki, H.; Hieshima, K.; Yoshie, O.; Nomiyama, H. RANKL-induced DC-STAMP is essential for osteoclastogenesis. *J Exp Med* **2004,** 200, (7), 941-6.

95. Yang, M.; Birnbaum, M. J.; MacKay, C. A.; Mason-Savas, A.; Thompson, B.; Odgren, P. R. Osteoclast stimulatory transmembrane protein (OC-STAMP), a novel protein induced by RANKL that promotes osteoclast differentiation. *J Cell Physiol* **2008,** 215, (2), 497-505.

96. Jay, S. M.; Skokos, E.; Laiwalla, F.; Krady, M. M.; Kyriakides, T. R. Foreign body giant cell formation is preceded by lamellipodia formation and can be attenuated by inhibition of Rac1 activation. *Am J Pathol* **2007,** 171, (2), 632-40.

97. Ishii, M.; Iwai, K.; Koike, M.; Ohshima, S.; Kudo-Tanaka, E.; Ishii, T.; Mima, T.; Katada, Y.; Miyatake, K.; Uchiyama, Y.; Saeki, Y. RANKL-induced expression of tetraspanin CD9 in lipid raft membrane microdomain is essential for cell fusion during osteoclastogenesis. *J Bone Miner Res* **2006,** 21, (6), 965-76.

98. Tachibana, I.; Hemler, M. E. Role of transmembrane 4 superfamily (TM4SF) proteins CD9 and CD81 in muscle cell fusion and myotube maintenance. *J Cell Biol* **1999,** 146, (4), 893-904.

99. Kaji, K.; Oda, S.; Shikano, T.; Ohnuki, T.; Uematsu, Y.; Sakagami, J.; Tada, N.; Miyazaki, S.; Kudo, A. The gamete fusion process is defective in eggs of Cd9-deficient mice. *Nat Genet* **2000,** 24, (3), 279-82.

100. Crean, S. M.; Meneski, J. P.; Hullinger, T. G.; Reilly, M. J.; DeBoever, E. H.; Taichman, R. S. N-linked sialyated sugar receptors support haematopoietic cell-osteoblast adhesions. *Br J Haematol* **2004,** 124, (4), 534-46.

101. Takahata, M.; Iwasaki, N.; Nakagawa, H.; Abe, Y.; Watanabe, T.; Ito, M.; Majima, T.; Minami, A. Sialylation of cell surface glycoconjugates is essential for osteoclastogenesis. *Bone* **2007,** 41, (1), 77-86.

102. Battaglino, R. A.; Pham, L.; Morse, L. R.; Vokes, M.; Sharma, A.; Odgren, P. R.; Yang, M.; Sasaki, H.; Stashenko, P. NHA-oc/NHA2: a mitochondrial cation-proton antiporter selectively expressed in osteoclasts. *Bone* **2008,** 42, (1), 180-92.

103. Brett, C. L.; Donowitz, M.; Rao, R. Evolutionary origins of eukaryotic sodium/proton exchangers. *Am J Physiol Cell Physiol* **2005,** 288, (2), C223-39.

104. Yang, M.; Mailhot, G.; Birnbaum, M. J.; MacKay, C. A.; Mason-Savas, A.; Odgren, P. R. Expression of and role for ovarian cancer G-protein-coupled receptor 1 (OGR1) during osteoclastogenesis. *J Biol Chem* **2006,** 281, (33), 23598-605.

105. Kehrl, J. H. Heterotrimeric G protein signaling: roles in immune function and fine-tuning by RGS proteins. *Immunity* **1998,** 8, (1), 1-10.

106. Beadling, C.; Druey, K. M.; Richter, G.; Kehrl, J. H.; Smith, K. A. Regulators of G protein signaling exhibit distinct patterns of gene expression and target G protein specificity in human lymphocytes. *J Immunol* **1999,** 162, (5), 2677-82.

107. Yowe, D.; Weich, N.; Prabhudas, M.; Poisson, L.; Errada, P.; Kapeller, R.; Yu, K.; Faron, L.; Shen, M.; Cleary, J.; Wilkie, T. M.; Gutierrez-Ramos, C.; Hodge, M. R. RGS18 is a myeloerythroid lineage-specific regulator of G-protein-signalling molecule highly expressed in megakaryocytes. *Biochem J* **2001,** 359, (Pt 1), 109-18.

108. Iwai, K.; Koike, M.; Ohshima, S.; Miyatake, K.; Uchiyama, Y.; Saeki, Y.; Ishii, M. RGS18 acts as a negative regulator of osteoclastogenesis by modulating the acid-sensing OGR1/NFAT signaling pathway. *J Bone Miner Res* **2007,** 22, (10), 1612-20.

109. Ludwig, M. G.; Vanek, M.; Guerini, D.; Gasser, J. A.; Jones, C. E.; Junker, U.; Hofstetter, H.; Wolf, R. M.; Seuwen, K. Proton-sensing G-protein-coupled receptors. *Nature* **2003,** 425, (6953), 93-8.

110. Yang, S.; Li, Y. P. RGS12 is essential for RANKL-evoked signaling for terminal differentiation of osteoclasts in vitro. *J Bone Miner Res* **2007,** 22, (1), 45-54.

111. Humphrey, M. B.; Ogasawara, K.; Yao, W.; Spusta, S. C.; Daws, M. R.; Lane, N. E.; Lanier, L. L.; Nakamura, M. C. The signaling adapter protein DAP12 regulates multinucleation during osteoclast development. *J Bone Miner Res* **2004,** 19, (2), 224-34.

112. Humphrey, M. B.; Daws, M. R.; Spusta, S. C.; Niemi, E. C.; Torchia, J. A.; Lanier, L. L.; Seaman, W. E.; Nakamura, M. C. TREM2, a DAP12-associated receptor, regulates osteoclast differentiation and function. *J Bone Miner Res* **2006,** 21, (2), 237-45.

113. Yuvaraj, S.; Blanchard, J. J.; Daughtridge, G.; Kolb, R. J.; Shanmugarajan, S.; Bateman, T. A.; Reddy, S. V. Microarray profile of gene expression during osteoclast differentiation in modeled microgravity. *J Cell Biochem* **2010,** 111, (5), 1179-87.

114. Noman, A. S.; Koide, N.; Iftakhar, E. K. I.; Dagvadorj, J.; Tumurkhuu, G.; Naiki, Y.; Komatsu, T.; Yoshida, T.; Yokochi, T. Retinoblastoma protein-interacting zinc finger 1 (RIZ1) participates in RANKL-induced osteoclast formation via regulation of NFATc1 expression. *Immunol Lett* **2010,** 131, (2), 166-9.

115. Huang, S.; Shao, G.; Liu, L. The PR domain of the Rb-binding zinc finger protein RIZ1 is a protein binding interface and is related to the SET domain functioning in chromatin-mediated gene expression. *J Biol Chem* **1998,** 273, (26), 15933-9.

116. Carling, T.; Kim, K. C.; Yang, X. H.; Gu, J.; Zhang, X. K.; Huang, S. A histone methyltransferase is required for maximal response to female sex hormones. *Mol Cell Biol* **2004,** 24, (16), 7032-42.

117. Abbondanza, C.; de Nigris, F.; De Rosa, C.; Rossiello, R.; Puca, G. A.; Napoli, C. Silencing of YY1 downregulates RIZ1 promoter in human osteosarcoma. *Oncol Res* **2008,** 17, (1), 33-41.

118. GuezGuez, A.; Prod'homme, V.; Mouska, X.; Baudot, A.; Blin-Wakkach, C.; Rottapel, R.; Deckert, M. 3BP2 Adapter protein is required for receptor activator of NFkappaB ligand (RANKL)-induced osteoclast differentiation of RAW264.7 cells. *J Biol Chem* **2010,** 285, (27), 20952-63.

119. Le Bras, S.; Moon, C.; Foucault, I.; Breittmayer, J. P.; Deckert, M. Abl-SH3 binding protein 2, 3BP2, interacts with CIN85 and HIP-55. *FEBS Lett* **2007,** 581, (5), 967-74.

120. Shukla, U.; Hatani, T.; Nakashima, K.; Ogi, K.; Sada, K. Tyrosine phosphorylation of 3BP2 regulates B cell receptor-mediated activation of NFAT. *J Biol Chem* **2009,** 284, (49), 33719-28.

121. Jevremovic, D.; Billadeau, D. D.; Schoon, R. A.; Dick, C. J.; Leibson, P. J. Regulation of NK cell-mediated cytotoxicity by the adaptor protein 3BP2. *J Immunol* **2001,** 166, (12), 7219-28.

122. Foucault, I.; Le Bras, S.; Charvet, C.; Moon, C.; Altman, A.; Deckert, M. The adaptor protein 3BP2 associates with VAV guanine nucleotide exchange factors to regulate NFAT activation by the B-cell antigen receptor. *Blood* **2005,** 105, (3), 1106-13.

123. Deckert, M.; Tartare-Deckert, S.; Hernandez, J.; Rottapel, R.; Altman, A. Adaptor function for the Syk kinases-interacting protein 3BP2 in IL-2 gene activation. *Immunity* **1998,** 9, (5), 595-605.

124. Schlondorff, J.; Blobel, C. P. Metalloprotease-disintegrins: modular proteins capable of promoting cell-cell interactions and triggering signals by protein-ectodomain shedding. *J Cell Sci* **1999,** 112 (Pt 21), 3603-17.

125. Yoshida, S.; Setoguchi, M.; Higuchi, Y.; Akizuki, S.; Yamamoto, S. Molecular cloning of cDNA encoding MS2 antigen, a novel cell surface antigen strongly expressed in murine monocytic lineage. *Int Immunol* **1990,** 2, (6), 585-91.

126. Choi, S. J.; Han, J. H.; Roodman, G. D. ADAM8: a novel osteoclast stimulating factor. *J Bone Miner Res* **2001,** 16, (5), 814-22.

127. Ainola, M.; Li, T. F.; Mandelin, J.; Hukkanen, M.; Choi, S. J.; Salo, J.; Konttinen, Y. T. Involvement of a disintegrin and a metalloproteinase 8 (ADAM8) in osteoclastogenesis and pathological bone destruction. *Ann Rheum Dis* **2009,** 68, (3), 427-34.

128. Raisz, L. G.; Simmons, H. A.; Sandberg, A. L.; Canalis, E. Direct stimulation of bone resorption by epidermal growth factor. *Endocrinology* **1980,** 107, (1), 270-3.

129. Normanno, N.; De Luca, A.; Aldinucci, D.; Maiello, M. R.; Mancino, M.; D'Antonio, A.; De Filippi, R.; Pinto, A. Gefitinib inhibits the ability of human bone marrow stromal cells to induce osteoclast differentiation: implications for the pathogenesis and treatment of bone metastasis. *Endocr Relat Cancer* **2005,** 12, (2), 471-82.

130. Yi, T.; Lee, H. L.; Cha, J. H.; Ko, S. I.; Kim, H. J.; Shin, H. I.; Woo, K. M.; Ryoo, H. M.; Kim, G. S.; Baek, J. H. Epidermal growth factor receptor regulates osteoclast differentiation and survival through cross-talking with RANK signaling. *J Cell Physiol* **2008,** 217, (2), 409-22.

131. Blair, H. C.; Zaidi, M. Osteoclastic differentiation and function regulated by old and new pathways. *Rev Endocr Metab Disord* **2006,** 7, (1-2), 23-32.

132. Xing, L.; Schwarz, E. M.; Boyce, B. F. Osteoclast precursors, RANKL/RANK, and immunology. *Immunol Rev* **2005,** 208, 19-29.

133. Hayashi, H.; Nakahama, K.; Sato, T.; Tuchiya, T.; Asakawa, Y.; Maemura, T.; Tanaka, M.; Morita, M.; Morita, I. The role of Mac-1 (CD11b/CD18) in osteoclast differentiation induced by receptor activator of nuclear factor-kappaB ligand. *FEBS Lett* **2008,** 582, (21-22), 3243-8.

134. Wiley, S. R.; Schooley, K.; Smolak, P. J.; Din, W. S.; Huang, C. P.; Nicholl, J. K.; Sutherland, G. R.; Smith, T. D.; Rauch, C.; Smith, C. A.; et al. Identification and characterization of a new member of the TNF family that induces apoptosis. *Immunity* **1995,** 3, (6), 673-82.

135. Zauli, G.; Rimondi, E.; Nicolin, V.; Melloni, E.; Celeghini, C.; Secchiero, P. TNF-related apoptosis-inducing ligand (TRAIL) blocks osteoclastic differentiation induced by RANKL plus M-CSF. *Blood* **2004,** 104, (7), 2044-50.

136. Roux, S.; Lambert-Comeau, P.; Saint-Pierre, C.; Lepine, M.; Sawan, B.; Parent, J. L. Death receptors, Fas and TRAIL receptors, are involved in human osteoclast apoptosis. *Biochem Biophys Res Commun* **2005,** 333, (1), 42-50.

137. Zauli, G.; Rimondi, E.; Stea, S.; Baruffaldi, F.; Stebel, M.; Zerbinati, C.; Corallini, F.; Secchiero, P. TRAIL inhibits osteoclastic differentiation by counteracting RANKL-dependent p27Kip1 accumulation in pre-osteoclast precursors. *J Cell Physiol* **2008,** 214, (1), 117-25.

138. Okahashi, N.; Murase, Y.; Koseki, T.; Sato, T.; Yamato, K.; Nishihara, T. Osteoclast differentiation is associated with transient upregulation of cyclin-dependent kinase inhibitors p21(WAF1/CIP1) and p27(KIP1). *J Cell Biochem* **2001,** 80, (3), 339-45.

139. Sankar, U.; Patel, K.; Rosol, T. J.; Ostrowski, M. C. RANKL coordinates cell cycle withdrawal and differentiation in osteoclasts through the cyclin-dependent kinase inhibitors p27KIP1 and

p21CIP1. *J Bone Miner Res* **2004,** 19, (8), 1339-48.

140. Saftig, P.; Hunziker, E.; Wehmeyer, O.; Jones, S.; Boyde, A.; Rommerskirch, W.; Moritz, J. D.; Schu, P.; von Figura, K. Impaired osteoclastic bone resorption leads to osteopetrosis in cathepsin-K-deficient mice. *Proc Natl Acad Sci U S A* **1998,** 95, (23), 13453-8.

141. Corisdeo, S.; Gyda, M.; Zaidi, M.; Moonga, B. S.; Troen, B. R. New insights into the regulation of cathepsin K gene expression by osteoprotegerin ligand. *Biochem Biophys Res Commun* **2001,** 285, (2), 335-9.

142. Shalhoub, V.; Faust, J.; Boyle, W. J.; Dunstan, C. R.; Kelley, M.; Kaufman, S.; Scully, S.; Van, G.; Lacey, D. L. Osteoprotegerin and osteoprotegerin ligand effects on osteoclast formation from human peripheral blood mononuclear cell precursors. *J Cell Biochem* **1999,** 72, (2), 251-61.

143. Pang, M.; Martinez, A. F.; Fernandez, I.; Balkan, W.; Troen, B. R. AP-1 stimulates the cathepsin K promoter in RAW 264.7 cells. *Gene* **2007,** 403, (1-2), 151-8.

144. Kafienah, W.; Bromme, D.; Buttle, D. J.; Croucher, L. J.; Hollander, A. P. Human cathepsin K cleaves native type I and II collagens at the N-terminal end of the triple helix. *Biochem J* **1998,** 331 (Pt 3), 727-32.

145. Johnson, M. R.; Polymeropoulos, M. H.; Vos, H. L.; Ortiz de Luna, R. I.; Francomano, C. A. A nonsense mutation in the cathepsin K gene observed in a family with pycnodysostosis. *Genome Res* **1996,** 6, (11), 1050-5.

146. Selinger, C. I.; Day, C. J.; Morrison, N. A. Optimized transfection of diced siRNA into mature primary human osteoclasts: inhibition of cathepsin K mediated bone resorption by siRNA. *J Cell Biochem* **2005,** 96, (5), 996-1002.

147. Phan, T. C.; Xu, J.; Zheng, M. H. Interaction between osteoblast and osteoclast: impact in bone disease. *Histol Histopathol* **2004,** 19, (4), 1325-44.

148. Lee, Z. H.; Kim, H. H. Signal transduction by receptor activator of nuclear factor kappa B in osteoclasts. *Biochem Biophys Res Commun* **2003,** 305, (2), 211-4.

149. Lomaga, M. A.; Yeh, W. C.; Sarosi, I.; Duncan, G. S.; Furlonger, C.; Ho, A.; Morony, S.; Capparelli, C.; Van, G.; Kaufman, S.; van der Heiden, A.; Itie, A.; Wakeham, A.; Khoo, W.; Sasaki, T.; Cao, Z.; Penninger, J. M.; Paige, C. J.; Lacey, D. L.; Dunstan, C. R.; Boyle, W. J.; Goeddel, D. V.; Mak, T. W. TRAF6 deficiency results in osteopetrosis and defective interleukin-1, CD40, and LPS signaling. *Genes Dev* **1999,** 13, (8), 1015-24.

150. Kobayashi, N.; Kadono, Y.; Naito, A.; Matsumoto, K.; Yamamoto, T.; Tanaka, S.; Inoue, J. Segregation of TRAF6-mediated signaling pathways clarifies its role in osteoclastogenesis. *Embo J* **2001,** 20, (6), 1271-80.

151. Angel, P.; Karin, M. The role of Jun, Fos and the AP-1 complex in cell-proliferation and transformation. *Biochim Biophys Acta* **1991,** 1072, (2-3), 129-57.

152. Kim, H. J.; Lee, Y.; Chang, E. J.; Kim, H. M.; Hong, S. P.; Lee, Z. H.; Ryu, J.; Kim, H. H. Suppression of osteoclastogenesis by N,N-dimethyl-D-erythro-sphingosine: a sphingosine kinase inhibition-independent action. *Mol Pharmacol* **2007,** 72, (2), 418-28.

153. Li, Y. P.; Chen, W.; Liang, Y.; Li, E.; Stashenko, P. Atp6i-deficient mice exhibit severe osteopetrosis due to loss of osteoclast-mediated extracellular acidification. *Nat Genet* **1999,** 23, (4), 447-51.

154. Frattini, A.; Orchard, P. J.; Sobacchi, C.; Giliani, S.; Abinun, M.; Mattsson, J. P.; Keeling, D. J.; Andersson, A. K.; Wallbrandt, P.; Zecca, L.; Notarangelo, L. D.; Vezzoni, P.; Villa, A. Defects in TCIRG1 subunit of the vacuolar proton pump are responsible for a subset of human autosomal recessive osteopetrosis. *Nat Genet* **2000,** 25, (3), 343-6.

155. Hu, Y.; Nyman, J.; Muhonen, P.; Vaananen, H. K.; Laitala-Leinonen, T. Inhibition of the osteoclast V-ATPase by small interfering RNAs. *FEBS Lett* **2005,** 579, (22), 4937-42.

156. Xu, J.; Cheng, T.; Feng, H. T.; Pavlos, N. J.; Zheng, M. H. Structure and function of V-ATPases in osteoclasts: potential therapeutic targets for the treatment of osteolysis. *Histol Histopathol* **2007,** 22, (4), 443-54.

157. Forgac, M. Structure and properties of the vacuolar (H+)-ATPases. *J Biol Chem* **1999,** 274, (19), 12951-4.

158. Xu, T.; Vasilyeva, E.; Forgac, M. Subunit interactions in the clathrin-coated vesicle vacuolar (H(+))-ATPase complex. *J Biol Chem* **1999,** 274, (41), 28909-15.

159. Sun-Wada, G. H.; Yoshimizu, T.; Imai-Senga, Y.; Wada, Y.; Futai, M. Diversity of mouse proton-translocating ATPase: presence of multiple isoforms of the C, d and G subunits. *Gene* **2003,** 302, (1-2), 147-53.

160. Feng, S.; Deng, L.; Chen, W.; Shao, J.; Xu, G.; Li, Y. P. Atp6v1c1 is an essential component of the osteoclast proton pump and in F-actin ring formation in osteoclasts. *Biochem J* **2009,** 417, (1), 195-203.

161. Kornak, U.; Kasper, D.; Bosl, M. R.; Kaiser, E.; Schweizer, M.; Schulz, A.; Friedrich, W.; Delling, G.; Jentsch, T. J. Loss of the ClC-7 chloride channel leads to osteopetrosis in mice and man. *Cell* **2001,** 104, (2), 205-15.

162. Okamoto, F.; Kajiya, H.; Toh, K.; Uchida, S.; Yoshikawa, M.; Sasaki, S.; Kido, M. A.; Tanaka, T.; Okabe, K. Intracellular ClC-3 chloride channels promote bone resorption in vitro through organelle acidification in mouse osteoclasts. *Am J Physiol Cell Physiol* **2008,** 294, (3), C693-701.

163. Kajiya, H.; Okamoto, F.; Li, J. P.; Nakao, A.; Okabe, K. Expression of mouse osteoclast K-Cl Co-transporter-1 and its role during bone resorption. *J Bone Miner Res* **2006,** 21, (7), 984-92.

164. Lauf, P. K.; Bauer, J.; Adragna, N. C.; Fujise, H.; Zade-Oppen, A. M.; Ryu, K. H.; Delpire, E. Erythrocyte K-Cl cotransport: properties and regulation. *Am J Physiol* **1992,** 263, (5 Pt 1), C917-32.

165. Reuss, L. Basolateral KCl co-transport in a NaCl-absorbing epithelium. *Nature* **1983,** 305, (5936), 723-6.

166. Philipson, K. D.; Nicoll, D. A.; Ottolia, M.; Quednau, B. D.; Reuter, H.; John, S.; Qiu, Z. The Na+/Ca2+ exchange molecule: an overview. *Ann N Y Acad Sci* **2002,** 976, 1-10.

167. Philipson, K. D.; Longoni, S.; Ward, R. Purification of the cardiac Na+-Ca2+ exchange protein. *Biochim Biophys Acta* **1988,** 945, (2), 298-306.

168. Nicoll, D. A.; Hryshko, L. V.; Matsuoka, S.; Frank, J. S.; Philipson, K. D. Mutation of amino acid residues in the putative transmembrane segments of the cardiac sarcolemmal Na+-Ca2+ exchanger. *J Biol Chem* **1996,** 271, (23), 13385-91.

169. Li, J. P.; Kajiya, H.; Okamoto, F.; Nakao, A.; Iwamoto, T.; Okabe, K. Three Na+/Ca2+ exchanger (NCX) variants are expressed in mouse osteoclasts and mediate calcium transport during bone resorption. *Endocrinology* **2007,** 148, (5), 2116-25.

170. Kefalas, P.; Brown, T. R.; Brickell, P. M. Signalling by the p60c-src family of protein-tyrosine kinases. *Int J Biochem Cell Biol* **1995,** 27, (6), 551-63.

171. Soriano, P.; Montgomery, C.; Geske, R.; Bradley, A. Targeted disruption of the c-src proto-oncogene leads to osteopetrosis in mice. *Cell* **1991,** 64, (4), 693-702.

172. Schwartzberg, P. L.; Xing, L.; Hoffmann, O.; Lowell, C. A.; Garrett, L.; Boyce, B. F.; Varmus, H. E. Rescue of osteoclast function by transgenic expression of kinase-deficient Src in src-/- mutant mice. *Genes Dev* **1997,** 11, (21), 2835-44.

173. Tanaka, S.; Takahashi, N.; Udagawa, N.; Sasaki, T.; Fukui, Y.; Kurokawa, T.; Suda, T. Osteoclasts express high levels of p60c-src, preferentially on ruffled border membranes. *FEBS Lett* **1992,** 313, (1), 85-9.

174. Boyce, B. F.; Yoneda, T.; Lowe, C.; Soriano, P.; Mundy, G. R. Requirement of pp60c-src expression for osteoclasts to form ruffled borders and resorb bone in mice. *J Clin Invest* **1992,** 90, (4), 1622-7.

175. Winograd-Katz, S. E.; Brunner, M. C.; Mirlas, N.; Geiger, B. Analysis of the signaling pathways regulating Src-dependent remodeling of the actin cytoskeleton. *Eur J Cell Biol* **2011,** 90, (2-3), 143-56.

176. Wu, L. W.; Baylink, D. J.; Lau, K. H. Molecular cloning and expression of a unique rabbit osteoclastic phosphotyrosyl phosphatase. *Biochem J* **1996,** 316 (Pt 2), 515-23.

177. Amoui, M.; Sheng, M. H.; Chen, S. T.; Baylink, D. J.; Lau, K. H. A transmembrane osteoclastic protein-tyrosine phosphatase regulates osteoclast activity in part by promoting osteoclast survival through c-Src-dependent activation of NFkappaB and JNK2. *Arch Biochem Biophys* **2007,** 463, (1), 47-59.

178. Yang, J. H.; Amoui, M.; Lau, K. H. Targeted deletion of the osteoclast protein-tyrosine phosphatase (PTP-oc) promoter prevents RANKL-mediated osteoclastic differentiation of RAW264.7 cells. *FEBS Lett* **2007,** 581, (13), 2503-8.

179. Teitelbaum, S. L. Bone resorption by osteoclasts. *Science* **2000,** 289, (5484), 1504-8.

180. Lakkakorpi, P.; Tuukkanen, J.; Hentunen, T.; Jarvelin, K.; Vaananen, K. Organization of osteoclast microfilaments during the attachment to bone surface in vitro. *J Bone Miner Res* **1989,** 4, (6), 817-25.

181. Biswas, R. S.; Baker, D.; Hruska, K. A.; Chellaiah, M. A. Polyphosphoinositides-dependent regulation of the osteoclast actin cytoskeleton and bone resorption. *BMC Cell Biol* **2004,** 5, 19.

182. Chellaiah, M. A. Regulation of actin ring formation by rho GTPases in osteoclasts. *J Biol Chem* **2005,** 280, (38), 32930-43.

183. Chellaiah, M.; Kizer, N.; Silva, M.; Alvarez, U.; Kwiatkowski, D.; Hruska, K. A. Gelsolin deficiency blocks podosome assembly and produces increased bone mass and strength. *J Cell Biol* **2000,** 148, (4), 665-78.

184. Calle, Y.; Jones, G. E.; Jagger, C.; Fuller, K.; Blundell, M. P.; Chow, J.; Chambers, T.; Thrasher,

A. J. WASp deficiency in mice results in failure to form osteoclast sealing zones and defects in bone resorption. *Blood* **2004,** 103, (9), 3552-61.

185. Rohatgi, R.; Ma, L.; Miki, H.; Lopez, M.; Kirchhausen, T.; Takenawa, T.; Kirschner, M. W. The interaction between N-WASP and the Arp2/3 complex links Cdc42-dependent signals to actin assembly. *Cell* **1999,** 97, (2), 221-31.

186. Insall, R. H.; Machesky, L. M. Regulation of WASP: PIP2 Pipped by Toca-1? *Cell* **2004,** 118, (2), 140-1.

187. Glogauer, M.; Hartwig, J.; Stossel, T. Two pathways through Cdc42 couple the N-formyl receptor to actin nucleation in permeabilized human neutrophils. *J Cell Biol* **2000,** 150, (4), 785-96.

188. Rozelle, A. L.; Machesky, L. M.; Yamamoto, M.; Driessens, M. H.; Insall, R. H.; Roth, M. G.; Luby-Phelps, K.; Marriott, G.; Hall, A.; Yin, H. L. Phosphatidylinositol 4,5-bisphosphate induces actin-based movement of raft-enriched vesicles through WASP-Arp2/3. *Curr Biol* **2000,** 10, (6), 311-20.

189. Machesky, L. M.; Gould, K. L. The Arp2/3 complex: a multifunctional actin organizer. *Curr Opin Cell Biol* **1999,** 11, (1), 117-21.

190. Hurst, I. R.; Zuo, J.; Jiang, J.; Holliday, L. S. Actin-related protein 2/3 complex is required for actin ring formation. *J Bone Miner Res* **2004,** 19, (3), 499-506.

191. Torres, E.; Rosen, M. K. Protein-tyrosine kinase and GTPase signals cooperate to phosphorylate and activate Wiskott-Aldrich syndrome protein (WASP)/neuronal WASP. *J Biol Chem* **2006,** 281, (6), 3513-20.

192. Wu, X.; Suetsugu, S.; Cooper, L. A.; Takenawa, T.; Guan, J. L. Focal adhesion kinase regulation of N-WASP subcellular localization and function. *J Biol Chem* **2004,** 279, (10), 9565-76.

193. Cory, G. O.; Cramer, R.; Blanchoin, L.; Ridley, A. J. Phosphorylation of the WASP-VCA domain increases its affinity for the Arp2/3 complex and enhances actin polymerization by WASP. *Mol Cell* **2003,** 11, (5), 1229-39.

194. Chellaiah, M. A.; Kuppuswamy, D.; Lasky, L.; Linder, S. Phosphorylation of a Wiscott-Aldrich syndrome protein-associated signal complex is critical in osteoclast bone resorption. *J Biol Chem* **2007,** 282, (13), 10104-16.

195. Chellaiah, M. A.; Schaller, M. D. Activation of Src kinase by protein-tyrosine phosphatase-PEST in osteoclasts: comparative analysis of the effects of bisphosphonate and

protein-tyrosine phosphatase inhibitor on Src activation in vitro. *J Cell Physiol* **2009,** 220, (2), 382-93.

196. Weaver, A. M.; Karginov, A. V.; Kinley, A. W.; Weed, S. A.; Li, Y.; Parsons, J. T.; Cooper, J. A. Cortactin promotes and stabilizes Arp2/3-induced actin filament network formation. *Curr Biol* **2001,** 11, (5), 370-4.

197. Ma, T.; Sadashivaiah, K.; Madaylputhlya, N.; Chellaiah, M. A. Regulation of sealing ring formation by L-plastin and cortactin in osteoclasts. *J Biol Chem* **2011,** 285, (39), 29911-24.

198. Cui, J.; Matkovich, S. J.; deSouza, N.; Li, S.; Rosemblit, N.; Marks, A. R. Regulation of the type 1 inositol 1,4,5-trisphosphate receptor by phosphorylation at tyrosine 353. *J Biol Chem* **2004,** 279, (16), 16311-6.

199. Yaroslavskiy, B. B.; Turkova, I.; Wang, Y.; Robinson, L. J.; Blair, H. C. Functional osteoclast attachment requires inositol-1,4,5-trisphosphate receptor-associated cGMP-dependent kinase substrate. *Lab Invest* **2010,** 90, (10), 1533-42.

200. Bonnelye, E.; Saltel, F.; Chabadel, A.; Zirngibl, R. A.; Aubin, J. E.; Jurdic, P. Involvement of the orphan nuclear estrogen receptor-related receptor alpha in osteoclast adhesion and transmigration. *J Mol Endocrinol* **2010,** 45, (6), 365-77.

201. Tyska, M. J.; Warshaw, D. M. The myosin power stroke. *Cell Motil Cytoskeleton* **2002,** 51, (1), 1-15.

202. McMichael, B. K.; Cheney, R. E.; Lee, B. S. Myosin X regulates sealing zone patterning in osteoclasts through linkage of podosomes and microtubules. *J Biol Chem* **2010,** 285, (13), 9506-15.

203. Berg, J. S.; Derfler, B. H.; Pennisi, C. M.; Corey, D. P.; Cheney, R. E. Myosin-X, a novel myosin with pleckstrin homology domains, associates with regions of dynamic actin. *J Cell Sci* **2000,** 113 Pt 19, 3439-51.

204. Weber, K. L.; Sokac, A. M.; Berg, J. S.; Cheney, R. E.; Bement, W. M. A microtubule-binding myosin required for nuclear anchoring and spindle assembly. *Nature* **2004,** 431, (7006), 325-9.

205. Okumura, S.; Mizoguchi, T.; Sato, N.; Yamaki, M.; Kobayashi, Y.; Yamauchi, H.; Ozawa, H.; Udagawa, N.; Takahashi, N. Coordination of microtubules and the actin cytoskeleton is important in osteoclast function, but calcitonin disrupts sealing zones without affecting microtubule networks. *Bone* **2006,** 39, (4), 684-93.

206. Jurdic, P.; Saltel, F.; Chabadel, A.; Destaing, O. Podosome and sealing zone: specificity of the osteoclast model. *Eur J Cell Biol* **2006,** 85, (3-4), 195-202.

207. Chang, E. J.; Ha, J.; Oerlemans, F.; Lee, Y. J.; Lee, S. W.; Ryu, J.; Kim, H. J.; Lee, Y.; Kim, H. M.; Choi, J. Y.; Kim, J. Y.; Shin, C. S.; Pak, Y. K.; Tanaka, S.; Wieringa, B.; Lee, Z. H.; Kim, H. H. Brain-type creatine kinase has a crucial role in osteoclast-mediated bone resorption. *Nat Med* **2008,** 14, (9), 966-72.

208. Wyss, M.; Kaddurah-Daouk, R. Creatine and creatinine metabolism. *Physiol Rev* **2000,** 80, (3), 1107-213.

209. Zhang, D.; Udagawa, N.; Nakamura, I.; Murakami, H.; Saito, S.; Yamasaki, K.; Shibasaki, Y.; Morii, N.; Narumiya, S.; Takahashi, N.; et al. The small GTP-binding protein, rho p21, is involved in bone resorption by regulating cytoskeletal organization in osteoclasts. *J Cell Sci* **1995,** 108 (Pt 6), 2285-92.

210. van Beek, E.; Pieterman, E.; Cohen, L.; Lowik, C.; Papapoulos, S. Farnesyl pyrophosphate synthase is the molecular target of nitrogen-containing bisphosphonates. *Biochem Biophys Res Commun* **1999,** 264, (1), 108-11.

211. Lacal, J. C. Regulation of proliferation and apoptosis by Ras and Rho GTPases through specific phospholipid-dependent signaling. *FEBS Lett* **1997,** 410, (1), 73-7.

212. Reinholz, G. G.; Getz, B.; Sanders, E. S.; Karpeisky, M. Y.; Padyukova, N.; Mikhailov, S. N.; Ingle, J. N.; Spelsberg, T. C. Distinct mechanisms of bisphosphonate action between osteoblasts and breast cancer cells: identity of a potent new bisphosphonate analogue. *Breast Cancer Res Treat* **2002,** 71, (3), 257-68.

213. Wang, Y. P., A.; Grainger, D.W. Small interfering RNA knocks down the molecular target of alendronate, farnesyl pyrophosphate synthase, in osteoclast and osteoblast cultures. *Molecular Pharmaceutics* **2011,** 8, (4), 1016-24.

214. Shankar, G.; Davison, I.; Helfrich, M. H.; Mason, W. T.; Horton, M. A. Integrin receptor-mediated mobilisation of intranuclear calcium in rat osteoclasts. *J Cell Sci* **1993,** 105 (Pt 1), 61-8.

215. Nesbitt, S.; Nesbit, A.; Helfrich, M.; Horton, M. Biochemical characterization of human osteoclast integrins. Osteoclasts express alpha v beta 3, alpha 2 beta 1, and alpha v beta 1 integrins. *J Biol Chem* **1993,** 268, (22), 16737-45.

216. McHugh, K. P.; Hodivala-Dilke, K.; Zheng, M. H.; Namba, N.; Lam, J.; Novack, D.; Feng, X.;

Ross, F. P.; Hynes, R. O.; Teitelbaum, S. L. Mice lacking beta3 integrins are osteosclerotic because of dysfunctional osteoclasts. *J Clin Invest* **2000,** 105, (4), 433-40.

217. Horton, M. A.; Taylor, M. L.; Arnett, T. R.; Helfrich, M. H. Arg-Gly-Asp (RGD) peptides and the anti-vitronectin receptor antibody 23C6 inhibit dentine resorption and cell spreading by osteoclasts. *Exp Cell Res* **1991,** 195, (2), 368-75.

218. Han, H. D.; Mangala, L. S.; Lee, J. W.; Shahzad, M. M.; Kim, H. S.; Shen, D.; Nam, E. J.; Mora, E. M.; Stone, R. L.; Lu, C.; Lee, S. J.; Roh, J. W.; Nick, A. M.; Lopez-Berestein, G.; Sood, A. K. Targeted gene silencing using RGD-labeled chitosan nanoparticles. *Clin Cancer Res* **2010,** 16, (15), 3910-22.

219. Engleman, V. W.; Nickols, G. A.; Ross, F. P.; Horton, M. A.; Griggs, D. W.; Settle, S. L.; Ruminski, P. G.; Teitelbaum, S. L. A peptidomimetic antagonist of the alpha(v)beta3 integrin inhibits bone resorption in vitro and prevents osteoporosis in vivo. *J Clin Invest* **1997,** 99, (9), 2284-92.

220. Komano, Y.; Nanki, T.; Hayashida, K.; Taniguchi, K.; Miyasaka, N. Identification of a human peripheral blood monocyte subset that differentiates into osteoclasts. *Arthritis Res Ther* **2006,** 8, (5), R152.

221. Tucci, M.; De Palma, R.; Lombardi, L.; Rodolico, G.; Berrino, L.; Dammacco, F.; Silvestris, F. beta(3) Integrin subunit mediates the bone-resorbing function exerted by cultured myeloma plasma cells. *Cancer Res* **2009,** 69, (16), 6738-46.

222. Kim, S. H.; Dass, C. R. p53-targeted cancer pharmacotherapy: move towards small molecule compounds. *J Pharm Pharmacol* **2011,** 63, (5), 603-10.

223. Michael, D.; Oren, M. The p53-Mdm2 module and the ubiquitin system. *Semin Cancer Biol* **2003,** 13, (1), 49-58.

224. Vassilev, L. T.; Vu, B. T.; Graves, B.; Carvajal, D.; Podlaski, F.; Filipovic, Z.; Kong, N.; Kammlott, U.; Lukacs, C.; Klein, C.; Fotouhi, N.; Liu, E. A. In vivo activation of the p53 pathway by small-molecule antagonists of MDM2. *Science* **2004,** 303, (5659), 844-8.

225. Carvajal, D.; Tovar, C.; Yang, H.; Vu, B. T.; Heimbrook, D. C.; Vassilev, L. T. Activation of p53 by MDM2 antagonists can protect proliferating cells from mitotic inhibitors. *Cancer Res* **2005,** 65, (5), 1918-24.

226. Zauli, G.; Rimondi, E.; Corallini, F.; Fadda, R.; Capitani, S.; Secchiero, P. MDM2 antagonist Nutlin-3 suppresses the proliferation and differentiation of human pre-osteoclasts through a p53-dependent pathway. *J Bone Miner Res* **2007,** 22, (10), 1621-30.

227. Komarova, S. V.; Pereverzev, A.; Shum, J. W.; Sims, S. M.; Dixon, S. J. Convergent signaling by acidosis and receptor activator of NF-kappaB ligand (RANKL) on the calcium/calcineurin/NFAT pathway in osteoclasts. *Proc Natl Acad Sci U S A* **2005,** 102, (7), 2643-8.

228. Coxon, F. P.; Helfrich, M. H.; Van't Hof, R.; Sebti, S.; Ralston, S. H.; Hamilton, A.; Rogers, M. J. Protein geranylgeranylation is required for osteoclast formation, function, and survival: inhibition by bisphosphonates and GGTI-298. *J Bone Miner Res* **2000,** 15, (8), 1467-76.

229. Fisher, J. E.; Rogers, M. J.; Halasy, J. M.; Luckman, S. P.; Hughes, D. E.; Masarachia, P. J.; Wesolowski, G.; Russell, R. G.; Rodan, G. A.; Reszka, A. A. Alendronate mechanism of action: geranylgeraniol, an intermediate in the mevalonate pathway, prevents inhibition of osteoclast formation, bone resorption, and kinase activation in vitro. *Proc Natl Acad Sci U S A* **1999,** 96, (1), 133-8.

230. Harada, H.; Kukita, T.; Kukita, A.; Iwamoto, Y.; Iijima, T. Involvement of lymphocyte function-associated antigen-1 and intercellular adhesion molecule-1 in osteoclastogenesis: a possible role in direct interaction between osteoclast precursors. *Endocrinology* **1998,** 139, (9), 3967-75.

231. Tani-Ishii, N.; Penninger, J. M.; Matsumoto, G.; Teranaka, T.; Umemoto, T. The role of LFA-1 in osteoclast development induced by co-cultures of mouse bone marrow cells and MC3T3-G2/PA6 cells. *J Periodontal Res* **2002,** 37, (3), 184-91.

232. Wong, B. R.; Rho, J.; Arron, J.; Robinson, E.; Orlinick, J.; Chao, M.; Kalachikov, S.; Cayani, E.; Bartlett, F. S., 3rd; Frankel, W. N.; Lee, S. Y.; Choi, Y. TRANCE is a novel ligand of the tumor necrosis factor receptor family that activates c-Jun N-terminal kinase in T cells. *J Biol Chem* **1997,** 272, (40), 25190-4.

233. Okada, Y.; Morimoto, I.; Ura, K.; Watanabe, K.; Eto, S.; Kumegawa, M.; Raisz, L.; Pilbeam, C.; Tanaka, Y. Cell-to-Cell adhesion via intercellular adhesion molecule-1 and leukocyte function-associated antigen-1 pathway is involved in 1alpha,25(OH)2D3, PTH and IL-1alpha-induced osteoclast differentiation and bone resorption. *Endocr J* **2002,** 49, (4), 483-95.

234. Pierce, W. M., Jr.; Waite, L. C. Bone-targeted carbonic anhydrase inhibitors: effect of a proinhibitor on bone resorption in vitro. *Proc Soc Exp Biol Med* **1987,** 186, (1), 96-102.

235. Hosain, F.; Spencer, R. P.; Couthon, H. M.; Sturtz, G. L. Targeted delivery of antineoplastic agent to bone: biodistribution studies of technetium-99m-labeled gem-bisphosphonate conjugate of methotrexate. *J Nucl Med* **1996,** 37, (1), 105-7.

236. Uludag, H.; Yang, J. Targeting systemically administered proteins to bone by bisphosphonate

conjugation. *Biotechnol Prog* **2002,** 18, (3), 604-11.

237. Soutschek, J.; Akinc, A.; Bramlage, B.; Charisse, K.; Constien, R.; Donoghue, M.; Elbashir, S.; Geick, A.; Hadwiger, P.; Harborth, J.; John, M.; Kesavan, V.; Lavine, G.; Pandey, R. K.; Racie, T.; Rajeev, K. G.; Rohl, I.; Toudjarska, I.; Wang, G.; Wuschko, S.; Bumcrot, D.; Koteliansky, V.; Limmer, S.; Manoharan, M.; Vornlocher, H. P. Therapeutic silencing of an endogenous gene by systemic administration of modified siRNAs. *Nature* **2004,** 432, (7014), 173-8.

238. Minakuchi, Y.; Takeshita, F.; Kosaka, N.; Sasaki, H.; Yamamoto, Y.; Kouno, M.; Honma, K.; Nagahara, S.; Hanai, K.; Sano, A.; Kato, T.; Terada, M.; Ochiya, T. Atelocollagen-mediated synthetic small interfering RNA delivery for effective gene silencing in vitro and in vivo. *Nucleic Acids Res* **2004,** 32, (13), e109.

239. Takeshita, F.; Minakuchi, Y.; Nagahara, S.; Honma, K.; Sasaki, H.; Hirai, K.; Teratani, T.; Namatame, N.; Yamamoto, Y.; Hanai, K.; Kato, T.; Sano, A.; Ochiya, T. Efficient delivery of small interfering RNA to bone-metastatic tumors by using atelocollagen in vivo. *Proc Natl Acad Sci U S A* **2005,** 102, (34), 12177-82.

240. Bumcrot, D.; Manoharan, M.; Koteliansky, V.; Sah, D. W. RNAi therapeutics: a potential new class of pharmaceutical drugs. *Nat Chem Biol* **2006,** 2, (12), 711-9.

241. Tomita, T.; Takeuchi, E.; Tomita, N.; Morishita, R.; Kaneko, M.; Yamamoto, K.; Nakase, T.; Seki, H.; Kato, K.; Kaneda, Y.; Ochi, T. Suppressed severity of collagen-induced arthritis by in vivo transfection of nuclear factor kappaB decoy oligodeoxynucleotides as a gene therapy. *Arthritis Rheum* **1999,** 42, (12), 2532-42.

242. Roman-Blas, J. A.; Jimenez, S. A. NF-kappaB as a potential therapeutic target in osteoarthritis and rheumatoid arthritis. *Osteoarthritis Cartilage* **2006,** 14, (9), 839-48.

243. Schiffelers, R. M.; Xu, J.; Storm, G.; Woodle, M. C.; Scaria, P. V. Effects of treatment with small interfering RNA on joint inflammation in mice with collagen-induced arthritis. *Arthritis Rheum* **2005,** 52, (4), 1314-8.

244. Khoury, M.; Louis-Plence, P.; Escriou, V.; Noel, D.; Largeau, C.; Cantos, C.; Scherman, D.; Jorgensen, C.; Apparailly, F. Efficient new cationic liposome formulation for systemic delivery of small interfering RNA silencing tumor necrosis factor alpha in experimental arthritis. *Arthritis Rheum* **2006,** 54, (6), 1867-77.

245. Hoshika, S.; Minakawa, N.; Matsuda, A. Synthesis and physical and physiological properties of 4'-thioRNA: application to post-modification of RNA aptamer toward NF-kappaB. *Nucleic Acids Res* **2004,** 32, (13), 3815-25.

246. Allerson, C. R.; Sioufi, N.; Jarres, R.; Prakash, T. P.; Naik, N.; Berdeja, A.; Wanders, L.; Griffey, R. H.; Swayze, E. E.; Bhat, B. Fully 2'-modified oligonucleotide duplexes with improved in vitro potency and stability compared to unmodified small interfering RNA. *J Med Chem* **2005,** 48, (4), 901-4.

247. Li, B. J.; Tang, Q.; Cheng, D.; Qin, C.; Xie, F. Y.; Wei, Q.; Xu, J.; Liu, Y.; Zheng, B. J.; Woodle, M. C.; Zhong, N.; Lu, P. Y. Using siRNA in prophylactic and therapeutic regimens against SARS coronavirus in Rhesus macaque. *Nat Med* **2005,** 11, (9), 944-51.

248. Choung, S.; Kim, Y. J.; Kim, S.; Park, H. O.; Choi, Y. C. Chemical modification of siRNAs to improve serum stability without loss of efficacy. *Biochem Biophys Res Commun* **2006,** 342, (3), 919-27.

249. Dande, P.; Prakash, T. P.; Sioufi, N.; Gaus, H.; Jarres, R.; Berdeja, A.; Swayze, E. E.; Griffey, R. H.; Bhat, B. Improving RNA interference in mammalian cells by 4'-thio-modified small interfering RNA (siRNA): effect on siRNA activity and nuclease stability when used in combination with 2'-O-alkyl modifications. *J Med Chem* **2006,** 49, (5), 1624-34.

250. Song, E.; Zhu, P.; Lee, S. K.; Chowdhury, D.; Kussman, S.; Dykxhoorn, D. M.; Feng, Y.; Palliser, D.; Weiner, D. B.; Shankar, P.; Marasco, W. A.; Lieberman, J. Antibody mediated in vivo delivery of small interfering RNAs via cell-surface receptors. *Nat Biotechnol* **2005,** 23, (6), 709-17.

251. Wang, D.; Miller, S.; Sima, M.; Kopeckova, P.; Kopecek, J. Synthesis and evaluation of water-soluble polymeric bone-targeted drug delivery systems. *Bioconjug Chem* **2003,** 14, (5), 853-9.

252. Newa, M.; Bhandari, K. H.; Tang, L.; Kalvapalle, R.; Suresh, M.; Doschak, M. R. Antibody-mediated "Universal" osteoclast targeting platform using calcitonin as a model drug. *Pharm Res* **2011,** 28, (5), 1131-43.

253. Wang, D.; Miller, S. C.; Kopeckova, P.; Kopecek, J. Bone-targeting macromolecular therapeutics. *Adv Drug Deliv Rev* **2005,** 57, (7), 1049-76.

254. Yokogawa, K.; Miya, K.; Sekido, T.; Higashi, Y.; Nomura, M.; Fujisawa, R.; Morito, K.; Masamune, Y.; Waki, Y.; Kasugai, S.; Miyamoto, K. Selective delivery of estradiol to bone by aspartic acid oligopeptide and its effects on ovariectomized mice. *Endocrinology* **2001,** 142, (3), 1228-33.

255. Kasugai, S.; Fujisawa, R.; Waki, Y.; Miyamoto, K.; Ohya, K. Selective drug delivery system to bone: small peptide (Asp)6 conjugation. *J Bone Miner Res* **2000,** 15, (5), 936-43.

256. Aouadi, M.; Tesz, G. J.; Nicoloro, S. M.; Wang, M.; Chouinard, M.; Soto, E.; Ostroff, G. R.; Czech, M. P. Orally delivered siRNA targeting macrophage Map4k4 suppresses systemic inflammation. *Nature* **2009,** 458, (7242), 1180-4.

257. Wu, S. Y.; McMillan, N. A. Lipidic systems for in vivo siRNA delivery. *Aaps J* **2009,** 11, (4), 639-52.

258. Krebs MD; E, A. Localized, targeted, and sustained siRNA delivery. . *Chemistry* **2011,** 17, (11), 3054-3062.

259. Song, E.; Lee, S. K.; Wang, J.; Ince, N.; Ouyang, N.; Min, J.; Chen, J.; Shankar, P.; Lieberman, J. RNA interference targeting Fas protects mice from fulminant hepatitis. *Nat Med* **2003,** 9, (3), 347-51.

260. Yasuhiko Tabata, Y. I. Phagocytosis of polymer microspheres by macrophages *Adv. Polym. Sci* **1990,** 94, 110-141.

261. Marsh, M.; McMahon, H. T. The structural era of endocytosis. *Science* **1999,** 285, (5425), 215-20.

262. Kobzik, L.; Huang, S.; Paulauskis, J. D.; Godleski, J. J. Particle opsonization and lung macrophage cytokine response. In vitro and in vivo analysis. *J Immunol* **1993,** 151, (5), 2753-9.

263. Cejka, D.; Losert, D.; Wacheck, V. Short interfering RNA (siRNA): tool or therapeutic? *Clin Sci (Lond)* **2006,** 110, (1), 47-58.

264. Taljanovic, M. S.; Jones, M. D.; Ruth, J. T.; Benjamin, J. B.; Sheppard, J. E.; Hunter, T. B. Fracture fixation. *Radiographics* **2003,** 23, (6), 1569-90.

265. Zhang, Y.; Song, J.; Shi, B.; Wang, Y.; Chen, X.; Huang, C.; Yang, X.; Xu, D.; Cheng, X.; Chen, X. Combination of scaffold and adenovirus vectors expressing bone morphogenetic protein-7 for alveolar bone regeneration at dental implant defects. *Biomaterials* **2007,** 28, (31), 4635-42.

266. Perry, A.; Mahar, A.; Massie, J.; Arrieta, N.; Garfin, S.; Kim, C. Biomechanical evaluation of kyphoplasty with calcium sulfate cement in a cadaveric osteoporotic vertebral compression fracture model. *Spine J* **2005,** 5, (5), 489-93.

267. Dreinhöfer Karsten, L. L., Maalouf Ghassan Bone Augmentation in Osteoporosis – An Update on Vertebroplasty and Kyphoplasty *European Musculoskeletal Review* **2008,** 3, (1), 14-6.

268. John Jackson, F. L., Clive Duncan,Clement Mugabe, Helen Burt. The use of bone cement for

the localized, controlled release of the antibiotics vancomycin, linezolid, or fusidic acid: effect of additives on drug release rates and mechanical strength. *Drug Deliv. and Transl. Res.* **2011,** 1, 121-131.

269. Neut, D.; Kluin, O. S.; Thompson, J.; van der Mei, H. C.; Busscher, H. J. Gentamicin release from commercially-available gentamicin-loaded PMMA bone cements in a prosthesis-related interfacial gap model and their antibacterial efficacy. *BMC Musculoskelet Disord* **2010,** 11, 258.

270. W.J.E.M.Habraken; J.G.C.Wolke; A.G.Mikos; J.A.Jansen. Injectable PLGA microsphere/calcium phosphate cements: physical properties and degradation characteristics. *J.Biomater.Sci.Polymer Edn* **2006,** 17, (9), 1057-1074.

271. Ginebra, M. P.; Traykova, T.; Planell, J. A. Calcium phosphate cements: competitive drug carriers for the musculoskeletal system? *Biomaterials* **2006,** 27, (10), 2171-7.

272. Wu, F.; Su, J.; Wei, J.; Guo, H.; Liu, C. Injectable bioactive calcium-magnesium phosphate cement for bone regeneration. *Biomed Mater* **2008,** 3, (4), 44105.

273. Bohner, M.; Gbureck, U.; Barralet, J. E. Technological issues for the development of more efficient calcium phosphate bone cements: a critical assessment. *Biomaterials* **2005,** 26, (33), 6423-9.

274. A. Tofighi, S. M., P. Chakravarthy, C. Rey, D.Lee. Setting reactions involved in injectable cements based on amorphous calcium phosphate. *Key Eng. Mater.* **2000,** 192-195, 769-772.

275. Constantz, B. R.; Ison, I. C.; Fulmer, M. T.; Poser, R. D.; Smith, S. T.; VanWagoner, M.; Ross, J.; Goldstein, S. A.; Jupiter, J. B.; Rosenthal, D. I. Skeletal repair by in situ formation of the mineral phase of bone. *Science* **1995,** 267, (5205), 1796-9.

276. Takechi, M.; Miyamoto, Y.; Ishikawa, K.; Nagayama, M.; Kon, M.; Asaoka, K.; Suzuki, K. Effects of added antibiotics on the basic properties of anti-washout-type fast-setting calcium phosphate cement. *J Biomed Mater Res* **1998,** 39, (2), 308-16.

277. Ratier, A.; Gibson, I. R.; Best, S. M.; Freche, M.; Lacout, J. L.; Rodriguez, F. Setting characteristics and mechanical behaviour of a calcium phosphate bone cement containing tetracycline. *Biomaterials* **2001,** 22, (9), 897-901.

278. Ethell, M. T.; Bennett, R. A.; Brown, M. P.; Merritt, K.; Davidson, J. S.; Tran, T. In vitro elution of gentamicin, amikacin, and ceftiofur from polymethylmethacrylate and hydroxyapatite cement. *Vet Surg* **2000,** 29, (5), 375-82.

279. Takechi, M.; Miyamoto, Y.; Momota, Y.; Yuasa, T.; Tatehara, S.; Nagayama, M.; Ishikawa, K.; Suzuki, K. The in vitro antibiotic release from anti-washout apatite cement using chitosan. *J Mater Sci Mater Med* **2002,** 13, (10), 973-8.

280. Otsuka, M.; Matsuda, Y.; Suwa, Y.; Fox, J. L.; Higuchi, W. I. A novel skeletal drug delivery system using a self-setting calcium phosphate cement. 5. Drug release behavior from a heterogeneous drug-loaded cement containing an anticancer drug. *J Pharm Sci* **1994,** 83, (11), 1565-8.

281. Otsuka, M.; Matsuda, Y.; Fox, J. L.; Higuchi, W. I. A novel skeletal drug delivery system using self-setting calcium phosphate cement. 9: Effects of the mixing solution volume on anticancer drug release from homogeneous drug-loaded cement. *J Pharm Sci* **1995,** 84, (6), 733-6.

282. Blom, E. J.; Klein-Nulend, J.; Klein, C. P.; Kurashina, K.; van Waas, M. A.; Burger, E. H. Transforming growth factor-beta1 incorporated during setting in calcium phosphate cement stimulates bone cell differentiation in vitro. *J Biomed Mater Res* **2000,** 50, (1), 67-74.

283. R.B Edwards III, H. J. S., J.J. Bogdanske, J.Devitt, R.Vanderby, M.D. Markee. Percutaneous injection of recombinant human bone morphogenetic protein-2 in a calcium phosphate paste accelerates healing of a canine tibial osteotomy. *J. Bone Jt. Surg.* **2004,** A 86, 1425-1438.

284. Dong, L.; Huang, Z.; Cai, X.; Xiang, J.; Zhu, Y. A.; Wang, R.; Chen, J.; Zhang, J. Localized Delivery of Antisense Oligonucleotides by Cationic Hydrogel Suppresses TNF-alpha Expression and Endotoxin-Induced Osteolysis. *Pharm Res* **2011,** 28, (6), 1349-56.

285. Christie, R. J.; Grainger, D. W. Design strategies to improve soluble macromolecular delivery constructs. *Adv Drug Deliv Rev* **2003,** 55, (3), 421-37.

286. Shen, J.; Samul, R.; Silva, R. L.; Akiyama, H.; Liu, H.; Saishin, Y.; Hackett, S. F.; Zinnen, S.; Kossen, K.; Fosnaugh, K.; Vargeese, C.; Gomez, A.; Bouhana, K.; Aitchison, R.; Pavco, P.; Campochiaro, P. A. Suppression of ocular neovascularization with siRNA targeting VEGF receptor 1. *Gene Ther* **2006,** 13, (3), 225-34.

287. Alexopoulou, L.; Holt, A. C.; Medzhitov, R.; Flavell, R. A. Recognition of double-stranded RNA and activation of NF-kappaB by Toll-like receptor 3. *Nature* **2001,** 413, (6857), 732-8.

288. Yamamoto, M.; Sato, S.; Hemmi, H.; Hoshino, K.; Kaisho, T.; Sanjo, H.; Takeuchi, O.; Sugiyama, M.; Okabe, M.; Takeda, K.; Akira, S. Role of adaptor TRIF in the MyD88-independent toll-like receptor signaling pathway. *Science* **2003,** 301, (5633), 640-3.

289. Aderem, A. Role of Toll-like receptors in inflammatory response in macrophages. *Crit Care Med* **2001,** 29, (7 Suppl), S16-8.

CHAPTER 2

SIRNA KNOCKDOWN OF RANK SIGNALING TO CONTROL

OSTEOCLAST-MEDIATED BONE RESORPTION

Abstract

This chapter demonstrates the potential for small interfering (si)RNA control of osteoclast function. RANK and RANK ligand can act together to activate osteoclast formation and its intrinsic bone resorption activities. Suppression of RANK reduces osteoclast-mediated bone resorption in vitro. Delivery of siRNA targeting RANK to both RAW264.7 and primary bone marrow cell cultures produces short-term repression of RANK expression without off-targeting effects, and significantly inhibits both osteoclast formation as determined by tartrate-resistant acid phosphatase (TRAP) assay, and subsequent bone resorption by resorption pit assay.

Introduction

With mean life expectancy increasing worldwide, degenerative skeletal diseases become more significant. Age-related hormonal changes are correlated with enhanced osteoclast activity observed in this patient population. Reduced bone density is highly associated clinically with the risk of fragility fractures,[1-3] decreasing the eligibility for orthopedic implants, significantly impairing many patients' quality of life. The osteoclast is the major cell type responsible for bone resorption.

Together with the bone-forming osteoblast, the osteoclast regulates the homeostasis of skeletal mass and continual turnover.[4] Increased osteoclast function induces excessive osteoclast-mediated bone resorption, leading to bone loss-associated diseases, including Paget's disease,[5] osteoporosis,[6] hypercalcemia [7] and metastatic bone disease.[8]

As large multinucleated cells, osteoclasts originate from mononuclear precursors of the monocyte-macrophage cell lineage.[9] Osteoclastogenesis, cell maintenance and activation involve complex pathways with intricate relationships between multiple signaling molecules. Macrophage colony-stimulating factor (M-CSF), receptor activator of nuclear factor κB (RANK) and RANK ligand (RANKL) are known to be key molecules initiating osteoclast formation. Interaction between M-CSF and its receptor, c-Fms, generates signals for osteoclast precursor cell survival and proliferation.[10] By contrast, osteoclastogenesis is modulated by positive interactions between RANK and RANKL and negative interactions between RANKL and osteoprotegerin (OPG). RANK is a transmembrane signaling receptor expressed on haematopoietic precursor cells and osteoclasts.[11] Interaction of RANKL is required for osteoclast formation, activation and calcium homeostasis.[11, 12] It has also been reported that interaction of RANK and RANKL increases survival of the mature osteoclast in vitro and in vivo.[13] RANK signals through the key adapter molecule, TNF receptor-associated factor (TRAF) 6, and RANK cytoplasmic domains, to regulate formation and activation through osteoclast-specific gene expression.[11] Mice lacking RANK, TRAF 6 or RANKL are deficient in osteoclasts and lack osteoclastogenesis.[12, 14-16] OPG, a soluble protein of the TNF receptor family, secreted by osteoblasts, competitively binds RANKL,[11, 17] consequently acting as a decoy receptor to block osteoclastogenesis and suppress osteoclast survival.[18, 19] Thus,

positive regulator RANKL and negative regulator OPG are normally coordinated to modulate bone degradation and formation homeostasis by competitive interactions with RANK. RANK is therefore a central factor in this bone metabolic regulatory pathway.

RNA interference (RNAi) [20] is a relatively recent development with increasing utility as a sequence-specific posttranscriptional gene silencing tool.[21] Because systemic siRNA targeting has proven very challenging, local or topical siRNA therapeutics have been most actively investigated. Successful delivery approaches include ocular, respiratory, CNS, skin and vaginal sites where local siRNA delivery accesses desired cell target populations directly.[22-26] To date, siRNA targeting of RANK responsible for osteoclast formation and function has not been reported. The purpose of this study is to assess the utility of RNA interference (RNAi) methods to target RANK in regulating osteoclast formation and function in vitro. Reduction of RANK expression using siRNA specific to RANK is expected to suppress bone resorption by osteoclasts, ultimately increasing bone density and potentially preventing bone mass loss. In order to determine the efficacy of this RANK-targeting siRNA, both RAW and primary cells were evaluated for RANK message and protein expression after siRNA delivery. Functional assessments included inhibition of osteoclast formation by TRAP assay, and functional suppression of osteoclasts by bone resorption pit assay. Results show that osteoclast formation and osteoclast-mediated bone resorption can be significantly suppressed using siRNAs targeting RANK.

<u>Materials and Methods</u>

Cell culture

<u>Immortalized murine monocyte-macrophage cell line culture.</u>   A subclonal line of murine

monocytic pre-osteoclastic RAW264.7 cells, purchased from the American Type Culture Collection

(ATCC), was cultured in Dulbecco's modified Eagle's medium (DMEM, Gibco) supplemented with

10% heat-inactivated fetal bovine serum (FBS, Hyclone®, UT) and 1% penicillin-streptomycin

(Gibco), defined for all cell cultures as "complete media". To induce osteoclast formation in vitro,

RAW cells (passage number controlled to less than 10) were cultured on 24-well plates in

complete media at the density of 4×10^4 cells per well supplemented with 100ng/ml of RANKL.

Complete media with RANKL was changed every other day.

<u>Primary murine cell harvest and differentiation.</u>   C57BL/6 male mice (6-8-week-old, Jackson

labs) were maintained in a specific pathogen-free facility at the University of Utah. All procedures

were performed as approved by the Institutional Animal Care and Use Committee of University of

Utah. Bone marrow cells (BMC) were harvested from murine tibias and femurs of C57BL/6 male

mice and differentiated into osteoclast precursors using previously described methods.[27-29] Briefly,

BMCs were cultured in α-MEM (Gibco) containing 10% FBS and 1% penicillin-streptomycin

overnight at a density of 1×10^6 cells/ml. Nonadherent cells were harvested the next day and

immediately seeded into 24-well tissue culture plates in complete media with 30 ng/ml M-CSF

(R&D Systems) at a density of 1×10^6 cells per well. After 2 days of culture, attached cells were

used as osteoclast precursors. To generate osteoclasts, precursor cells were incubated in

200ng/ml RANKL and 30ng/ml M-CSF (R&D Systems) in complete media, refreshed every other

day. RANKL working concentrations to reliably generate osteoclasts from both RAW264.7 and primary cell cultures in serum media were experimentally determined.

sRANKL expression. A glutathione-S-transferase (GST)-tagged sRANKL construct was generated by cloning the murine sRANKL SalI/NotI fragment, coding 470-951 nucleotides, into the plasmid pGEX-4T-1 (a generous gift of Dr. M. F. Manolson, University of Toronto). The expressed protein was harvested as previously described.[29-31] GST-tagged sRANKL was purified by Glutathione Sepharose 4B affinity resin (Amersham Pharmacia Biotech), dialyzed against phosphate buffered saline (PBS, Gibco) and concentrated using Amicon Ultra centrifuge tubes (Millipore). Protein concentration was determined by BCA protein assay kit (Pierce).

siRNA transfection of cells. An siGENOME SMARTpool (Dharmacon) containing four different siRNA sequences all designed to target murine RANK, as well as four pure individual siRNAs (**1**, sense 5'-GAGCAGAACUGACUCUAUGUU- 3', antisense 5'-CAUAGAGUCAGUUC UGCUCUU-3'; **2**, sense 5'-GCGCAGACUUCACUCCAUAUU-3', antisense 5'-UAUGGAGUGAAG UCUGCGCUU-3'; **3**, sense 5'-CCAAGGAGGCCCAGGCUUAUU-3', antisense 5'-UAAGCCUGGG CCUCCUUGGUU-3'; **4**, sense 5'-CAAGAAGUGUGUGAAGGUAUU-3', antisense 5'-UACCUU CACACACUUCUUGUU-3'), and a non-targeting control siRNA (sense: 5'-UAGCGACUAAA CACAUCAAUU-3', antisense: 5'-UUAUCGCUGAUUUGUGUAGUU-3') were purchased from Dharmacon. DharmaFECT 4 (DF4, Dharmacon) was used as the cationic lipid cell transfection reagent. RAW cells were seeded at a density of 4×10^4 cells per well in 24-well plates in DMEM at 37°C with 5% CO_2 overnight. Transfection with siRNA/DF4 complexes was then carried out in complete media. Primary BMC were seeded at 1×10^6 cells per well in 24-well plates in complete

media containing 30ng/ml M-CSF for 2 days. Subsequently, siRNA transfection was immediately performed. Transfection reagent DF4 and siRNA were prepared according to manufacturer's instructions (Dharmacon). Final dosing concentrations of all siRNAs provided to each well were 125 nM in a total volume of 1.0 microliter DF4. Cell uptake of siRNA complexes was performed by incubating cells with siRNA complexes in complete media at 37°C with 5% CO_2. In osteoclast formation and pit formation assays, cells were transfected by siRNA complexes in complete media with 100ng/ml RANKL (RAW cells) or 30 ng/ml M-CSF and 200 ng/ml RANKL (BMC). Nonspecific knockdown of DF4 was assessed by using non-targeting siRNA dosed under identical conditions. Multiple cell transfections were carried out identically each day over the successive first 3 days, or on alternating days, as specified in each figure. In the case of transfection of osteoclast cultures, RAW cells and primary BMCs were seeded in 24-well plates and treated as mentioned above to generate osteoclasts. Mature osteoclasts were purified essentially as described elsewhere [28, 32] by gently washing with PBS without Ca^{2+} and Mg^{2+} (Gibco). By tapping the plate, most mononuclear cells were detached, while multinucleated osteoclasts remained on the plate. Osteoclasts were transfected by incubating with siRNA complexes prepared as above in complete media containing 100ng/ml RANKL (RAW cells) or 200ng/ml RANKL and 30ng/ml M-CSF (BMC).

Reverse transcriptase-polymerase chain reaction (RT-PCR). Total RNA was isolated 48 hours after siRNA transfection using an RNeasy Mini Kit (Qiagen). Up to 4 micrograms of RNA were used to make cDNA with the SuperScript III 1st strand RT kit for PCR (Invitrogen). PCR primers were designed for RANK (5'-AGATGTGGTCTGCAGCTCTTCCAT-3', 5'- ACACACTTC TTGCTGACTGGAGGT-3') and cyclophilin B (housekeeping control, 5'- AGCGCTTCCCAGATG

AGAACTTCA-3', 5'-GCAATGGCAAAGGGTTTCTCCACT-3') using Primerquest software

purchased from Integrated DNA Technologies (IDT). PCR was performed with iTaq DNA

polymerase (Bio-Rad), 1.5 mM magnesium chloride, 200 µM each of dNTPs, 500 nM of each

primer and 2 µL of the cDNA. Reactions were performed using the following protocol: $95^{o}C$ melt,

$60^{o}C$ anneal and $72^{o}C$ extension in the iCycler Thermal cycler (Bio-Rad). PCR products were

analyzed on ethidium bromide-stained TBE-based 2% agarose gels run at 100V for 30 minutes

and visualized with UV light.

Real-time quantitative PCR (qPCR) analysis. cDNA was prepared as described above.

Primers for RANK (5'-TAGGACGTCAGGCCAAAGGACAAA-3', 5'-AGGGCCTACTGC

CTAAGTGTGTTT-3', Probe: 56-FAM/TGAAGGTGCCAGGGAAATTCAAGAAAGA/36-TAMSp)

and cyclophilin B (5'-TCCGGCAAGATCGAAGTGGAGAAA-3', 5'-AACCTTGTGACTGGCTACCTT

CGT-3', Probe: 56-FAM/TCATCCCTCTAAGCAGCTGTCTG TGT/36-TAMSp) were designed using

Primerquest software purchased from IDT. Experiments were performed using 7900HT Sequence

Detection System and data were analyzed using SDS RQ manager (Applied Biosystems).

RANK Western immunoblot assay. Cells were lysed in RIPA buffer (Sigma) supplied with 1×

protease inhibitor cocktail (Pierce) and 1mM phenylmethylsulfonyl fluoride (Sigma).[32] Insoluble

material was removed by centrifuging at 15,000 rpm at 4℃ for 5 minutes after 20 minutes on ice.

Protein concentration was measured with a BCA protein assay kit (Pierce). Heat-denatured

samples were separated on 4-12% SDS-polyacrylamide gels (Invitrogen) and blotted on PVDF

filters (Bio-Rad). After blocking with 5% (w/v) dry milk in 0.5% Tween 20 in TBS (TBST), the filter

was incubated overnight in primary antibody against RANK (BAF692; R&D systems) in 5%

BSA/TBST with constant shaking. After three washes with TBST, the membrane was incubated

with streptravidin-HRP (RPN 1231; Amersham Pharmacia Biotech Ltd). The housekeeping control

was detected with antibody against cyclophilin B (PA1-027; Affinity BioReagents) and

HRP-conjugated donkey antirabbit antibody (SA1-200, Affinity BioReagents). Secondary

antibodies were detected with chemiluminescence reagent (Santa Cruz Biotechnology) and band

images were captured using a Molecular Imager Gel Doc XR System (Bio-Rad).

Tartrate-resistant acid phosphatase (TRAP) assay. Cells were stained for TRAP using a

leukocyte acid phosphatase kit (Sigma) according to the instructions. Osteoclasts staining positive

with at least three nuclei were counted as TRAP-positive cells.

Bone resorption pit assay. Bovine bone was sawed into 0.2-0.3 mm thick slices (a gift from

Dr. S. Miller, University of Utah) and washed as described [29] before placing small pieces into

24-well plates. A total of 4×10^4 RAW cells were plated and cultured on bone slices in DMEM for 12

hours and then cells were transfected with siRNA in complete media with 100ng/ml RANKL (Day

1). BMCs were plated on bone slices at a density of 1×10^6 per well in 30ng/ml M-CSF complete

media for 2 days. Thereafter, siRNA transfection was performed in 200ng/ml RANKL and 30ng/ml

M-CSF-containing complete media (Day 1). The media was changed every other day. To observe

osteoclast-generated bone resorption, slices were stained using a previous described method.[29]

Pit numbers per frame were counted from random fields under microscopic observation.

Cell imaging. Live adherent cells, TRAP-stained images and pit images were photographed

using a Nikon Eclipse TE 2000-U microscope, with Photometrics Coolsnap ES camera (gray scale,

Roper Scientific) or QImagine RETIGA EXi color 12-bit camera (color, Canda), using Metamorph[TM]

software (Molecular Devices) or QCapture™ software (QImaging). An average of 15 frames per

well were taken randomly for TRAP assay analysis and 10 frames were acquired randomly from

each bone slice for pit formation analysis (except for triple siRNA transfection sequences in

primary BMC where 5 frames were acquired).

 <u>Statistical analysis.</u> Analysis of variance (ANOVA) followed by two-tailed student's t-test was

used for statistical analysis. For multiple comparisons, Bonferroni correction was applied. All

experiments were repeated three times. Error bars represent the standard error of the mean.

<div align="center">

<u>Results</u>

Transfection in culture of RAW cells

</div>

 <u>Optimization of siRNA transfection in cultures of RAW cells.</u> DharmaFECT 4 (DF4) was

chosen as a siRNA transfection reagent since it was appropriate for mouse and rat cell lines based

on the manufacturer's instructions. Transfection conditions in serum-containing media were

optimized using a commercial murine-targeted siRNA pool (SMARTpool). Each siRNA sequence

was then tested individually for their effectiveness to knock down RANK expression in cells in

complete media. While qPCR results for sample siRNA-1 and -2 RANK knockdown were

statistically indistinguishable, siRNA-2 was selected for further study since it produced the greatest

overall knockdown effect (Figure 2.1A, p=0.009). RANK siRNA-2, therefore, was used for all

further siRNA transfections of RAW cultures. Nonspecific knockdown of RANK by DF4 evaluated

using non-targeting siRNA and DF4 demonstrates little effect by PCR analysis, shown in Figure

2.1B. Similarly, treatment of mature osteoclasts with RANK siRNA-2 also significantly suppressed
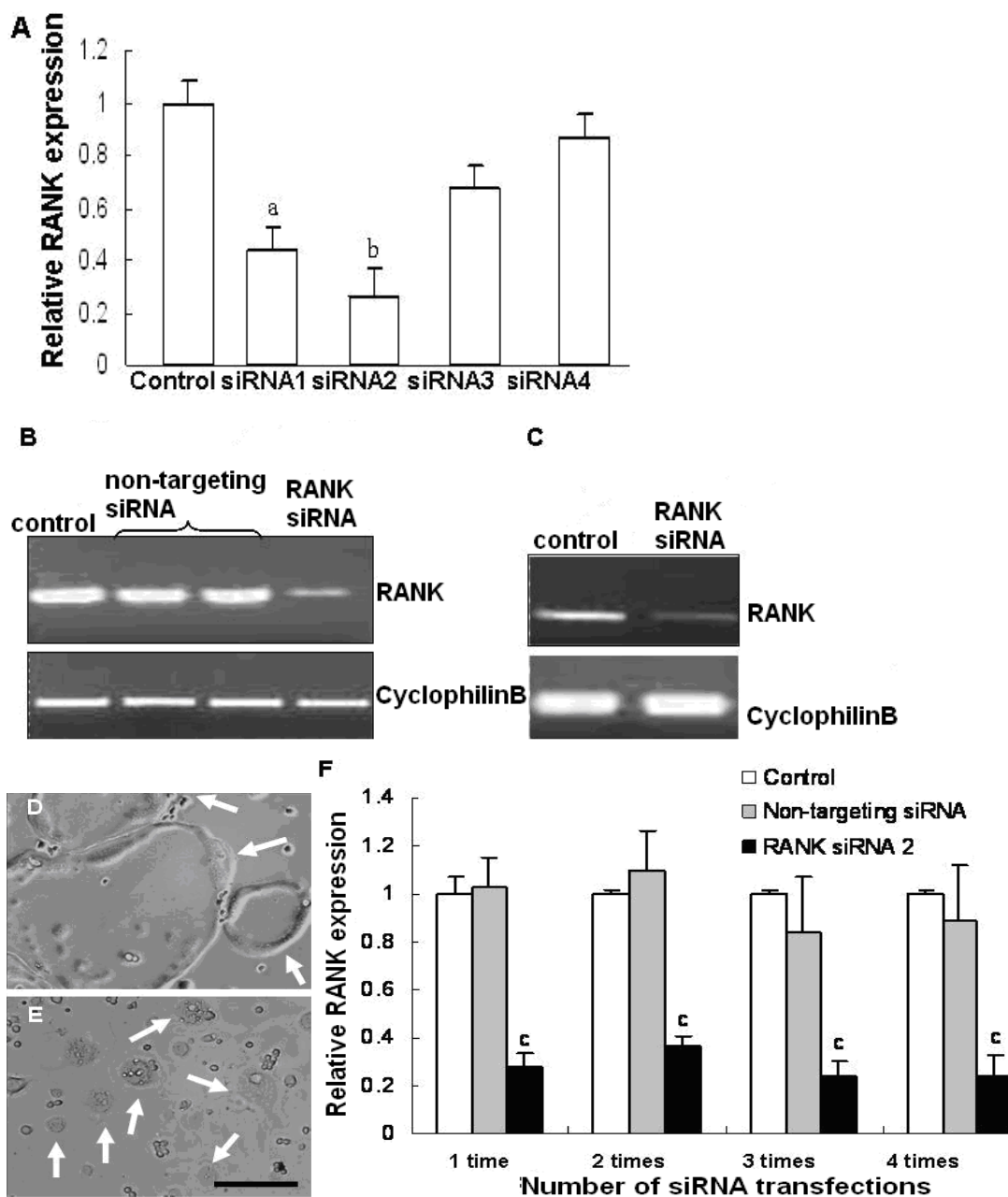
Figure 2.1 RANK mRNA expression knockdown in cultured RAW cells. RNA was harvested 48 hours posttransfection. (A) Four RANK siRNAs were assayed by qPCR analysis for the greatest knockdown effects. ([a]$p<0.05$, [b]$p<0.01$, each compared with controls without treatment). (B) DF4 was tested for nonspecific knockdown of RANK using non-targeting siRNA. (C) RANK siRNA-2 was used to knock down the RANK gene expression in RAW-derived mature osteoclasts. Representative images of (E) RAW-derived osteoclasts (arrows) after a 48-hours knockdown by RANK siRNA, compared with (D) controls with no treatment. (10X magnification) (F) RANK mRNA expression knockdown in RAW cell culture after multiple serial transfections determined by performing qPCR. ([c]$p<0.001$, RANK targeting groups vs. controls with no treatment).

RANK expression in cultures compared with untreated osteoclasts (Figure 2.1C). Additionally, in the presence of RANKL, small osteoclasts continued to fuse into larger ones in control cultures (Figure 2.1D), while in RANK siRNA-treated cultures (Figure 2.1E), the speed of cell fusion was suppressed after treatment, and the osteoclast size was smaller than those in controls. RANK expression knockdown by multiple serial RANK and non-targeting siRNA transfections of RAW cells were tested using qPCR analysis (Figure 2.1F). Serial transfections were performed every other day. mRNA was extracted on Day 3 (single siRNA transfection on Day 1), Day 5 (double siRNA transfections on Day 1 and 3), Day 7 (three siRNA transfections on Day 1, 3, and 5) and Day 9 (four siRNA transfections on Day 1, 3, 5, and 7), respectively. Compared to control (no treatment) groups, RANK siRNA-2 significantly suppressed RANK expression in all four situations ($p < 0.001$). There was no significant difference between the control groups and the non-targeting siRNA groups on RANK expression for one ($p = 0.2$), two ($p = 0.49$), three ($p = 0.23$), or four ($p = 0.51$) serial transfections, indicating that DF4 had no significant effect on expression of RANK in the absence of specific siRNA. In addition, compared with non-targeting siRNA transfections, the RANK siRNA-2 groups showed significant reduction of RANK expression for all four dosing situations: one ($p = 0.00163$), two ($p = 0.0007$), three ($p = 0.0056$), and four ($p = 0.0049$) serial siRNA transfections ($p < 0.01$). RANK protein expression was detected by Western blotting after single and multiple transfections, respectively. For a single transfection, RANK protein was at most suppressed 3 days posttransfection and then began to recover (Figure 2.2A). Multiple transfections were performed in two ways. First, RAW cells were transfected successively daily in the first 3 culture days (Day 1 to Day 3). Protein was harvested on Day 5, 6 and 7. RANK
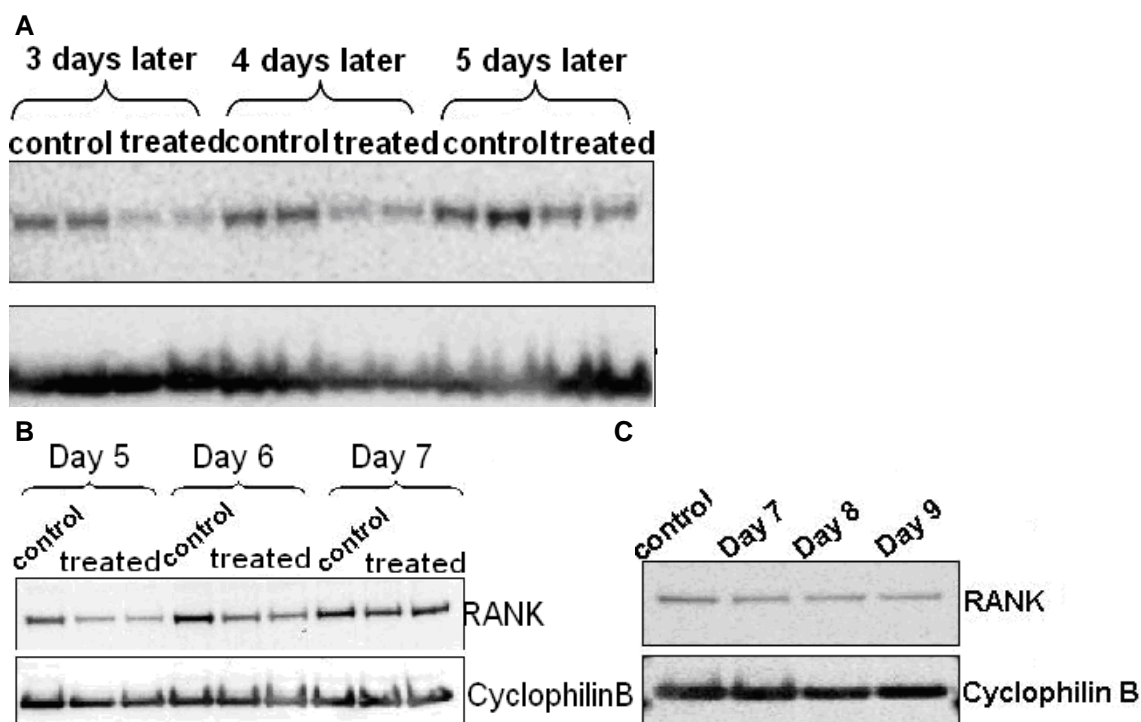
Figure 2.2 Western blot analysis of RANK protein knockdown in RAW cell cultures. Western blotting analyzed 30µg of cell lysate per sample. (A) Protein was harvested at 3, 4, and 5 days after single RANK siRNA-2 transfection. (B) RANK protein expression after three successive RANK siRNA-2 transfections. Protein was harvested on Day 5, 6, and 7. (C) RANK protein expression after three serial RANK siRNA-2 transfections on Day 1, 3 and 5. Protein was harvested on Day 7, 8 and 9.

knockdown was maintained until Day 6 and then started to return from Day 7 (Figure 2.2B).

Second, RAW cells were transfected three times serially but on every other day (Day 1, 3 and 5), and protein was harvested from Day 7 to Day 9. Figure 2.2C clearly shows that protein knockdown effects could be prolonged until Day 9 with serial transfections.

Effects of RANK siRNA on osteoclast formation and pit resorption in RAW cells. RAW cells were transfected with RANK siRNA or non-targeting siRNA in complete media with 100ng/ml RANKL. For each siRNA, cells were dosed either once (Day 1), or three times serially on alternate days (Day 1, 3, and 5). To evaluate osteoclast formation, TRAP assay was performed on Day 7.

Results are summarized in Figure 2.3F. Both controls with no siRNA exposure (Figure 2.3A) and cells treated with non-targeting siRNA (single transfection, Figure 2.3B; three transfections, Figure 2.3C) showed strongly TRAP-positive multinucleate giant cells. Compared to controls, both single-(Figure 2.3D, p=0.007) and three-dose transfections with RANK siRNA (Figure 2.3E, p=0.00015) showed significant reductions in numbers of TRAP-positive multinucleate cells in culture. There was no significant difference in the number of osteoclasts between controls and the single non-targeting siRNA transfection groups (p=0.17). Although three serial non-targeting transfections exert some influence on osteoclast formation by the transfection reagent (p=0.042), comparisons between three serial transfections of non-targeting versus RANK siRNA show that osteoclast numbers were significantly reduced in the RANK siRNA-treated groups (p<0.001). The same trend exists for comparisons between single transfections of non-targeting versus RANK targeting siRNAs (p=0.017). Three-dose RANK siRNA transfection groups showed reduced osteoclast numbers compared with single dose groups, but not significantly different (p=0.13). Resorption pit assay was performed 6 days postsingle transfection. Formation of resorption pits on bone slices was markedly curtailed in the siRNA-treated groups (Figure 2.3G, p=0.02) compared to controls (no treatment) that displayed many pits formed by osteoclasts.

   Effects of siRNA on RANK mRNA and protein expression in primary BMC cultures. To ensure that RANK siRNA-2 retained the most powerful knockdown effects, differences in siRNA knockdown for the 4 different RANK siRNAs were tested on primary BMC cultures in serum media. RT-PCR results clearly demonstrated that RANK siRNA-2 was the most efficient at down-regulating BMC RANK mRNA expression (Figure 2.4A). Therefore, RANK siRNA-2 was
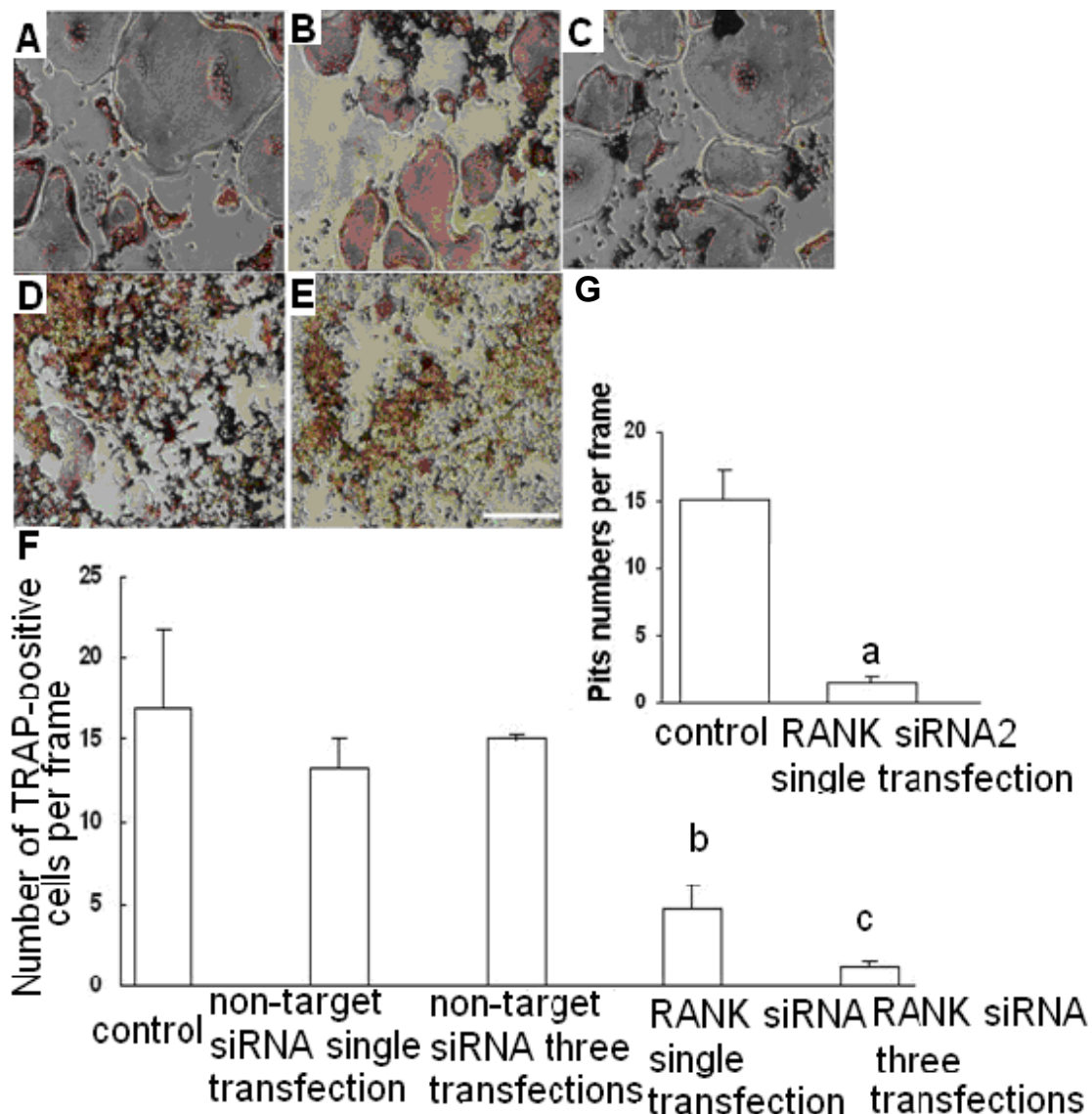
Figure 2.3   Effects of RANK siRNA and non-targeting siRNA on osteoclast formation determined by TRAP assay in RAW cell cultures. Cultures were performed in the presence of RANKL (A) with no siRNA treatment for positive controls, (B) transfected with non-targeting siRNA once on Day 1, (C) transfected with non-targeting siRNA three times serially every other day, (D) transfected with RANK siRNA once on Day 1, (E) three times serially every other day. (F) Comparison of the number of TRAP-positive multinucleate cells formed after siRNA dosing. ([b]$p<0.01$, [c]$p<0.001$, RANK siRNA-2 single and three transfection groups vs. controls). (scale bar = 250μm) Inhibition of osteoclast-mediate bone resorption by RANK siRNA was evaluated by pit formation assay. (G) Difference of resorption pit numbers per frame (10X magnification) between RANK siRNA untreated and treated RAW cells ([a]$p<0.05$).
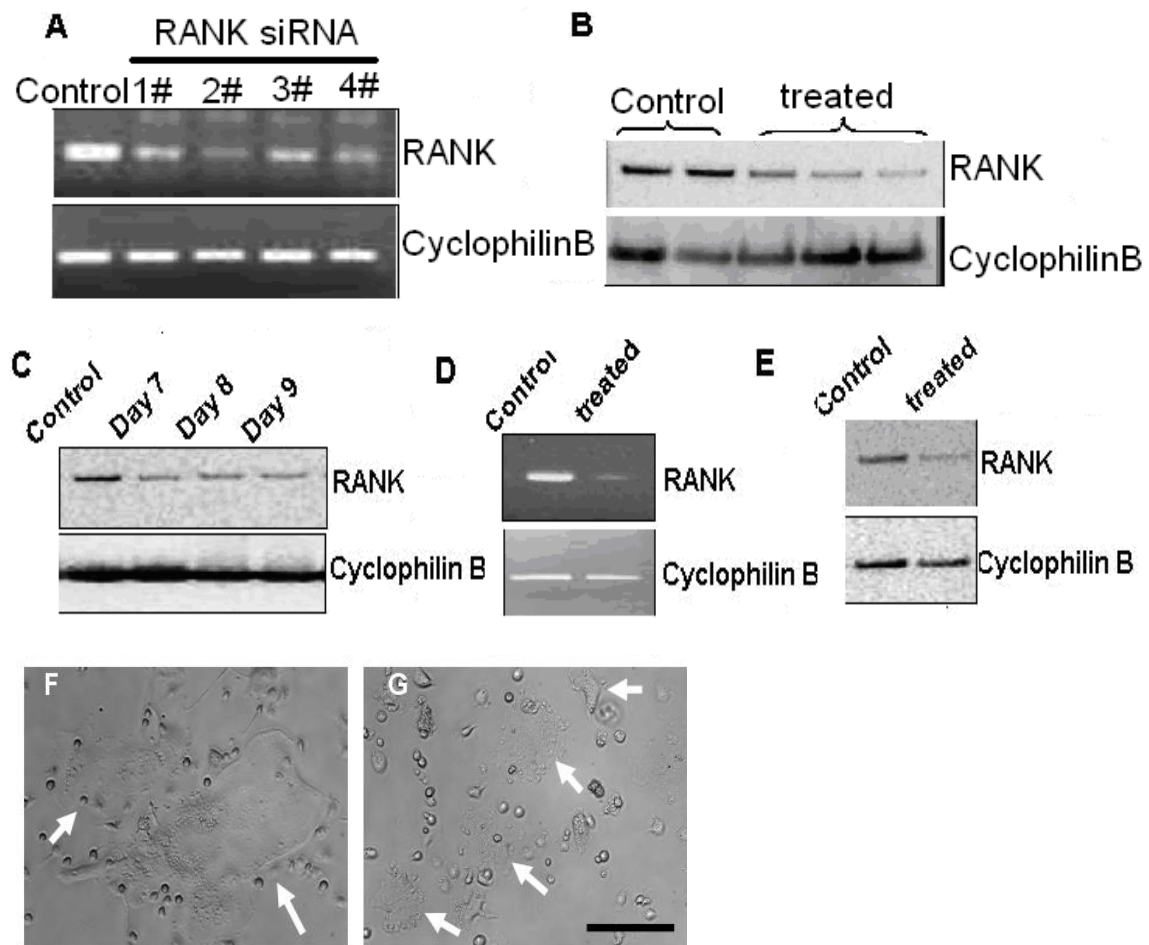
Figure 2.4 RANK knockdown by RANK siRNA dosing to primary BMC and BMC-derived osteoclasts in serum-based culture. RNA was harvested 48 hours posttransfection. Protein was harvested 3 days posttransfection, except from the mature osteoclasts, the RNA was 48 hours posttransfection. Western blotting analyzed 30µg of cell lysate per sample. (A) Four RANK siRNAs were analyzed by RT-PCR for the greatest knockdown effect. (B) Lysates analyzed by Western blot for RANK protein expression suppression by a single dose of RANK siRNA. (C) RANK protein expression after three serial siRNA transfections on every other day. Protein was harvested on Day 7, 8, and 9. (D) Inhibition of target RANK gene expression in primary cell-induced osteoclasts at the mRNA and protein level as shown by PCR (D) and Western blot (E). Representative images of primary BMC-derived osteoclasts (arrows) after 48-hours knockdown by RANK siRNA (G) compared with controls (F). (10X magnification)

used for subsequent transfections in primary BMCs. Consistently, RANK protein production was reduced both by single siRNA transfection (Figure 2.4B) and three serial transfections on alternate days (Figure 2.4C). Furthermore, RANK siRNA transfection was also able to suppress RANK message expression in primary BMC-induced mature osteoclasts. PCR products showed significantly reduced RANK mRNA expression in osteoclast cultures after single transfection (Figure 2.4D), as well as reduced RANK protein expression by Western blot assay (Figure 2.4E). Similarly to RAW cell cultures, BMC-induced osteoclasts had reduced rates of cell fusion after transfection (Figure 2.4G) compared to large osteoclasts formed in control cultures (Figure 2.4F).

Effects of RANK siRNA in primary BMC cultures

TRAP assays were performed on Day 5 cell cultures for single siRNA transfections. Compared with controls (Figure 2.5B), significant reductions in numbers of TRAP-positive multinucleate giant cells posttransfection (Figure 2.5C, p=0.001) were observed. Results are summarized in Figure 2.5A. Primary osteoclast precursor cells were cultured on bovine bone slices. Resorption pit assay was performed on Day 5 for single transfections. Controls without siRNA treatment produced abundant resorption pits on bone slices as detected by microscopy (4X magnification). RANK siRNA treatment inhibited osteoclastic bone resorption with significant reductions in resorption pit numbers (Figure 2.5D, p=0.04).

Discussion

We provide evidence that siRNA delivered to cells in serum-containing media can successfully and specifically inhibit RANK expression both in osteoclast precursors and mature
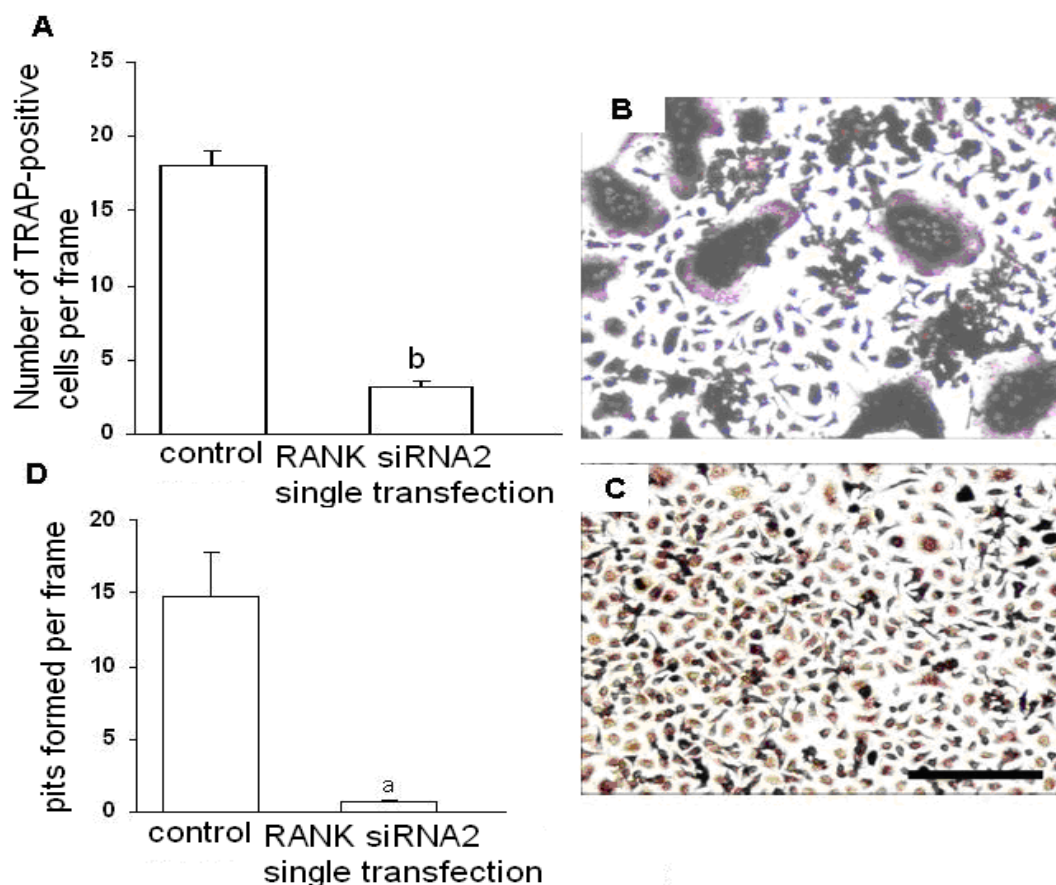
Figure 2.5   Inhibition of primary cell-induced osteoclast formation and activity by RANK siRNA. (A) Inhibition of osteoclast formation by a single RANK siRNA dose (Day 1). TRAP assay was performed on Day 5 ([b]$p<0.01$). Resorption pit assay was performed on same day. Representative image of TRAP-stained cells in (B) control groups with no treatment, and (C) treated groups with single siRNA dose. (D) Comparison of average pit number for cell-treated bovine bone slices per frame (4X magnification) between controls (no treatment) and single dose of RANK siRNA-2 ([a]$p<0.05$). (scale bar = 250μm).

osteoclasts from RAW secondary and primary BMC. This results in suppression of cell-based bone resorption mechanisms by reducing the number and activity of osteoclasts in cultures.

RANK plays an essential role in regulating osteoclastogenesis.[33] Activation of RANK by its ligand, RANKL, is required for the formation and activation of osteoclasts.[12, 15] Similar to RANK, OPG can also bind RANKL to act as a competitive inhibitor by blocking RANK interaction.[17, 34, 35] Since the elucidation of the RANK/RANKL/OPG signaling pathways, RANKL and OPG have been

actively investigated as therapeutic targets. Several OPG-based approaches to regulate bone mass and reduce bone resorption have been reported in animal models [17, 18, 36] and in a human trial.[37] However, reliable delivery of a large protein therapeutic poses several challenges, including limited stability, relevant dosing and bioavailability (short half-life), possible host immune responses to recombinant products, patient compliance (parenteral requirements) and complex formulating issues for sustained protein release.[38-40] A fully human monoclonal antibody targeting RANKL, denosumab, is currently investigated as a subcutaneous injection in late-stage clinical development for bone metabolic therapies.[41-43] Possible safety issues of this anti-RANKL antibody regard cross-reactions with OPG or RANK-activated endogenous antibodies. Therefore, other therapeutic options are necessary. RNAi is an alternative approach to RANK and RANKL control in this same context. In this approach, siRNA molecules silence gene expression in a sequence-specific manner by causing degradation of corresponding endogenous mRNA.[20, 44, 45] In fact, complete absence of either RANKL or RANK (as shown in RANKL and RANK knockout mice) eliminates RANKL-RANK signaling between osteoblasts and immature osteoclasts.[12, 15] This depletes functioning mature osteoclasts, removes intrinsic bone deposition control mechanisms and eventually causes osteopetrosis in these knockout mutants. Therefore, due to these concerns as well as other side effects (i.e., targeting undesired cell populations expressing RANK, and general nonspecific targeting), site- and temporally selective, as well as reversible control over RANK-RANKL activity, rather than its complete, irreversible abolition, is considered more appealing for developing new clinical approaches to osteoporosis therapies. In this study, siRNA targeting RANK was transfected into serum-based secondary macrophage cultures,

primary monocyte-macrophage cultures, and culture-generated osteoclasts to observe RANK

mRNA knockdown and suppression of protein expression. While RNAi has noted issues with

mammalian cell delivery efficiency and specific targeting,[46] one advantage of siRNA in the context

of RANK is the transient gene knock-down experienced (5~6 days, depending on the target, cell

type and frequency of target protein expression typical to that cell) with relatively small amounts of

siRNA dosed. This provides an alternative control feature for RANK suppression in cells compared

to mutants completely lacking RANK or protein-based systemic antagonism approaches.

Additionally, clinical osteoporosis bone augmentation approaches [47, 48] permit local placement of

siRNA-releasing carriers directly into osteoporotic sites by injection, permitting renewable, local

siRNA delivery to bone RANK at these sites and avoiding systemic delivery issues. As osteoclasts

central to both bone metabolic control and RANK presentation derive from fusions of

haematopoietically sourced circulating cells and tissue-resident differentiated macrophages,

assessing and comparing the utility of siRNA knockdown effects in both secondary and primary

macrophage cultures was considered an important milestone. Immortalized commercial

RAW264.7 monocyte-macrophages are commonly cultured as macrophage surrogates despite

the general lack of reporting of phenotypic indicators or fidelity to primary macrophages, and their

relatively high rates of contamination from commercial sources.[49] Some limitations with the

accuracy of RAW cell comparisons to primary macrophages in model assays have already been

noted.[27, 50] Aggressive endocytosis and proliferation rates in RAWs, characteristic of

tumor-derived cell lines, as well as higher frequency and intensity of both gene up-regulation and

protein expression, may all alter the intensity and duration of siRNA effects.[51] Nevertheless, as

RAW264.7 cells have been frequently used for in vitro generation of osteoclasts,[32, 52-54] this study compared RAW cells to primary BMC for effects of siRNA on osteoclast behavior.

RANK siRNA-2 provides the highest knockdown of the RANK mRNA for both RAW and primary BMC cultures. A dose of 125 nM RANK siRNA and the commercial cationic lipid transfection reagent, DF4 demonstrated successful inhibition of the target RANK gene expression at the mRNA level 48 hours after transfection in serum-based culture conditions. In addition, evidence indicates that RANK message knockdown is not caused by the transfection reagent, as there was no significant reduction of RANK mRNA expression in cells transfected with non-targeting siRNA/DF4 complexes. Moreover, the accumulating effects of multiple serial transfections were evaluated in RAW cells, showing sustained knockdown effects in serum-containing culture media. A likely explanation for the similar RANK knockdown effects observed with the three and four transfection cycles could be the increasing cell numbers by the third and fourth transfection cycles, diluting effects of constant siRNA dosing.

Protein expression analysis of both cell cultures further confirmed RANK knock-down using siRNA. In RAW cell cultures, with single transfections, RANK protein levels were suppressed after 3 days in culture. Subsequently, RANK protein production began to recover, due possibly to rapid cell proliferation and dilution of siRNA within cells. Multiple transfections (i.e., 3 serial doses) were performed, successively in the first 3 days or serially every other day throughout the culture period. In the latter case, RANK protein expression can be suppressed until Day 9. The same prolonged protein suppression was observed in BMCs as well, suggesting that changing the frequency of multiple siRNA transfections can extend protein knockdown. Therefore, serial siRNA transfections

performed every other day was considered more effective and hence used for multiple transfections in subsequent assays.

Since RANK also resides on mature osteoclasts and positively regulates osteoclast activation and survival, it was also important to target RANK on mature osteoclasts. We found that mature osteoclasts induced from both RAW and primary BMC cultures can be successfully transfected by siRNA, producing significant reductions in both RANK message and protein compared with untreated controls. In support of this, we found that in both secondary and primary cultures, after osteoclasts were transfected by RANK siRNA, further fusion was suppressed. This corresponds to a previous report showing that RANKL stimulation is essential for cell fusion of osteoclasts.[55] Large osteoclasts have much greater bone resorbing capability than small osteoclasts under same conditions,[32, 56, 57] therefore, the bone resorbing activity of osteoclasts is suppressed after RANK siRNA transfection at least in part by controlling osteoclast fusion and size. We further assessed RANK siRNA effects on osteoclast formation. In RAW cell cultures, osteoclast numbers were reduced significantly in both single and three serial RANK-siRNA treated groups. No significant changes were observed in the number of osteoclasts in single non-targeting siRNA-treated cultures compared with controls, consistent with minimal apoptosis and cell viability influences from transfection. Three serial transfections of non-targeting siRNA showed significant differences when compared to controls, though the average numbers were similar. A likely explanation may be a negative role played by the transfection reagent in multiple dosing. However, comparisons between three serial transfections of non-targeting siRNA and RANK siRNA showed significant differences in osteoclast number, which confirms the inhibition effects on osteoclast differentiation

by specific siRNA transfection. Though the average osteoclast number in three serially RANK siRNA transfected cell cultures was lower than that for single-dose groups, there was no significant difference within the 7 culture days, indicating that osteoclast formation is sensitive to RANK expression level and a single transfection at culture initiation is sufficient to inhibit both osteoclast formation and activity for a cycle of osteoclast formation in RAW cells. Hence, single doses of siRNA were applied for evaluation of effects on osteoclast bone-resorption activity. Similar results were obtained in primary BMC cultures; a single dose of RANK siRNA leads to a significant reduction in numbers of TRAP-positive cells. Furthermore, we have established that RANK siRNA is a potent inhibitor of osteoclast-mediated bone resorption, resulting in significant reduction of bone resorption pit number. Bone resorption activity was largely inhibited by RANK siRNA in both cultures. We attribute this in part to fewer osteoclasts formed, demonstrated by TRAP assay results, consistent with RANK mRNA and protein knockdown specific to siRNA introduction in monocyte-macrophage precursor and mature osteoclast serum-based cultures. All experiments with primary cells duplicated the results and conclusions from RAW cell cultures, confirming the general knockdown effect of RANK siRNA in these cell types in serum-based culture.

In summary, we conclude that siRNA can be successfully used to specifically inhibit RANK expression both in RAW and primary macrophage cell cultures, and also in osteoclast precursors and mature osteoclasts in serum-based transfections. Since RANK is an essential receptor in the membranes of both osteoclast precursors and osteoclasts and plays a key role in osteoclast formation and function, control of RANK has important fundamental and translational implications. The experimental results follow theoretical predictions: formation of osteoclasts is strongly

suppressed after siRNA treatment and the bone resorption pit numbers are largely reduced as well.

In addition, our analysis demonstrates that a single dose of RANK siRNA is sufficient to inhibit both osteoclast formation and activity for a cycle of osteoclast formation. These data suggest that siRNA against RANK could be a powerful tool for inhibiting osteoclast-mediated bone resorption and improving bone mass maintenance. Extensions of this concept to treatment of osteoporosis or low bone mass using siRNA administration could be interesting if reasonably RANK control at desired locations could be achieved.

Acknowledgements

References

1.   LaFleur, J.; McAdam-Marx, C.; Kirkness, C.; Brixner, D. I. Clinical risk factors for fracture in postmenopausal osteoporotic women: a review of the recent literature. *Ann Pharmacother* **2008,** 42, (3), 375-86.

2.   Lewiecki, E. M. Managing osteoporosis: challenges and strategies. *Cleve Clin J Med* **2009,** 76, (8), 457-66.

3.   Watts, N. B. Bone: bone density screening leads to reduced fracture risk. *Nat Rev Endocrinol* **2010,** 6, (1), 17-8.

4.   Ducy, P.; Schinke, T.; Karsenty, G. The osteoblast: a sophisticated fibroblast under central surveillance. *Science* **2000,** 289, (5484), 1501-4.

5.   Langston, A. L.; Ralston, S. H. Management of Paget's disease of bone. *Rheumatology*

(Oxford) **2004,** 43, (8), 955-9.

6.   NIH Consensus Development Panel on Osteoporosis Prevention, D., and Therapy. Osteoporosis prevention, diagnosis, and therapy. *Jama* **2001,** 285, (6), 785-95.

7.   Berenson, J. R. Treatment of hypercalcemia of malignancy with bisphosphonates. *Semin Oncol* **2002,** 29, (6 Suppl 21), 12-8.

8.   Coleman, R. E. Bisphosphonates: clinical experience. *Oncologist* **2004,** 9 Suppl 4, 14-27.

9.   Raisz, L. G. Physiology and pathophysiology of bone remodeling. *Clin Chem* **1999,** 45, (8 Pt 2), 1353-8.

10.   Corral, D. A.; Amling, M.; Priemel, M.; Loyer, E.; Fuchs, S.; Ducy, P.; Baron, R.; Karsenty, G. Dissociation between bone resorption and bone formation in osteopenic transgenic mice. *Proc Natl Acad Sci U S A* **1998,** 95, (23), 13835-40.

11.   Dougall, W. C.; Glaccum, M.; Charrier, K.; Rohrbach, K.; Brasel, K.; De Smedt, T.; Daro, E.; Smith, J.; Tometsko, M. E.; Maliszewski, C. R.; Armstrong, A.; Shen, V.; Bain, S.; Cosman, D.; Anderson, D.; Morrissey, P. J.; Peschon, J. J.; Schuh, J. RANK is essential for osteoclast and lymph node development. *Genes Dev* **1999,** 13, (18), 2412-24.

12.   Li, J.; Sarosi, I.; Yan, X. Q.; Morony, S.; Capparelli, C.; Tan, H. L.; McCabe, S.; Elliott, R.; Scully, S.; Van, G.; Kaufman, S.; Juan, S. C.; Sun, Y.; Tarpley, J.; Martin, L.; Christensen, K.; McCabe, J.; Kostenuik, P.; Hsu, H.; Fletcher, F.; Dunstan, C. R.; Lacey, D. L.; Boyle, W. J. RANK is the intrinsic hematopoietic cell surface receptor that controls osteoclastogenesis and regulation of bone mass and calcium metabolism. *Proc Natl Acad Sci U S A* **2000,** 97, (4), 1566-71.

13.   Lacey, D. L.; Tan, H. L.; Lu, J.; Kaufman, S.; Van, G.; Qiu, W.; Rattan, A.; Scully, S.; Fletcher, F.; Juan, T.; Kelley, M.; Burgess, T. L.; Boyle, W. J.; Polverino, A. J. Osteoprotegerin ligand modulates murine osteoclast survival in vitro and in vivo. *Am J Pathol* **2000,** 157, (2), 435-48.

14.   Jochum, W.; David, J. P.; Elliott, C.; Wutz, A.; Plenk, H., Jr.; Matsuo, K.; Wagner, E. F. Increased bone formation and osteosclerosis in mice overexpressing the transcription factor Fra-1. *Nat Med* **2000,** 6, (9), 980-4.

15. Kong, Y. Y.; Yoshida, H.; Sarosi, I.; Tan, H. L.; Timms, E.; Capparelli, C.; Morony, S.; Oliveira-dos-Santos, A. J.; Van, G.; Itie, A.; Khoo, W.; Wakeham, A.; Dunstan, C. R.; Lacey, D. L.; Mak, T. W.; Boyle, W. J.; Penninger, J. M. OPGL is a key regulator of osteoclastogenesis, lymphocyte development and lymph-node organogenesis. *Nature* **1999,** 397, (6717), 315-23.

16. Lomaga, M. A.; Yeh, W. C.; Sarosi, I.; Duncan, G. S.; Furlonger, C.; Ho, A.; Morony, S.; Capparelli, C.; Van, G.; Kaufman, S.; van der Heiden, A.; Itie, A.; Wakeham, A.; Khoo, W.; Sasaki, T.; Cao, Z.; Penninger, J. M.; Paige, C. J.; Lacey, D. L.; Dunstan, C. R.; Boyle, W. J.; Goeddel, D. V.; Mak, T. W. TRAF6 deficiency results in osteopetrosis and defective interleukin-1, CD40, and LPS signaling. *Genes Dev* **1999,** 13, (8), 1015-24.

17. Simonet, W. S.; Lacey, D. L.; Dunstan, C. R.; Kelley, M.; Chang, M. S.; Luthy, R.; Nguyen, H. Q.; Wooden, S.; Bennett, L.; Boone, T.; Shimamoto, G.; DeRose, M.; Elliott, R.; Colombero, A.; Tan, H. L.; Trail, G.; Sullivan, J.; Davy, E.; Bucay, N.; Renshaw-Gegg, L.; Hughes, T. M.; Hill, D.; Pattison, W.; Campbell, P.; Sander, S.; Van, G.; Tarpley, J.; Derby, P.; Lee, R.; Boyle, W. J. Osteoprotegerin: a novel secreted protein involved in the regulation of bone density. *Cell* **1997,** 89, (2), 309-19.

18. Akatsu, T.; Murakami, T.; Nishikawa, M.; Ono, K.; Shinomiya, N.; Tsuda, E.; Mochizuki, S.; Yamaguchi, K.; Kinosaki, M.; Higashio, K.; Yamamoto, M.; Motoyoshi, K.; Nagata, N. Osteoclastogenesis inhibitory factor suppresses osteoclast survival by interfering in the interaction of stromal cells with osteoclast. *Biochem Biophys Res Commun* **1998,** 250, (2), 229-34.

19. Emery, J. G.; McDonnell, P.; Burke, M. B.; Deen, K. C.; Lyn, S.; Silverman, C.; Dul, E.; Appelbaum, E. R.; Eichman, C.; DiPrinzio, R.; Dodds, R. A.; James, I. E.; Rosenberg, M.; Lee, J. C.; Young, P. R. Osteoprotegerin is a receptor for the cytotoxic ligand TRAIL. *J Biol Chem* **1998,** 273, (23), 14363-7.

20. Fire, A.; Xu, S.; Montgomery, M. K.; Kostas, S. A.; Driver, S. E.; Mello, C. C. Potent and specific genetic interference by double-stranded RNA in Caenorhabditis elegans. *Nature* **1998,** 391, (6669), 806-11.

21. Aagaard, L.; Rossi, J. J. RNAi therapeutics: principles, prospects and challenges. *Adv Drug Deliv Rev* **2007,** 59, (2-3), 75-86.

22. Woodrow, K. A.; Cu, Y.; Booth, C. J.; Saucier-Sawyer, J. K.; Wood, M. J.; Saltzman, W. M. Intravaginal gene silencing using biodegradable polymer nanoparticles densely loaded with small-interfering RNA. *Nat Mater* **2009,** 8, (6), 526-33.

23. Reich, S. J.; Fosnot, J.; Kuroki, A.; Tang, W.; Yang, X.; Maguire, A. M.; Bennett, J.; Tolentino, M. J. Small interfering RNA (siRNA) targeting VEGF effectively inhibits ocular neovascularization in a mouse model. *Mol Vis* **2003,** 9, 210-6.

24. Takanashi, M.; Oikawa, K.; Sudo, K.; Tanaka, M.; Fujita, K.; Ishikawa, A.; Nakae, S.; Kaspar, R. L.; Matsuzaki, M.; Kudo, M.; Kuroda, M. Therapeutic silencing of an endogenous gene by siRNA cream in an arthritis model mouse. *Gene Ther* **2009,** 16, (8), 982-9.

25. Massaro, D.; Massaro, G. D.; Clerch, L. B. Noninvasive delivery of small inhibitory RNA and other reagents to pulmonary alveoli in mice. *Am J Physiol Lung Cell Mol Physiol* **2004,** 287, (5), L1066-70.

26. Thakker, D. R.; Natt, F.; Husken, D.; Maier, R.; Muller, M.; van der Putten, H.; Hoyer, D.; Cryan, J. F. Neurochemical and behavioral consequences of widespread gene knockdown in the adult mouse brain by using nonviral RNA interference. *Proc Natl Acad Sci U S A* **2004,** 101, (49), 17270-5.

27. Chamberlain, L. M.; Godek, M. L.; Gonzalez-Juarrero, M.; Grainger, D. W. Phenotypic non-equivalence of murine (monocyte-) macrophage cells in biomaterial and inflammatory models. *J Biomed Mater Res A* **2009,** 88, (4), 858-71.

28. Takami, M.; Kim, N.; Rho, J.; Choi, Y. Stimulation by toll-like receptors inhibits osteoclast differentiation. *J Immunol* **2002,** 169, (3), 1516-23.

29. Wang, Y.; Lebowitz, D.; Sun, C.; Thang, H.; Grynpas, M. D.; Glogauer, M. Identifying the relative contributions of Rac1 and Rac2 to osteoclastogenesis. *J Bone Miner Res* **2008,** 23, (2), 260-70.

30. Lambrinoudaki, I.; Christodoulakos, G.; Botsis, D. Bisphosphonates. *Ann N Y Acad Sci* **2006,** 1092, 397-402.

31. Hausler, K. D.; Horwood, N. J.; Chuman, Y.; Fisher, J. L.; Ellis, J.; Martin, T. J.; Rubin, J. S.; Gillespie, M. T. Secreted frizzled-related protein-1 inhibits RANKL-dependent osteoclast formation. *J Bone Miner Res* **2004,** 19, (11), 1873-81.

32. Trebec, D. P.; Chandra, D.; Gramoun, A.; Li, K.; Heersche, J. N.; Manolson, M. F. Increased expression of activating factors in large osteoclasts could explain their excessive activity in osteolytic diseases. *J Cell Biochem* **2007,** 101, (1), 205-20.

33. Nakagawa, N.; Kinosaki, M.; Yamaguchi, K.; Shima, N.; Yasuda, H.; Yano, K.; Morinaga, T.; Higashio, K. RANK is the essential signaling receptor for osteoclast differentiation factor in osteoclastogenesis. *Biochem Biophys Res Commun* **1998,** 253, (2), 395-400.

34. Boyle, W. J.; Simonet, W. S.; Lacey, D. L. Osteoclast differentiation and activation. *Nature* **2003,** 423, (6937), 337-42.

35. Suda, T.; Takahashi, N.; Udagawa, N.; Jimi, E.; Gillespie, M. T.; Martin, T. J. Modulation of osteoclast differentiation and function by the new members of the tumor necrosis factor receptor and ligand families. *Endocr Rev* **1999,** 20, (3), 345-57.

36. Kostenuik, P. J.; Capparelli, C.; Morony, S.; Adamu, S.; Shimamoto, G.; Shen, V.; Lacey, D. L.; Dunstan, C. R. OPG and PTH-(1-34) have additive effects on bone density and mechanical strength in osteopenic ovariectomized rats. *Endocrinology* **2001,** 142, (10), 4295-304.

37. Bekker, P. J.; Holloway, D.; Nakanishi, A.; Arrighi, M.; Leese, P. T.; Dunstan, C. R. The effect of a single dose of osteoprotegerin in postmenopausal women. *J Bone Miner Res* **2001,** 16, (2), 348-60.

38. Breimer, D. D. Future challenges for drug delivery. *J Control Release* **1999,** 62, (1-2), 3-6.

39. DeFelippis, M. R.; Chance, R. E.; Frank, B. H. Insulin self-association and the relationship to pharmacokinetics and pharmacodynamics. *Crit Rev Ther Drug Carrier Syst* **2001,** 18, (2), 201-64.

40. Akers, M. J., DeFelippis, M.R., Peptides and proteins as parenteral solutions. In *Pharmaceutical Formulation Development of Peptides and Proteins*., ed.; Frokjaer, S., Hovgaard, L., 'Ed.'^'Eds.' Taylor & Francis: London, 2000; 'Vol.' p^pp 145-177.

41. Miller, P. D. Denosumab: anti-RANKL antibody. *Curr Osteoporos Rep* **2009,** 7, (1), 18-22.

42. Lewiecki, E. M. Is denosumab better than alendronate in the treatment of osteoporosis? *Nat Clin Pract Rheumatol* **2009,** 5, (2), 72-3.

43. Gerstenfeld, L. C.; Sacks, D. J.; Pelis, M.; Mason, Z. D.; Graves, D. T.; Barrero, M.; Ominsky, M. S.; Kostenuik, P. J.; Morgan, E. F.; Einhorn, T. A. Comparison of Effects of the Bisphosphonate Alendronate Versus the RANKL Inhibitor Denosumab on Murine Fracture Healing. *J Bone Miner Res* **2009,** 24, (3), 196-208.

44. Almeida, R.; Allshire, R. C. RNA silencing and genome regulation. *Trends Cell Biol* **2005,** 15, (5), 251-8.

45. Myers, J. W.; Jones, J. T.; Meyer, T.; Ferrell, J. E., Jr. Recombinant Dicer efficiently converts large dsRNAs into siRNAs suitable for gene silencing. *Nat Biotechnol* **2003,** 21, (3), 324-8.

46. Kumar, L. D.; Clarke, A. R. Gene manipulation through the use of small interfering RNA (siRNA): from in vitro to in vivo applications. *Adv Drug Deliv Rev* **2007,** 59, (2-3), 87-100.

47. Bajammal, S. S.; Zlowodzki, M.; Lelwica, A.; Tornetta, P., 3rd; Einhorn, T. A.; Buckley, R.; Leighton, R.; Russell, T. A.; Larsson, S.; Bhandari, M. The use of calcium phosphate bone cement in fracture treatment. A meta-analysis of randomized trials. *J Bone Joint Surg Am* **2008,** 90, (6), 1186-96.

48. An, Y. H., *Internal Fixation in Osteoporotic Bone*. ed.; Thieme Medical Publishers: New York, 2002; 'Vol.' p 207-216.

49. Hughes, P.; Marshall, D.; Reid, Y.; Parkes, H.; Gelber, C. The costs of using unauthenticated, over-passaged cell lines: how much more data do we need? *Biotechniques* **2007,** 43, (5), 575, 577-8, 581-2 passim.

50. Godek, M. L.; Sampson, J. A.; Duchsherer, N. L.; McElwee, Q.; Grainger, D. W. Rho GTPase protein expression and activation in murine monocytes/macrophages is not modulated by model biomaterial surfaces in serum-containing in vitro cultures. *J Biomater Sci Polym Ed* **2006,** 17, (10), 1141-1158.

51. Bartlett, D. W.; Davis, M. E. Insights into the kinetics of siRNA-mediated gene silencing from live-cell and live-animal bioluminescent imaging. *Nucleic Acids Res* **2006,** 34, (1), 322-33.

52. Liu, X. H.; Kirschenbaum, A.; Yao, S.; Levine, A. C. Interactive effect of interleukin-6 and prostaglandin E2 on osteoclastogenesis via the OPG/RANKL/RANK system. *Ann N Y Acad Sci* **2006,** 1068, 225-33.

53. Hsu, H.; Lacey, D. L.; Dunstan, C. R.; Solovyev, I.; Colombero, A.; Timms, E.; Tan, H. L.; Elliott, G.; Kelley, M. J.; Sarosi, I.; Wang, L.; Xia, X. Z.; Elliott, R.; Chiu, L.; Black, T.; Scully, S.; Capparelli, C.; Morony, S.; Shimamoto, G.; Bass, M. B.; Boyle, W. J. Tumor necrosis factor receptor family member RANK mediates osteoclast differentiation and activation induced by osteoprotegerin ligand. *Proc Natl Acad Sci U S A* **1999,** 96, (7), 3540-5.

54. Manolson, M. F.; Yu, H.; Chen, W.; Yao, Y.; Li, K.; Lees, R. L.; Heersche, J. N. The a3 isoform of the 100-kDa V-ATPase subunit is highly but differentially expressed in large (>or=10 nuclei) and small (<or= nuclei) osteoclasts. *J Biol Chem* **2003,** 278, (49), 49271-8.

55. Iwasaki, R.; Ninomiya, K.; Miyamoto, K.; Suzuki, T.; Sato, Y.; Kawana, H.; Nakagawa, T.; Suda, T.; Miyamoto, T. Cell fusion in osteoclasts plays a critical role in controlling bone mass and osteoblastic activity. *Biochem Biophys Res Commun* **2008,** 377, (3), 899-904.

56. Lees, R. L.; Sabharwal, V. K.; Heersche, J. N. Resorptive state and cell size influence intracellular pH regulation in rabbit osteoclasts cultured on collagen-hydroxyapatite films. *Bone* **2001,** 28, (2), 187-94.

57. Lees RL, H. J. Differences in regulation of pH(i) in large (≥10 nuclei) and small (≤5 nuclei) osteoclasts. *Am J Cell Physiol* **2000,** 279, C751-C761.

CHAPTER 3

SMALL INTERFERING RNA KNOCKS DOWN THE MOLECULAR TARGET

OF ALENDRONATE, FARNESYL PYROPHOSPHATE SYNTHASE,

IN OSTEOCLAST AND OSTEOBLAST CULTURES

Abstract

Farnesyl pyrophosphate synthase (FPPS), an enzyme in the mevalonate pathway, is the inhibition target of alendronate, a potent FDA-approved nitrogen-containing bisphosphonate (N-BP) drug, at the molecular level. Alendronate not only inhibits osteoclasts, but also has been reported to positively affect osteoblasts. This study assesses the knockdown effects of siRNA targeting FPPS compared with alendronate in both osteoclast and osteoblast cultures. Primary murine bone marrow cell-induced osteoclasts and the preosteoblast MC3T3-E1 cell line were used to assess effects of anti-FPPS siRNA compared with alendronate. Results show that both FPPS mRNA message and protein knockdown in serum-based culture is correlated with reduced osteoclast viability. FPPS siRNA is more potent than 10µM alendronate, but less potent than 50µM alendronate on reducing osteoclast viability. Despite FPPS knockdown, no significant changes were observed in osteoblast proliferation. FPPS knockdown promotes osteoblast differentiation

significantly but not cell mineral deposition. However, compared with 50μM alendronate dosing,

FPPS siRNA does not exhibit cytotoxic effects on osteoblasts while producing significant effects on

ostoblast differentiation. Both siRNA and alendronate at tested concentrations do not have

significant effects on cultured osteoblast mineralization. Overall, results indicate that FPPS siRNA

could be useful for selectively inhibiting osteoclast-mediated bone resorption and improving bone

mass maintenance by influencing both osteoclasts and osteoblasts in distinct ways.

Introduction

Osteoporosis, a metabolic bone disease and leading cause of osteoporotic fragility fractures

in both men and women, is rapidly becoming a global healthcare crisis as average life expectancy

increases worldwide. It is defined as a disorder of calcium and phosphate metabolism

characterized by low bone mass and micro-architectural deterioration.[1] With decades of clinical

experience, bisphosphonates are the most used pharmacological approach to treat osteoporosis

currently,[2] due to their significant inhibition of osteoclast-mediated bone resorption.

Nitrogen-containing bisphosphonates (N-BPs) are more potent than their non-nitrogen-containing

bisphosphonate analogs in suppressing osteoclast activity. However, since "avascular

osteonecrosis" in patients receiving pamidronate (N-BP) therapy was first described by Marx in

2003,[3] their general side effects, including gastrointestinal irritation, bone/joint pain and jaw

osteonecrosis,[3-5] and their long half-life [6] have clouded their therapeutic efficacy. Furthermore, due

to their severe suppression of bone turnover,[7, 8] long-term bisphosphonate therapy can increase

the risk of fractures, such as atypical fracture as a potential complication which was first reported

in 2005.[9, 10] Therefore, designing an improved therapeutic that retains N-BPs' inhibition of bone

resorption with significant reductions in its side effects will be highly significant.

The major intracellular target of alendronate, one of the most potent N-BPs, is farnesyl

pyrophosphate (FPP) synthase (FPPS), a key enzyme in the mevalonate pathway.[11-15] The

mevalonate pathway is ubiquitous in mammalian cells, producing essential lipids including

cholesterol and isoprenoids that are critical for posttranslational prenylation of proteins regulating

cell apoptosis, such as Ras and Rho.[16, 17] FPPS catalyzes the synthesis of the C_{15} metabolite

farnesyl pyrophosphate (FPP) through the sequential condensation of isopentenyl pyrophosphate

(IPP), starting with dimethylallyl pyrophosphate (DMAPP) and then with the resultant geranyl

pyrophosphate (GPP). FPP is also used as the substrate to produce the C_{20} isoprenoid

geranylgeranyl pyrophosphate (GGPP). Both FPP and GGPP are required for posttranslational

prenylation of small GTPases. FPP is therefore an essential isoprenoid intermediate in the

mevalonate pathway required for the posttranslational prenylation of essential GTPase signaling

proteins.[18] Crystallography studies reveal that as potent inhibitors of osteoclastic activity,

alendronate competitively binds with FPPS in the GPP/DMAPP binding site and the

FPPS/alendronate complex can be further stabilized by binding with IPP.[13, 15] Down-regulation of

posttranslational prenylation of GTP-binding proteins results in perturbed cell activity and the

induction of osteoclast apoptosis.[19] However, interestingly, increasing evidence suggests that

these bisphosphonates also have an anabolic effect on osteoblasts. Specifically, N-BPs were

shown to induce human osteoblast differentiation and mineralization in culture by inhibiting the

mevalonate pathway.[20] Therefore, a therapeutic that avoids known side effects for N-BPs but

reliably suppresses FPPS to inhibit the mevalonate pathway in both osteoclasts and osteoblasts could increase bone formation in the control of osteoporosis.

RNAi is a potent therapeutic gene silencing tool to transiently knock down gene-specific mRNA expression levels by exploiting a natural intracellular cytoplasmic mRNA regulatory phenomenon in mammalian species.[21-23] Gene silencing using short interfering RNAs (siRNAs) has many potential therapeutic applications.[24] We therefore examined the potential of administering small interfering RNA (siRNA) to suppress N-BP's molecular target, FPPS, in both osteoclasts and osteoblasts in vitro and compared its effects with the clinically familiar N-BP, alendronate. Ostoclasts were obtained from murine primary bone marrow monocytes.[25, 26] The preosteoblastic cell line MC3T3-E1 was used since it has been widely exploited as a culture model for osteoblast differentiation.[27] Expression levels of FPPS message and protein are monitored after siRNA transfections. Osteoclast viability and osteoblast proliferation, differentiation and mineral deposition posttransfections in serum culture were evaluated.

<u>Materials and Methods</u>

In vitro experimental data

<u>Primary murine cell harvest and differentiation.</u>   C57BL/6 male mice (6-8-week-old, Jackson Labs) were maintained in a specific pathogen-free facility at the University of Utah. All procedures were performed as approved by the Institutional Animal Care and Use Committee of University of Utah. Bone marrow cells (BMCs) were harvested from murine tibias and femurs of C57BL/6 male mice and differentiated into osteoclast precursors using previously described methods.[25, 26, 28]

Briefly, BMCs were cultured in α-MEM (Gibco) containing 10% heat-inactivated fetal bovine serum (FBS, Hyclone®, UT) and 1% penicillin-streptomycin (Gibco) overnight at a density of 1×10^6 cells/ml, defined for all cell cultures as "complete media". Nonadherent cells were harvested the next day and immediately seeded into 24-well tissue culture plates in complete media with 30 ng/ml M-CSF (R&D Systems) at a density of 1×10^6 cells per well. After 2 days of culture, adherent cells were used as osteoclast precursors. To generate osteoclasts, these precursor cells were incubated in 200ng/ml RANKL and 30ng/ml M-CSF (R&D Systems) in complete media, refreshed every other day. RANKL working concentrations to reliably generate osteoclasts from primary cell cultures in serum media were experimentally determined. Mature osteoclasts, distinguished by multinucleated, large cell bodies were purified essentially as described elsewhere by gently washing with PBS without Ca^{2+} and Mg^{2+} (Gibco).[26, 29] It usually took 5 days incubation for at least 80% of the plate remains to be covered with osteoclasts. By tapping the plate, most mononuclear cells were detached and removed, while multinucleated osteoclasts remained on the plate.

Osteoblast culture.   The immature osteoblast-like cell line MC3T3-E1 (subclone 4, ATCC, USA) cells were cultured at 4×10^4 cells/well in 24-well plates. To induce differentiation, cells were maintained in complete media with 50µg/ml ascorbic acid (AA, Sigma) and 10mM β-glycerophosphate (Sigma).[30] Media was refreshed every other day.

sRANKL expression.   A glutathione-S-transferase (GST)-tagged sRANKL construct was generated by cloning the murine sRANKL SalI/NotI fragment, coding 470-951 nucleotides, into the plasmid pGEX-4T-1 (a generous gift of Dr. M. F. Manolson, University of Toronto). The expressed protein was harvested as previously described.[25, 31, 32] GST-tagged sRANKL was purified by

Glutathione Sepharose 4B affinity resin (Amersham Pharmacia Biotech), dialyzed against phosphate buffered saline (PBS, Gibco) and concentrated using Amicon Ultra centrifuge tubes (Millipore). Protein concentration was determined by a BCA protein assay kit (Pierce).

siRNA transfection of osteoclasts and osteoblasts. Four ON-TARGETplus siRNAs all designed to target murine FPPS, (Target sequences: siRNA1, 5'-GUC AAG UAC AAG ACG GCUU-3'; siRNA2, 5'-GAA AAG AGG UAC AAA UCGA-3'; siRNA3, 5'-AGA AAG UGA CCC CGG AAUU-3'; siRNA4, 5'-CCU AGA GUA CAA UGC CUUA-3'), and a non-targeting control siRNA (sense: 5'-UAG CGA CUA AAC ACA UCA AUU-3', antisense: 5'-UUA UCG CUG AUU UGU GUA GUU-3') were purchased from Dharmacon (USA). DharmaFECT 4 (DF4, Dharmacon) was used as the cationic lipid cell transfection reagent in complete media. Mature osteoclasts were prepared as described above, residual monocytes were removed from culture, and siRNA transfection was immediately performed. Transfection reagent DF4 and siRNA were prepared according to manufacturer's instructions (Dharmacon). Final dosing concentrations of all siRNAs provided to each well were 125nM in a total volume of 1.0 microliter DF4. Cell uptake of siRNA complexes was performed by incubating cells with siRNA complexes in complete media with 30ng/ml M-CSF and 200ng/ml RANKL at 37°C with 5% CO_2. Nonspecific knockdown from DF4 transfection was assessed by using non-targeting siRNA dosed under identical conditions. Multiple repeated siRNA cell transfections were performed on alternating days as specified in each figure legend.

MC3T3-E1 cells were cultured at 4×10^4 cells/well in 24-well plates in complete media overnight. Transfections were performed early the next day. Final dosing concentrations of all siRNAs provided to each well were identical to osteoclasts. Cell uptake of siRNA complexes was

performed by incubating the cells with siRNA complexes in complete media with 50µg/ml AA and

10mM β-glycerophosphate at 37℃ with 5% CO_2.

Reverse transcriptase-polymerase chain reaction (RT-PCR). Total cellular RNA was isolated

from each well at different time points after siRNA transfection using an RNeasy Mini Kit (Qiagen).

Up to 4 micrograms of RNA were used to make cDNA with the SuperScript III 1st strand RT kit for

PCR (Invitrogen). PCR primers were designed for FPPS (5'-TGC TGG TAT CAG AAG CCA GGC

ATA-3', 5'-TGC TGG TAT CAG AAG CCA GGC ATA-3') and cyclophilin B (housekeeping control,

5'- AGC GCT TCC CAG ATG AGA ACT TCA-3', 5'-GCA ATG GCA AAG GGT TTC TCC ACT-3')

using Primerquest software and purchased from Integrated DNA Technologies (IDT). PCR was

performed by routine methods described previously.[33]

Western immunoblot assay. The assay was performed as described previously.[33] Briefly,

cells were lysed and protein concentration was measured using a BCA protein assay kit (Pierce).

Heat-denatured samples were separated on 4-12% SDS-polyacrylamide gels (Invitrogen) and

blotted on PVDF filters (Bio-Rad). The filter was incubated overnight in primary antibody human

antimouse FPPS (HCA012, AbD SeroTec) in 5% BSA/TBST. Then the membrane was incubated

with goat antihuman IgG (0500-0099, AbD SeroTec). The housekeeping control was detected with

antibody against cyclophilin B (PA1-027; Affinity BioReagents) and HRP-conjugated donkey

antirabbit antibody (SA1-200, Affinity BioReagents). Secondary antibodies were detected with

chemiluminescence reagent (Santa Cruz Biotechnology) and band images were captured using a

Molecular Imager Gel Doc XR System (Bio-Rad).

Cell viability. The relative number of viable osteoclasts or osteoblasts in each well was

determined using the Cell Titer 96 Aqueous One Solution Cell Proliferation Assay (Promega, WI, USA). To terminate culture, media was replaced with 300µl/well of fresh complete media with the addition of 60µl of Cell Titer 96 Aqueous One Solution, including three wells containing only media for background subtraction. Cells were then incubated at 37°C with 5% CO_2 for 2 hours and optical absorbance at 490nm was then determined using a plate reader (TECAN GENIOS Plus).

Alkaline phosphatase activity. To evaluate the differentiation of MC3T3-E1 cells, alkaline phosphatase (ALP) activity was determined. MC3T3-E1 cells were seeded at 4×10^4 cells/well in 24-well plate and transfected with siRNA or incubated with complete media containing various concentrations of alendronate (gift from Prof. J. Kopecek, University of Utah). ALP activity was determined using a QuantiChromTM Alkaline Phosphatase Assay Kit (BioAssay Systems, CA). Alkaline phosphatase activity values were normalized to the relative number of viable cells as determined directly using the above-mentioned cell proliferation assay.

Cell mineralization. The degree of mineralization of cultured MC3T3-E1 cells was determined using Alizarin red staining,[20] sensitive to the identification of cell calcification in vitro. Briefly, media was aspirated and the cells were rinsed twice with PBS. Then cells were fixed with ice-cold 70% (v/v) ethanol for 1 hour. Ethanol was removed and the cells were then stained with 2% Alizarin Red S (Sigma) in deionized water (pH 4.2) for half an hour at room temperature. The staining solution was removed and the cells were rinsed five times with deionized water. After removing the water, cells were incubated in PBS for 15 minutes at room temperature on a shaker. After PBS was removed, the cells were rinsed with PBS again. Dye destaining was performed by incubating the cells with 10% (w/v) cetylpyridinium chloride in 10mM sodium phosphate (pH 7)

washing buffer at room temperature. The washing buffer was then transferred to a 96-well plate and the optical absorbance at 562 nm was measured using a plate reader (TECAN GENIOS Plus). The concentration of Alizarin Red S in the wash buffer was determined according to Alizarin Red S standards. Mineralization values were normalized to the relative number of viable cells determined by using Cell Titer 96 Aqueous One Solution Cell Proliferation Assay as described above. Mineralization produced in culture after triplicate serial siRNA transfections was measured the day following the last transfection.

Statistical analysis.   MTT, ALP and mineralization results are reported as mean ± standard deviation relative to control. Significance is determined using the two-tailed Student's t-test with Bonferroni corrections. All experiments were repeated three times.

Results

In vitro knockdown effects

Successful FPPS message and protein knockdown in both osteoclast and osteoblast cultures. Since this study's focus was not on assessing transfection efficiency but rather on assessing posttransfection knockdown of target, the established commercial cationic cell transfection surfactant, DharmaFECT 4 (DF4), was used for siRNA transfection based on its frequency of successful use and manufacturer's instructions claiming it "appropriate" for mouse and rat cell lines. Importantly, siRNA transfections were all performed in serum-containing media to avoid serum-free media-induced cell stress. Each siRNA sequence was tested individually for effectiveness to knock down FPPS expression in osteoclasts in complete media. siRNA-2

produced the greatest overall knockdown effect from the commercial library, and therefore, was used for all further siRNA transfections of both osteoclast and osteoblast cultures. Nonspecific knockdown of FPPS target by DF4, evaluated using non-targeting siRNA and DF4 in both cultures, is not significant by PCR analysis (Figure 3.1). Significant down-regulation of FPPS gene and protein expression was observed in osteoclast cultures (Figure 3.1A,C). Since all assays on osteoblasts were performed 5 days posttransfection, gene and protein expression levels were monitored prior to this on Days 2 to 5. Treatment of osteoblasts with FPPS siRNA-2 also significantly suppressed FPPS message expression in cultures until Day 4 when cell assays were performed, compared to untreated and non-targeting siRNA-transfected osteoblasts (Figure 3.1B).
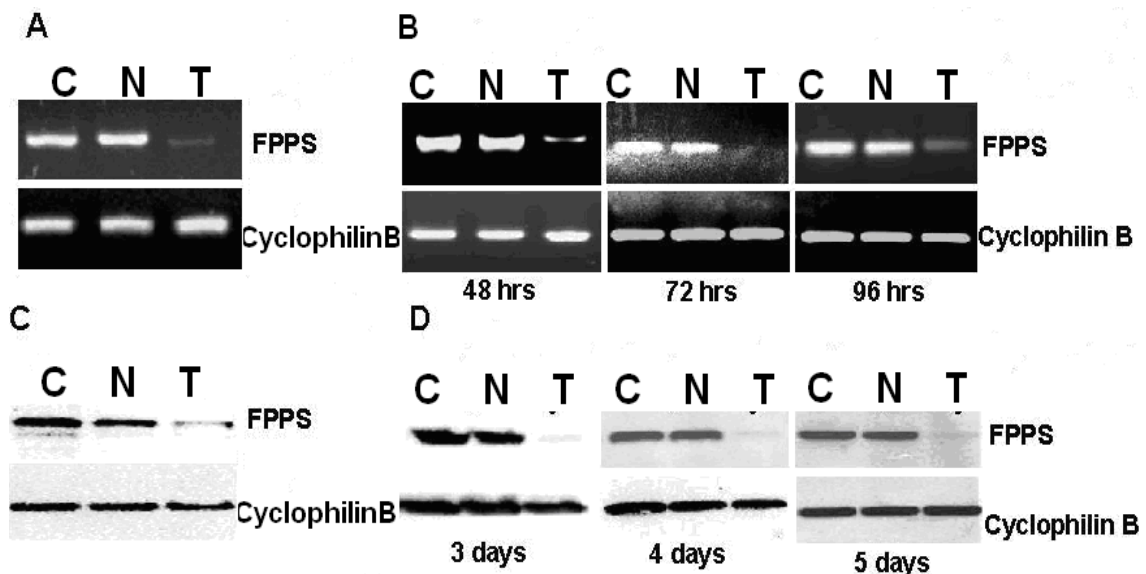

Figure 3.1 Successful FPPS message and protein knockdown in both osteoclast and osteoblast cultures. FPPS message knockdown by FPPS siRNA in (A) osteoclast culture 48 hours posttransfection and (B) osteoblast culture 48 to 96 hours postsingle transfection compared with untreated cells and cells transfected with non-targeting siRNA. Inhibition of target FPPS gene expression at the mRNA level is shown by PCR. FPPS protein knockdown by FPPS siRNA in (C) osteoclast 3 days postsingle transfection and (D) osteoblast cultures 3 to 5 days posttransfection compared with untreated cells and cells transfected with non-targeting siRNA. Protein expression was evaluated by Western blotting. (C, control; N, non-targeting siRNA; T, FPPS siRNA)

Significantly, sustained down-regulation of FPPS protein expression was also observed 5 days posttransfection (Figure 3.1D).

Comparison of FPPS siRNA and alendronate on osteoclast cytotoxicity. Osteoclast viability assays were performed 3 days after siRNA transfections in serum-based cultures. Osteoclasts numbers were significantly reduced in FPPS siRNA-treated groups compared with control groups (70.3% of the control, *p=0.03, Figure 3.2A). Compared with non-targeting siRNA which showed 98.4% viability of the untreated control, FPPS siRNA significantly suppressed viability (*p=0.015), indicating that reduced cell viability results from specific FPPS gene knockdown, but not from nonspecific effects of siRNA or transfection reagent dosing. Osteoclasts were treated with alendronate at two different concentrations (10µM and 50µM). After 3-day culture, (the same duration as siRNA transfection), cell viability was reduced to 95.5% (*p=0.025) in the 10µM
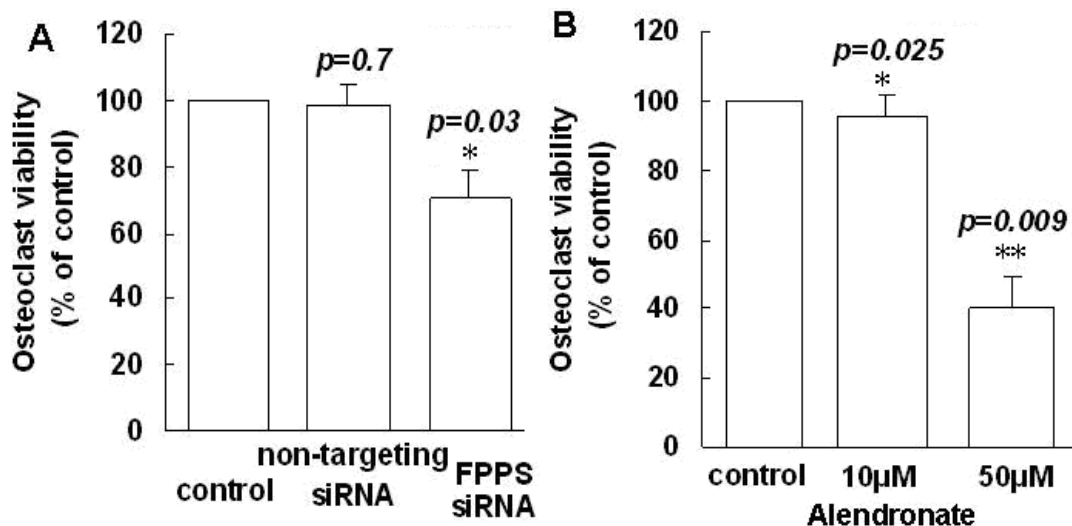

Figure 3.2 Both FPPS siRNA and alendronate reduce osteoclast cell viability. Cytotoxicity was determined using the Cell Titer 96 Aqueous One Solution Cell Proliferation assay. (A) Cultured osteoclast viability comparing non-targeting siRNA and FPPS siRNA 3 days posttransfection. (B) osteoclast viability compared for 10µM and 50µM alendronate 3 days postdosing to cultures (p values shown are obtained by comparing each group with controls, n=3).

alendronate-treated group and to 40.3% (**p=0.009) in the 50µM alendronate-treated group. Both

cell viability decreases are significant compared with control (Figure 3.2B).

Comparison of FPPS siRNA and alendronate treatments on MC3T3-E1 preosteoblast cell

proliferation.   FPPS siRNA and alendronate effects on MC3T3-E1 preosteoblast cell proliferation

were compared 5 days posttreatment. As shown in Figure 3.3A, FPPS siRNA had little effect on

cell proliferation (95.9% of the control) compared with nontreated control groups, as well as

non-targeting siRNA-treated groups (103.7% of the control). Furthermore, there is no significant

difference between FPPS siRNA and non-targeting siRNA groups (p=0.55). For alendronate, three

different concentrations (10µM, 50µM and 100µM) were initially used. The 100µM alendronate

dose showed significant evidence of cell death (>90%), a likely result of bisphosphonate toxicity,
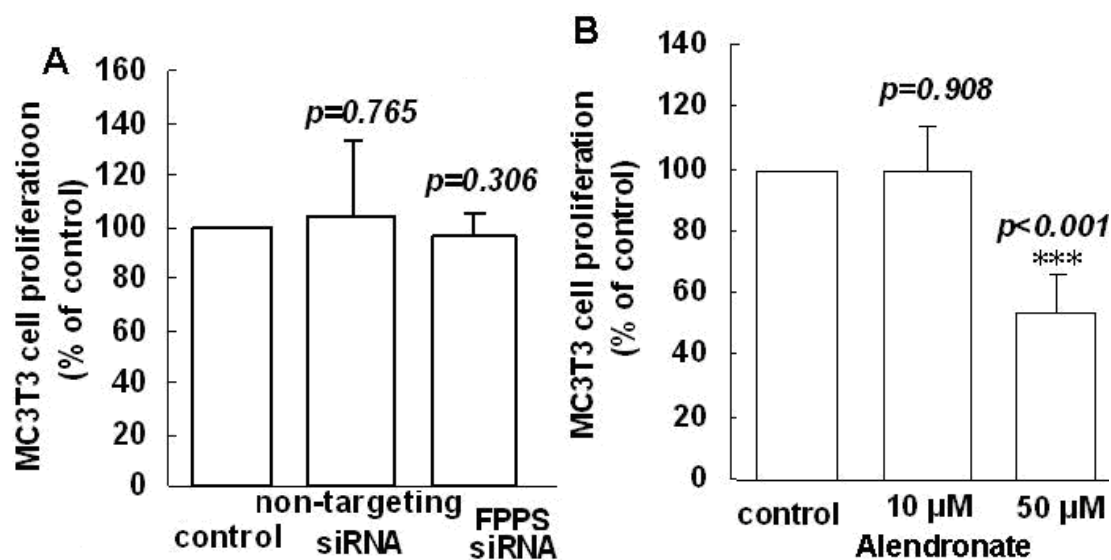

Figure 3.3 FPPS siRNA is not as potent as alendronate (50µM) on reducing cultured MC3T3-E1 pre-osteoblast cell proliferation. Cell proliferation was determined using the Cell Titer 96 Aqueous One Solution Cell Proliferation assay. (A) osteoblast viability comparing non-targeting siRNA and FPPS siRNA 5 days postsingle transfection in serum-based cultures. (B) The comparison of osteoblast viability compared for 10µM and 50µM alendronate 5 days postdosing to cultures. (p values shown are obtained by comparing each group with controls, n=3).

and this concentration was not continued. Compared with nontreated controls, there is no

significant inhibition of cell proliferation at 10µM (Figure 3.3B, p=0.908), but when alendronate's

concentration increased to 50µM, cell viability is reduced to 54% compared to control (Figure 3.3B,

***p<0.001). There is also a significant difference in cell viability between the 50µM and 10µM

groups (***p<0.001).

Comparison of FPPS siRNA and alendronate treatments on MC3T3-E1 preosteoblast cell

differentiation and mineralization.   MC3T3-E1 pre-osteoblast cell differentiation was detected by

measuring ALP activity. After 5-day culture, the effects of non-targeting siRNA, FPPS siRNA and

alendronate (10µM and 50µM) on MC3T3 cell differentiation were compared. As shown in Figure

3.4A, non-targeting siRNA had no effect on osteoblastic differentiation compared with control

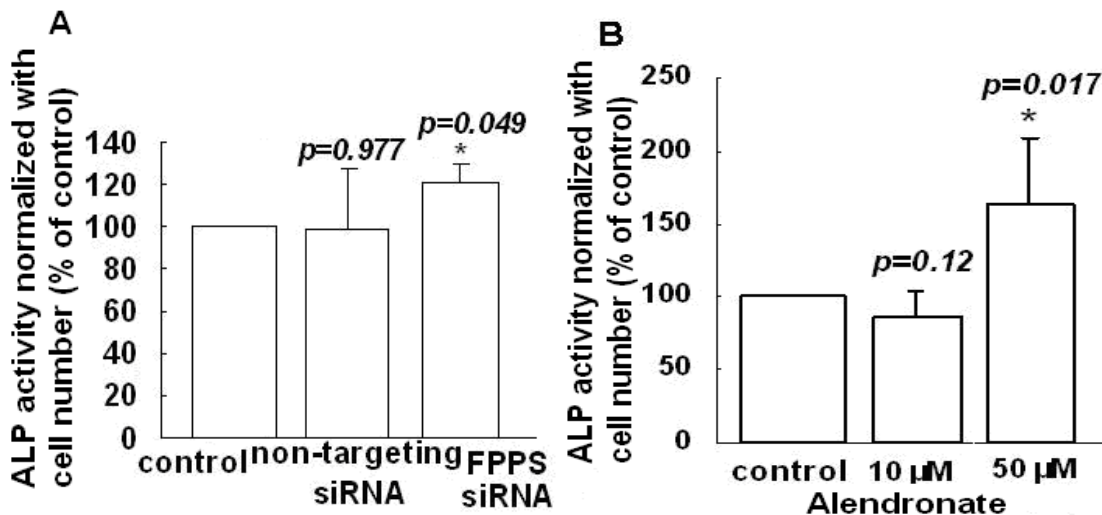(99.5%, p=0.977). However, FPPS siRNA treatment increased cell ALP activity and showed a

**Figure 3.4 Both FPPS siRNA and alendronate (50µM) significantly increase ALP activity
during MC3T3-E1 pre-osteoblast differentation.** Cell differentiation was monitored by measuring
ALP activity. (A) osteoblast ALP activity compared for non-targeting siRNA and FPPS siRNA 5 days
postsingle transfection in serum-containing cultures. (B) osteoblast ALP activity compared for 10µM
and 50µM alendronate 5 days postdosing to cultures (p values shown are obtained by comparing
each group to controls, (n=3).

significant 21% increase compared to nontreated control groups (*p=0.049). When alendronate

concentration was 10µM, cell ALP activity was reduced to 85.9% compared to control, but was not

significant (p=0.12). However, 50µM alendronate treatment significantly increased cell ALP activity

to 164% (*p=0.017).

Full comparison of these effects on cell mineralization among non-targeting siRNA, FPPS

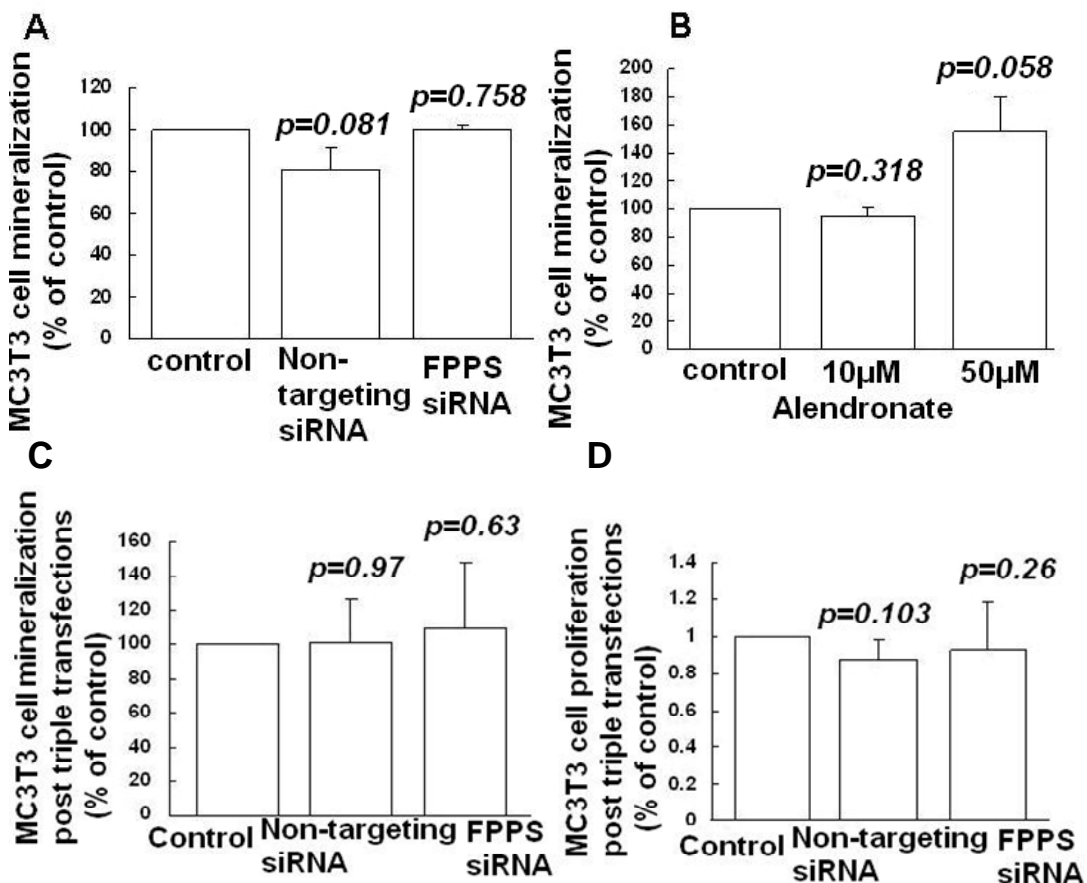siRNA and alendronate (10µM and 50µM) is summarized in Figure 3.5. Non-targeting siRNA

Figure 3.5 Neither FPPS siRNA nor alendronate significantly affect MC3T3-E1 pre-osteoblast cell mineralization. (A) osteoblast mineral deposition compared for non-targeting siRNA and FPPS siRNA 5 days postsingle transfection, and (C) posttriple transfections in serum-based cultures; (B) osteoblast mineral deposition compared for 10µM and 50µM alendronate 5 days postdosing to cultures. (D) osteoblast proliferation after triplicate non-targeting and FPPS siRNA transfections (p values shown are obtained by comparing each group to controls, n=3).

reduced MC3T3 cell mineralization to 81% of control (p=0.081). FPPS siRNA of single dose had

no significant effect on cell mineralization (99.5%, p=0.758) after 5-day culture compared with

control (p value between non-targeting siRNA and FPPS siRNA groups is 0.078). There is no

significant influence of 10μM alendronate on cell mineralization (95.3%, p=0.318). However, 50μM

alendronate increased cell mineralization to 155.5% compared to controls (p=0.058). Cell

mineralization under triplicate FPPS siRNA transfections on every other day showed 9.98%

increase compared with control (not significantly different). Triplicate non-targeting siRNA

transfection showed only 0.51% increase compared with control (Figure 3.5C). In addition, both

non-targeting and FPPS siRNA (single and triple dosing) have no observed influence on

osteoblast proliferation (Figure 3.5D).

<div align="center">Discussion</div>

Bisphosphonates are potent inhibitors of bone resorption and widely used in clinic to treat

postmenopausal osteoporosis. However, more attention has been drawn recently to their side

effects, such as bisphosphonate-associated osteonecrosis and their long half-life that complicates

fracture healing.[7] Inhibition of FPPS in the mevalonate pathway has been implicated as the

mechanism of action for select N-BPs at the molecular level in both osteoclasts and

osteoblasts.[11-13, 20, 34] Osteoclasts and osteoblasts are closely correlated with each other; therefore,

in our study, use of siRNA to knock down FPPS expression in both osteoclasts and osteoblasts

was examined and compared with N-BP alendronate. Alendronate is one of the most potent

FDA-approved N-BPs,[35] commonly prescribed for the treatment and prevention of osteoporosis.

Actual dosing ranges of alendronate to which bone cells are exposed under pharmacological conditions are unknown. Many studies have shown that bisphosphonate affects cells in a dose-dependent manner in cultures.[20, 36, 37] We therefore employed three alendronate concentrations (10μM, 50μM and 100μM) in cell cultures. Alendronate at 100μM concentration significantly reduced cell viability in both cell types, consistent with the observation of Im et al.[38] who showed inhibited cellular proliferation when alendronate was used at 100μM. We chose alendronate working concentration within the range of 10-100μM since significant effects on cells have been observed in other studies.[20, 36, 37, 39]

FPPS siRNA-2 provides the highest knockdown of FPPS mRNA in primary BMC cultures in our preliminary studies (data not shown) and was used for all experiments. A dose of 125nM siRNA and the commercial cationic lipid transfection reagent, DF4, demonstrated successful inhibition of both the target FPPS gene and protein expression 48 hours and 72 hours, respectively, after transfection in serum-based culture for osteoclasts. In osteoblast cultures, successfully sustained gene and protein knockdown were obtained up to 5 days posttransfections. In addition, evidence indicates that FPPS message knockdown is not caused by the transfection reagent, as there was no significant reduction of FPPS mRNA or protein expression in cells transfected with non-targeting siRNA/DF4 complexes.

Classically, the majority of reports regarding bisphosphonates have been focused on their effects on reducing osteoclast bone resorbing activities.[40-45] A variety of modes of drug action on osteoclasts have been explored. The present study focused on cytotoxic depletion of osteoclasts since both in vitro and in vivo studies provide evidence that bisphosphonates reduce osteoclast

numbers and activity.[43] FPPS siRNA showed significant inhibition on growth of cultured murine bone marrow cell-induced osteoclasts. This suppression is stronger than that from 10µM alendronate, but not as potent as that from alendronate at 50µM. Cell viability can be reduced to 40% by alendronate at 50µM compared with the nontreated control. FPPS siRNA effects on cell viability are less than expected based on the substantial mRNA and protein knockdown results, exhibiting about 30% reduction compared with control. A possible explanation for this could be intrinsic disproportionate relationships between cell viability and FPPS enzyme activity. Unlike other functional cell proteins, e.g., cell receptors where decreased protein expression leads to proportionate decreases in functions, enzymatic turn-over activity can remain significant despite relative knock-down, distinguishing functional differences between knockdown and knockout. Inhibition of the mevalonate pathway has been linked to bisphosphonate-induced apoptosis in macrophages and human myeloma cells in vitro.[46, 47] These reports suggest that reduced osteoclast viability results from FPPS siRNA-induced cell apoptosis by preventing protein prenylation in osteoclasts.

Except for the effect of bisphosphonate on osteoclast apoptosis, it was also reported to be able to inhibit osteoclast formation in long-term human marrow culture alone[40] or by acting on osteoblastic cells.[48] In addition, mevalonate pathway is essential for producing DMAPP and IPP which are involved in the biosynthesis of molecules for cell memebrane maintenance. Taken together, it would be interesting to further investigate the effects of FPPS siRNA on osteoclastogenesis and osteoclast podosome assembly and actin ring formation which play a critical role of osteoclastic bone resorption.

Increasing evidence showing that N-BPs directly affect osteoblast proliferation, differentiation

and mineralization [37, 49, 50] in ways distinct from those of osteoclasts prompted study of the role of

FPPS siRNA on the mevalonate pathway in MC3T3-E1 pre-osteoblast cells cultures. Changes in

MC3T3-E1 cell viability in response to FPPS siRNA addition to cultures was compared to single

alendronate treatments. As expected, non-targeting siRNA does not significantly influence cultured

cell proliferation compared with controls without any treatment. However, FPPS siRNA addition

does not significantly change cell proliferation compared with both control and non-targeting

siRNA. This suggests that FPPS knockdown is not sufficient to influence MC3T3-E1 viability within

5 days. No difference is observed on cell viability between cells without any treatment and those

treated with 10µM alendronate. However, when alendronate concentration increases to 50µM, cell

viability was inhibited dramatically. During culture, significant numbers of dead cells were not

evident, suggesting that the decreased cell viability results from suppression of cell proliferation,

but not cytotoxicity. This observation is not surprising since similar alendronate inhibition of cell

proliferation is also reported with human fetal osteoblast cells,[37] osteoclasts [43, 51] and primary

osteoblasts.[50, 52] Though some opposing effects have been reported,[38, 53, 54] this may be due to

variations in experiments, including cell types, culture duration, bisphosphonate analogue

chemistries and concentrations applied.

While FPPS siRNA did not influence osteoblast viability significantly, it increases total alkaline

phosphatase activity significantly compared with controls lacking any treatment. These

observations indicate that FPPS knockdown enhances osteoblast differentiation without affecting

cell proliferation. Stronger induction of alkaline phosphatase activity was obtained by treating these

cells with 50μM alendronate. These findings concur with those of a previous study suggesting that

bisphosphonates enhance osteoblast progression from the proliferation stage to the matrix

maturation stage.[37] However, culture mineralization was increased in MC3T3 cells treated with

50μM alendronate by 55.5%, nearly significant compared with control (p=0.058) and correlates

with previous reports[20] showing increased human fetal osteoblast cell mineralization by

pamidronate and zoledronate. Thus, N-BP alendronate augments cultured cell mineralization

within 5 days posttreatment. In contrast, for osteoblasts treated with siRNA, there is no significant

difference in mineralization between the control and non-targeting siRNA or FPPS siRNA after

single transfections. To investigate the possibility for disproportionate functional knockdown of cell

enzyme (ALP) activity, triplicate siRNA transfections dosed every other day were performed to

minimize FPPS expression during the subsequent cell assay period. While triplicate dosing of

non-targeting siRNA produces no observable effects on cell mineralization, multiple FPPS

transfections generate about 10% increase of cell mineralization compared with control. This

observed increase may suggest some small cell mineralization enhancement from FPPS

knockdown. However, FPPS knockdown did not enhance cell mineralization compared with

50μM alendronate. Although alendronate at 50μM can promote cell mineralization by 56%, this

effect is obscured by its severe suppression of cell proliferation. Cell mineral deposition by 50μM

alendronate in term of percentage of cell proliferation (mineralization%×proliferation%) is 84%

compared to the controls, while mineralization from FPPS single transfection is 95% and by triple

transfections is 101.7% of the controls. Overall, the effect of FPPS knockdown on cell

mineralization is not significant. Based on the siRNA results, the direct effect of FPPS changes on

cell mineralization is not clear. Osteoclasts and osteoblasts closely communicate and interact with each other in vivo to regulate bone remodeling. Bisphosphonates can act indirectly on osteoclasts through their action on osteoblast lineage cells.[39, 55-58] Therefore, further study is required to determine whether FPPS siRNA effects on osteoblasts seen in this study indirectly influence osteoclasts.

In summary, single-dose FPPS siRNA, unlike results obtained from osteoclast cultures, did not show any significant cytotoxicity in MC3T3-E1 preosteoblasts. Compared with 50µM alendronate which exhibits potent inhibition of cell viability, FPPS siRNA has much milder effects on cell proliferation. Both FPPS siRNA and 50µM alendronate can promote cell differentiation significantly, but FPPS siRNA increases ALP activity without significantly inhibiting cell proliferation. Within 5 days posttreatment, FPPS siRNA did not evidence an influence on cell mineral deposition.

<div align="center">Conclusions</div>

Significantly, to the best of our knowledge, this is the first report to knock down the molecular target of clinically common nitrogen-containing bisphosphonates using siRNA, and comparing these effects to alendronate, both on osteoclasts and osteoblasts in similar cultures. Results from both the culture of primary murine bone marrow cell-induced osteoclasts and MC3T3-E1 preosteoblast cells showed that FPPS siRNA suppresses osteoclast viability significantly, but with less potency than alendronate at 50µM. There is no observed effect of FPPS siRNA on osteoblast proliferation. However, osteoblast differentiation can be significantly increased by FPPS siRNA.

Both FPPS siRNA and alendronate show no significant effects on osteoblast mineral deposition. In summary, siRNA targeting FPPS has a beneficial effect at the cellular level of inhibiting excessive bone resorption and increasing overall bone mass maintenance by its effects on both osteoblasts and osteoclasts and suggest that it has clinical potential.

Acknowledgements

References

1.   NIH Consensus Development Panel on Osteoporosis Prevention, and Therapy. Osteoporosis prevention, diagnosis, and therapy. *Jama* **2001,** 285, (6), 785-95.

2.   Rogers, M. J.; Watts, D. J.; Russell, R. G. Overview of bisphosphonates. *Cancer* **1997,** 80, (8 Suppl), 1652-60.

3.   Marx, R. E. Pamidronate (Aredia) and zoledronate (Zometa) induced avascular necrosis of the jaws: a growing epidemic. *J Oral Maxillofac Surg* **2003,** 61, (9), 1115-7.

4.   Dodson, T. B.; Guralnick, W. C.; Donoff, R. B.; Kaban, L. B. Massachusetts General Hospital/Harvard Medical School MD oral and maxillofacial surgery program: a 30-year review. *J Oral Maxillofac Surg* **2004,** 62, (1), 62-5.

5.   Ruggiero, S. L.; Mehrotra, B.; Rosenberg, T. J.; Engroff, S. L. Osteonecrosis of the jaws associated with the use of bisphosphonates: a review of 63 cases. *J Oral Maxillofac Surg* **2004,** 62, (5), 527-34.

6.   Khan, S. A.; Kanis, J. A.; Vasikaran, S.; Kline, W. F.; Matuszewski, B. K.; McCloskey, E. V.; Beneton, M. N.; Gertz, B. J.; Sciberras, D. G.; Holland, S. D.; Orgee, J.; Coombes, G. M.; Rogers, S. R.; Porras, A. G. Elimination and biochemical responses to intravenous alendronate in postmenopausal osteoporosis. *J Bone Miner Res* **1997,** 12, (10), 1700-7.

7.	Yang, K. H.; Won, J. H.; Yoon, H. K.; Ryu, J. H.; Choo, K. S.; Kim, J. S. High concentrations of pamidronate in bone weaken the mechanical properties of intact femora in a rat model. *Yonsei Med J* **2007,** 48, (4), 653-8.

8.	Sebba, A. Osteoporosis: how long should we treat? *Curr Opin Endocrinol Diabetes Obes* **2008,** 15, (6), 502-7.

9.	Sellmeyer, D. E. Atypical fractures as a potential complication of long-term bisphosphonate therapy. *Jama* **2010,** 304, (13), 1480-4.

10.	Odvina, C. V.; Zerwekh, J. E.; Rao, D. S.; Maalouf, N.; Gottschalk, F. A.; Pak, C. Y. Severely suppressed bone turnover: a potential complication of alendronate therapy. *J Clin Endocrinol Metab* **2005,** 90, (3), 1294-301.

11.	van Beek, E.; Pieterman, E.; Cohen, L.; Lowik, C.; Papapoulos, S. Farnesyl pyrophosphate synthase is the molecular target of nitrogen-containing bisphosphonates. *Biochem Biophys Res Commun* **1999,** 264, (1), 108-11.

12.	Bergstrom, J. D.; Bostedor, R. G.; Masarachia, P. J.; Reszka, A. A.; Rodan, G. Alendronate is a specific, nanomolar inhibitor of farnesyl diphosphate synthase. *Arch Biochem Biophys* **2000,** 373, (1), 231-41.

13.	Kavanagh, K. L.; Guo, K.; Dunford, J. E.; Wu, X.; Knapp, S.; Ebetino, F. H.; Rogers, M. J.; Russell, R. G.; Oppermann, U. The molecular mechanism of nitrogen-containing bisphosphonates as antiosteoporosis drugs. *Proc Natl Acad Sci U S A* **2006,** 103, (20), 7829-34.

14.	Dunford, J. E.; Thompson, K.; Coxon, F. P.; Luckman, S. P.; Hahn, F. M.; Poulter, C. D.; Ebetino, F. H.; Rogers, M. J. Structure-activity relationships for inhibition of farnesyl diphosphate synthase in vitro and inhibition of bone resorption in vivo by nitrogen-containing bisphosphonates. *J Pharmacol Exp Ther* **2001,** 296, (2), 235-42.

15.	Rondeau, J. M.; Bitsch, F.; Bourgier, E.; Geiser, M.; Hemmig, R.; Kroemer, M.; Lehmann, S.; Ramage, P.; Rieffel, S.; Strauss, A.; Green, J. R.; Jahnke, W. Structural basis for the exceptional in vivo efficacy of bisphosphonate drugs. *ChemMedChem* **2006,** 1, (2), 267-73.

16.	Lacal, J. C. Regulation of proliferation and apoptosis by Ras and Rho GTPases through specific phospholipid-dependent signaling. *FEBS Lett* **1997,** 410, (1), 73-7.

17.	Constantz, B. R.; Ison, I. C.; Fulmer, M. T.; Poser, R. D.; Smith, S. T.; VanWagoner, M.; Ross, J.; Goldstein, S. A.; Jupiter, J. B.; Rosenthal, D. I. Skeletal repair by in situ formation of the mineral phase of bone. *Science* **1995,** 267, (5205), 1796-9.

18. Rogers, M. J. New insights into the molecular mechanisms of action of bisphosphonates. *Curr Pharm Des* **2003,** 9, (32), 2643-58.

19. Tenenbaum, H. C.; Shelemay, A.; Girard, B.; Zohar, R.; Fritz, P. C. Bisphosphonates and periodontics: potential applications for regulation of bone mass in the periodontium and other therapeutic/diagnostic uses. *J Periodontol* **2002,** 73, (7), 813-22.

20. Reinholz, G. G.; Getz, B.; Sanders, E. S.; Karpeisky, M. Y.; Padyukova, N.; Mikhailov, S. N.; Ingle, J. N.; Spelsberg, T. C. Distinct mechanisms of bisphosphonate action between osteoblasts and breast cancer cells: identity of a potent new bisphosphonate analogue. *Breast Cancer Res Treat* **2002,** 71, (3), 257-68.

21. Hammond, S. M.; Bernstein, E.; Beach, D.; Hannon, G. J. An RNA-directed nuclease mediates post-transcriptional gene silencing in Drosophila cells. *Nature* **2000,** 404, (6775), 293-6.

22. Calle, Y.; Jones, G. E.; Jagger, C.; Fuller, K.; Blundell, M. P.; Chow, J.; Chambers, T.; Thrasher, A. J. WASp deficiency in mice results in failure to form osteoclast sealing zones and defects in bone resorption. *Blood* **2004,** 103, (9), 3552-61.

23. Aigner, A. Delivery systems for the direct aplication of siRNAs to induce RNA interference (RNAi) in vivo. *J Biomed Biotechnol* **2006,** 2006, 1-15.

24. de Fougerolles, A.; Vornlocher, H. P.; Maraganore, J.; Lieberman, J. Interfering with disease: a progress report on siRNA-based therapeutics. *Nat Rev Drug Discov* **2007,** 6, (6), 443-53.

25. Wang, Y.; Lebowitz, D.; Sun, C.; Thang, H.; Grynpas, M. D.; Glogauer, M. Identifying the relative contributions of Rac1 and Rac2 to osteoclastogenesis. *J Bone Miner Res* **2008,** 23, (2), 260-70.

26. Takami, M.; Kim, N.; Rho, J.; Choi, Y. Stimulation by toll-like receptors inhibits osteoclast differentiation. *J Immunol* **2002,** 169, (3), 1516-23.

27. Issack, P. S.; Lauerman, M. H.; Helfet, D. L.; Doty, S. B.; Lane, J. M. Alendronate Inhibits PTH (1-34)-induced Bone Morphogenetic Protein Expression in MC3T3-E1 Preosteoblastic Cells. *Hss J* **2007,** 3, (2), 169-72.

28. Chamberlain, L. M.; Godek, M. L.; Gonzalez-Juarrero, M.; Grainger, D. W. Phenotypic non-equivalence of murine (monocyte-) macrophage cells in biomaterial and inflammatory models. *J Biomed Mater Res A* **2009,** 88, (4), 858-71.

29. Trebec, D. P.; Chandra, D.; Gramoun, A.; Li, K.; Heersche, J. N.; Manolson, M. F. Increased

expression of activating factors in large osteoclasts could explain their excessive activity in osteolytic diseases. *J Cell Biochem* **2007,** 101, (1), 205-20.

30.   Lee, Y. K.; Song, J.; Lee, S. B.; Kim, K. M.; Choi, S. H.; Kim, C. K.; LeGeros, R. Z.; Kim, K. N. Proliferation, differentiation, and calcification of preosteoblast-like MC3T3-E1 cells cultured onto noncrystalline calcium phosphate glass. *J Biomed Mater Res A* **2004,** 69, (1), 188-95.

31.   Lambrinoudaki, I.; Christodoulakos, G.; Botsis, D. Bisphosphonates. *Ann N Y Acad Sci* **2006,** 1092, 397-402.

32.   Hausler, K. D.; Horwood, N. J.; Chuman, Y.; Fisher, J. L.; Ellis, J.; Martin, T. J.; Rubin, J. S.; Gillespie, M. T. Secreted frizzled-related protein-1 inhibits RANKL-dependent osteoclast formation. *J Bone Miner Res* **2004,** 19, (11), 1873-81.

33. Wang, Y.; Grainger, D. W. siRNA knock-down of RANK signaling to control osteoclast-mediated bone resorption. *Pharm Res* **2010,** 27, (7), 1273-84.

34.   Naidu, A.; Dechow, P. C.; Spears, R.; Wright, J. M.; Kessler, H. P.; Opperman, L. A. The effects of bisphosphonates on osteoblasts in vitro. *Oral Surg Oral Med Oral Pathol Oral Radiol Endod* **2008,** 106, (1), 5-13.

35.   Sato, M.; Grasser, W.; Endo, N.; Akins, R.; Simmons, H.; Thompson, D. D.; Golub, E.; Rodan, G. A. Bisphosphonate action. Alendronate localization in rat bone and effects on osteoclast ultrastructure. *J Clin Invest* **1991,** 88, (6), 2095-105.

36. Kim, H. K.; Kim, J. H.; Abbas, A. A.; Yoon, T. R. Alendronate enhances osteogenic differentiation of bone marrow stromal cells: a preliminary study. *Clin Orthop Relat Res* **2009,** 467, (12), 3121-8.

37.   Reinholz, G. G.; Getz, B.; Pederson, L.; Sanders, E. S.; Subramaniam, M.; Ingle, J. N.; Spelsberg, T. C. Bisphosphonates directly regulate cell proliferation, differentiation, and gene expression in human osteoblasts. *Cancer Res* **2000,** 60, (21), 6001-7.

38.   Im, G. I.; Qureshi, S. A.; Kenney, J.; Rubash, H. E.; Shanbhag, A. S. Osteoblast proliferation and maturation by bisphosphonates. *Biomaterials* **2004,** 25, (18), 4105-15.

39.   Sahni, M.; Guenther, H. L.; Fleisch, H.; Collin, P.; Martin, T. J. Bisphosphonates act on rat bone resorption through the mediation of osteoblasts. *J Clin Invest* **1993,** 91, (5), 2004-11.

40.   Hughes, D. E.; MacDonald, B. R.; Russell, R. G.; Gowen, M. Inhibition of osteoclast-like cell formation by bisphosphonates in long-term cultures of human bone marrow. *J Clin Invest* **1989,** 83,

(6), 1930-5.

41. Cecchini, M. G.; Felix, R.; Fleisch, H.; Cooper, P. H. Effect of bisphosphonates on proliferation and viability of mouse bone marrow-derived macrophages. *J Bone Miner Res* **1987,** 2, (2), 135-42.

42. Lowik, C. W.; van der Pluijm, G.; van der Wee-Pals, L. J.; van Treslong-De Groot, H. B.; Bijvoet, O. L. Migration and phenotypic transformation of osteoclast precursors into mature osteoclasts: the effect of a bisphosphonate. *J Bone Miner Res* **1988,** 3, (2), 185-92.

43. Hughes, D. E.; Wright, K. R.; Uy, H. L.; Sasaki, A.; Yoneda, T.; Roodman, G. D.; Mundy, G. R.; Boyce, B. F. Bisphosphonates promote apoptosis in murine osteoclasts in vitro and in vivo. *J Bone Miner Res* **1995,** 10, (10), 1478-87.

44. Ito, M.; Amizuka, N.; Nakajima, T.; Ozawa, H. Ultrastructural and cytochemical studies on cell death of osteoclasts induced by bisphosphonate treatment. *Bone* **1999,** 25, (4), 447-52.

45. Fisher, J. E.; Rogers, M. J.; Halasy, J. M.; Luckman, S. P.; Hughes, D. E.; Masarachia, P. J.; Wesolowski, G.; Russell, R. G.; Rodan, G. A.; Reszka, A. A. Alendronate mechanism of action: geranylgeraniol, an intermediate in the mevalonate pathway, prevents inhibition of osteoclast formation, bone resorption, and kinase activation in vitro. *Proc Natl Acad Sci U S A* **1999,** 96, (1), 133-8.

46. Shipman, C. M.; Croucher, P. I.; Russell, R. G.; Helfrich, M. H.; Rogers, M. J. The bisphosphonate incadronate (YM175) causes apoptosis of human myeloma cells in vitro by inhibiting the mevalonate pathway. *Cancer Res* **1998,** 58, (23), 5294-7.

47. Luckman, S. P.; Hughes, D. E.; Coxon, F. P.; Graham, R.; Russell, G.; Rogers, M. J. Nitrogen-containing bisphosphonates inhibit the mevalonate pathway and prevent post-translational prenylation of GTP-binding proteins, including Ras. *J Bone Miner Res* **1998,** 13, (4), 581-9.

48. Nishikawa, M.; Akatsu, T.; Katayama, Y.; Yasutomo, Y.; Kado, S.; Kugal, N.; Yamamoto, M.; Nagata, N. Bisphosphonates act on osteoblastic cells and inhibit osteoclast formation in mouse marrow cultures. *Bone* **1996,** 18, (1), 9-14.

49. Giuliani, N.; Pedrazzoni, M.; Negri, G.; Passeri, G.; Impicciatore, M.; Girasole, G. Bisphosphonates stimulate formation of osteoblast precursors and mineralized nodules in murine and human bone marrow cultures in vitro and promote early osteoblastogenesis in young and aged mice in vivo. *Bone* **1998,** 22, (5), 455-61.

50. Garcia-Moreno, C.; Serrano, S.; Nacher, M.; Farre, M.; Diez, A.; Marinoso, M. L.; Carbonell, J.;

Mellibovsky, L.; Nogues, X.; Ballester, J.; Aubia, J. Effect of alendronate on cultured normal human osteoblasts. *Bone* **1998,** 22, (3), 233-9.

51. Reszka, A. A.; Halasy-Nagy, J. M.; Masarachia, P. J.; Rodan, G. A. Bisphosphonates act directly on the osteoclast to induce caspase cleavage of mst1 kinase during apoptosis. A link between inhibition of the mevalonate pathway and regulation of an apoptosis-promoting kinase. *J Biol Chem* **1999,** 274, (49), 34967-73.

52. Khokher, M. A.; Dandona, P. Diphosphonates inhibit human osteoblast secretion and proliferation. *Metabolism* **1989,** 38, (2), 184-7.

53. Klein, B. Y.; Ben-Bassat, H.; Breuer, E.; Solomon, V.; Golomb, G. Structurally different bisphosphonates exert opposing effects on alkaline phosphatase and mineralization in marrow osteoprogenitors. *J Cell Biochem* **1998,** 68, (2), 186-94.

54. Plotkin, L. I.; Weinstein, R. S.; Parfitt, A. M.; Roberson, P. K.; Manolagas, S. C.; Bellido, T. Prevention of osteocyte and osteoblast apoptosis by bisphosphonates and calcitonin. *J Clin Invest* **1999,** 104, (10), 1363-74.

55. Giuliani, N.; Pedrazzoni, M.; Passeri, G.; Girasole, G. Bisphosphonates inhibit IL-6 production by human osteoblast-like cells. *Scand J Rheumatol* **1998,** 27, (1), 38-41.

56. Vitte, C.; Fleisch, H.; Guenther, H. L. Bisphosphonates induce osteoblasts to secrete an inhibitor of osteoclast-mediated resorption. *Endocrinology* **1996,** 137, (6), 2324-33.

57. Pan, B.; Farrugia, A. N.; To, L. B.; Findlay, D. M.; Green, J.; Lynch, K.; Zannettino, A. C. The nitrogen-containing bisphosphonate, zoledronic acid, influences RANKL expression in human osteoblast-like cells by activating TNF-alpha converting enzyme (TACE). *J Bone Miner Res* **2004,** 19, (1), 147-54.

58. Viereck, V.; Emons, G.; Lauck, V.; Frosch, K. H.; Blaschke, S.; Grundker, C.; Hofbauer, L. C. Bisphosphonates pamidronate and zoledronic acid stimulate osteoprotegerin production by primary human osteoblasts. *Biochem Biophys Res Commun* **2002,** 291, (3), 680-6.

CHAPTER 4

LOCAL DELIVERY OF RANK SIRNA TO BONE USING INJECTABLE PLGA

MICROSPHERE/CALCIUM PHOSPHATE CEMENT

AUGMENTATION BIOMATERIALS

Abstract

This chapter describes design of a new delivery strategy for RNA interfering technology to knock down RANK and inhibit osteoclast formation and function. For this purpose, well-known resorbable polyester (PLGA) microparticles were utilized as a carrier to deliver RANK siRNA to both osteoclast precursors and osteoclasts. As natural phagocytes, osteoclast and osteoclast precursors should selectively internalize micron-sized particles versus most other non-targeted cells, producing a natural osteoclast and phagocyte cell targeting capability. PLGA-siRNA particles were dispersed into clinical-grade injectable calcium-based injectable bone cement, a clinically familiar biomaterial used in osteoporosis bone augmentation and fragility fracture fixation. SiRNA released from this formulation in vitro retains bioactivity against RANK in cultured osteoclast precursor cells, inhibiting their progression toward the osteoclastic phenotype without killing them. These data support the proof-of-concept to utilize a clinically relevant approach to improve fragility fracture healing in the context of osteoporosis by delivering functional siRNA directly to sites of osteoporosis from bone augmentation materials and fracture fixation hardware.

Introduction

Osteoporosis is a disease characterized by low bone density and quality, with a primary clinical presentation of hip, wrist and spine fractures, severely impairing patients' quality of life.[1] Such fragility fractures affect thousands of patients annually.[2] Most osteoporotic fractures require operative reduction and stabilization. Fracture healing processes in the context of ongoing osteoporosis pathology are especially difficult. Specifically, osteoporotic bone loss is a strong setback in healing prognosis. Low bone quality and excessive bone resorption decrease the mechanical strength necessary for acceptable, durable fracture healing. Fracture fixation is therefore employed with surgically implanted hardware and bone augmentation materials in osteoporotic fracture sites, and augmentation is increasingly used prophylactically at high-risk sites of potential fracture. Nonetheless, loosening occurs commonly around such implants, producing hardware "cut out", mandating fixation tooling removal and retarding fracture healing. After implantation, large numbers of differentiating osteoclast precursors in the form of monocyte macrophages are recruited to the peri-implant area, especially at the bone-implant interface.[3, 4] Their presence often correlates with enhanced bone resorption and osteoclastogenic activities. This reduced bone-implant interface area results in aseptic loosening and finally prosthetic failure.

Two cytokines -- RANK ligand (RANKL) and macrophage colony-stimulating factor (M-CSF) -- are essential for the process of osteoclastogenesis.[5, 6] RANKL is the key cytokine for promoting osteoclastogenesis. Interactions between RANKL and RANK receptor on the surface of osteoclast precursors are essential for expression of osteoclast-specific genes,[7] bone resorption and survival of mature osteoclasts.[8] Osteoclastogenesis is negatively regulated by osteoprotegerin (OPG),

which is also expressed by stromal cells and osteoblasts.[9] OPG is a decoy receptor that competes with RANK for binding RANKL.[10] In this RANKL/RANK/OPG axis, positive regulator RANKL and negative regulator OPG are coordinated through interaction with RANK on osteoclast precursor cells in bone sites to regulate normal bone formation and degradation.

Clinical approaches to improving bone quality in osteoporosis fixation include reinforcement of porous, weakened bones prior to fracture or device implantation (i.e., prophylaxis) by direct augmentation of bone around the fracture and fixation hardware using injected prosthetic bulking materials.[11-15] Bone augmentation using bone cement has already been investigated and widely used with vertebral fractures,[16] femur fractures,[17] humerus fractures,[18] and calcaneum fractures.[19] The technique utilizes various biomaterials, including polymethylmethacrylate (PMMA), calcium phosphate substitutes (as bone cements, shaped blocks, coatings), various bone grafts, and modified implants.[20] PMMA is commonly clinically used and shows acceptable compressive strength. However, recognized problems with PMMA hinder its applications. These include excessive heat generation during in situ polymerization, lack of quality control during in situ preparation, dense nondegrading foreign body, poor control of antibiotic release when drug-loaded and poor removal during revision surgeries.[21, 22] Studies show that often less than 50% of a drug load is bioavailable from PMMA injected in and around bone.[23, 24] Compared to PMMA, calcium phosphate cements (CPC) have several unique properties for bone, including intrinsic osteoconductivity (degradable by osteoclasts), osteoinductivity (infiltrated by osteoblasts and replaced with new bone), deployment as viscous setting fluid matrices by local injection and acceptable in situ biocompatibility.[25-27] Due to its relatively poor mechanical properties, CPC is

FDA-approved for treatment of nonloaded bone defects (i.e., generally craniomaxilofacial). In vivo

degradation of CPC-based cements can vary widely depending on formulation and chemistry,

induced by both passive physiologic dissolution and active cell-mediated phagocytosis.[28]

Individual CPC degradation rate depends on patients' metabolic health, anatomic site, age and

sex, as well as cement's chemistry, density, formulation, porosity, Powder/Liquid (P/L) ratio

(loading) and resulting particle size. The self-setting ability of CPC within the bone cavity enables it

to be used in an injectable formulation, which largely expands its utility.[29, 30] To date, substantial

experience supports the feasibility and value of using CPC as a drug carrier in bone augmentation.

Pharmacologically active molecules of diverse chemistries are readily distributed within the liquid

bone cement formulation prior to setting, making CPC a controlled drug release medium. Several

drugs have formulated for release from CPC, such as antibiotics to decrease postsurgical

infections,[31, 32] anticancer drugs to reduce tumorogenesis[33] and growth factors to promote bone

healing.[34] However, release rates of encapsulated drugs are limited since most CPC formulations

are dense monoliths and its in vivo resorption is very slow. To enhance release and CPC

degradation, soluble poragens can be incorporated into the CPC to more rapidly dissolve and

enhance CPC porosity and dissolution.[35] Additionally, degradable poly(lactic-co-glycolic acid)

(PLGA) particles are also used within the cement to deliberately introduce large macropores upon

their degradation, facilitating further active and passive in vivo degradation of cement and

enhancing bone in-growth at surgical sites.[25, 36] Furthermore, the resultant changes of CPC

handling properties and cement setting are maintained within desired workable ranges.[25] This

provides an opportunity to load both the CPC matrix and encapsulated PLGA particles with drug

loads for controlled release strategies from the injectable hybrid biomaterial.

PLGA is a well-studied degradable polymer long FDA-approved in microsphere and microparticle formulations for delivery of several human drugs.[37] Bioactive molecule microencapsulation in both animals and humans and versatile capacity for sustaining long-term controlled drug release in these systems is well-established.[38, 39] As a dual-use drug delivery medium, PLGA particles have also been tested in combination with CPC to deliver protein bone growth factors (rhBMP-2) while also acting as a poragen.[40] Historically, PLGA has been widely investigated as a delivery vehicle of small molecule drugs[41] and proteins,[42] and with some promise as a delivery vehicle for nucleic acids, including plasmid DNA[43] and siRNA.[43, 44] Significantly, PLGA particles 3-6 μm in diameter are selectively scavenged by host phagocytic cells, providing a particle size-selective cell-specific drug targeting and dosing mechanism.[45] Therefore, specific osteoclast and phagocyte cell uptake can be achieved by controlling PLGA particle sizes to those internalized by professional phagocytes while avoiding other cell types in the tissue bed.

RNA interference (RNAi) is a powerful tool to down-regulate specific mRNA/protein expression utilizing a natural intracellular regulatory mechanism in mammalian species. Gene silencing using siRNA has many potential therapeutic applications due to several advantages intrinsic to RNAi.[46] SiRNAs are well known for their very short circulating half-lives in vivo,[47] and current challenges in systemic targeting from parenteral siRNA formulations. These unresolved issues have produced the current emphasis on local delivery of therapeutic siRNA as a more direct clinical goal.[48] We have shown recently that siRNA against RANK provides potent in vitro inhibition of osteoclast-mediated bone resorption.[49] Here we describe a novel strategy to deliver RANK

siRNA locally to bone in an injectable CPC matrix, loaded within PLGA microspheres for local uptake by bone-resident osteoclast precursors. PLGA particles served to limit siRNA degradation and facilitate phagocyte cell-targeted delivery, demonstrating in vitro efficacy in knocking down RANK target in osteoclastic cell cultures from a protective osteoclast-targeted siRNA delivery carrier released from injectable calcium-based cement reservoir.

Materials and Methods

Materials

Reagents.   PLGA (50:50 monomer ratio, molecular weight (mw) 57kDa) with lauryl ester end groups was purchased from Lakeshore Biomaterials (AL, USA). Branched polyethylenimine (bPEI) (mw: 25kDa) and poly(vinyl alcohol) (PVA, average mw 30,000-70,000) were bought from Sigma-Aldrich (USA). RNase-free water was prepared using diethyl pyrocarbonate (DEPC) (Sigma-Aldrich). RANK siRNA (sense 5'-GCGCAGACUUCACUCCAUAUU-3', antisense 5'-UAU GGAGUGAAGUCUGCGCUU-3') and RNase-free siRNA buffer were purchased from Dharmacon (CO, USA). RANK siRNA's DNA analogues (5'-GCGCAGACTTCACTCCATATT-3', 5'-TATGGAG TGAAGTCTGCGCTT-3') were purchased from Integrated DNA Technologies (IA, USA).

Methods

Primary murine cell harvesting and differentiation.   C57BL/6 male mice (6-8-week-old, Jackson Labs, ME, USA) were maintained in a specific pathogen-free facility at the University of Utah. All procedures were performed as approved by the Institutional Animal Care and Use Committee, University of Utah. Bone marrow cells (BMC) were harvested from murine tibias and

femurs of C57BL/6 male mice and differentiated into osteoclast precursors using previously

described methods.[49] Briefly, BMCs were cultured in α-MEM (Gibco) containing 10% FBS and 1%

penicillin-streptomycin (defined for all cell cultures as "complete media") overnight at a density of

1×10^6 cells/ml. Nonadherent cells were harvested the next day and immediately seeded into

24-well tissue culture plates in complete media with 30 ng/ml M-CSF (R&D Systems) at a density

of 1×10^6 cells per well. After 2 days of culture, attached cells were used as osteoclast precursors.

To generate osteoclasts, precursor cells were incubated in 200ng/ml RANKL and 30ng/ml M-CSF

(R&D Systems) in complete media (defined as "osteoclast-specific media"), refreshed every other

day.[45] RANKL was expressed using a previously described detailed procedure.[49]

Reverse transcriptase-polymerase chain reaction (RT-PCR).   Total RNA was isolated using

an RNeasy Mini Kit (Qiagen). Up to 4 micrograms of RNA were used to make cDNA with the

SuperScript III 1st strand RT kit for PCR (Invitrogen). PCR primers were designed for RANK

(5'-AGATGTGGTCTGCAGCTCTTCCAT-3', 5'-ACACACTTCTTGCTGACTGGAGGT -3') and

cyclophilin B (housekeeping control, 5'-AGCGCTTCCCAGATGAGAACTTCA-3', 5'-GCAATGG

CAAAGGGTTTCTCCACT-3') using Primerquest software purchased from Integrated DNA

Technologies (USA). PCR was performed with iTaq DNA polymerase (Bio-Rad, USA), 1.5 mM

magnesium chloride, 200 μM each of dNTPs, 500 nM of each primer and 2 μL of the cDNA.

Reactions were performed using the following protocol: 95^oC melt, 60^oC anneal and 72^oC

extension in the iCycler Thermal cycler (Bio-Rad). PCR products were analyzed on ethidium

bromide-stained TBE-based 2% agarose gels run at 100V for 30 min and visualized with UV light.

Preparation of siRNA/bPEI complexes and siRNA transfection in vitro.   To prepare

siRNA/bPEI complexes at various anion/cation charge (NP) ratios, 2μl of 10μM RANK siRNA aqueous solution was mixed with 2μl of bPEI solutions of different concentrations (0.016-0.16μg). The complex mixed solutions were kept at room temperature for 20 minutes. Then, 4μl of each mixture was electrophoresed using ethidium bromide-stained TBE-based 2% agarose gels run at 100V for 20 minutes, followed by visualization with UV light to assess the siRNA-bPEI complex formation. Cell transfections with siRNA/bPEI complexes at fixed NP ratios in complete media were performed subsequently. siRNA/bPEI complexes for each well are prepared by mixing 2.5ul of 20μM siRNA aqueous solution with 1.6μl, 1.2μl, 0.8μl and 0μl (NP 20, 15, 10 and 0) of 1mg/ml bPEI, respectively, in a total volume of 20μl with RNase-free water. After incubation at room temperature for 20 minutes, complete media was added to achieve the final volume of 1ml, yielding a final amount of siRNA in each well of 1.675μg. The dose was determined based on our published results.[49] Cell siRNA transfections were always performed in complete media. After 24-hour incubation at $37^{o}C$ under 5% CO_2, culture media was refreshed with 1ml complete media and the transfected cells were further incubated. RNA was harvested 2 days later and RANK expression was analyzed by PCR.

PLGA microparticle preparation. Microparticles of PLGA were prepared using a known double-emulsion solvent evaporation technique.[50] In brief, siRNA or DNA analog/bPEI complexes were prepared by mixing equal volumes of 33.5μg of siRNA/DNA analog and 1mg/ml bPEI in RNase-free siRNA buffer. Complex-containing PLGA microspheres were prepared by dispersing the siRNA/bPEI aqueous solution into a solution of 50mg PLGA dissolved in 2ml methylene chloride with intense probe sonication (Biologics, Inc. Ultrasonic 3000, 20s sonication with 10s

pause). Then, the w/o dispersion was added into an aqueous 4% PVA solution while vortexing. The solvent was extracted by transferring the final w/o/w emulsion into a beaker containing aqueous 0.6% PVA solution and stirred for 3~4 hours at room temperature. The solidified microspheres were washed using RNase-free water three times followed by lyophilization.

Particle size distribution, zeta potential and surface morphology.   Particle size distribution and zeta potential (surface charge) of PLGA microparticles with siRNA was determined using a Malvern Instruments Zetasizer Nano ZS (Westborough, USA) in 10mM NaCl at pH 7.4. To further confirm measured particle sizes and surface morphology, scanning electron microscopy (SEM) was performed. PLGA microspheres were attached to a metal stub using conductive tape and coated with gold in a sputter coater. SEM images of coated samples were captured on Hitachi S2460N.

siRNA loading and encapsulation efficiency.   Following a previously described procedure,[38] 3-5 mg PLGA particles were dissolved in DMSO. The siRNA was extracted by adding equal volumes of Tris-EDTA buffer (10mM Tris-HCl containing 1mM EDTA, pH 7.4). Aqueous layers were removed, and siRNA concentration was measured using the QuantIT[TM] PicoGreenTM assay (Invitrogen, USA). Encapsulation efficiency is calculated as the percent of the PLGA-extracted siRNA versus the initial feed siRNA amount. The siRNA was then precipitated from the aqueous solution by adding 0.3M sodium acetate and 70% (v/v) ethanol. After 30 min incubation at -20°C, the solution was centrifuged at 12,000 rpm at 4°C for 30 min. The pellet was dried and analyzed on a 2% agarose gel.

Evaluation of in vitro siRNA controlled release.   DNA analog loaded PLGA particles (1 mg)

were suspended in 1ml RNase-free siRNA buffer (pH 7.4), and kept at 37°C under constant gentle

shaking for 4 weeks. To collect the supernatant, the suspension was centrifuged at 12,000 rpm for

15 minutes, and supernatant was removed for analysis followed by replacement with the same

volume of fresh buffer. The siRNA content in supernatant was measured using the QuantlT^{TM}

PicoGreenTM assay.

Cytotoxicity assay.   Murine bone marrow cells were cultured in osteoclast-specific media

with 1 mg PLGA particles loaded with either RANK siRNA or the DNA analogue negative control.

After 3-day incubation in 37°C, cytotoxicity was measured using CellTiter-Blue Cell Viability Assay

kit (Promega, USA).

Particle intracellular degradation studies and RANK knockdown efficiency in culture.

Fluorescently labeled PLGA particles were prepared by adding 0.5% (weight percentage vs. PLGA)

6-coumarin dye to methylene chloride.[51] Murine bone marrow cells were seeded at 1×10^{6} cells/well

and incubated with 1 mg fluorescently-labeled PLGA particles in a 24-well plate in complete media

containing M-CSF and RANKL at 37°C. Particle intracellular degradation studies were performed

using fluorescence microscopy. Culture media was refreshed every other day. Disappearance of

punctate fluorescence indicates particle degradation. Murine bone marrow cells were incubated

with PLGA particles in 24-well plates in osteoclast-specific media. The dose of siRNA per well (125

nM) was determined using previous published results.[49]   The RANK siRNA-loaded PLGA

particle-treated groups were compared with control groups treated with PLGA particles without

siRNA, and also with DNA analogue-loaded PLGA particle-treated groups. PLGA particles was

diluted in 1 ml osteoclast-specific media and added to cultures. Total RNA was isolated 4 days

posttransfection using an RNeasy Mini Kit (Qiagen). PCR products were analyzed on ethidium bromide-stained TBE-based 2% agarose gels and visualized under UV light.

Loading of siRNA-containing PLGA particles into CPC. A commercially available injectable CPC (62.5 wt% tricalcium phosphate (α-TCP), 26.8 wt% dicalcium phosphate anhydrous (DCPA), 8.9 wt% calcium carbonate ($CaCO_3$), and 1.8 wt% hydroxyapatite (HAP)) was a gift from BioMet Osteobiologics (NJ, USA). Pure CPC cement was prepared according to the manufacturer's instructions and used as the control. PLGA microparticles were loaded into dry CPC powder at 10% (w/w). This mixture was added into a 5-ml syringes (Becton Dickinson, NJ) filled with aqueous solution provided in the kit to achieve the liquid/powder ratio of 0.35 ml/g.[25] Subsequently, thorough mixing required manual stirring within the syringe barrel for 60 seconds. The resulting CPC suspension containing PLGA microparticles was then injected into a clean rubber mold (circular cylinder shape: 6 mm diameter, 6 mm height) to cure CPC samples.

Characterization of the PLGA-modified CP cement. The total porosity of PLGA microparticle-loaded CPC was determined by heating CPC specimens at 650°C for 2 hours to pyrolyze the PLGA particles. CPC sample weight is measured before and after pyrolysis. Total porosity and macroporosity is calculated from the following equations[52]:

$$\varepsilon_{macro} = \left(1 - \frac{m_{burnt}}{m_{pureCPC}}\right) \times 100\% \qquad <1>; \qquad\qquad \varepsilon_{tot} = \left(1 - \frac{m_{burnt}}{v \times \rho_{HAP}}\right) \times 100\% \qquad <2>$$

Equation <1> calculates macropores produced by PLGA particles. Equation <2> yields the sample's total porosity, including micropores representing the porosity of the pure CPC sample,

where m_{burnt} is the weight of samples after PLGA removal by heating, v (cm^3) is the volume of the sample, $m_{pureCPC}$ is the weight of pure CPC sample, and ρ_{HAP} (g/cm^3) is the density of hydroxyapatite (3.156 g/cm^3).[53]

CPC mechanical testing.   CPC samples were vacuum-dried overnight. Compression strength was measured using an Instron (Instron TT-CM; Instron, Canton, Massachusetts). Samples were placed in the mechanical testing bench and compressive strength was measured at a crosshead speed of 0.5 mm/min. Mechanical stiffness was determined and compared between CPC alone and 10:90 PLGA/CPC samples.

CPC composite matrix morphology.   Cross-sections of CPC samples (vacuum dried overnight) were visualized for porosity and morphology by SEM.

RANK knockdown efficacy by siRNA released from modified cement in vitro.   In order to fabricate CPC composite wafers to deploy into 24-well plate cell cultures for siRNA release and bioactivity assays in cell culture, 1 mg PLGA microparticles carrying 1.675µg were mixed thoroughly with 9 mg CPC powder (10:90) on a sterilized plastic weighing plate, and dissolved in aqueous solution to reach the same liquid/powder ratio of 0.35 ml/g as used for mechanical samples. A flat medicine spoon was used to mold the CPC mixture into a flat disc. After curing the CPC into a hard wafer, a razor blade was used to cut and remove pieces of the plate to fit into wells of 24-well culture plate. Murine bone marrow cells were then seeded onto these CPC wafers at 1×10^6 per well in the wells. Cells were then incubated with 30 ng/ml M-CSF in complete media for the first 2 days and followed by incubation with osteoclast-specific media. Cell RNA was harvested 8 days posttreatment and subject to RT-PCR. PCR products were analyzed on ethidium

bromide-stained TBE-based 2% agarose gels run at 100V for 30 min and visualized with UV light.

Cell imaging and statistical analysis. Fluorescent images of adherent cells in culture were captured using a Coolsnap color CCD camera attached to a Nikon E600 microscope using Image Pro Plus 4.0 software. All images were captured using the same exposure time period and corrected for unequal field illumination. Analysis of variance (ANOVA) followed by two-tailed student's t-test was used for statistical analysis. All experiments were repeated three times. Error bars represent the standard error of the mean. Statistically significant was considered if $p < 0.05$.

Results

Particle preparation

Optimization of RANK siRNA/bPEI complexes. To determine the NP threshold for stable siRNA polyplex formation, different amounts of bPEI were mixed with 0.14nmol RANK siRNA at NP ratios of 0, 0.5, 1, 2 and 5. Figure 4.1A shows migration of siRNA/bPEI complexes by gel electrophoresis. With NP ratios of 0, 0.5 and 1, siRNA bands migrate separately on the gel, indicating uncomplexed, excess siRNA. When the NP ratio is equal to 2, the density of the siRNA band is substantially weaker. When the NP ratio is 5, no siRNA migrates freely in the gel, indicating that all siRNA molecules are initially entrapped in bPEI complexes through electrostatic interactions. Knowing that an NP value of 5 is the threshold, RANK expression was assayed after cells were incubated with NP 10, 15 and 20 for 2 days. RANK gene expression starts to decrease when NP is 15, and significant down-regulation was shown when NP is 20 (Figure 4.1B). Therefore, NP 20 was used for the following delivery experiments.
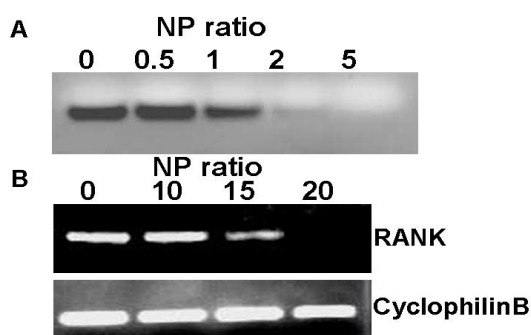
Figure 4.1 siRNA polyplex preparation. (A) Gel migration of RANK siRNA/bPEI complexes at different NP ratios (0-5). (B) RANK expression in BMC cultures 3 days post-BMC treatment with RANK siRNA/bPEI complexes at different NP ratios (0-20) in serum-based media.

Characterization of PLGA microspheres. PLGA SEM images (Figure 4.2A) revealed that microspheres display the expected spherical morphology with an average size of 5.45 ± 0.88 µm as detetmined from light scattering particle size analysis. PLGA microparticle surface charge was -21.07 ± 1.42 mV. The siRNA encapsulation efficiency in these PLGA particles using the double-emlusion method is 80.75 ± 4.1%. (n=3)

RANK knockdown effects, cytotoxicity and intracellular degradation of PLGA microspheres. Cytotoxicity from PLGA microparticle exposure in culture was determined: no significant cell toxicity differences were observed between controls without treatment and cells treated with particles (Figure 4.2B). Gel electrophoresis showed that the charge and molecular weight of RANK siRNA extracted from PLGA particles was similar to the control stock siRNA (Figure 4.2C). RNA harvested from murine-derived primary bone marrow cells incubated with microparticles for 4 days was subject to RT-PCR. Cells incubated with RANK-siRNA-loaded PLGA particles showed significant down-regulation of RANK expression, compared with controls without microparticle incubation and cells treated with microparticles loaded with dummy DNA analogues as controls
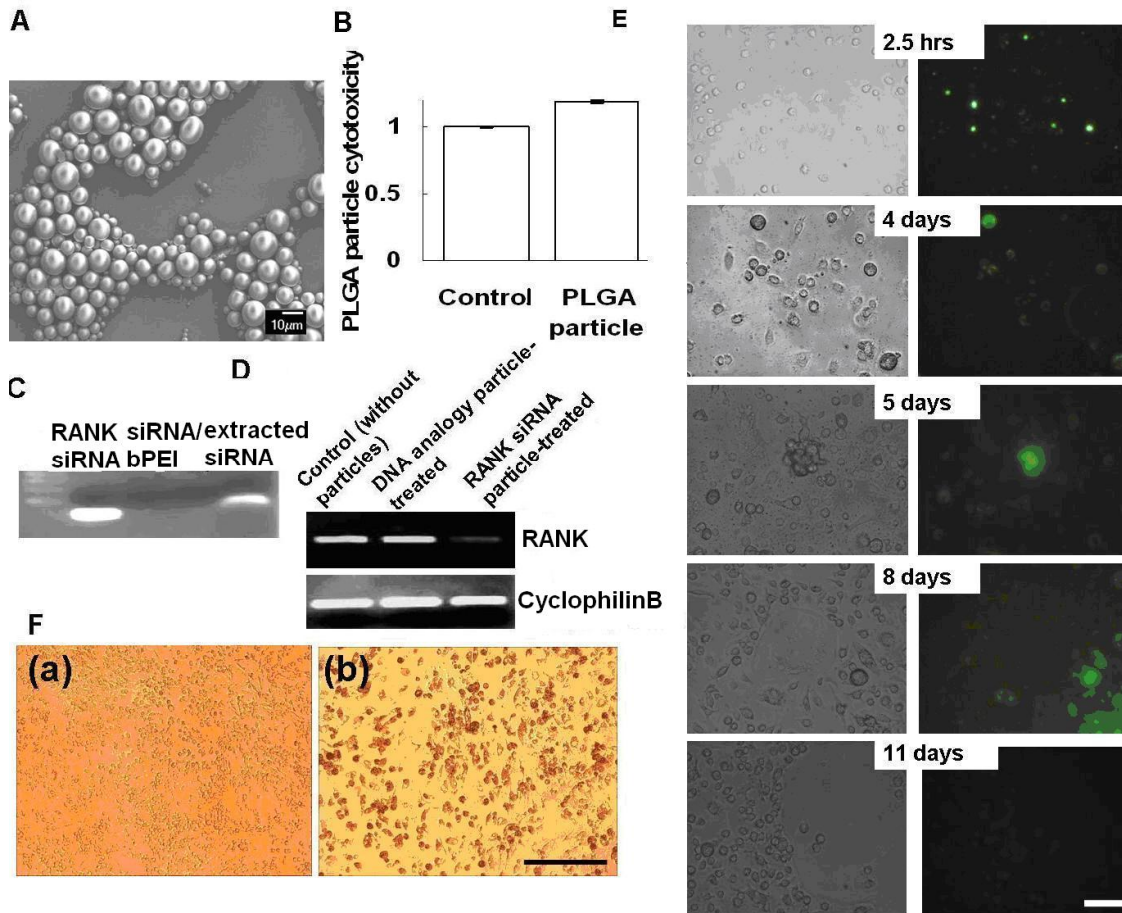
Figure 4.2 Physicochemical and functional properties of siRNA encapsulated in PLGA microparticles. (A) SEM image of PLGA particles. (B) Murine BMC cell cytotoxicity of RANK siRNA/bPEI complexes incorporated in PLGA particles in serum-based cultures after 3 days. (C) Gel electrophoresis comparison of the RANK siRNA extracted from PLGA particles versus control stock siRNA. (D) Significant down-regulation of RANK in murine BMC cultures by siRNA-loaded PLGA particles. RANK siRNA DNA analogue-loaded PLGA particles served as negative control. (E) Degradation of fluorescent-labeled PLGA particles in BMC over time. (F) PLGA particles were phagocytosed by BMCs compared to nonphagocytic cells. (a) No particle treatment; (b) entire bone marrow cells incubated with PLGA particles.

(Figure 4.2D). Efficient cell phagocytosis of PLGA microspheres was also confirmed. Particles were readily taken up by cells and started to degrade after particle uptake. After 11 days in culture, microspheres disappeared and the enclosed fluorescence marker was distributed evenly throughout the cell volume (Figure 4.2E). Figure 4.2F shows PLGA particles were selective phagocytosed by BMCs compared to nonphagocytic cell cultures.

In vitro release of DNA analogues of RANK siRNA from PLGA microparticles. Murine RANK DNA analogue-loaded PLGA microparticles were used (Figure 4.3) to evaluate the in vitro release profile of siRNA from microparticles due to its similar physical chemistry and structure, higher stability and lower cost compared to siRNA. There was little or no release from the PLGA particles over 50 days in culture media alone.

Preparation of PLGA/CPC composite

Characterization of PLGA microparticle/CPC composite matrix. Table 4.1 shows calculated results for the microparticle porosity and macroporosity (ave. ± SE, n=3). The microporous pure
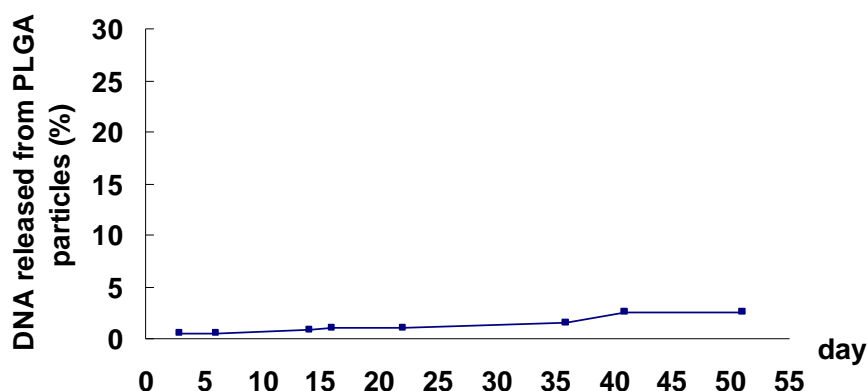

Figure 4.3 Release kinetics of RANK siRNA analogue DNA from PLGA microparticles. 1mg PLGA particles incubated in 1ml RNase-free water. (n=3)

Table 4.1 SUMMARY RESULTS OF THE CPC MATRIX POROSITY MEASUREMENTS

	Average mass (g)	Density (g/cm³)	porosity (%)	Macroporosity(%)
Microporous cement	0.2522±0.0045	1.769825±0.015951	55.02±0.422	----
10:90 PLGA/CPC	0.2241±0.0066	1.572456±0.023224	63.68±0.56	35.23±0.99

CPC samples had a porosity of 55%, while the PLGA-loaded CPC samples (10% w/w particle load) displayed a higher porosity of 63%. The macroporosity introduced by PLGA particles is 35%.

CPC morphology and mechanical characteristics. Figures 4.4A and 4.4B show SEM images of the cross-sections of pure CPC and PLGA particles within the cured 10:90 PLGA/CPC matrix, respectively. PLGA microparticles are shown distributed homogeneously within the CPC matrix (Figure 4.4B). CPC matrix stiffness is expressed as maximum compressive load (N) versus maximum compressive extension (mm). Control samples (CPC alone) showed a stiffness of 251.8 ±27.14 N/mm. The 10% PLGA incorporated CPC samples had an average value of 200.5±9.57 N/mm. No significant difference in stiffness was observed between the CPC alone and the 10:90 CPC samples (Figure 4.4C).

Down-regulation of RANK gene expression by RANK siRNA-loaded PLGA/CPC composite microparticles. Murine BMC RNA was harvested 8 days after these cells were seeded on CPC wafers. PCR results shows significant suppression of RANK expression in cells incubated with RANK siRNA-loaded PLGA/CPC compared with control without particle treatments and DNA analogue-loaded PLGA/CPC matrices (Figure 4.4D).
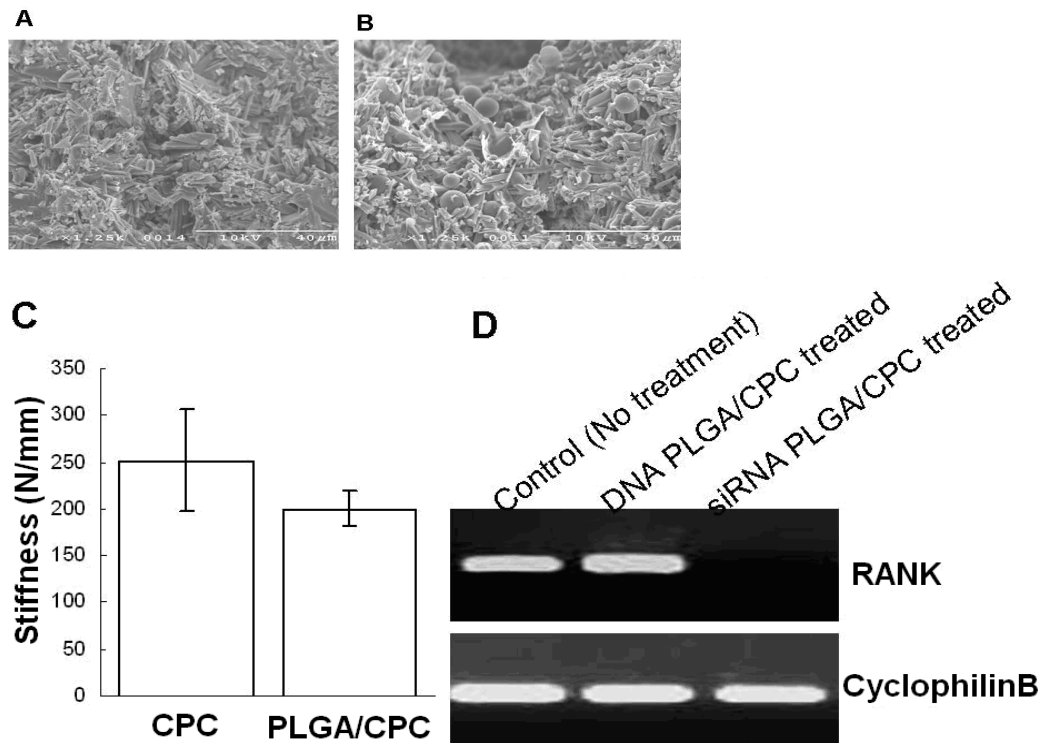
Figure 4.4 Characteristics of CPC matrices: morphology, mechanical and functional properties. (A) SEM of cross-section of pure CPC, (B) SEM of cross-section of PLGA/CPC composite, (C) Comparison of mechanical stiffness between CPC alone and 10:90 PLGA/CPC samples. (D) significantly reduced RANK expression in murine BMC cultures by treatment with RANK siRNA-PLGA particle-loaded CPC matrices for 8 days. RANK siRNA DNA analogue-loaded PLGA/CPC matrices served as negative control with no observable effects in cultures.

Discussion

Increasing incidence of osteoporotic fragility fractures and their prolonged healing requirements postfixation constitute major clinical challenges that require better clinical solutions to improve osteoporosis patient outcomes. Though bisphosphonate drugs are effective against generalized osteoporosis, their severe suppression of bone turnover largely inhibits fracture healing.[54, 55] Currently, no therapy has yet produced significant improvements in osteoporotic bone augmentation for improved fragility fracture healing. RNA interference is a new promising drug

class with unique mechanisms to selectively target pathological pathways. Yet, effective siRNA delivery to target tissues is difficult, mandating primarily local or topical routing to produce therapeutic efficacy to date. Importantly, siRNA has not yet been studied to ameliorate osteoclast-mediated bone loss in the context of fragility fractures and fixation tooling. This opportunity is explored in this study with in vitro assays of siRNA delivery using injectable bone augmentation biomaterials (CPC) clinically applied in osteoporosis as delivery matrices.

As RANK is recognized to play an essential role in regulating osteoclastogenesis, it is a natural target for siRNA bioactivity in the context of osteoporosis therapy.[56] Activation of RANK by its ligand, RANKL, is required for the formation and activation of osteoclasts.[57, 58] Our previous RANK siRNA delivery methods show specific siRNA silencing of RANK in both macrophage-like secondary cell line cultures (RAW264.7) and primary murine bone marrow cultures to inhibit osteoclast formation and bone resorption in vitro, and collectively support proof-of-concept to deliver therapeutic RANK siRNA to osteoclasts locally.[49] Therefore, this current study continues the development of this concept for locally delivered siRNA targeting RANK from bone cement, assessing in vitro siRNA delivery and RANK knockdown efficacy from PLGA particles within CPC bone augmentation materials to target osteoclasts and osteoclast precursors and suppress osteoclast-mediated bone resorption.

To increase the stability and loading efficiency of siRNA in PLGA microparticles, RANK siRNA was complexed with bPEI at different NP ratios (i.e., NP ~ 0-5) because of bPEI's known utility as a nonviral nucleic acid delivery vector.[59-61] The siRNA/bPEI migration assay demonstrates that siRNA forms stable complexes with bPEI when the NP ratio ≥ 5. Transfection of RANK siRNA in

mouse bone marrow cells in serum-based cultures with these polyplexes showed produced RANK

gene silencing monitored by PCR 2 days posttransfection. Compared to controls without treatment,

RANK gene expression in BMC cultures shows no significant gene expression reduction when the

NP ratio was 10, but begins to decrease when the NP ratio equals 15. Significant RANK gene

silencing is achieved when the NP ratio reached 20, indicating that siRNA specifically

down-regulates RANK message RNA expression in BMCs. Therefore, NP 20 was used for the

following experiments. RANK knockdown effect is comparable with using DharmaFECT 4

transfection reagent in our previous published results.[49]

The established double emulsion method was used to prepare all PLGA microspheres. For

maximum particle loading and protection of siRNA payloads from nucleases, 4% (w/v) PVA was

used for microparticle preparation.[50, 62] With modifications of the fabrication process, including the

time and power of sonication, microparticle size was controlled within the range of 1~10 µm, to

selectively target particle uptake exclusively by professional phagocytosis.[45] PEI has been proven

previously to increase oligoDNA encapsulation in PLGA particles at least 2-fold relative to that

without PEI, especially for preformed PEI-oligoDNA polyplexes, and to increase cellular

accumulation of nanoparticles.[63] For this study, use of bPEI improves the siRNA PLGA particle

encapsulation efficiency to 81%, which is comparable with previous published encapsulation

efficiency of preformed siRNA-PEI in PLGA particles. Cytotoxicity from siRNA-loaded PLGA

particles was analyzed by culturing BMCs with PLGA particles in serum-containing complete

media at minimum effective dose determined before.[49] No significant cytotoxicity was observed.

Electrophoresis results showed that the extracted siRNA from these particles maintained a similar

charge, migration and molecular weight as the uncomplexed siRNA. Microparticles were readily phagocytosed by BMCs compared to nonphagocytic cell cultures, establishing this particle size-dependent targeting mode, and gradual intracellular particle degradation was observed using fluorescence imaging. Complete microparticle degradation was achieved in 11 days of incubation in cell cultures.

In vitro release profiles of DNA from PLGA microparticles have been shown to be dependent on the molecular mass of the PLGA; increasing PLGA molecular weight reduced the encapsulated DNA release rate.[64] Little or no release of DNA from PLGA particles was shown from PLGA microspheres where the PLGA molecular weight was greater than 30kDa.[65] OligoDNA release results from polyplexes in PLGA microparticls are consistent with this previous report. Only 3% of loaded oligoDNA, as a stable siRNA analogue for this study, was released from the PLGA particles of molecular weight 57kDa over 7 weeks in siRNA buffer. High molecular weight PLGA particles protect encapsulated DNA and maintain the particle integrity until particles are released from CPC to target cell candidates by phagocytosis. Clearly, there is a difference between particle degradation to release the nucleic acid payload within cells (i.e., 11 days, Figure 4.2D) versus to water (negligible release after 50 days to water, Figure 4.3). OligoDNA analogue/bPEI polyplex-loaded PLGA particles posses similar polyplex charge as RANK siRNA and the same particle surface charge when loaded into PLGA particles (Table 4.1). However, as expected, the actual siRNA/bPEI PLGA particles effectively reduced RANK expression in BMC cultures, compared with control oligoDNA analogue/bPEI-loaded PLGA particles, indicating that decreased RANK expression is due to specific siRNA taken up by phagocytes and subsequent gene

sequence-specific knockdown. The retention of physicochemical and functional integrity of RANK siRNA during the encapsulation also suggests that the polyplex polymer effectively protects siRNA during particle fabrication. Taken together, these results support the utility of siRNA/bPEI-loaded PLGA microparticles for specific suppression of RANK expression in osteoclast precursors in serum-based cultures of NP ratios of 20.

CPC has been used by the orthopaedic community for osteoporotic fracture healing.[66, 67] Similarly, PLGA particles have been previously loaded into CPC as drug delivery vehicles and as an additive to increase CPC macropore-mediated bone integration. Extending this concept to PLGA microparticles encapsulating RANK siRNA as CPC injectable composite structural and drug delivery materials with dosing and bioactivity sufficient to suppress osteoclast formation and function and increase the periprosthetic bone density was the goal of this study.   The design calls for particle-selective delivery to professional host-resident phagocytes responsible for bone loss in osteoporosis, and application of the CPC matrix as a bone augmentation material adjunct to fixation.

PLGA particles formulated into injectable clinical-grade CPC are known to increase total CPC porosity and function as a delivery vehicle.[35] Addition of 10% or 20% (w/w) PLGA in CPC retains all CPC physical parameters within surgically workable ranges, but 20% (w/w) PLGA particle loading is the maximum loading to maintain composite cement injectability.[36, 40, 68, 69] CPC containing 10% PLGA microspheres has similar properties with CPC alone.[25] Therefore, the 10% (w/w) PLGA particle/CPC composite formulations were selected for siRNA delivery in this study. After cement curing and setting, the PLGA/CPC formulation formed a rigid scaffold with

homogeneously distributed PLGA microspheres. Addition of these PLGA microparticles significantly increased the porosity of the cement (Table 4.1), implying the improvement of interconnectivity in the cement. Significantly, as long as pore interconnectivity is obtained, PLGA particle release will not be dependent on slow CPC degradation or dissolution kinetics, yielding a versatile sustained release system. In addition, such interconnectivity also can accelerate overall aqueous access, penetration and degradation of CPC.

Matrix mechanical properties could also be compromised with higher PLGA particle incorporation. Based on mechanical testing results from the 10% formulations of PLGA-loaded CPC, no significant differences are observable in stiffness between CPC alone and PLGA/CPC composites at their as-cured initial stage. A previous published study showed significant differences in compression strength after 3 days of the matrix degradation time.[35]

For cell cultures, thin, flat CPC wafers were used to accelerate PLGA particle release to produce an experimentally accessible cell culture period. Successful knockdown of RANK gene by incubating osteoclast precursor phagocytic cells with RANK siRNA/PEI PLGA particle-incorporated CPC proves the facility of this bone targeting delivery system. Unchanged RANK expression observed from DNA analogue/bPEI PLGA-incorporated CPC and blank CPC control cell cultures implies the desired specific knockdown by the released siRNA sequences in cell culture. We have previously shown specific siRNA-induced suppression of RANK expression and significant inhibition of osteoclast formation and bone resorption in both secondary RAW264.7 and primary cultures.[49] PLGA particle release must start with the particles exposed on the CPC matrix surface and newly generated CPC pores can then increase their interconnectivity over time

to facilitate further particle release and make cement more porous and susceptible for further degradation. However, this in vitro release profile will be very different from in vivo kinetics, due to body fluid transport, bone mechanical stress influences and individual pathological conditions. In vitro studies have shown that the overall pH of the medium around 10:90 PLGA/CPC samples decreased to 4.4 after 12 weeks' incubation from PLGA acid by-product production and the significant pH decrease started to show after week 4.[35] In vivo, however, the local tissue system may be buffered sufficiently, depending on the deployed CPC volume and the CPC-PLGA intrinsic acid-base interactions.

Future in vivo studies will exploit local siRNA delivery to bone from bone augmentation devices and injected liquid depots. This strategy seeks to provide a novel, clinically relevant approach to improve osteoporotic fragility fracture healing using current clinical bone augmentation strategies in osteoporosis, while also remaining amenable to local siRNA therapeutic drug delivery directly from bone defects and common fracture fixation hardware.

Conclusions

We have shown that siRNA can be encapsulated within PLGA microspheres without significantly impairing its functional integrity. As a result, targeted phagocytic cell-specific delivery can be achieved by controlling particle sizes within the microrange. This study supports the concept of applying the unique combination of bone augmenting CPC and local siRNA cell-targeted particle delivery achieved by PLGA-encapsulation of siRNA molecules and siRNA cell uptake targeted from CPC matrices injected into bone augmentation sites. RANK-targeted

knockdown in osteoclasts and their precursor phagocytic cells can be achieved by particle size-cell phagocyte discrimination. This selectively targets osteoclastic phenotypes in augmentation zones where osteoporosis has produced low bone density and allowed CPC injection. PLGA particle release and degradation produces CPC macropores known to facilitate further particle release, and promote bone in-growth, simultaneously, with suppression of bone resorption in peri-implant areas needed to facilitate healing and mechanical stabilization processes.

References

1.   Dong, L.; Huang, Z.; Cai, X.; Xiang, J.; Zhu, Y. A.; Wang, R.; Chen, J.; Zhang, J. Localized delivery of antisense oligonucleotides by cationic hydrogel suppresses TNF-alpha expression and endotoxin-induced osteolysis. *Pharm Res* **2011,** 28, (6), 1349-56.

2.   Johnell, O.; Kanis, J. A. An estimate of the worldwide prevalence and disability associated with osteoporotic fractures. *Osteoporos Int* **2006,** 17, (12), 1726-33.

3.   Kadoya, Y.; al-Saffar, N.; Kobayashi, A.; Revell, P. A. The expression of osteoclast markers on foreign body giant cells. *Bone Miner* **1994,** 27, (2), 85-96.

4.   Sabokbar, A.; Fujikawa, Y.; Neale, S.; Murray, D. W.; Athanasou, N. A. Human arthroplasty derived macrophages differentiate into osteoclastic bone resorbing cells. *Ann Rheum Dis* **1997,** 56, (7), 414-20.

5.   Yasuda, H.; Shima, N.; Nakagawa, N.; Yamaguchi, K.; Kinosaki, M.; Mochizuki, S.; Tomoyasu,

A.; Yano, K.; Goto, M.; Murakami, A.; Tsuda, E.; Morinaga, T.; Higashio, K.; Udagawa, N.; Takahashi, N.; Suda, T. Osteoclast differentiation factor is a ligand for osteoprotegerin/osteoclastogenesis-inhibitory factor and is identical to TRANCE/RANKL. *Proc Natl Acad Sci U S A* **1998,** 95, (7), 3597-602.

6.   Lacey, D. L.; Timms, E.; Tan, H. L.; Kelley, M. J.; Dunstan, C. R.; Burgess, T.; Elliott, R.; Colombero, A.; Elliott, G.; Scully, S.; Hsu, H.; Sullivan, J.; Hawkins, N.; Davy, E.; Capparelli, C.; Eli, A.; Qian, Y. X.; Kaufman, S.; Sarosi, I.; Shalhoub, V.; Senaldi, G.; Guo, J.; Delaney, J.; Boyle, W. J. Osteoprotegerin ligand is a cytokine that regulates osteoclast differentiation and activation. *Cell* **1998,** 93, (2), 165-76.

7.   Dougall, W. C.; Glaccum, M.; Charrier, K.; Rohrbach, K.; Brasel, K.; De Smedt, T.; Daro, E.; Smith, J.; Tometsko, M. E.; Maliszewski, C. R.; Armstrong, A.; Shen, V.; Bain, S.; Cosman, D.; Anderson, D.; Morrissey, P. J.; Peschon, J. J.; Schuh, J. RANK is essential for osteoclast and lymph node development. *Genes Dev* **1999,** 13, (18), 2412-24.

8.   Lacey, D. L.; Tan, H. L.; Lu, J.; Kaufman, S.; Van, G.; Qiu, W.; Rattan, A.; Scully, S.; Fletcher, F.; Juan, T.; Kelley, M.; Burgess, T. L.; Boyle, W. J.; Polverino, A. J. Osteoprotegerin ligand modulates murine osteoclast survival in vitro and in vivo. *Am J Pathol* **2000,** 157, (2), 435-48.

9.   Simonet, W. S.; Lacey, D. L.; Dunstan, C. R.; Kelley, M.; Chang, M. S.; Luthy, R.; Nguyen, H. Q.; Wooden, S.; Bennett, L.; Boone, T.; Shimamoto, G.; DeRose, M.; Elliott, R.; Colombero, A.; Tan, H. L.; Trail, G.; Sullivan, J.; Davy, E.; Bucay, N.; Renshaw-Gegg, L.; Hughes, T. M.; Hill, D.; Pattison, W.; Campbell, P.; Sander, S.; Van, G.; Tarpley, J.; Derby, P.; Lee, R.; Boyle, W. J. Osteoprotegerin: a novel secreted protein involved in the regulation of bone density. *Cell* **1997,** 89, (2), 309-19.

10. Yasuda, H.; Shima, N.; Nakagawa, N.; Mochizuki, S. I.; Yano, K.; Fujise, N.; Sato, Y.; Goto, M.; Yamaguchi, K.; Kuriyama, M.; Kanno, T.; Murakami, A.; Tsuda, E.; Morinaga, T.; Higashio, K. Identity of osteoclastogenesis inhibitory factor (OCIF) and osteoprotegerin (OPG): a mechanism by which OPG/OCIF inhibits osteoclastogenesis in vitro. *Endocrinology* **1998,** 139, (3), 1329-37.

11. Tanzer, M.; Karabasz, D.; Krygier, J. J.; Cohen, R.; Bobyn, J. D. The Otto Aufranc Award: bone augmentation around and within porous implants by local bisphosphonate elution. *Clin Orthop Relat Res* **2005,** 441, 30-9.

12. von der Linden, P.; Gisep, A.; Boner, V.; Windolf, M.; Appelt, A.; Suhm, N. Biomechanical evaluation of a new augmentation method for enhanced screw fixation in osteoporotic proximal femoral fractures. *J Orthop Res* **2006,** 24, (12), 2230-7.

13. Cook, S. D.; Salkeld, S. L.; Patron, L. P.; Barrack, R. L. The effect of demineralized bone

matrix gel on bone ingrowth and fixation of porous implants. *J Arthroplasty* **2002,** 17, (4), 402-8.

14. Sumner, D. R.; Turner, T. M.; Purchio, A. F.; Gombotz, W. R.; Urban, R. M.; Galante, J. O. Enhancement of bone ingrowth by transforming growth factor-beta. *J Bone Joint Surg Am* **1995,** 77, (8), 1135-47.

15. Tanzer, M.; Harvey, E.; Kay, A.; Morton, P.; Bobyn, J. D. Effect of noninvasive low intensity ultrasound on bone growth into porous-coated implants. *J Orthop Res* **1996,** 14, (6), 901-6.

16. Heini, P. F.; Berlemann, U. Bone substitutes in vertebroplasty. *Eur Spine J* **2001,** 10 Suppl 2, S205-13.

17. Szpalski, M.; Descamps, P. Y.; Hayez, J. P.; Raad, E.; Gunzburg, R.; Keller, T. S.; Kosmopoulos, V. Prevention of hip lag screw cut-out by cement augmentation: description of a new technique and preliminary clinical results. *J Orthop Trauma* **2004,** 18, (1), 34-40.

18. Maldonado, Z. M.; Seebeck, J.; Heller, M. O.; Brandt, D.; Hepp, P.; Lill, H.; Duda, G. N. Straining of the intact and fractured proximal humerus under physiological-like loading. *J Biomech* **2003,** 36, (12), 1865-73.

19. Cassidy, C.; Jupiter, J. B.; Cohen, M.; Delli-Santi, M.; Fennell, C.; Leinberry, C.; Husband, J.; Ladd, A.; Seitz, W. R.; Constanz, B. Norian SRS cement compared with conventional fixation in distal radial fractures. A randomized study. *J Bone Joint Surg Am* **2003,** 85-A, (11), 2127-37.

20. Larsson, S. Treatment of osteoporotic fractures. *Scand J Surg* **2002,** 91, (2), 140-6.

21. Lewis, G. Injectable bone cements for use in vertebroplasty and kyphoplasty: state-of-the-art review. *J Biomed Mater Res B Appl Biomater* **2006,** 76, (2), 456-68.

22. Moroni, A.; Hoang-Kim, A.; Lio, V.; Giannini, S. Current augmentation fixation techniques for the osteoporotic patient. *Scand J Surg* **2006,** 95, (2), 103-9.

23. Wu, P.; Grainger, D. W. Drug/device combinations for local drug therapies and infection prophylaxis. *Biomaterials* **2006,** 27, (11), 2450-67.

24. Moojen, D. J.; Hentenaar, B.; Charles Vogely, H.; Verbout, A. J.; Castelein, R. M.; Dhert, W. J. In vitro release of antibiotics from commercial PMMA beads and articulating hip spacers. *J Arthroplasty* **2008,** 23, (8), 1152-6.

25. W.J.E.M.Habraken; J.G.C.Wolke; A.G.Mikos; J.A.Jansen. Injectable PLGA microsphere/calcium phosphate cements: physical properties and degradation characteristics.

J.Biomater.Sci.Polymer Edn **2006,** 17, (9), 1057-1074.

26. Ginebra, M. P.; Traykova, T.; Planell, J. A. Calcium phosphate cements: competitive drug carriers for the musculoskeletal system? *Biomaterials* **2006,** 27, (10), 2171-7.

27. Wu, F.; Su, J.; Wei, J.; Guo, H.; Liu, C. Injectable bioactive calcium-magnesium phosphate cement for bone regeneration. *Biomed Mater* **2008,** 3, (4), 44105.

28. Jarcho, M. Calcium phosphate ceramics as hard tissue prosthetics. *Clin Orthop Relat Res* **1981**, (157), 259-78.

29. A. Tofighi, S. M., P. Chakravarthy, C. Rey, D.Lee. Setting reactions involved in injectable cements based on amorphous calcium phosphate. *Key Eng. Mater.* **2000,** 192-195, 769-772.

30. Constantz, B. R.; Ison, I. C.; Fulmer, M. T.; Poser, R. D.; Smith, S. T.; VanWagoner, M.; Ross, J.; Goldstein, S. A.; Jupiter, J. B.; Rosenthal, D. I. Skeletal repair by in situ formation of the mineral phase of bone. *Science* **1995,** 267, (5205), 1796-9.

31. Takechi, M.; Miyamoto, Y.; Ishikawa, K.; Nagayama, M.; Kon, M.; Asaoka, K.; Suzuki, K. Effects of added antibiotics on the basic properties of anti-washout-type fast-setting calcium phosphate cement. *J Biomed Mater Res* **1998,** 39, (2), 308-16.

32. Ratier, A.; Gibson, I. R.; Best, S. M.; Freche, M.; Lacout, J. L.; Rodriguez, F. Setting characteristics and mechanical behaviour of a calcium phosphate bone cement containing tetracycline. *Biomaterials* **2001,** 22, (9), 897-901.

33. Otsuka, M.; Matsuda, Y.; Fox, J. L.; Higuchi, W. I. A novel skeletal drug delivery system using self-setting calcium phosphate cement. 9: Effects of the mixing solution volume on anticancer drug release from homogeneous drug-loaded cement. *J Pharm Sci* **1995,** 84, (6), 733-6.

34. Blom, E. J.; Klein-Nulend, J.; Klein, C. P.; Kurashina, K.; van Waas, M. A.; Burger, E. H. Transforming growth factor-beta1 incorporated during setting in calcium phosphate cement stimulates bone cell differentiation in vitro. *J Biomed Mater Res* **2000,** 50, (1), 67-74.

35. Habraken W.J.E.M, W. G. G. C., Mikos AG, Jansen JA. Injectable PLGA microsphere/calcium phosphate cements: physical properties and degradation characteristics. *J.Biomater.Sci.Polymer Edn* **2006,** 17, (9), 1057-1074.

36. Link, D. P.; van den Dolder, J.; van den Beucken, J. J.; Cuijpers, V. M.; Wolke, J. G.; Mikos, A. G.; Jansen, J. A. Evaluation of the biocompatibility of calcium phosphate cement/PLGA microparticle composites. *J Biomed Mater Res A* **2008,** 87, (3), 760-9.

37. Berkland, C.; Kim, K.; Pack, D. W. Fabrication of PLG microspheres with precisely controlled and monodisperse size distributions. *J Control Release* **2001,** 73, (1), 59-74.

38. Woodrow, K. A.; Cu, Y.; Booth, C. J.; Saucier-Sawyer, J. K.; Wood, M. J.; Saltzman, W. M. Intravaginal gene silencing using biodegradable polymer nanoparticles densely loaded with small-interfering RNA. *Nat Mater* **2009,** 8, (6), 526-33.

39. Panyam, J.; Labhasetwar, V. Biodegradable nanoparticles for drug and gene delivery to cells and tissue. *Adv Drug Deliv Rev* **2003,** 55, (3), 329-47.

40. Ruhe, P. Q.; Hedberg, E. L.; Padron, N. T.; Spauwen, P. H.; Jansen, J. A.; Mikos, A. G. rhBMP-2 release from injectable poly(DL-lactic-co-glycolic acid)/calcium-phosphate cement composites. *J Bone Joint Surg Am* **2003,** 85-A Suppl 3, 75-81.

41. Dutt, M.; Khuller, G. K. Chemotherapy of Mycobacterium tuberculosis infections in mice with a combination of isoniazid and rifampicin entrapped in Poly (DL-lactide-co-glycolide) microparticles. *J Antimicrob Chemother* **2001,** 47, (6), 829-35.

42. Garbuz, D. S.; Hu, Y.; Kim, W. Y.; Duan, K.; Masri, B. A.; Oxland, T. R.; Burt, H.; Wang, R.; Duncan, C. P. Enhanced gap filling and osteoconduction associated with alendronate-calcium phosphate-coated porous tantalum. *J Bone Joint Surg Am* **2008,** 90, (5), 1090-100.

43. Jensen, D. M.; Cun, D.; Maltesen, M. J.; Frokjaer, S.; Nielsen, H. M.; Foged, C. Spray drying of siRNA-containing PLGA nanoparticles intended for inhalation. *J Control Release* **2009**.

44. Luo, G.; Jin, C.; Long, J.; Fu, D.; Yang, F.; Xu, J.; Yu, X.; Chen, W.; Ni, Q. RNA interference of MBD1 in BxPC-3 human pancreatic cancer cells delivered by PLGA-poloxamer nanoparticles. *Cancer Biol Ther* **2009,** 8, (7), 594-8.

45. Hasegawa, T.; Hirota, K.; Tomoda, K.; Ito, F.; Inagawa, H.; Kochi, C.; Soma, G.; Makino, K.; Terada, H. Phagocytic activity of alveolar macrophages toward polystyrene latex microspheres and PLGA microspheres loaded with anti-tuberculosis agent. *Colloids Surf B Biointerfaces* **2007,** 60, (2), 221-8.

46. Achenbach, T. V.; Brunner, B.; Heermeier, K. Oligonucleotide-based knockdown technologies: antisense versus RNA interference. *Chembiochem* **2003,** 4, (10), 928-35.

47. Soutschek, J.; Akinc, A.; Bramlage, B.; Charisse, K.; Constien, R.; Donoghue, M.; Elbashir, S.; Geick, A.; Hadwiger, P.; Harborth, J.; John, M.; Kesavan, V.; Lavine, G.; Pandey, R. K.; Racie, T.; Rajeev, K. G.; Rohl, I.; Toudjarska, I.; Wang, G.; Wuschko, S.; Bumcrot, D.; Koteliansky, V.; Limmer, S.; Manoharan, M.; Vornlocher, H. P. Therapeutic silencing of an endogenous gene by systemic

administration of modified siRNAs. *Nature* **2004,** 432, (7014), 173-8.

48.   Cejka, D.; Losert, D.; Wacheck, V. Short interfering RNA (siRNA): tool or therapeutic? *Clin Sci (Lond)* **2006,** 110, (1), 47-58.

49.   Wang, Y.; Grainger, D. W. siRNA knock-down of RANK signaling to control osteoclast-mediated bone resorption. *Pharm Res* **2010,** 27, (7), 1273-84.

50.   Abbas, A. O.; Donovan, M. D.; Salem, A. K. Formulating poly(lactide-co-glycolide) particles for plasmid DNA delivery. *J Pharm Sci* **2008,** 97, (7), 2448-61.

51.   Walter, E.; Dreher, D.; Kok, M.; Thiele, L.; Kiama, S. G.; Gehr, P.; Merkle, H. P. Hydrophilic poly(DL-lactide-co-glycolide) microspheres for the delivery of DNA to human-derived macrophages and dendritic cells. *J Control Release* **2001,** 76, (1-2), 149-68.

52.   Habraken, W. J.; Zhang, Z.; Wolke, J. G.; Grijpma, D. W.; Mikos, A. G.; Feijen, J.; Jansen, J. A. Introduction of enzymatically degradable poly(trimethylene carbonate) microspheres into an injectable calcium phosphate cement. *Biomaterials* **2008,** 29, (16), 2464-76.

53.   J´an Majling, P. Z. a., Angela Palov´a, and Stefan Svet´ık. Sintering of the ultrahigh pressure densified hydroxyapatite monolithic xerogels. *Journal of Materials Research* **1997,** 12, (1), 198-202.

54.   Yang, K. H.; Won, J. H.; Yoon, H. K.; Ryu, J. H.; Choo, K. S.; Kim, J. S. High concentrations of pamidronate in bone weaken the mechanical properties of intact femora in a rat model. *Yonsei Med J* **2007,** 48, (4), 653-8.

55.   Sebba, A. Osteoporosis: how long should we treat? *Curr Opin Endocrinol Diabetes Obes* **2008,** 15, (6), 502-7.

56.   Nakagawa, N.; Kinosaki, M.; Yamaguchi, K.; Shima, N.; Yasuda, H.; Yano, K.; Morinaga, T.; Higashio, K. RANK is the essential signaling receptor for osteoclast differentiation factor in osteoclastogenesis. *Biochem Biophys Res Commun* **1998,** 253, (2), 395-400.

57.   Li, J.; Sarosi, I.; Yan, X. Q.; Morony, S.; Capparelli, C.; Tan, H. L.; McCabe, S.; Elliott, R.; Scully, S.; Van, G.; Kaufman, S.; Juan, S. C.; Sun, Y.; Tarpley, J.; Martin, L.; Christensen, K.; McCabe, J.; Kostenuik, P.; Hsu, H.; Fletcher, F.; Dunstan, C. R.; Lacey, D. L.; Boyle, W. J. RANK is the intrinsic hematopoietic cell surface receptor that controls osteoclastogenesis and regulation of bone mass and calcium metabolism. *Proc Natl Acad Sci U S A* **2000,** 97, (4), 1566-71.

58.   Kong, Y. Y.; Yoshida, H.; Sarosi, I.; Tan, H. L.; Timms, E.; Capparelli, C.; Morony, S.;

Oliveira-dos-Santos, A. J.; Van, G.; Itie, A.; Khoo, W.; Wakeham, A.; Dunstan, C. R.; Lacey, D. L.; Mak, T. W.; Boyle, W. J.; Penninger, J. M. OPGL is a key regulator of osteoclastogenesis, lymphocyte development and lymph-node organogenesis. *Nature* **1999,** 397, (6717), 315-23.

59. Choung, S.; Kim, Y. J.; Kim, S.; Park, H. O.; Choi, Y. C. Chemical modification of siRNAs to improve serum stability without loss of efficacy. *Biochem Biophys Res Commun* **2006,** 342, (3), 919-27.

60. Wang, D. A.; Narang, A. S.; Kotb, M.; Gaber, A. O.; Miller, D. D.; Kim, S. W.; Mahato, R. I. Novel branched poly(ethylenimine)-cholesterol water-soluble lipopolymers for gene delivery. *Biomacromolecules* **2002,** 3, (6), 1197-207.

61. Jiang, G.; Park, K.; Kim, J.; Kim, K. S.; Oh, E. J.; Kang, H.; Han, S. E.; Oh, Y. K.; Park, T. G.; Kwang Hahn, S. Hyaluronic acid-polyethyleneimine conjugate for target specific intracellular delivery of siRNA. *Biopolymers* **2008,** 89, (7), 635-42.

62. Capan, Y.; Woo, B. H.; Gebrekidan, S.; Ahmed, S.; DeLuca, P. P. Preparation and characterization of poly (D,L-lactide-co-glycolide) microspheres for controlled release of poly(L-lysine) complexed plasmid DNA. *Pharm Res* **1999,** 16, (4), 509-13.

63. Patil, Y.; Panyam, J. Polymeric nanoparticles for siRNA delivery and gene silencing. *Int J Pharm* **2009,** 367, (1-2), 195-203.

64. Alonso, M. J.; Cohen, S.; Park, T. G.; Gupta, R. K.; Siber, G. R.; Langer, R. Determinants of release rate of tetanus vaccine from polyester microspheres. *Pharm Res* **1993,** 10, (7), 945-53.

65. Wang, D.; Robinson, D. R.; Kwon, G. S.; Samuel, J. Encapsulation of plasmid DNA in biodegradable poly(D, L-lactic-co-glycolic acid) microspheres as a novel approach for immunogene delivery. *J Control Release* **1999,** 57, (1), 9-18.

66. Bajammal, S. S.; Zlowodzki, M.; Lelwica, A.; Tornetta, P., 3rd; Einhorn, T. A.; Buckley, R.; Leighton, R.; Russell, T. A.; Larsson, S.; Bhandari, M. The use of calcium phosphate bone cement in fracture treatment. A meta-analysis of randomized trials. *J Bone Joint Surg Am* **2008,** 90, (6), 1186-96.

67. Larsson, S.; Bauer, T. W. Use of injectable calcium phosphate cement for fracture fixation: a review. *Clin Orthop Relat Res* **2002**, (395), 23-32.

68. Link, D. P.; van den Dolder, J.; Jurgens, W. J.; Wolke, J. G.; Jansen, J. A. Mechanical evaluation of implanted calcium phosphate cement incorporated with PLGA microparticles. *Biomaterials* **2006,** 27, (28), 4941-7.

69. Bohner, M.; Baroud, G. Injectability of calcium phosphate pastes. *Biomaterials* **2005,** 26, (13), 1553-63.

CHAPTER 5

SUMMARY AND PROPOSED FUTURE WORK

This dissertation research focuses on the development of a novel clinically relevant approach to improve osteoporotic fragility fracture healing using locally delivered small interfering RNA (siRNA) to osteoporotic sites using clinically familiar interventional technology. Two cellular targets have been investigated for their efficacy in inhibiting osteoclast-mediated excessive bone resorption. A combination device strategy has been designed to introduce siRNA as a therapeutic approach locally to bone.

<u>Major Accomplishments of This Dissertation Research</u>

○　Both osteoclast precursors and mature osteoclasts can be successfully transfected by siRNA in serum cultures without toxicity; both the RANK gene and protein expression can be successfully knocked down by RANK siRNA; both osteoclast formation and specific functions can be significantly suppressed without toxicity in vitro. Significantly, our in vitro studies support RANK as a potent and attractive target for siRNA control in osteoporosis fracture healing.

○　We first reported the knockdown of the molecular target of clinically common nitrogen-containing bisphosphonates, farnesyl pyrophosphate synthase (FPPS) using siRNA, and compared these effects to alendronate, both on osteoclasts and osteoblasts in

similar cultures. Results from both the culture of primary murine bone marrow cell-induced osteoclasts and MC3T3-E1 preosteoblast cells showed that siRNA targeting FPPS has substantial effects at the cellular level of inhibiting excessive cell-based bone resorption and increasing overall bone mass maintenance by its effects on both osteoblasts and osteoclasts, suggesting clinical potential.

○ We have designed a novel strategy to deliver anti-RANK siRNA-incorporated PLGA particles from injectable calcium phosphate cement (CPC) carriers to demonstrate their efficacy in inhibiting osteoclast-mediated bone resorption in vitro.

Proposed Future Work

With several important in vitro studies accomplished as significant proof-of-concept, the next step moves to critical in vivo evaluations of the designed PLGA/CPC system using an animal model of osteoporosis. Two ovariectomized rat bone defect models are proposed for this extension. The objective of this in vivo work is to show biological transformations in osteoporotic bone from this therapeutics approach. Expected deliverables include proof of concept of the local siRNA delivery approach for reversal of surgically imposed osteopenia and loss of bone mineral density in an animal model, and dose-response evaluations to permit extrapolation to human bone therapies.

Human osteoporosis is defined by World Health Organization as BMD showing 2.5 standard deviations (SD) below the average value of healthy adults (T-score). Laboratory animals models for osteopenia include rodents (rats, mice, rabbits), dogs, nonhuman primates (monkeys, large

apes), and ruminants (sheep). Each species exhibits strengths and weaknesses in modeling this disease, and each species has limited appropriate characteristics for modeling certain aspects of bone demineralization diseases. As osteoporosis is a hormonally induced disease occurring late in life, most animals do not experience osteoporosis as they die soon after their reproductive maturity is finished. Since the advent of improved healthcare and nutrition in most societies in the 20th century, most humans are an exception to this rule, living decades after their reproductive potential is completed. Only the larger apes can manifest osteopenia at advanced ages, such as monkeys.[1] BMD decreases are difficult to compare among different species due to different methods and equipments used in studies. However, BMD reduction by ovariectomy and calcium-restricted diet in animals is lower than osteoporotic humans.[1] In addition, human osteoporotic vertebral bodies are quite different from animal species. Interspecies differences in bone architecture result from different anatomical features and weight bearing, and site-specific differences should be carefully considered. Hence, use of animal models for a strictly human disease is always difficult. Ovariectomized rats have been studied most as approximate osteoporotic models. Estrogen deficiency-induced rat skeletal bone loss mimics postmenopausal cancellous bone loss. However, the absence of a Haversian system in cortical bone and different bone remodeling in young rats largely limit its application.[2] Nonhuman primates, naturally developing osteoporosis when living to advanced age, are closer to human physiological conditions. Ovariectomy can result in a bone loss of -1.4SD compared with control animals.[3] Monkeys can develop age-related osteopenia,[4] but monkeys must be over 30 years old, which largely restricts the practical application of this experimental model.[5] This nonhuman primate

model was pivotal for Mercks' approval of bisphosphonate drugs to allow them to proceed to human trials. However, problems of cost, handling and ethics largely restrict use of this nonhuman primate model. Using sheep, decreases in BMD or bone mass were reported at distal femur and spine in ovariectomized sheep model.[1] Additionally, sheep have intrinsic advantages in their ease of maintenance and more human-relevant bone size and anatomy/physiology compared with other large animal models.[6] A major problem in using the sheep for disease models requiring genetic monitoring is that its genome database is not as well-developed as other species. Dog models are more appropriate for intracortical bone remodeling compared to other animal models and well-established.[5] However, ovariectomy does not change BMD values in dogs.[1] Compared to other species, rats and mice are much less expensive and easy to maintain, and widely available both as in-bred wildtypes and numerous mutant knockouts and knockins. Some transgenic mouse models, such as OPG knockout mutants, exhibit osteoporosis. Among various osteopenia models, the well-established ovariectomized (OVX) wildtype (Wistar) rat model is the most commonly used due to its pathologic reproducibility and relative efficiency.[5] Ovariectomy in rats was reported to reduce mean BMD by about 7% compared to controls in the femur and 16% reduction in bone mechanical properties at the femoral neck.[1] Moreover, the rat is a well-established model for bone cement use, fracture healing and bone implantation with a relatively short lifespan and well-characterized skeleton.[1] Substantial published data available for this OVX rat model make it preferred for preliminary in vivo therapy studies in experimental therapies. After important proof-of-concept in rodentia, a large animal model is better justified but not simple to accomplish.

Future work to evaluate locally injected RANK siRNA-encapsulated PLGA particle delivery in

CPC carriers to improve healing of large segmental bone defects in osteoporotic rat femurs under external fixation. The large segmental femoral defect model is well-established[7-9] and used to evaluate bone healing in long bone osteoporosis under external fixation. The AO Foundation's Rat-Fix™ commercial external fixator tooling kit also makes this the model of choice for fragility fracture modeling under human-relevant orthopedic fixation conditions. The objective of this in vivo work is to test the improvement of large segmental bone defect healing by our modified CPC.

A significant 40% reduction in the cross-sectional area of fracture callus was found in osteoporotic rats, and 23% reduction in bone mineral density (BMD) in their bone healing was reported between the osteotomized and wildtype rat femurs.[10] Reduced rates of fracture callus are induced by ovariectomy in rats.[11] A study of ovariectomized sheep showed a dramatic 33% decrease in torsional stiffness in healed osteoporotic fractured animals.[12] Osteoporosis bone mineral density is expected 6 weeks after the ovariectomy in the rat as a concomitant 60% reduction in femur bone mineral density was reported.[13] Therefore, 6-week postovariectomy is chosen as the starting point for in vivo surgery models.

The large segmental rodent defect model has been extensively used for evaluating bone grafting materials [7, 8, 14, 15] and hence chosen to test our modified CPC for bone regeneration in the context of rat osteoporosis fragility fracture. A 5 mm mid-diaphyseal segmental defect will be created, since published data show 100% femoral nonunion at 5 mm after 9 weeks in the rat.[7, 8] Furthermore, it has been shown that 9 weeks are sufficient to show formation of bone shell and significant bone healing in the model treated with rhBMP-2.[8] Therefore, 5 mm excision and 9 week experimental duration are initially chosen for our studies. However, we realize that longer periods

might be required to differentiate significantly from controls since callus and shell are not mature bone healing modes. Bone healing efficacy using the proposed CPC formulation with siRNA/PLGA particles will be compared to 1) CPC alone, 2) CPC with unloaded PLGA particles, and 3) CPC with two siRNA incorporation levels (see Table 5.1). Rats will be assigned (n=42/cohort, see Section 2.3) to each group: nine rats for histological examination/cohort (3 rats per time point at three time points (3-, 6- and 9-week sacrifice endpoints),[7, 8] and 33 rats for all other analyses. Group sample size was determined from power analysis based on torsional strength analyses from a previously study using the same rat model.[8] This power analysis determined that, with a significant difference of torsional strength between rats without treatment and CPC alone-treated groups, and the alpha set at 0.05, 28 animals per group provided a power above 80%. An additional 20% increase (5 rats) is included to account for pilot studies, inevitable animal loss due to infection, transport and other unforeseen complications.

Methods

PLGA/CPC composite preparation.   PLGA microparticles prepared as described in Chapter 4 (Materials and Methods-PLGA particle preparation) will be sterilized by ethylene oxide, assayed

TABLE 5.1 LARGE SEGMENTAL DEFECT OVARIECTOMIZED RAT COHORT DESIGNS FOR SIRNA DELIVERY FROM CPC MATRICES

Group 1	Sham control	Segmental defect created but the segmental bone is replaced into the defect site
Group 2	Control A	Defect with 100% CPC implant alone
Group 3	Control B	Defect with CPC implant with 15% w/w nonloaded 5μm PLGA particles
Group 4	Treated/high dose	Defect with CPC with 20% w/w 5μm siRNA/PLGA particles
Group 5	Treated/low dose	Defect with CPC with 15% w/w 5μm siRNA/PLGA particles

for LPS contamination, tested for siRNA bioactivity in vitro as established on osteoclast cultures and reconstituted with CPC powders for injection as described in D.2.A. A glass mold of 4 mm (diameter) × 5 mm (height) with a central hole of 1.5 mm will be used for cement cylinder preparation.

Animal model preparation.   Osteoporotic female Wistar rats (n=210 total, ~250g) will be used, ovariectomized at the age of 5 months. A bilateral ovariectomy using a dorsal approach will be performed following well-established protocols.[16] Briefly, after anaesthesia, a 1 cm incision will be made on the rat's back.   Both ovaries will be excised and fallopian tubes ligated using absorbable suture material. The peritoneum and muscle will be sutured and the skin closed with wound clips. Osteopenia is expected 6 weeks postovariectomy as a reduction in femur bone mineral density of 60% assessed in-house by dual-energy x-ray absorptiometry (DEXA, Hologic QDR-1000/W).[13] Bone surgeries to establish defects and to place various CPC implants will be performed (see below) after that time point. All rats will be housed individually in cages in the University of Utah-approved animal facilities and have access to standard medical care, calcium-deficient chow and water ad libitum.

Femoral defect surgical protocols.   One day before surgery, all rats will undergo dual-energy X-ray absorptiometry (Core facility, University of Utah) of both femurs and basal bone mineral density will be recorded. Each rat will receive one implant in the right femur with external fixation. The entire surgical protocol will be performed as routinely described.[7-9, 14] Rats will be anesthetized by intraperitoneal injection of sodium pentobarbital (50 mg/kg) prior to the operation. A 3 to 4 cm longitudinal incision will be made along the right femoral axis.   An external fixator six-hole 1.2 mm

LC-DCP mini-plate (Mouse-Fix™, AO/ASIF Synthes, PA, USA, see Figure 5.1) will be fixed to the

anterior portion of the femur with four threaded Kirchner pins 1.2 mm in diameter (Zimmer). A 5

mm middiaphyseal segmental defect will then be created using a dental burr. The operating field

will be irrigated thoroughly, the cement cylinder implants inserted into the defect and the wound

closed with sutures.

Evaluation of siRNA-mediated bone defect healing

Radiographic evaluation.   At 3, 6 and 9 weeks postsurgery, rats will be anesthetized and live

radiographs and microCT scans of the right femur will be collected (School of Medicine Core

facilities, University of Utah). The criterion of a united defect is the observation of continuity of

femurs restored by a bone shell or bridging callus formed from radiographs and 3-D CT imaging.

The number of united femurs in each group at each time point will be recorded.

Explant histology/histomorphometry: At each experimental time point (3, 6 and 9 weeks

postsurgery), three rats will be sacrificed and tissue from the area of the defect and the adjacent

bone will be removed and preserved using a well-established procedure: fixation in formalin, serial
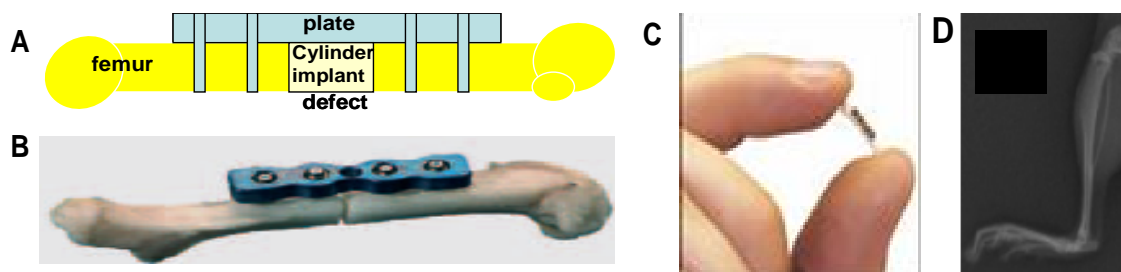

Figure 5.1: (A) Concept of femoral large segmental rat defect model with the RatFix™ LC-DCP plate external fixation stabilizer and implanted siRNA-loaded CPC bone cement device and (B) MouseFix™ plate on explanted murine femur. (C) AO Foundation's Mousefix-ator plate, actual size, and (D) micro-CT image of the plate on murine femur.

alcohol dehydration and polymerization in MMA. Sections with 500 μm thickness will be cut parallel to the long axis of the bone and further polished to 10 μm (ARUP, University of Utah) for histochemistry. Three sections will be made for each implant from central sections, and some stained with hematoxylin and eosin for general histological analysis. Others will be immediately stained with methylene blue/basic fuchsin for identification of cement line.[17] Specifically, thin sections will be first incubated in mouse antirat RANK for 1 hour followed by peroxidase conjugated rabbit antimouse IgG incubation for half an hour. Then 3,3'-diaminobenzidine tetrahydrochloride will produce a brownish color by reaction with peroxidase. Methylene blue/basic fuchsin will then be stained. After washing in PBS, sections will be subjected to TRAP assay (marker for osteoclasts). All sections will be investigated by light microscopy to analyze bone formation, RANK expression (immunohistochemistry) and osteoclast numbers (staining and antibody markers) in the periprosthetic and defect areas. Ten images from each section will be averaged for numbers of osteoclasts per image.

Dual energy x-ray absorptiometry.   At week 9, 33 rats from each group will be sacrificed. Both femurs will be harvested, wrapped in saline-saturated filter paper and stored in sealed plastic bags at 4°C until testing.[7] The surrounding soft tissue and the fixation plates together with pins will be removed. The harvested femurs will be subjected to dual energy x-ray absorptiometry (Hologic QDR-1000/W, School of Medicine Core facility, University of Utah). Bone specimens will be oriented with the anterior-posterior plane along the scanner beam axis. A constant area of 5×10 mm, including the defect region, will be scanned and analyzed. Data of BMD and area of bone formation (BA) will be obtained by software analysis.

microCT determination of bone defect healing quality. Postmortem μCT at final postmortem follow-up (General Electric EVS-RS9 micro-CT, Utah School of Medicine Core facility, or S. Miller lab) will be used to produce a cross-sectional area of callus relative to bone and high-resolution (36 micron voxel) images of bridging callus, defect site mineralization and polar moment of inertia in femurs. The micro-CT data will be analyzed with imaging software (Northern Eclipse, PA) to determine any differences in defect sizes and bone mineralization amounts.[18, 19]

Explanted femur mechanical testing. Following absorptiometry and microCT analyses, femurs will be mechanically tested. Both bone ends of each femur will be placed in purpose-built aluminum potting fixtures with a height of 10 mm each. The fixtures will then be filled with plastic padding (Bondo), so that the bone ends became immovably embedded, leaving the remaining section of the femurs between the fixtures free for testing. A custom jig will be used to ensure correct alignment of the bone axis along the loading axis of the testing machine. All specimens will be tested to failure in torsion at room temperature on an electromechanical testing machine (MZ500S, Maruto Instrument Co., Japan) at a rate of 6°/sec, with no axial load during the testing. Values for angulation and torque will be collected 50 times per second until failure, using commercially available software (LabVIEW, National Instruments, Texas). The collected data will be digitally stored and will include the variables of time, angulation and torque. Based on the data collected, maximum torque, torsion at failure (angulation at failure) and torsional stiffness will be calculated. The torsional rigidity will be calculated by using the angulation and torque data to define a slope, from which the tangent of the maximal slope for each sample will be used to define the torsional stiffness. The mechanical properties of the right femurs will be first compared with

their contralateral left femurs to reduce the effect of animal variation in treated groups and then compared with the right femurs from the other groups.

Future work to deliver PLGA microparticles containing RANK siRNA from calcium phosphate cement (CPC) in an in vivo rat bone hole osteopenia model.   The potential issue with femoral large segmental defect model is that bone defect is generated at the diaphysis which is composed largely of cortical bone.   This dense bone may not show significant bone loss in this area during experimental period, even after ovariectomization as cancellous bone is the primary issue in osteoporosis. Therefore, another rat model with bone defect at a cancellous bone area that can be resorbed rapidly is proposed as an alternative. Protocols for preparing ovariectomized rats, animal grouping and postsurgery evaluation will be the same as femoral large segmental rat defect model.

Surgical protocol.   The bone mineral density (BMD), CT scans and x-rays of all experimental rats' right femurs will be recorded by DEXA and CT scanner (GE EVS-RS9, Core facility, University of Utah) before surgery. The surgical protocol has already been described in detail.[20] Rats will be anesthetized by intraperitoneal injection of sodium pentobarbital (50 mg/kg) prior to the operation. Each rat will receive one cement injection in the right femur. The untreated left femur will be used as control. The midline of the rat right knee will be cut, and patella will be lifted. A drill with 1.8 mm diameter will be used to remove the medulla ossium from the intercondylar area to expose the intertrochanteric area. At the same time, CPC will be prepared. TSK Surecut Biopsy Needles (TochigiSeiko, Japan) will be used for injection. After the injection of the cement composite, the wound will be closed with sutures. DEXA and CT scan will be performed on the next day of surgery

for rats' implanted femur. Six months after implantation, all rat right femurs will be scanned by

DEXA and CT again for BMD and sacrificed by CO_2 asphyxiation.   Both femurs will be harvested

and all soft tissues removed. All specimens will be wrapped in saline-saturated filter paper and

stored in sealed plastic bags at $-20^{\circ}C$ until testing.

Animal grouping.   Group sample size was determined from power analysis based on

torsional strength analyses from a previously study using the same rat model.[8] This power

analysis determined that, with a significant difference of torsional strength between rats without

treatment and CPC alone-treated groups, and the alpha set at 0.05, 28 animals per group

provided a power above 80%. An additional 20% increase (5 rats) is included to account for pilot

studies, inevitable animal loss due to infection, transport and other unforeseen complications. CPC

without modification will serve as control.

Anticipated results.   The successful local siRNA bone delivery system is anticipated to show:

(1) resorption of the CPC matrix, and 2) newly formed bone around the cement implant at 3 or 6

weeks in siRNA-treated groups. In case of the first model mentioned, a large bone shell forms

(microCT) to bridge these defects; in contrast, fracture nonunions should be significant in control A

and B groups, (3) treated groups should show significantly higher BMD and/or bone formation than

the other groups, (4) a significant resorption of the cement and incorporation of the remaining

matrix into the bone tissue is expected in both models, (5) a significantly reduced expression of

RANK and number of osteoclasts should be evident in the periprosthetic areas, and (6) treated

femurs in treated groups are expected to show a higher maximum torque, failure torque and

torsional stiffness than the other groups.   Should CPC not provide sufficient dosing or release

kinetics in vivo, alternative siRNA injectable carriers will be studied.

References

1.   Egermann, M.; Goldhahn, J.; Schneider, E. Animal models for fracture treatment in osteoporosis. *Osteoporos Int* **2005,** 16 Suppl 2, S129-38.

2.   Miller, S. C.; Wronski, T. J. Long-term osteopenic changes in cancellous bone structure in ovariectomized rats. *Anat Rec* **1993,** 236, (3), 433-41.

3.   Kasra, M.; Grynpas, M. D. Effect of long-term ovariectomy on bone mechanical properties in young female cynomolgus monkeys. *Bone* **1994,** 15, (5), 557-61.

4.   Pope, N. S.; Gould, K. G.; Anderson, D. C.; Mann, D. R. Effects of age and sex on bone density in the rhesus monkey. *Bone* **1989,** 10, (2), 109-12.

5.   Turner, R. T.; Maran, A.; Lotinun, S.; Hefferan, T.; Evans, G. L.; Zhang, M.; Sibonga, J. D. Animal models for osteoporosis. *Rev Endocr Metab Disord* **2001,** 2, (1), 117-27.

6.   Turner, A. S. The sheep as a model for osteoporosis in humans. *Vet J* **2002,** 163, (3), 232-9.

7.   Lee, S. C.; Shea, M.; Battle, M. A.; Kozitza, K.; Ron, E.; Turek, T.; Schaub, R. G.; Hayes, W. C. Healing of large segmental defects in rat femurs is aided by RhBMP-2 in PLGA matrix. *J Biomed Mater Res* **1994,** 28, (10), 1149-56.

8.   Ohura, K.; Hamanishi, C.; Tanaka, S.; Matsuda, N. Healing of segmental bone defects in rats induced by a beta-TCP-MCPM cement combined with rhBMP-2. *J Biomed Mater Res* **1999,** 44, (2), 168-75.

9.   Yasko, A. W.; Lane, J. M.; Fellinger, E. J.; Rosen, V.; Wozney, J. M.; Wang, E. A. The healing of segmental bone defects, induced by recombinant human bone morphogenetic protein (rhBMP-2). A radiographic, histological, and biomechanical study in rats. *J Bone Joint Surg Am* **1992,** 74, (5), 659-70.

10.   Namkung-Matthai, H.; Appleyard, R.; Jansen, J.; Hao Lin, J.; Maastricht, S.; Swain, M.; Mason, R. S.; Murrell, G. A.; Diwan, A. D.; Diamond, T. Osteoporosis influences the early period of fracture healing in a rat osteoporotic model. *Bone* **2001,** 28, (1), 80-6.

11.   Walsh, W. R.; Sherman, P.; Howlett, C. R.; Sonnabend, D. H.; Ehrlich, M. G. Fracture healing in a rat osteopenia model. *Clin Orthop Relat Res* **1997**, (342), 218-27.

12. Lill, C. A.; Hesseln, J.; Schlegel, U.; Eckhardt, C.; Goldhahn, J.; Schneider, E. Biomechanical evaluation of healing in a non-critical defect in a large animal model of osteoporosis. *J Orthop Res* **2003,** 21, (5), 836-42.

13. Bagi, C. M.; Ammann, P.; Rizzoli, R.; Miller, S. C. Effect of estrogen deficiency on cancellous and cortical bone structure and strength of the femoral neck in rats. *Calcif Tissue Int* **1997,** 61, (4), 336-44.

14. Reichert, J. C.; Saifzadeh, S.; Wullschleger, M. E.; Epari, D. R.; Schutz, M. A.; Duda, G. N.; Schell, H.; van Griensven, M.; Redl, H.; Hutmacher, D. W. The challenge of establishing preclinical models for segmental bone defect research. *Biomaterials* **2009,** 30, (12), 2149-63.

15. Vogelin, E.; Jones, N. F.; Huang, J. I.; Brekke, J. H.; Lieberman, J. R. Healing of a critical-sized defect in the rat femur with use of a vascularized periosteal flap, a biodegradable matrix, and bone morphogenetic protein. *J Bone Joint Surg Am* **2005,** 87, (6), 1323-31.

16. Plas-Roser, S.; Aron, C. New data concerning the control by the adrenals of sexual receptivity in the rat. *Physiol Behav* **1977,** 19, (1), 57-60.

17. Gruber, H. E.; Marshall, G. J.; Kirchen, M. E.; Kang, J.; Massry, S. G. Improvements in dehydration and cement line staining for methacrylate embedded human bone biopsies. *Stain Technol* **1985,** 60, (6), 337-44.

18. Kalpakcioglu, B. B.; Morshed, S.; Engelke, K.; Genant, H. K. Advanced imaging of bone macrostructure and microstructure in bone fragility and fracture repair. *J Bone Joint Surg Am* **2008,** 90 Suppl 1, 68-78.

19. Strube, P.; Mehta, M.; Baerenwaldt, A.; Trippens, J.; Wilson, C. J.; Ode, A.; Perka, C.; Duda, G. N.; Kasper, G. Sex-specific compromised bone healing in female rats might be associated with a decrease in mesenchymal stem cell quantity. *Bone* **2009,** 45, (6), 1065-72.

20. Kajiwara, H.; Yamaza, T.; Yoshinari, M.; Goto, T.; Iyama, S.; Atsuta, I.; Kido, M. A.; Tanaka, T. The bisphosphonate pamidronate on the surface of titanium stimulates bone formation around tibial implants in rats. *Biomaterials* **2005,** 26, (6), 581-7.

CHAPTER 6

DEVICE-BASED LOCAL DELIVERY OF SIRNA AGAINST MAMMALIAN

TARGET OF RAPAMYCIN (MTOR) IN A MURINE SUBCUTANEOUS

IMPLANT MODEL TO INHIBIT FIBROUS ENCAPSULATION

Abstract

Fibrous encapsulation of surgically implanted devices is associated with elevated proliferation and activation of fibroblasts in tissues surrounding these implants, frequently causing foreign body complications. Here we test the hypothesis that inhibition of the expression of mammalian target of rapamycin (mTOR) in fibroblasts can mitigate the soft tissue implant foreign body response by suppressing fibrotic responses around implants. In this study, mTOR was knocked down using small interfering RNA conjugated with branched cationic polyethylenimine (bPEI) in fibroblastic lineage cells in serum-based cell culture as shown by both gene and protein analysis. This mTOR knockdown led to an inhibition in fibroblast proliferation by 70% and simultaneous down-regulation in the expression of type I collagen in fibroblasts in vitro. These siRNA/bPEI complexes were released from poly(ethylene glycol) (PEG)-based hydrogel coatings surrounding model polymer implants in a subcutaneous rodent model in vivo. No significant reduction in fibrous capsule

thickness and mTOR expression in the foreign body capsules was observed. Observed siRNA inefficacy in this in vivo implant model was attributed to siRNA dosing limitations in the gel delivery system, and lack of targeting ability of the siRNA complex specifically to fibroblasts. While in vitro data supported mTOR knockdown in fibroblast cultures, in vivo siRNA delivery must be further improved to produce clinically relevant effects on fibrotic encapsulation around implants.

Introduction

The foreign body reaction (FBR) at the tissue/material interface commonly contributes to abnormal inflammation, wound healing responses and tissue fibrosis without effective mitigation.[1,2] In general, monocytes/macrophages are activated at implant surfaces and modulate local host fibroblast function, contributing to often-excessive deposition of collagen matrix around implanted materials (fibrotic capsule), a component of the FBR.[1,3] Recent work [4] demonstrated that macrophage fusion observed around implants alone does not necessarily produce implant fibrotic encapsulation. Instead, an alternative hypothesis is that fibro-proliferation is regulated by growth factors secreted by activated macrophages.[3,5,6] Fibrogenesis induced by implants is characterized by macrophage activation and associated elevated proliferation and activation of fibroblasts that up-regulate collagen production. Therefore, control of inflammation around implants by locally released drugs to reduce cell activation and limit collagen encapsulation of implanted biomaterials has been reported.[7-9]

Mammalian target of rapamycin (mTOR) plays a critical role in cell cycle regulation. Rapamycin, a known inhibitor for mTOR,[10] can inactivate mTOR specifically. Because mTOR

regulates cell proliferation, it has been extensively investigated as a potent target for both anticancer [11] and antirestenotic [12] therapies. Inhibition of mTOR in fibroblasts influences not only proliferation but also collagen production.[13, 14] Rapamycin and its analogues are reported to effectively prevent cardiac and pulmonary fibrosis in vivo. [15, 16] These previous reports describing modulation of mTOR in fibroblasts indicate that mTOR could also be a potent target to prevent implant-induced fibrosis in the context of the FBR.

RNAi is a powerful tool to knock down specific mRNA expression levels by exploiting a natural intracellular regulatory phenomenon in mammalian species.[17-19] Gene silencing using siRNAs has many potential therapeutic applications.[20] However, RNAi technology has not yet been used clinically largely due to challenges in dosing and effective targeted siRNA delivery systems. Local or topical siRNA therapeutics have been most actively investigated and successful delivery approaches include ocular delivery, respiratory delivery, CNS delivery, skin delivery and vaginal delivery where local delivery accesses cell target populations directly.[21-25] One unexplored and promising delivery route is via combination implantable devices for local drug delivery.[26] We therefore demonstrate device-based local delivery of siRNA, testing the hypothesis that delivery of mTOR siRNA from poly(ethylene glycol) (PEG)-based hydrogel-coated biomaterials can suppress collagen encapsulation elicited from a soft tissue implant FBR.

Materials and Methods

Branched polyethylenimine (bPEI) (m.w..: 25,000) and dithiothreitol (DTT) were obtained from Sigma-Aldrich (USA). Poly(ethylene glycol) dimethacrylate (PEGDM; m.w.: 7500) was synthesized

as reported previously.[27] RNase-free water was prepared using diethyl pyrocarbonate (DEPC) (Sigma-Aldrich). All siRNA molecules were purchased from Dharmacon (CO, USA).

Methods

Preparation of siRNA/bPEI complexes.   To prepare siRNA/bPEI complexes at various anion/cation charge (NP) ratios, 2 µl of 10 µM mTOR siRNA aqueous solution (sense: GCG GAU GGC UCC UGA CUA UUU, antisense: AUA GUC AGG AGC CAU CCG CUU) was mixed with 2 µl of bPEI solutions of different concentrations (0.016-0.64 µg). The complex mixed solutions were kept at room temperature for 20 minutes. Then 4 µl of each mixture was electrophoresed using ethidium bromide-stained TBE-based 2% agarose gels run at 80V for 20 minutes, followed by visualization with UV light to assess the siRNA-bPEI complex formation.

Cell culture and siRNA transfection in vitro.   Murine NIH 3T3 fibroblasts (American Type Culture Collection, ATCC) were plated at 3×10^4 cells/well in a 12-well plate in Dulbecco's modified Eagle's medium (DMEM, GIBCO) supplemented with 10% heat-inactivated fetal bovine serum (FBS, Hyclone®, USA) and 1% penicillin-streptomycin (GIBCO), defined for all cell cultures as "complete media", at 37^oC with 5% CO_2 overnight. Cell transfections with siRNA/bPEI complexes at fixed NP ratios in complete media were performed subsequently. siRNA/bPEI complexes for each well are prepared by mixing 7 ul of 20 µM siRNA aqueous solution with 4.48 µl, 2.24 µl, 1.12 µl and 0 µl (NP 20, 10, 5 and 0) of 1mg/ml bPEI, respectively, in a total volume of 18 µl with RNase-free water. After incubation at room temperature for 20 minutes, complete media was added to achieve the final volume of 1ml, yielding a final concentration of siRNA in each well of

140nM. Cell siRNA transfections were always performed in complete media. After 24 hours incubation at 37^oC under 5% CO_2, culture media was refreshed with 1ml complete media and the transfected cells were further incubated.

Cell cytotoxicity and proliferation.   3T3 murine fibroblasts were seeded at 3×10^3 cells/well in 96-well plates in complete media. After overnight incubation, cells were transfected with mTOR siRNA/bPEI complexes at different NP ratios (1, 2, 5, 10, 20 and 40 prepared as described above) in complete media, maintaining siRNA concentration at 140nM. Cytotoxicity of the siRNA/bPEI complexes was determined at 24 hours after initial transfection using the CellTiter 96 Aqueous One Solution Cell Proliferation Assay (Promega, USA). Media for each well was replaced with 100μl fresh complete media containing 20μl of Cell Titer 96 Aqueous One Solution including three wells without cells for background subtraction. Cells were then incubated at 37^oC for 2 hours and optical absorbance at 490nm was then determined using a plate reader (TECAN GENIOS Plus). To evaluate mTOR siRNA effects on cell proliferation, cells were plated at 3×10^4 cells/well in 6-well plates and transfected with mTOR siRNA/bPEI complexes at an NP ratio of 20 in complete media. Non-targeting siRNA/bPEI complexes with the same NP ratio were used as control. Cultures were refreshed with complete media 24 hours later. After incubation at 37^oC for 5 days, relative numbers of cells in each well were determined using the Cell Proliferation Assay (Promega, USA). CellTiter 96 solution-containing media was transferred to 96-well plates for optical reading at 490 nm. In addition, cultured cells were imaged at Day 5 with phase contrast microscopy prior to this assay.

Western immunoblotting.   Cells were lysed by using M-PER Mammalian Protein Extraction reagent (Pierce, USA) with 1X Halt^{TM} protease inhibitor cocktail (Pierce). Insoluble material was

removed by centrifuging at 15,000 rpm at 4°C for 5 minutes after 20 minutes on ice. Protein

concentrations were measured with the Bio-Rad protein assay system (Bio-Rad, USA).

Heat-denatured protein samples (8µg) were separated on 4-12% SDS-polyacrylamide gels

(Invitrogen) and blotted onto cellulose membranes (Bio-Rad). After blocking with bovine serum

albumin (BSA) in phosphate-buffered saline containing 0.5% Tween 20 (PBST) for 1 hour at RT,

the filter was incubated overnight with antibody against murine mTOR (2983, Cell Signaling) in 5%

BSA/PBST with constant shaking. After three washes with PBST, the membrane was incubated

with horseradish peroxidase (HRP)-conjugated antirabbit IgG (SA1-200, Affinity BioReagents).

Housekeeping controls were detected with an antibody against mouse cyclophilin B (PA1-027,

Affinity BioReagents) and HRP-conjugated antirabbit IgG. Chemiluminescence was produced with

western blotting luminol reagent (Santa Cruz Biotechnology) and gel images captured using a

Molecular Imager Gel Doc XR System (Bio-Rad).

Reverse transcript polymerase chain reaction (RT-PCR). Total RNA harvests from

transfected cells were isolated 48 hours after siRNA transfection using an RNeasy Mini Kit

(Qiagen). Up to 0.5 µg of RNA was converted to cDNA with the SuperScript III 1st strand RT kit for

PCR (Invitrogen). PCR primers were designed for mTOR (forward: 5'-AGC GTA TTG TTG AGG

ACT GGC AGA-3', reverse: 5'-ATC CTG GAG GTT GTT GCC TCT TGA-3'), cyclophilin B

(housekeeping control, forward: 5'-GCA ATG GCA AAG GGT TTC TCC ACT-3', reverse: 5'-AGC

GCT TCC CAG ATG AGA ACT TCA-3'), and collagen type 1 alpha 1 (COL1A1) (forward: 5'-AAG

AAT GGC GAT CGT GGT GAG ACT-3', reverse: 5'-TTG AGT CCG TCT TTG CCA GGA GAA-3')

using Primerquest software from Integrated DNA Technologies (IDT, USA). PCR was performed

with iTaq DNA polymerase (Bio-Rad), 1.5 mM magnesium chloride, 200 µM each of dNTPs, 500

nM of each primer, and 2 µl of the cDNA. PCR reaction for mTOR was 95°C for 3 minutes,

followed by 25 cycles with 95°C for 30 seconds, 63.9^{o}C for 30 seconds, and finally at 72°C for 1

minute. PCR reactions for cyclophilin B and COL1A1 were 95°C for 3 minutes, followed by 30

cycles with 95°C for 30 seconds, 60°C for 30 seconds, and finally at 72°C for 1 minute. PCR

products were collected for all three genes and electrophoresed using ethidium bromide-stained

TBE-based 2% agarose gels run at 100V for 30 minutes.

Preparation of PEG-based hydrogel release matrix and in vitro controlled release of
siRNA/bPEI complexes to cultured cells.   Crosslinked hydrogels releasing siRNA were prepared

using PEGDM and DTT at a 1:1 stoichiometric ratio of thiols to acrylates by Michael-type addition

reactions.[28, 29] FITC-labeled siRNA (FITC-siRNA, siGLO® Green, Dharmacon) was used for

determining siRNA release kinetics from the PEG-based hydrogels. To encapsulate siRNA in the

hydrogels, 2 µg of siRNA and 4.77 µl of 1 mg/ml bPEI (NP = 20) were mixed first and incubated at

room temperature for 15 minutes. Volumes of stock solutions equal to either 4.25 or 8.5 mg of

PEGDM and 0.09 or 0.18 mg of DTT in RNase-free water were added respectively to the

siRNA/bPEI complex mixtures successively in a circular plastic mold with a parafilm bottom (6 mm)

diameter. Final polymerization volume was adjusted to 20 µl with RNase-free water. After 5 hours

incubations at 37°C, the resulting hydrogels were used for releasing study after washes with PBS

at least three times to remove free siRNA and unreacted reagents.

The siRNA-containing hydrogels were immersed in 1ml of PBS buffer for 14 days, and the

supernatant was collected and refreshed at different time points for fluorescence intensity

measurements using a plate reader (TECAN GENIOS Plus, excitation 485 nm/emission 528 nm). The standard curve was prepared by using FITC-labeled siRNA PBS solutions (0, 0.0125, 0.25, 0.5, 1 and 2 µg/ml).

To further confirm that siRNA can be released as intact polyplexes, delivery of siRNA/bPEI complexes to cells was evaluated by incubating fibroblast cultures with hydrogel-released siRNA/bPEI complexes. Hydrogels were incubated in 1ml complete media at 37°C. The complex suspension was collected at several time intervals over 15 days. At each sampling time except the last one, supernatant (1 ml) was removed and an equivolume of fresh media was replaced for continued collection.   Cells were plated at 3×10^4 cells/well in a 12-well plate and then treated with the collected media. Protein harvested 3 days later was followed by Western blotting.

In vivo subcutaneous siRNA-releasing device implantation.   All procedures were conducted as approved by the Institutional Animal Care and Use Committee of the University of Utah. C57/BL-6 female mice (12-week-old, 20-25 g, Jackson Laboratories) were maintained in a pathogen-free facility at the University of Utah. Circular Millipore filters (mixed cellulose ester, pore size: 0.45 µm, diameter: 4 mm) were coated with siRNA-containing PEG-based hydrogel under sterile conditions in a cell culture hood. PEGDM, DTT and siRNA/bPEI were mixed in a circular plastic mold with a parafilm bottom (6 mm diameter) and then one filter was placed into the middle of the viscous solution. After incubation at 37°C for 5 hours, the resulting hydrogel (6 mm diameter, 0.7 mm thickness) containing the embedded filter was used for implantation. Mice were anesthetized by intraperitoneal injection of ketamine/xylazine mixture (ketamine: 75 mg/kg, xylazine: 25 mg/kg). Their backs were shaved and cleaned. Dorsal incisions about 1 cm long were

made perpendicularly to the longitudinal axis at the same level as the diaphragm with sterilized surgical scissors. Subcutaneous pockets on both sides of the incision were created by blunt curved forceps and the hydrogel-coated filters were implanted subcutaneously into the dorsal region of mice essentially as described previously.[4] Identical filter pieces covered with PEG-hydrogel without siRNA were used as negative controls. Hydrogels with siRNAs targeting TGF-β1 (sense: GCA ACA ACG CCA UCU AUG AdTdT, antisense: UCA UAG AUG GCG UUG UUG CdTdT) were used as positive controls (sequence sourced from Dr. M. Gonzalez-Juarrero, Colorado State University, showing significant TGF-β1 knockdown efficacy in a chronic pulmonary tuberculosis murine model, unpublished data). Cellulosic (filter paper) circular discs coated with polymer hydrogels containing mTOR-specific siRNAs were compared to both controls. For mTOR siRNA delivery, two doses, 2 μg and 10 μg per implant, were tested, while a single control TGF-β1 siRNA dose (10 μg) was used. After implantation, each surgical incision was closed with standard 4-0 silk sutures. Each mouse received two bilateral implants dorsally of different siRNA doses, providing 4 implants per siRNA per dose. All subjects were euthanized after 2 weeks and surrounding tissues with implants were harvested by necropsy and fixed in 10% neutralized formalin for histological analysis as described below.

Histological analyses and immunohistochemistry. Tissue samples were embedded in paraffin and cut into 5 μm sections after 24 hours' fixation in 10% formalin. Three longitudinal ground sections were generated per sample and were stained with Hematoxylin and eosin (H&E) for cell nuclei and Masson's trichrome (MTS) for collagen encapsulation assessments (conducted at ARUP, University of Utah).[8, 30] Capsule thickness for each section was estimated

microscopically as the average thickness at six different random locations, and was determined

per filter implant as the average thickness of 3 sections per filter explant.

Immunohistochemical staining was performed by ARUP Laboratories (Salt Lake City, UT).

Briefly, slides were cut at 4 μm, then melted at $55^{o}C$ to $60^{o}C$ for 30 minutes, deparaffinized and

rehydrated in graded alcohols (100% × 2, 95% × 2, 70% × 1) for 1 minute each. The following

steps were performed on the Ventana XT (Ventana Medical Systems, Tucson, AZ) at 37°C.

Slides were deparaffinized with EZ Prep solution on the XT, and pretreated with CC1 solution for

30 minutes (TGF beta) or 60 minutes (m-TOR) on the XT. Primary mTOR antibody were applied

for 2 hours (m-TOR 1:300), followed by the secondary antibody for 32 minutes (antirabbit IgG,

Sigma 1:100). Detection was done by staining with Alkaline Phosphatase Red, and the

counterstain was hematoxylin (Ventana) for 4 minutes. Slides were then dehydrated through

graded alcohols (70% × 1, 95% × 2, 100% × 2) for 30 seconds each, dipped in 4 changes of

xylene, and covered with a coverslip. Negative controls included sections treated with hydrogel

without siRNA loading. Microscopic analysis of the FBR was performed independently by two

investigators who were not aware of the identity of the samples.

Cell imaging. Live adherent cells and histological images were captured using a Nikon

Eclipse TE 2000-U microscope with Photometrics Coolsnap ES camera (Roper Scientific).

Statistical analysis. ANOVA followed by two-tailed student's t-test was used to evaluate

significant differences among groups. All in vitro experiments were repeated three times. Error

bars represent standard error of the mean. Results were considered statistically significant if $p <$

0.05.

<u>Results</u>

In vitro experimental data

<u>Optimization of mTOR siRNA/bPEI complexes and their cytotoxicity.</u> To determine the NP

threshold for stable siRNA complex formation, different amounts of bPEI were mixed with 0.14

nmol mTOR siRNA at NP ratios of 0, 0.5, 1, 2, 5, 10 and 20. Figure 6.1a shows migration of

siRNA/bPEI complexes by gel electrophoresis. With NP ratios of 0, 0.5 and 1, siRNA bands

migrate separately on the gel, indicating uncomplexed excess siRNA. When the NP ratio is equal

to 2, the density of the siRNA band is substantially weaker. When the NP ratios are ≥ 5, no siRNA

migrates freely in the gel, indicating that all siRNA molecules are initially entrapped in bPEI

complexes through electrostatic interactions. Therefore, the complex at NP > 5 should be
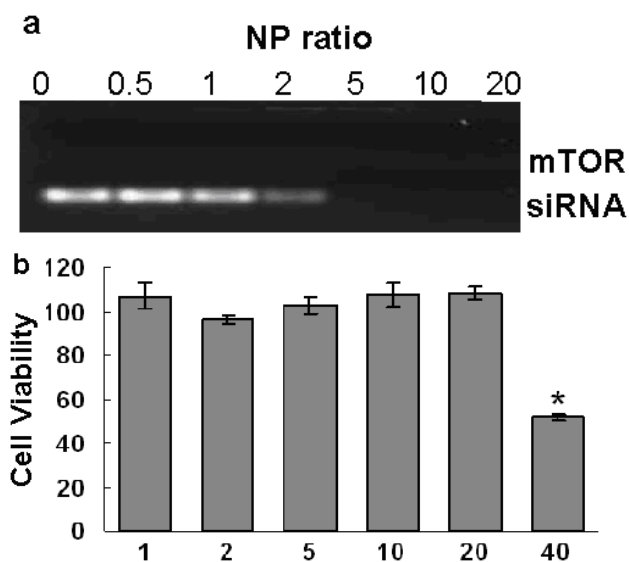
appropriate for siRNA transfection.

Figure 6.1. **Gel migration and cytotoxicity assays of mTOR siRNA/bPEI complexes.** (a)
Gel migration of mTOR siRNA/bPEI complexes at different NP ratios (1-40). (b) Cell
cytotoxicity of mTOR siRNA/bPEI complexes in 3T3 fibroblast in serum-based media. Assay
was performed 24 hours posttransfection. (*p=0.0004, compared with cultures without

Cytotoxicity from the siRNA complexes in serum-cultured fibroblasts in vitro was compared among the different NP ratios (NP = 0-40). As shown in Figure 6.1b, compared with cells without any treatment, cytotoxicity of the siRNA complexes is negligible when NP ratios are at or less than 20 (p = 0.18). In addition, there is no significant difference among the groups for NP ratios ≤ 20.

In vitro mTOR knockdown by siRNA/bPEI complexes on fibroblast cultures.   3T3 Fibroblasts transfected with siRNA/bPEI complexes of different NP ratios (0, 5, 10 and 20) were assayed for mTOR expression. Total protein was harvested 3 days after siRNA treatment. Western blot results showed significant reductions of mTOR expression by siRNA when the NP ratio was 20 (Figure 6.2a). Furthermore, an NP ratio of 20 is sufficient to knock down mTOR expression in fibroblasts in vitro using serum-based transfections. Therefore, the effect of mTOR siRNA/bPEI complexes on cellular mTOR gene expression was only evaluated by RT-PCR for NP = 20. Non-targeting
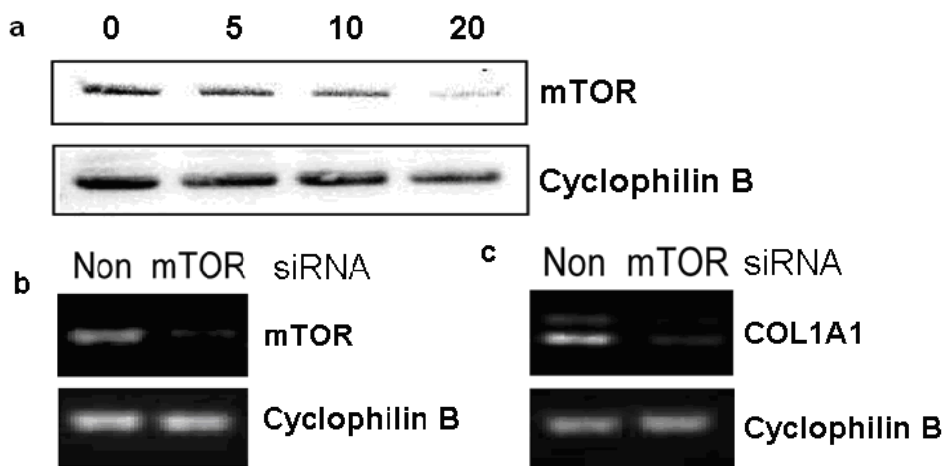

Figure 6.2. **RNA message knockdown in 3T3 fibroblast cultures in serum-based media**. (a) Western blot analysis for mTOR expression after mTOR siRNA/bPEI exposure. Cellular mRNA levels of (b) mTOR and (c) COL1A1 in cells treated with non-targeting siRNA (control) and mTOR siRNA/bPEI complexes were analyzed by RT-PCR. Cyclophilin B (housekeeping gene) mRNA was used as a control.

siRNA/bPEI complexes with the same NP ratio were used as controls. Compared to controls, mTOR siRNA complexed with bPEI reduces mTOR mRNA expression dramatically (Figure 6.2b) in 3T3 fibroblast cultures in vitro.

Since mTOR positively regulates collagen type I production,[13] COL1A1 mRNA levels were also assayed after mTOR siRNA transfection. Compared with non-targeting siRNA transfection, COL1A1 mRNA levels were significantly suppressed by mTOR siRNA treatment in vitro (Figure 6.2c).

Cell proliferation assays were performed 5 days after siRNA transfections in serum-based cultures. As shown in Figure 6.3c, cell numbers in mTOR siRNA groups under NP ratio 20 are much less than that for control siRNA transfection groups (<30%, *p = 0.028). Its representative microscopic images of fibroblasts for control (Figure 6.3a) and treated (Figure 6.3b) groups also demonstrate significant differences in cell density. PEG-based hydrogels were made with published methods [29] by reacting aqueous solutions of PEGDM and DTT. Within a 20 µl total
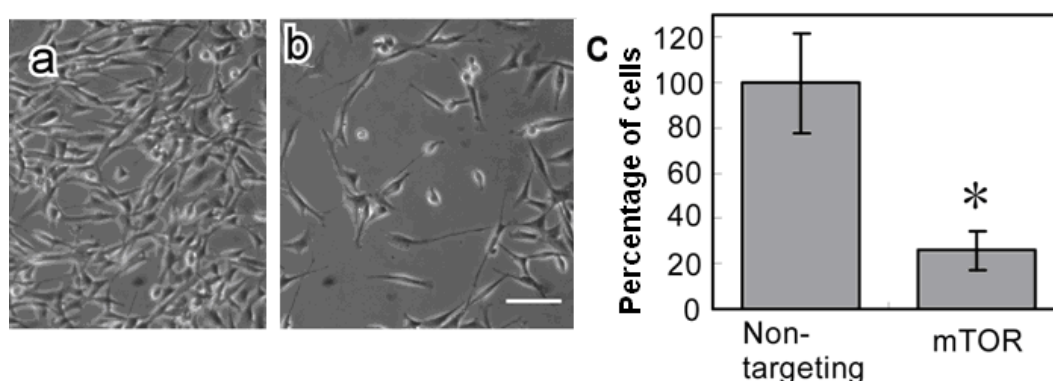

Figure 6.3. **Microscopic images of fibroblast serum-based cultures** (a) treated with non-targeting siRNA, (b) mTOR siRNA at NP ratio 20, and (c) cell proliferation in the siRNA-treated cells (NP 20, *p = 0.028), scale bar = 250µm. Images were taken 5 days after siRNA transfection. Numbers of cells treated with non-targeting siRNA was normalized to 100%.

reaction volume and an NP ratio of siRNA/bPEI equal to 20, 10 µg of siRNA is found to be the

maximum loading for successful in situ gelation with Michael addition network chemistry. Release

profiles for siRNA within the PEG-based hydrogels for two different siRNA/PEG gel formulations

were analyzed (Figure 6.4a). In Formulation 1 (PEGDM: 4.25 mg, DTT: 0.09 mg), approximately

50% of the siRNA was released from the gel within the first 24 hours incubation, and 80% of the

siRNA was released within 3 days. In Formulation 2 (PEGDM: 8.5 mg, DTT: 0.18 mg),

approximately 80% of the siRNA was released by day 7.   A prolonged protein knockdown effect
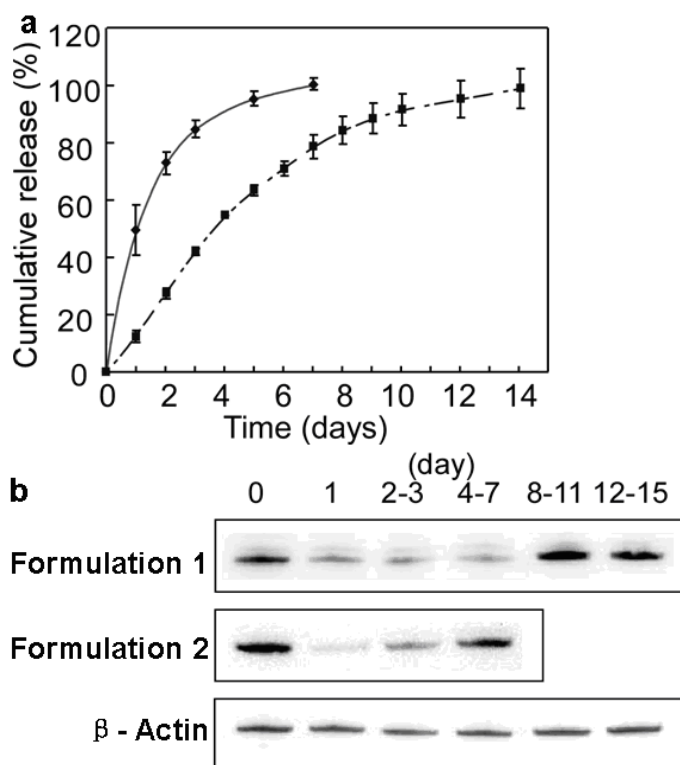

Figure 6.4. **Release of siRNA/bPEI complex from PEG-based hydrogels in vitro.** (a) Cumulative siRNA release profiles in PBS media sink conditions. NP ratio of the siRNA/bPEI complex was 20. Release profiles in Formulation 1 (PEGDM: 4.25mg, DTT: 0.09mg) and Formulation 2 (PEGDM: 8.5mg, DTT: 0.18mg) are indicated by the solid line and dash-dotted line, respectively. (b) Western blot analysis for mTOR expression in fibroblasts after incubating cells with hydrogel-released siRNA/bPEI complexes. Cell lysis was harvested after 3-day culture in this media. Numbers of days shown reflect the hydrogel release time prior to media collection and cell culture.

(up to 1 week) was also obtained by siRNA Formulation 2 compared with Formulation 1 (3 days), which was also supported by Western blot results (Figure 6.4b). Formulation 2 provides longer sustained release kinetics and protein expression suppression, and therefore was used for gel preparations for in vivo studies in subdermal implant-based siRNA release in mice. Tissue harvests surrounding hydrogel-coated filter implants were stained with MTC to identify collagen capsules (blue color). Collagen capsule thicknesses were calculated and compared among negative controls (hydrogels without siRNA: 71.95 ± 7.39 μm), positive controls (hydrogels loaded with TGF β1-specific siRNA: 66.82 ± 10.46 μm) and treated groups (hydrogels loaded with mTOR-specific siRNA: 2 μg dose, 96.60 ± 19.80 μm; 10μg dose, 63.22 ± 5.95 μm). Collagen capsule structure and thickness were evaluated from microscopic images (see Figure 6.5, foreign
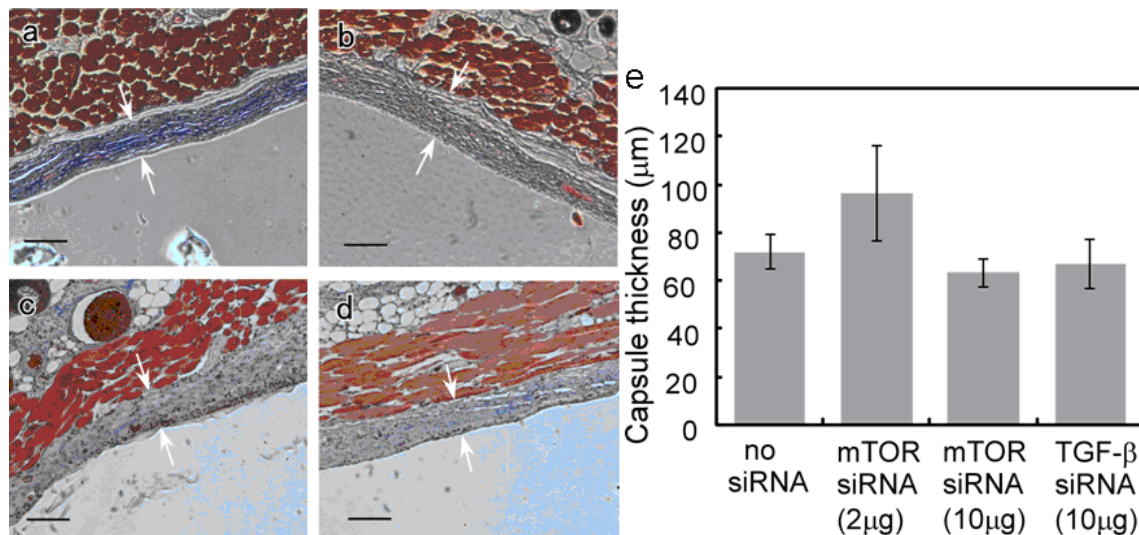

Figure 6.5. **Comparison of in vivo collagen capsule thickness for murine subdermal hydrogel-coated implants explanted after 2 weeks** for (a) negative control, no siRNA loaded, (b) 2μg mTOR siRNA loaded, (c) 10μg mTOR siRNA loaded and (d) positive control, 10 μg TGF-β siRNA loaded. Localization of fibrous capsule is marked by white arrows (scale bar = 100μm). (e) Summary of collagen capsule thickness data. P values for each individual group vs. negative control without siRNA treatment are: 0.3112 (2μg mTOR siRNA), 0.3954 (10μg mTOR siRNA), and 0.7045 (10μg TGF-ß siRNA).

body capsules are demarcated with arrows). However, no significant difference in capsule thickness or structure between these three groups was evident. In addition, H&E staining images indicate that mTOR siRNA does not significantly influence fibroblast density around these implants.

To further investigate whether mTOR inhibition modulates the fibrotic response, tissue mTOR expression was evaluated by immunohistochemistry. Immunostaining of mTOR in tissues adjacent to the capsule (2 µg and 10 µg siRNA dosing cohorts) indicated no significant differences in mTOR expression in foreign body capsules between siRNA-treated mice and the mice treated with blank gel. As shown in Figure 6.6, foreign body capsules contain fibroblasts, inflammatory cells and ECM. After 2-week implantations, no significant foreign body giant cells (FBGC) are observed around the implants. Numbers of macrophages were recruited to the interface, but there were no significant differences in numbers of macrophages around the implants among the groups. Therefore, despite in vitro knockdown success, it was concluded that mTOR siRNA treatments produced no significant reductions in FBR capsule thickness and protein knockdown in vivo.
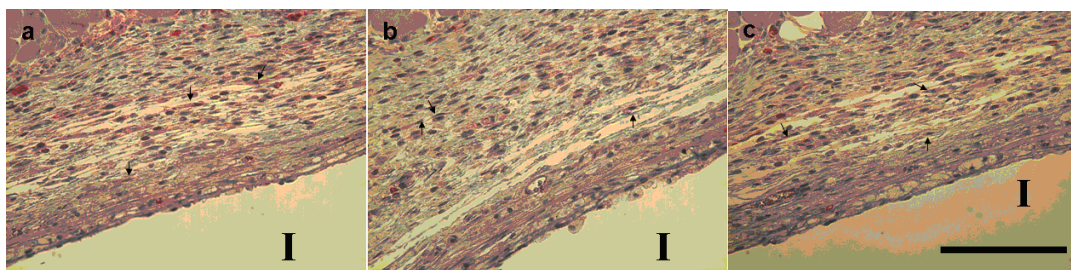

Figure 6.6 Immunostains of mTOR protein expression in foreign body capsules from murine histological sections. Tissue samples surrounding implants (I) were harvested from mice 2-week postimplantation. Immunohistochemical staining for mTOR in foreign body capsules around filter paper from (a) negative control group (no siRNA loaded), (b) 2µg mTOR siRNA-treated group, and (c) 10µg mTOR siRNA-treated group. Sections were stained with mTOR antibody, and counterstaining was done with hematoxylin. These treatments stain target proteins red and cell nuclei dark (blue). Arrows denote fibroblasts (scale bar = 125µm).

<u>Discussion</u>

siRNA is of substantial current interest as a sequence-specific posttranscriptional gene silencing tool for the genetic analysis and, significantly, for translational, therapeutic applications in various mammalian cells.[31, 32] In order to overcome several delivery challenges for siRNA in therapeutics, several approaches have been used, including conjugating siRNA with cholesterol [33], and delivery using cationic liposomes [34] and polymer carriers.[35] Some have also been successfully utilized for systemic siRNA delivery in mice.[34, 36] Viral vectors have been described for siRNA delivery as well.[37-39] Nevertheless, overcoming viral vector oncogenicity and immunogenicity remains a significant barrier for viral-based siRNA delivery. In general, efficiently targeting siRNA to systemic disease sites remains a significant problem. To overcome this, lipid or polymer-based siRNA delivery systems have been successfully used for local siRNA (e.g., topical) delivery, particularly to ophthalmic, vaginal, dermal, liver, neural, pulmonary and tumor targets.[21, 23-25, 40-44] Therefore, locally delivered siRNA from the surface of implantable subcutaneous devices was assessed for efficacy in targeting a major clinical complication of the foreign body response – implant-associated fibrosis.

To facilitate released siRNA internalization by mammalian cells in serum, mTOR siRNA was complexed with bPEI at different NP ratios (0-20) because of its known utility as a nonviral nucleic acid delivery vector.[45-47] The siRNA/bPEI migration assay (Figure 6.1a) demonstrates that siRNA forms stable complexes with bPEI when the NP ratio $\geq$ 5. Cytotoxicity from siRNA complexes was analyzed by culturing fibroblasts with siRNA complexes with different NP ratios up to 40 in serum complete media. Significant cytotoxicity was observed only when the NP ratio approached 40.

Taken together, these results indicate that siRNA/bPEI complexes can be used for specific suppression of mTOR expression in fibroblast serum-based cultures for NP ratios from 5 to 20.

Transfection of mTOR siRNA in 3T3 fibroblasts in serum-based cultures produced mTOR gene silencing monitored by Western blotting 3 days posttransfection. Knockdown of mTOR occurs only when the NP ratio was 20, indicating that siRNA specifically knocked down mTOR message RNA in fibroblasts. To further exclude the possibility of nonspecific knockdown of mTOR by the transfection reagent (bPEI), target gene expression was compared between non-targeting siRNA and mTOR siRNA in cells. Compared to non-targeting siRNA complexes, mTOR siRNA complexes reduced mTOR mRNA expression in fibroblasts dramatically as shown in Figure 6.2b. Thus, these data confirm that mTOR siRNA suppressed the targeted gene specifically through the RNAi mechanism.

In previous studies, mTOR was demonstrated to be essential for activating expression of the collagen type I gene (COL1A1) in dermal fibroblasts.[13, 48] A dramatic decrease (75%) in COL1A1 mRNA expression was induced by down-regulating mTOR expression level to 56%.[13] Hence, it is not surprising that mTOR siRNA also down-regulates COL1A1 mRNA expression by decreasing mTOR expression (Figure 6.2c). This supports the hypothesis that collagen production by fibroblasts would be blocked by mTOR siRNA transfection.

A significant role for mTOR is also promoting cell growth and proliferation by regulating protein synthesis.[49, 50] It is therefore conceivable that mTOR knockdown may also control or alter cell proliferation to some extent. Suppression of cell proliferation is shown after fibroblast transfection with mTOR siRNA in cultures (Figure 6.3). Nearly 70% decrease in cell number after

mTOR siRNA treatment is observed compared to non-targeting siRNA transfections, supporting that mTOR function specifically, not cytotoxicity, was successfully suppressed by the specific siRNA delivery to fibroblast cultures in serum.

These in vitro findings support siRNA targeting of mTOR to modulate collagen production and implant encapsulation, analogous to rapamycin's use against mTOR as an antifibrotic agent.[51-54] To move this in vivo, a local delivery strategy using release from an implant surface as a combination device model was used. PEG-based hydrogels were exploited for this in vivo delivery system since the Michael addition chemistry in water allows mild in situ polymerization at physiological temperatures and pH in the presence of siRNA/bPEI complexes, control of both loading and release rates, and in situ polymerization on or around an implant.[28, 29] To facilitate siRNA entry into cells, bPEI is used as a known complexing agent for nucleic acid delivery.[45, 46] SiRNA/bPEI complexes were loaded into and released from the swollen and degrading PEG-based hydrogel networks. Two different siRNA diffusion profiles were obtained from PEG hydrogels of two formulations, showing that encapsulated siRNA dosing release depends on hydrogel cross-linking. The higher cross-linked PEG hydrogels showed sustained release of siRNA to 14 days in vitro (Figure 6.4a). In addition, the sustained siRNA release resulted in prolonged protein knock-down to 7 days. Furthermore, this successful knockdown confirms that the released siRNA is active and complexed with PEI. Therefore, siRNA formulation 2 was selected for our in vivo studies.

Since encapsulated siRNA molecules exhibit both sustained release from PEG-based hydrogels and effective mTOR and collagen knockdown in the presence of serum in vitro, the

siRNA hydrogels were applied to a model soft tissue implant to reduce collagen expression and fibroblast proliferation in the context of the FBR. Based on in vitro release data showing complete siRNA release after 2 weeks, implants were harvested 2 weeks postsurgery. The thickness of the collagen fibrous capsule was evaluated for model circular membrane devices coated with PEG hydrogels in mice. As shown in Figure 6.5, no significant differences in collagen capsule formation were found among the three groups. Compared to negative controls, both mTOR and control TGF-β siRNA-releasing material groups exhibited no detectable antifibrotic activity in vivo. The capsule thickness for negative control groups is comparable to the published data for the same cellulose implants harvested 4 weeks postsurgery in the same animal model, (i.e., 63 ± 25μm in Ref [4], and 79 ± 40μm in Ref [55]). Previous studies have demonstrated that TGF-β is a potent target for antifibrotic therapy. [56-59] These studies show antifibrotic efficacy of TGF-β siRNA to prevent fibrosis in vivo using different delivery systems. However, TGF-β siRNA showed no detectable antifibrotic activity as collagen capsule thickness was unaffected by the TGF-β siRNA in the murine implant model. Possible explanations for these nondistinguishing results include insufficient siRNA dosing, inefficient cellular uptake by the target fibroblasts around the implant and siRNA scavenging by cells other than fibroblasts at the implant site. A limitation of this design is that PEG hydrogel gelation is inhibited when siRNA complex loading exceeds 10μg per polymerization. siRNA device-based dose loading cannot be increased in this formulation to address the dosing issue in vivo. Effective gene silencing dose of siRNA in many applications in vivo is 1-2.5mg/kg.[21] Here, our study administered 0.4~0.5mg/kg. Thus, inefficient silencing produced by the siRNA was due partially to low dosing.   As bPEI also has mild nucleophilicity and

some Michael addition capability with PEG acrylate,[60] increasing bPEI concentrations in the

gelation step could alter polymerization and also affect bPEI participation as a cell transfection

agent.

In situ tissue slice histology immunostaining for mTOR protein was performed to monitor in

vivo knockdown effects. In both 10µg and 2µg mTOR siRNA dose-treated groups, siRNA

treatment is unable to inhibit mTOR protein expression in the capsule. Therefore, similar capsule

thickness results from unchanged mTOR expression level in fibroblasts. For subcutaneous filter

paper implantation in our case, FBGCs were difficult to find at the implant interface with tissue

2-week postimplantation. Plenty of macrophages were recruited to the interface. However, there is

no significant difference of the number of macrophages at the implant and capsule interface

between siRNA treated groups and controls. Immunoreactivity appears comparable in all groups

and the addition of siRNA does not elicit significant changes in the FBR. In the early stage of the

FBR, macrophages recruited to the implant site fuse to form FBGCs. They adhere to the surface of

the hydrogel-coated implant and release several chemicals that affect the implant surface. In this

microenvironment, the hydrogel was also susceptible to degradation. Some fraction of siRNA/PEI

complexes are likely taken up by active capsule-associated cell endo- and phagocytosis

mechanisms, followed by their degradation in phagolysosomes where pH remains as low as 4.[61]

Hydrogel-released siRNA/PEI complexes escaping active cell phagocytosis must penetrate the

dense tissue extracellular matrix in the capsule to approach and enter target cells and then

successfully escape endosomes to produce siRNA bioactivity. Hence, despite local siRNA

dosing and direct release into the fibrous implant-associated capsule, siRNA polyplex dosing has

low percentage success in producing efficacy for mTOR knockdown in vivo. The apparent absence of protein knockdown in vivo is a testimony to the difficulty in getting sufficient siRNA from the implant to nearby fibroblast cells in the capsule. For device-based local siRNA delivery, the drug release system must overcome nonspecific macrophage/FBGC capture and degradation, unless these cells are specific targets for therapies. Therefore, device-based local siRNA delivery seeking to target collagen-producing local fibroblasts, but lacking specific cell-targeting features for fibroblasts, exhibits poor in vivo subcutaneous performance despite promising in vitro knockdown and antiproliferative efficacy in serum-based fibroblast monocultures.

Conclusions

In vitro cell culture results support siRNA targeting of mTOR to effectively suppress fibroblast proliferation and down-regulate type I collagen mRNA expression in serum-based fibroblast cultures. Thus, like commonly studied rapamycin, mTOR-targeted siRNA was expected to inhibit fibrotic responses around implants in vivo. Nonetheless, subcutaneous in vivo results demonstrated little translation of in vitro siRNA activity to alter implant-associated fibrous encapsulation using a PEG-based hydrogel-coated implant releasing mTOR siRNA in a murine subcutaneous implant model. Though mTOR remains a potent and attractive target for this therapeutic purpose, and local device-based delivery is attractive for combination device local siRNA delivery, further studies are warranted to improve in vivo efficacy in this application. These include new in vivo siRNA delivery systems, improvements in siRNA cell transfection efficacy, degradation-resistant siRNA chemistries, and specific siRNA targeting to fibroblasts under

physiological conditions and foreign body responses.

References

1.   Ratner, B. D. Reducing capsular thickness and enhancing angiogenesis around implant drug release systems. *J Control Release* **2002,** 78, (1-3), 211-8.

2.   Anderson, J. M.; Rodriguez, A.; Chang, D. T. Foreign body reaction to biomaterials. *Semin Immunol* **2008,** 20, (2), 86-100.

3.   Song, E.; Ouyang, N.; Horbelt, M.; Antus, B.; Wang, M.; Exton, M. S. Influence of alternatively and classically activated macrophages on fibrogenic activities of human fibroblasts. *Cell Immunol* **2000,** 204, (1), 19-28.

4.   Jay, S. M.; Skokos, E.; Laiwalla, F.; Krady, M. M.; Kyriakides, T. R. Foreign body giant cell formation is preceded by lamellipodia formation and can be attenuated by inhibition of Rac1 activation. *Am J Pathol* **2007,** 171, (2), 632-40.

5.   Martin, P.; Leibovich, S. J. Inflammatory cells during wound repair: the good, the bad and the ugly. *Trends Cell Biol* **2005,** 15, (11), 599-607.

6.   Miller, K. M.; Anderson, J. M. In vitro stimulation of fibroblast activity by factors generated from human monocytes activated by biomedical polymers. *J Biomed Mater Res* **1989,** 23, (8), 911-30.

7.   Norton, L. W.; Koschwanez, H. E.; Wisniewski, N. A.; Klitzman, B.; Reichert, W. M. Vascular endothelial growth factor and dexamethasone release from nonfouling sensor coatings affect the foreign body response. *J Biomed Mater Res A* **2007,** 81, (4), 858-69.

8.   Blanco, E.; Weinberg, B. D.; Stowe, N. T.; Anderson, J. M.; Gao, J. Local release of dexamethasone from polymer millirods effectively prevents fibrosis after radiofrequency ablation. *J*

Biomed Mater Res A **2006,** 76, (1), 174-82.

9. Patil, Y.; Panyam, J. Polymeric nanoparticles for siRNA delivery and gene silencing. *Int J Pharm* **2009,** 367, (1-2), 195-203.

10. Dumont, F. J.; Su, Q. Mechanism of action of the immunosuppressant rapamycin. *Life Sci* **1996,** 58, (5), 373-95.

11. Ruocco, M. G.; Maeda, S.; Park, J. M.; Lawrence, T.; Hsu, L. C.; Cao, Y.; Schett, G.; Wagner, E. F.; Karin, M. I{kappa}B kinase (IKK){beta}, but not IKK{alpha}, is a critical mediator of osteoclast survival and is required for inflammation-induced bone loss. *J Exp Med* **2005,** 201, (10), 1677-87.

12. Windecker, S.; Roffi, M.; Meier, B. Sirolimus eluting stent: a new era in interventional cardiology? *Curr Pharm Des* **2003,** 9, (13), 1077-94.

13. Shegogue, D.; Trojanowska, M. Mammalian target of rapamycin positively regulates collagen type I production via a phosphatidylinositol 3-kinase-independent pathway. *J Biol Chem* **2004,** 279, (22), 23166-75.

14. Poulalhon, N.; Farge, D.; Roos, N.; Tacheau, C.; Neuzillet, C.; Michel, L.; Mauviel, A.; Verrecchia, F. Modulation of collagen and MMP-1 gene expression in fibroblasts by the immunosuppressive drug rapamycin. A direct role as an antifibrotic agent? *J Biol Chem* **2006,** 281, (44), 33045-52.

15. Gao, X. M.; Wong, G.; Wang, B.; Kiriazis, H.; Moore, X. L.; Su, Y. D.; Dart, A.; Du, X. J. Inhibition of mTOR reduces chronic pressure-overload cardiac hypertrophy and fibrosis. *J Hypertens* **2006,** 24, (8), 1663-70.

16. Simler, N. R.; Howell, D. C.; Marshall, R. P.; Goldsack, N. R.; Hasleton, P. S.; Laurent, G. J.; Chambers, R. C.; Egan, J. J. The rapamycin analogue SDZ RAD attenuates bleomycin-induced pulmonary fibrosis in rats. *Eur Respir J* **2002,** 19, (6), 1124-7.

17. Hammond, S. M.; Bernstein, E.; Beach, D.; Hannon, G. J. An RNA-directed nuclease mediates post-transcriptional gene silencing in Drosophila cells. *Nature* **2000,** 404, (6775), 293-6.

18. Calle, Y.; Jones, G. E.; Jagger, C.; Fuller, K.; Blundell, M. P.; Chow, J.; Chambers, T.; Thrasher, A. J. WASp deficiency in mice results in failure to form osteoclast sealing zones and defects in bone resorption. *Blood* **2004,** 103, (9), 3552-61.

19. Aigner, A. Delivery systems for the direct aplication of siRNAs to induce RNA interference (RNAi) in vivo. *J Biomed Biotechnol* **2006,** 2006, 1-15.

20. de Fougerolles, A.; Vornlocher, H. P.; Maraganore, J.; Lieberman, J. Interfering with disease: a progress report on siRNA-based therapeutics. *Nat Rev Drug Discov* **2007,** 6, (6), 443-53.

21. Woodrow, K. A.; Cu, Y.; Booth, C. J.; Saucier-Sawyer, J. K.; Wood, M. J.; Saltzman, W. M. Intravaginal gene silencing using biodegradable polymer nanoparticles densely loaded with small-interfering RNA. *Nat Mater* **2009,** 8, (6), 526-33.

22. Reich, S. J.; Fosnot, J.; Kuroki, A.; Tang, W.; Yang, X.; Maguire, A. M.; Bennett, J.; Tolentino, M. J. Small interfering RNA (siRNA) targeting VEGF effectively inhibits ocular neovascularization in a mouse model. *Mol Vis* **2003,** 9, 210-6.

23. Takanashi, M.; Oikawa, K.; Sudo, K.; Tanaka, M.; Fujita, K.; Ishikawa, A.; Nakae, S.; Kaspar, R. L.; Matsuzaki, M.; Kudo, M.; Kuroda, M. Therapeutic silencing of an endogenous gene by siRNA cream in an arthritis model mouse. *Gene Ther* **2009,** 16, (8), 982-9.

24. Massaro, D.; Massaro, G. D.; Clerch, L. B. Noninvasive delivery of small inhibitory RNA and other reagents to pulmonary alveoli in mice. *Am J Physiol Lung Cell Mol Physiol* **2004,** 287, (5), L1066-70.

25. Thakker, D. R.; Natt, F.; Husken, D.; Maier, R.; Muller, M.; van der Putten, H.; Hoyer, D.; Cryan, J. F. Neurochemical and behavioral consequences of widespread gene knockdown in the adult mouse brain by using nonviral RNA interference. *Proc Natl Acad Sci U S A* **2004,** 101, (49), 17270-5.

26. Wu, P.; Grainger, D. W. Drug/device combinations for local drug therapies and infection prophylaxis. *Biomaterials* **2006,** 27, (11), 2450-67.

27. Christie, R. J.; Grainger, D. W. Design strategies to improve soluble macromolecular delivery constructs. *Adv Drug Deliv Rev* **2003,** 55, (3), 421-37.

28. van de Wetering, P.; Metters, A. T.; Schoenmakers, R. G.; Hubbell, J. A. Poly(ethylene glycol) hydrogels formed by conjugate addition with controllable swelling, degradation, and release of pharmaceutically active proteins. *J Control Release* **2005,** 102, (3), 619-27.

29. Metters, A.; Hubbell, J. Network formation and degradation behavior of hydrogels formed by Michael-type addition reactions. *Biomacromolecules* **2005,** 6, (1), 290-301.

30. Bryers, J. D.; Jarvis, R. A.; Lebo, J.; Prudencio, A.; Kyriakides, T. R.; Uhrich, K. Biodegradation of poly(anhydride-esters) into non-steroidal anti-inflammatory drugs and their effect on Pseudomonas aeruginosa biofilms in vitro and on the foreign-body response in vivo. *Biomaterials* **2006,** 27, (29), 5039-48.

31.   Aagaard, L.; Rossi, J. J. RNAi therapeutics: principles, prospects and challenges. *Adv Drug Deliv Rev* **2007,** 59, (2-3), 75-86.

32.   Almeida, R.; Allshire, R. C. RNA silencing and genome regulation. *Trends Cell Biol* **2005,** 15, (5), 251-8.

33.   Soutschek, J.; Akinc, A.; Bramlage, B.; Charisse, K.; Constien, R.; Donoghue, M.; Elbashir, S.; Geick, A.; Hadwiger, P.; Harborth, J.; John, M.; Kesavan, V.; Lavine, G.; Pandey, R. K.; Racie, T.; Rajeev, K. G.; Rohl, I.; Toudjarska, I.; Wang, G.; Wuschko, S.; Bumcrot, D.; Koteliansky, V.; Limmer, S.; Manoharan, M.; Vornlocher, H. P. Therapeutic silencing of an endogenous gene by systemic administration of modified siRNAs. *Nature* **2004,** 432, (7014), 173-8.

34.   Sorensen, D. R.; Leirdal, M.; Sioud, M. Gene silencing by systemic delivery of synthetic siRNAs in adult mice. *J Mol Biol* **2003,** 327, (4), 761-6.

35.   Khan, A.; Benboubetra, M.; Sayyed, P. Z.; Ng, K. W.; Fox, S.; Beck, G.; Benter, I. F.; Akhtar, S. Sustained polymeric delivery of gene silencing antisense ODNs, siRNA, DNAzymes and ribozymes: in vitro and in vivo studies. *J Drug Target* **2004,** 12, (6), 393-404.

36.   Sioud, M.; Sorensen, D. R. Cationic liposome-mediated delivery of siRNAs in adult mice. *Biochem Biophys Res Commun* **2003,** 312, (4), 1220-5.

37.   Rubinson, D. A.; Dillon, C. P.; Kwiatkowski, A. V.; Sievers, C.; Yang, L.; Kopinja, J.; Rooney, D. L.; Zhang, M.; Ihrig, M. M.; McManus, M. T.; Gertler, F. B.; Scott, M. L.; Van Parijs, L. A lentivirus-based system to functionally silence genes in primary mammalian cells, stem cells and transgenic mice by RNA interference. *Nat Genet* **2003,** 33, (3), 401-6.

38.   Tomar, R. S.; Matta, H.; Chaudhary, P. M. Use of adeno-associated viral vector for delivery of small interfering RNA. *Oncogene* **2003,** 22, (36), 5712-5.

39.   Matta, H.; Hozayev, B.; Tomar, R.; Chugh, P.; Chaudhary, P. M. Use of lentiviral vectors for delivery of small interfering RNA. *Cancer Biol Ther* **2003,** 2, (2), 206-10.

40.   Reich, S. J. e. a. Small interfering RNA (siRNA) targeting VEGF effectively inhibits ocular neovascularization in a mouse model. *Mol. Vision* **2004,** 9, 210-216.

41.   Humphrey, M. B.; Ogasawara, K.; Yao, W.; Spusta, S. C.; Daws, M. R.; Lane, N. E.; Lanier, L. L.; Nakamura, M. C. The signaling adapter protein DAP12 regulates multinucleation during osteoclast development. *J Bone Miner Res* **2004,** 19, (2), 224-34.

42.   Luo, M. C.; Zhang, D. Q.; Ma, S. W.; Huang, Y. Y.; Shuster, S. J.; Porreca, F.; Lai, J. An

efficient intrathecal delivery of small interfering RNA to the spinal cord and peripheral neurons. *Mol Pain* **2005,** 1, 29.

43.   Morrissey, D. V.; Lockridge, J. A.; Shaw, L.; Blanchard, K.; Jensen, K.; Breen, W.; Hartsough, K.; Machemer, L.; Radka, S.; Jadhav, V.; Vaish, N.; Zinnen, S.; Vargeese, C.; Bowman, K.; Shaffer, C. S.; Jeffs, L. B.; Judge, A.; MacLachlan, I.; Polisky, B. Potent and persistent in vivo anti-HBV activity of chemically modified siRNAs. *Nat Biotechnol* **2005,** 23, (8), 1002-7.

44.   Schiffelers, R. M.; Xu, J.; Storm, G.; Woodle, M. C.; Scaria, P. V. Effects of treatment with small interfering RNA on joint inflammation in mice with collagen-induced arthritis. *Arthritis Rheum* **2005,** 52, (4), 1314-8.

45.   Choung, S.; Kim, Y. J.; Kim, S.; Park, H. O.; Choi, Y. C. Chemical modification of siRNAs to improve serum stability without loss of efficacy. *Biochem Biophys Res Commun* **2006,** 342, (3), 919-27.

46.   Wang, D. A.; Narang, A. S.; Kotb, M.; Gaber, A. O.; Miller, D. D.; Kim, S. W.; Mahato, R. I. Novel branched poly(ethylenimine)-cholesterol water-soluble lipopolymers for gene delivery. *Biomacromolecules* **2002,** 3, (6), 1197-207.

47.   Jiang, G.; Park, K.; Kim, J.; Kim, K. S.; Oh, E. J.; Kang, H.; Han, S. E.; Oh, Y. K.; Park, T. G.; Kwang Hahn, S. Hyaluronic acid-polyethyleneimine conjugate for target specific intracellular delivery of siRNA. *Biopolymers* **2008,** 89, (7), 635-42.

48.   Kyriakides, T. R.; Zhu, Y. H.; Yang, Z.; Huynh, G.; Bornstein, P. Altered extracellular matrix remodeling and angiogenesis in sponge granulomas of thrombospondin 2-null mice. *Am J Pathol* **2001,** 159, (4), 1255-62.

49.   Achenbach, T. V.; Brunner, B.; Heermeier, K. Oligonucleotide-based knockdown technologies: antisense versus RNA interference. *Chembiochem* **2003,** 4, (10), 928-35.

50.   Burnett, P. E.; Barrow, R. K.; Cohen, N. A.; Snyder, S. H.; Sabatini, D. M. RAFT1 phosphorylation of the translational regulators p70 S6 kinase and 4E-BP1. *Proc Natl Acad Sci U S A* **1998,** 95, (4), 1432-7.

51.   Wu, M. J.; Wen, M. C.; Chiu, Y. T.; Chiou, Y. Y.; Shu, K. H.; Tang, M. J. Rapamycin attenuates unilateral ureteral obstruction-induced renal fibrosis. *Kidney Int* **2006,** 69, (11), 2029-36.

52.   Neef, M.; Ledermann, M.; Saegesser, H.; Schneider, V.; Reichen, J. Low-dose oral rapamycin treatment reduces fibrogenesis, improves liver function, and prolongs survival in rats with established liver cirrhosis. *J Hepatol* **2006,** 45, (6), 786-96.

53. Salminen, U. S.; Maasilta, P. K.; Taskinen, E. I.; Alho, H. S.; Ikonen, T. S.; Harjula, A. L. Prevention of small airway obliteration in a swine heterotopic lung allograft model. *J Heart Lung Transplant* **2000,** 19, (2), 193-206.

54. Poston, R. S.; Billingham, M.; Hoyt, E. G.; Pollard, J.; Shorthouse, R.; Morris, R. E.; Robbins, R. C. Rapamycin reverses chronic graft vascular disease in a novel cardiac allograft model. *Circulation* **1999,** 100, (1), 67-74.

55. Puolakkainen, P.; Bradshaw, A. D.; Kyriakides, T. R.; Reed, M.; Brekken, R.; Wight, T.; Bornstein, P.; Ratner, B.; Sage, E. H. Compromised production of extracellular matrix in mice lacking secreted protein, acidic and rich in cysteine (SPARC) leads to a reduced foreign body reaction to implanted biomaterials. *Am J Pathol* **2003,** 162, (2), 627-35.

56. Qi, Z.; Atsuchi, N.; Ooshima, A.; Takeshita, A.; Ueno, H. Blockade of type beta transforming growth factor signaling prevents liver fibrosis and dysfunction in the rat. *Proc Natl Acad Sci U S A* **1999,** 96, (5), 2345-9.

57. Kushibiki, T.; Nagata-Nakajima, N.; Sugai, M.; Shimizu, A.; Tabata, Y. Enhanced anti-fibrotic activity of plasmid DNA expressing small interference RNA for TGF-beta type II receptor for a mouse model of obstructive nephropathy by cationized gelatin prepared from different amine compounds. *J Control Release* **2006,** 110, (3), 610-7.

58. Kim, K. H.; Kim, H. C.; Hwang, M. Y.; Oh, H. K.; Lee, T. S.; Chang, Y. C.; Song, H. J.; Won, N. H.; Park, K. K. The antifibrotic effect of TGF-beta1 siRNAs in murine model of liver cirrhosis. *Biochem Biophys Res Commun* **2006,** 343, (4), 1072-8.

59. Ruiz-de-Erenchun, R.; Dotor de las Herrerias, J.; Hontanilla, B. Use of the transforming growth factor-beta1 inhibitor peptide in periprosthetic capsular fibrosis: experimental model with tetraglycerol dipalmitate. *Plast Reconstr Surg* **2005,** 116, (5), 1370-8.

60. Kunath, K.; von Harpe, A.; Petersen, H.; Fischer, D.; Voigt, K.; Kissel, T.; Bickel, U. The structure of PEG-modified poly(ethylene imines) influences biodistribution and pharmacokinetics of their complexes with NF-kappaB decoy in mice. *Pharm Res* **2002,** 19, (6), 810-7.

61. Haas, A. The phagosome: compartment with a license to kill. *Traffic* **2007,** 8, (4), 311-30.

APPENDIX

STANDARD OPERATING PROCEDURES

1. PRIMARY OSTEOCLAST DIFFERENTIATION

Components: Mice, Tissue culture hood, Dissection kit (2 pairs of tweezers and a pair of scissors), α-MEM, Ice bucket, 26 gauge needles (All cell culture reagents and tools should be sterilized before placing them into the hood or incubator!!!! All steps should be performed using sterile technique!!!! If you don't know sterile technique, find someone who does to show you before attempting)

At animal facility: Sacrifice mice

a.   Turn CO_2 on low to fill chamber, let run for at least 5 minutes.
b.   Turn CO_2 off and let gas sink to bottom of tank for about 5 minutes.   This creates a 1-2 inch layer of 95% CO_2, and will allow for faster, more humane killing of the mice.
c.   Gently add mice to tank, trying not to disrupt air too much (so the 95% CO_2 layer remains intact).
d.   Leave mice in tank for at least 2 minutes to ensure that they are all dead.
e.   Bring mice to our lab

Dissect out femurs and tibias

a.   Place mouse on dissection board on paper towel and soak both with 70% ethanol.
b.   Use tweezers to grab "hands" and pin them to the board so the mouse can be stretched out.
c.   Pick up abdominal skin with tweezers and make a small incision with the scissors, be careful not to cut through the abdominal muscles as that will expose more of the mouse than you will wish to see.
d.   Use tweezers to gently tear abdominal skin and reveal the lower half of the abdomen.
e.   Remove skin from legs using your fingers, as if "taking off his pants."
f.   Dislocate the hip and knee by pulling at the ankle while immobilizing the hip. If necessary, bend the knee backwards to dislocate (often necessary on older mice).
g.   In younger mice, the femur will "pop" through the muscle if you pull down on the shin while pushing up on the thigh.   Remove femur, then clip off foot and tease muscle off of tibia.   In older mice, this will not happen.   Clip off foot and tease muscle away from tibia, you may need to cut at the knee to remove.   Then use scissors and tweezers to tease away muscle

from femur, clip out once you can see the ball of the femur. Remove as much excess muscle as possible and store all bones in incomplete ice cold α-MEM.

h. Mouse carcasses should be wrapped in a black plastic bag and placed in the necropsy freezer located at the far south end of the basement.

<u>Flush bone marrow cells out of femurs and tibias</u>

a. Transfer all bones into a Petri dish containing ice cold incomplete α-MEM.

b. Use tweezers to clean off all bones of excess muscle.

c. Hold a bone with tweezers, use scissors to clip ends.

d. Using a 10mL syringe filled with ice cold incomplete α-MEM and a 26 gauge needle, hold bone vertically over a 50mL tube and flush marrow out of bones (5~10ml/bone). Use about 5mL per bone, and flush from both sides.

e. Resuspend bone marrow cells using a 5mL pipette, mix at least 20 times with pipette.

f. Spin down cells at 500g 5minutes.

g. Resuspend bone marrow cells in α-MEM and plate in 10cm-dish over night. We usually resuspend cells to be at a concentration of 10^7 cells per mL prior to plating.

h. Harvest flowing cells the next day. Spin down cells and resuspend cells in complete α-MEM with 20ng/ml M-CSF. Seed cells at 1.2 x 10^6/well into 24-well plate.

i. Two days later, renew the media with complete α-MEM with 20ng/ml M-CSF and 200ng/ml RANKL. The media should be replaced every other day.

Container	Volume	Number of cells
T-175	50mL	10 x 10^7
T-125 flask	35mL	5 x 10^7
100mm Petri dish	10mL	10^7
6-well plate	4mL	3 x 10^6
12-well plate	2mL	2 x 10^6
24-well plate	1mL	1 x 10^6

2. RANKL EXPRESSION

<u>Components:</u>

a. Autoclave the 2L flask with LB media (without Amp). Each flask contains 400ml LB (each flask contains 10g LB powder).
After autoclave, prepare AMP solution (water): weight 40mg AMP powder dissolves in 1ml pure water (di water + autoclave). Add 0.5ml to each 2L flask.
b. Using lysis buffer equilibrium the column, which keeps in 4°C. Wash 2.7 ml of the

glutathione-Sepharose (from Amersham Pharmacia, Cat. 17-0756-01; in a 75% slurry) with water to remove the ethanol, then twice in lysis buffer. Resuspend the Sepharose in 4 ml of lysis buffer, and pack the column (Bio-Rad Poly-Prep; 0.8 x 4 cm; #731-1550).

Bacterial lysates

a. Start two 3 ml culture (small glass tubes) of the 1~2 GST-OPGL clones in the early morning. Grow at 30°C in LBamp, 230rmp. In the evening, add each of them to 400 ml LB-amp separately, and grow O/N at 30.4°C.

b. Next early morning, induce the culture with the addition of 1 mM IPTG for 4 hours. (Prepare IPTG right before using: 0.2g into 1ml of water, and 0.5ml into each big flask)

c. Pellet the cells (7000rpm/6300g, 20 minutes), throw away the supernatant. (The pellet may be frozen at -70°C for an extended period of time). Transfer the pellet to the 50ml Nalgene high speed centrifuge tube (05-529-1D).

d. Resuspension the pellet once in 10ml lysis buffer (20 mM Tris pH 8.0; 150 mM NaCl; 1 mM EDTA + protease inhibitor cocktail, Pierce). Using spoon to help the dissolving/lysis process until all pellet resuspended uniformly.

e. Centrifuge at 7000 rpm for 20 minutes. Re-suspend the pellet in 10ml of the same buffer. Again, using spoon to help dissolving process.

f. Add lysozyme (10mg dissolved in 0.5ml pure water, prepare right before use) to a final concentration of 1 mg/ml, and 10ul of 500mM $MgCl_2$ (1ul/ml), mix up and down gently, and let sit at RT for 15 minutes.

g. Add 100ul Triton X-100 to a final concentration of 1%. Sonicate 1.5 minutes, 30 seconds each time, resting 10~20 seconds between, on ice (low setting-be careful not to generate froth). Add 10ul DNAase I (keep in the blue rack in -20°C) to a final concentration of 10 ug/ml. Leave on ice for 20-30 minutes.

h. Spin at 14,000-20,000rpm/25100-51300g for 20 minutes at 4°C and save the supernatant. The sup should be yellow, not clear. If it is clear, lysis was not complete. Load the entire sup on the top of the column, seal the column top and bottom with paraframe tightly. Rolling the column on the shaker in the refrigerator in chemical site O/N. Or the sup can be save O/N at 4°C.

Glutathione column

a. Wash the column with 2 x 10 ml of lysis buffer.

b. Wash the column with 2 x 10 ml of lysis buffer that lacks NaCl (20 mM Tris pH

c. 8.0, 1 mM EDTA).Using the blue color reagent (5X dilution before using) to check whether there is still protein in the flow through (If solution change to blue, means there is protein). If not, start elution.

d. Prepare reduced glutathione washing buffer: 30.7 mg reduced glutathione dissolve in 10ml lysis buffer with lacking NaCl.

e.   Add 4 ml of fresh (or frozen) 10 mM reduced glutathione (Sigma, Cat. No is G-4251) in 20 mM Tris pH 8.0, 1 mM EDTA to column. Cap the column, and leave it rocking O/N in cold room or rolling for 2 hours in 4°C.

f.   To elute, let the column sit at RT for 10 minutes first! Then collect 2 ml fractions by gravity flow. After that collect next 2 ml. During this process, use the blue color reagent (5X dilution before use) checking the protein containing amount.

g.   Add 2 more ml of the elution buffer. Collect flow through total reach to 5~6ml.

h.   Using Millipore concentration tubes to concentrate and desalting. First pour all flow through in the tube, centrifuge at highest speed for 20 minutes. Then after finishing, add 2ml of pure water to the tube, centrifuge again. At last, after finishing, add 2ml of PBS with 0.1% sodium azide again. After finishing this time, collect the concentrated sample (be careful do not tough the membrane).

i.   Using pure water clean the concentrated tube and pour 20% ethanol into the tube which can totally immerse the membrane.

j.   Please follow Amersham Pharmacia's instruction to clean and store the column.

k.   Measure protein concentration.

Buffers:

For 500 ml lysis buffer (20 mM Tris pH 8.0; 150 mM NaCl; 1 mM EDTA)--
10 ml 1 M Tris pH 8.0
15 ml 5 M NaCl
1 ml 0.5 M EDTA
For 200 ml lysis buffer lacking NaCl—
4 ml 1 M Tris pH 8.0
0.4 ml 0.5 M EDTA

3. PLGA PARTICLE PREPARATION

Components: prepare everything in RNase-free environment

a)   siRNA/bPEI solution in 160 ul Rnase-free buffer

b)   PLGA solution: dissolve 50 mg PLGA polymer (-20C freezer) into 2 ml methylene chloride (CH$_2$Cl$_2$) in a glass test tube. Wrap with foil paper and parafilm to prevent evaporation. Takes overnight to dissolve; also, methylene chloride evaporates quickly so on day of use, add additional methylene chloride if needed.

c)   Polyvinyl alcohol (PVA) solution: 5% stock PVA solution stored in 4°C fridge. Dilute to 4% before use.

Supplies: Beaker, magnetic stirrer, stir bar, vortex mixer and sonicator, glass culture tubes, ice

a. Add 160 ul siRNA/bPEI solution into 2 ml PLGA solution in CH_2Cl_2 drop-wise while vortexing and sonicate for 10 seconds at 10% output. Pause 10 seconds. Repeat sonication. This is emulsion 1.

b. (Add 2 ml 4% PVA drop-wise and slowly while vortexing. Sonicate for 10 seconds at 20% power output. Pause 10 seconds. Repeat sonication. This is emulsion 2 (this step is to make the PLGA solution easier to pour from the glass tube without losing PLGA polymer).)

c. Pour emulsion 2 into 6 ml 4% PVA in a 50 ml falcon tube while vortexing.   (Sonicate for 10 seconds at output 7. Pause 10 seconds. Repeat sonication. This is emulsion 3.)

d. Pour emulsion 3 to 4 ml 0.06% PVA solution in a glass beaker while stirring.

e. Stir for 3-4 hours to completely evaporate methylene chloride and allow PLGA particles to harden.

f. Collect particles and aliquot 1 ml into centrifuge tubes. But be sure to write the total volume and aliquot volume. Store the aliquots at -20 or -80 freezer.

g. Wash the particles 3 times with cold Milli-Q water for further analysis.

h. Perform steps shown in the parentheses can generate nanoscale particles

i. SEM preparation is subjected to different equipments. Dilute concentrated sample 100 times and dry 1~2 sample drops on the sample presenting matrix in the hood overnight.

4. PLGA/CPC PREPARATION

<u>Components:</u> Dried PLGA particles in powder, calcium phosphate cement (CPC) kit (BioMed)

<u>Mixing</u>

a. Add aqueous solution provided in the kit into a syringe at 0.35 g/ml of the PLGA/CPC.

b. Add weight percentage of 10% or 20% PLGA particles into CPC powder. Mix two powder using spoon provided in the kit and vertex. Transfer the mixture into the syringe.

c. Use spoon help dissolving process for 1minute.

d. Inject the mixture into mode provided in the kit.

e. The sitting reaction lasts 20 minutes. Be sure finishing injection within 15 minutes.